The Impact of sample scale on the compressibility parameters of saturated fine-grained soils

TEPONDJOU NGUEDIA ROSINE LARISSA

School of Computing, Science and Engineering
University of Salford, Salford, UK

Submitted in Partial Fulfilment of the Requirements of the Degree of Doctor of Philosophy in Civil Engineering

September 2015

Table of Contents

List of Tables

Table

List of Figures

Figure

Acknowledgement

This thesis is submitted in partial fulfilment of the requirements for the PhD degree at the University of Salford. This work has been conducted at the school of Computer, Science and Engineering from April 2012 to April 2015 under the supervision of Dr Gareth Swift, Dr Wayne Yu Wang and Dr Tahsin Toma Sabbagh.

I would like to thank my first supervisor, Dr Gareth Swift for guiding me through thorough experimental work and challenging project before leaving in December 2014. Special thanks to Dr Wayne Yu Wang for his continual assistance and support and his huge enthusiasm during my research. Great thanks to Dr Tahsin Toma Sabbagh, who took over Dr Gareth Swift for guiding me towards the modelling aspect of my research. Also in this regards, I will like to thank Mr Andy Gibbon for his assistance in operating the apparatus mainly used for my research and Mr Philip Latham and Mr Antony Burrage for their close collaboration in my experimental project. Additionally, I greatly appreciate the help from the Salford Analytical Service Enterprise staff for their assistance in assessing some soil specimens. Also, I would like to thanks my friends for their continued support and encouragement during my degree.

At the end but not the least, I am grateful to my parents. Words cannot express how thankful I am for their continuous support throughout my research. It was not easy for them to sponsor me but with dedication and belief they brought me here, and I am forever thankful.

Affirmation

Journal paper

Rosine T.N. & Sabbagh T.T. 2015. The impact of the diameter to height ratio on the compressibility parameters of saturated fine-grained soils. *International Journal of Research and Engineering Technology*, 4(5): 8 - 19

Conference paper accepted for publication

Rosine T.N. & Sabbagh T.T. Effect of initial moisture content and scale on the compression behaviour of fine-grained soils. 4th GeoChina International Conference 2016 July25-27, Shandong, China.

Journals under consideration

Rosine T.N. & Sabbagh T.T. Modelling of the effect of scale on the compressibility parameters of fine-grained soils. *Geomechanics and Geoengineering international journal*.

Rosine T.N. & Sabbagh T.T. Modelling of the effect of calculated coefficient of permeability on the scale effect of saturated fine-grained soils. *Soils and Foundation*.

List of symbols with their units

Annotations	Comments	Units
A	Cross-sectional area	mm^2
β and α	Slope intercepts	--------
a_v	Coefficient of compressibility	m^2/KN
c_c	Compression Index	-------
c_h	Coefficient of horizontal consolidation	m^2/yr
c_r	Recompression index	------
c_v	Coefficient of consolidation	m^2/yr
$c_{\alpha\varepsilon}$	Rate of secondary consolidation	m^2/yr
c_α	Axial rate of consolidation	-----
c_s	Swelling index	……
c_u	Undrained shear strength	kN/m^2
c_{uh}	Undrained horizontal shear strength	kN/m^2
c_{uv}	Undrained vertical shear strength	kN/m^2
d	Average particle size	mm
d_v	Vane diameter	mm
dV	Change in volume	m^3
d_{10}	Average particle size where 10% of the particles are finer	mm
D	Diameter of sample	mm
D_0	Deformation at zero consolidation	------
D_1 and D_2	Dial reading at t_1 and t_2	------
D_{90}	Deformation at 90% consolidation	------
D_{50}	Deformation at 50% consolidation	------
D_{100}	Deformation at 100% consolidation	------
DS	Diameter Scale	------
D/H	Diameter to height ratio	------
e	Void ratio	------
e_0	Initial void ratio	------
e_f	Final void ratio	------
e_1	Void ratio at σ_1	-------
e_2	Void ratio at σ_2	------

Δe	Change in void ratio	------
F	Measured force	N
G_s	Specific gravity	-----
h_v	Vane height	mm
H_D	Drainage path length	mm
H	Soil height	mm
HS	Height Scale	------
h_o	Initial height	mm
Δh	Change in height	mm
i	Hydraulic gradient	--------
k	Coefficient of permeability	m/s
LL	Liquid Limit	%
M_w	Mass of water	g
M_s	Mass of dry soil	g
m_v	Coefficient of volume compressibility	m^2/MN
m	Mass of rigid plate/porous stone	g
M	Slope of the initial segment	-------
n	Porosity	--------
PL	Plastic Limit	%
PI	Plasticity Index	%
P	Actual pressure	kPa
P_d	Diaphragm pressure	kPa
P_o	Initial pressure	kPa
ΔP	Change in pressure	kPa
δp	Pressure correction	kPa
ρ	Bulk density	Mg/m^3
ρ_w	Density of water	Mg/m^3
Q	Flow rate	m^3/sec
r	Radial distance to the centre of a drain well	mm
SEM	Scanning Electron Microscope	…….
SPSS	Statistical Package for the Social Sciences	……
S_r	Degree of saturation	%
SL	Shrinkage Limit	%

t	Consolidation time	Seconds
T	Transmitted load	N
T_v	Time factor	--------
t_1	Consolidation time at D_1	Seconds
t_2	Consolidation time at D_2	Seconds
t_p and t_s	Time at primary and secondary consolidation	Seconds
t_{50}	Consolidation time at 50% consolidation	Seconds
t_{90}	Consolidation time at 90% consolidation	Seconds
u	Pore water pressure	kPa
u_{excess}	Excess pore pressure	kPa
∂u	Change in excess pore pressure	kPa
U_{av}	Average degree of consolidation	%
V	Total soil volume	m^3
V_w	Volume of water	m^3
V_v	Volume of void	m^3
V_s	Volume of dry soil	m^3
w	Moisture content	%
W_s	Weight of solid	N
w_i	Initial moisture content	%
XRD	X-Ray Diffraction	…….
∂z	Change in soil depth	mm
γ_w	Unit weight of water	kN/m^3
σ_1'	Effective initial pressure	kPa
σ_2'	Effective final pressure	kPa
$\Delta\sigma'$	Change in effective stress	kPa
$\Delta\sigma$	Change in stress	kPa
ε	Strain	…….
δ	Settlement	mm
δ_T	Total ultimate settlement	mm
δ_i	Immediate settlement	mm
δ_c	Consolidation settlement	mm
δ_s	Secondary settlement	mm
τ_s	Frictional stress	kPa

τ	Torque	Kgcm
τ_h	Torque in the horizontal cylindrical surface	Kgcm
τ_v	Torque in the vertical cylindrical surface	Kgcm

Dedicated to my parents Mr and Mrs Tepondjou and all my brothers and sisters

ABSTRACT

The need for an improved understanding of the influence of sample scale on the compressibility behaviour of fine-grained soils is crucial in many applications, such as roads, embankments and foundations. The effect of sample scale represents a challenge when obtaining engineering parameters in the laboratory compared to those obtained in the field. This research therefore aimed at contributing to existing knowledge through both experimental and numerical studies. The experimental study was completed via a series of consolidation tests on fully saturated fine-grained soil (i.e. kaolin clay) at various sample scales, which were subsequently explored analytically using the finite element software PLAXIS 2D. This type of clay was chosen as it is easily sourced and well known. A Scanning Electron Microscope (SEM) and X-Ray Diffractometer (XRD) were employed in studying the micro-structure of the soil.

The Oedometer apparatus was used to obtain the combined effect of sample scale and initial moisture content on the compressibility parameters of kaolin clay. Compressibility parameters such as coefficient of consolidation (c_v), compression index (c_c) and coefficient of volume compressibility (m_v) were also investigated in this study. Three different methods were used to obtain c_v: Casagrande, Taylor's and Inflection methods. The sample scales were divided into three categories: soil sample height, diameter and diameter to height (D/H) ratio scale. Particular attention was given to the D/H ratio effect on the compressibility parameters due to the frictionless boundary conditions, and sample diameter scale due to drainage path length.

Based on the experimental data, Taylor's method was considered more reliable in deriving c_v as compared to the Casagrande and Inflection methods, due to the end of primary consolidation (EOP) observed at all sample scales. It was also observed that on average, sample scale has an effect on c_v with a correlation factor of 0.451 and that friction was reduced by 35%. The effect of sample scale on c_c and m_v was found to be insignificant. The investigation also showed a correlation factor between the initial moisture content and c_v of 0.546 and, 0.162 and 0.026 for c_c and m_v respectively. The new proposed model developed in PLAXIS 2D was found to show no significant difference with the laboratory data except where the calculated coefficient of permeability was used. A new proposed model was developed in PLAXIS to further study the effect of sample diameter scale on the behaviour of fine-grained soils.

CHAPTER 1

INTRODUCTION

1.1 Background

One of the uncertainties that arise when attempting to predict settlement of structures founded on fine-grained soils is in the laboratory determination of the soil design parameters using small soil samples, the behaviour of which may not correspond to the in situ (in the field) response of the soil mass. Larger soil samples may be more representative, particularly where the soil mass may contain micro- or macro- structural features. Some researchers have attempted to investigate the influence of sample scale on soil behaviour. These studies were conducted on the shear strength, bearing capacity, settlement, compaction-stress relationship and coefficient of consolidation with sample scale (Healy and Ramanjaneya, 1970; Grisso et al., 1984; Ortega, 1996; Cerato and Lutenegger, 2007 and Dirgeliene et al., 2007).

1.2 Research Gap

Over the past few decades, various methods have been developed to obtain the compressibility parameters, such as the coefficient of consolidation (c_v). c_v relates to the assessment of the time rate of settlement of a soil undergoing deformation under loading. Reviews of the consolidation variables discussed by previous researchers are as follows:

1. The coefficient of consolidation using different methods
2. Effect of soil sample diameter scale on c_v
3. Effect of soil sample height scale on c_v
4. Effect of soil sample diameter to height ratio scale on c_v
5. Effect of initial moisture content on compressibility parameters
6. Effect of soil sample scale on the compression index (c_c) and coefficient of volume compressibility (m_v)

1.2.1 The coefficient of consolidation (c_v) using different test methods

The value of c_v is obtained in the laboratory from the one-dimensional consolidation test using the curve-fitting procedures and based on Terzaghi's one-dimensional theory (Powrie,

2004). The value of c_v has been obtained from the observations of settlement under embankments and compared with values obtained in the laboratory (Leroueil, 1988 and Almeida and Marques, 2002). Leroueil (1988) collected data from 16 sites and showed the ratio of c_v (in situ) to c_v (laboratory) to vary between 3 and 200 (Tan, 2003). On the other hand, Almeida and Marques (2002) reported similar ratio values ranging from 20 to 30 for Sarapui clay deposits. The discrepancies between the in situ and laboratory values are due to various factors. These factors include the validity of assumptions underlying the consolidation theory, methods of evaluation of c_v using laboratory consolidation test data, and the difference between the laboratory testing conditions and those in the field. (Alshernawy, 2007). In the field, the value of c_v is affected by a number of factors: drainage conditions, soil layer thickness, applied load and macro- structural characteristics of the soil layer (Cortellazzo, 2002).

Some of the methods from which consolidation test data can be evaluated to obtain c_v include: Taylor's method (Taylor, 1942), Casagrande's method (Casagrande and Fadum, 1940), the velocity method (Parkin 1978, 1981, 1984), the rectangular hyperbola method (Sridharan et al., 1987), the inflection method (Mesri et al., 1999), the $\log(H_D^2/t) - U$ method (Sridharan et al., 1995) where U is the average degree of consolidation in percentage, H_D is the drainage path length (mm) and t is the consolidation time in minutes and the slope and settlement rate method (Al-Zoubi, 2013).

Taylor's method is affected by the initial compression and in some cases by secondary compression (Cortellazzo, 2002). The former increases the value of c_v while the latter decreases the value of c_v (this is shown in more detail in Chapter 2). The velocity method is also affected by the secondary compression but is less sensitive. The rectangular hyperbola method generates values that tend to be greater than the previous two methods but lower than those obtained with Taylor's method (Cortellazzo, 2002). The value of c_v obtained using the $\log (H_D^2/t) - U$ method was found to be closer to the value obtained in the laboratory (Sridharan et al., 1995). The inflection methods used only the inflection point of the compression versus log time curve to obtain the value of c_v. Its value was found to be similar to that of the Casagrande value (Mesri et al., 1999; Prakash et al., 2011; and Al-Zoubi, 2013). Al-Zoubi (2013) developed a new method of obtaining c_v using slope and settlement rate based on a direct analytical solution of Terzaghi's theory. The method utilises two consolidation points to back calculate the initial compression. The value of c_v was found

to be comparable to that obtained by the Casagrande method but lower than by Taylor's method (Al-Zoubi, 2013).

1.2.2 Effect of sample diameter on the value of c_v

Limited research has been completed on the effect of sample diameter on the value of c_v. Healy and Ramanjaneya (1970) looked at various sample scales under constant D/H = 3 on the value of c_v on Varved Clay with no emphases on sample diameter scale. During the investigation, the value of c_v was obtained using the Casagrande method, taking into account both vertical and horizontal (or radial) water flow within the soil sample. The value of c_v obtained under radial flow was found to be independent of sample scale (i.e. there was no significant difference in the value of c_v with a change in scale). Under vertical flow, the value of c_v obtained was found to differ greatly from that gained in the radial flow. The variation in c_v was due to the loading conditions, where loading on the Varved clay was applied either vertically or horizontally.

On the other hand, researchers such as Cerato and Lutenegger (2007), Al-Khuzaie (2011) and Dixit and Patil (2013) investigated the effect of sample diameter on soil behaviour. The sample diameter was studied on foundation footing sizes where various plate load tests were conducted at various sample diameters. This refers to the footing size and its effect on: friction angle and bearing capacity was investigated. The findings revealed that footing size has a significant influence on internal friction (between soil and foundation footing) and bearing capacity.

1.2.3 Effect of sample height on the value of c_v

Healy and Ramanjaneya (1970), Berry and Reid (1987), Ortega (1996), and Khan et al. (2012) carried out separate investigations into the relationship between soil thickness and c_v. c_v was found to increase with an increase in thickness. Berry and Reid (1987) carried out consolidation tests on samples prepared under two thicknesses; both tested under single drainage conditions. Findings revealed that the value of c_v obtained using the conventional size (75mm diameter by 20mm thickness according to the British Standard BS1377 Part 5 (BS, 1990)), ranges between 1 to 10 m^2/yr. However, as the soil thickness was increased, the value of c_v tended to exceed the upper limit, which confirms findings by Healy and Ramanjaneya (1970) and Ortega (1996). This relationship is examined in detail in this study.

1.2.4 Effect of sample diameter to height (D/H) scale on c_v

The diameter to height ratio (D/H) plays a significant role in obtaining accurate engineering properties. The American standard and British Standard recommend a minimum value of 2.5 and 4 respectively to minimise friction between the soil and the apparatus. However, there is little or no justification for these values given in the Standards, and there is very little supporting data in the literature to help explain how these ratios were derived. The British Standard 1377 Part 5 (BS, 1990) recommends a sample scale in terms of diameter and thickness and makes no reference to diameter-height (D/H) ratio; whereas the American Standard D2435 (ASTM, 2003) makes explicit reference to a limiting D/H ratio. Both the American and British Standard investigations were based on Terzaghi's theory. Previous investigations by Grisso et al. (1984), Dirgeliene et al. (2007), and Kotiya and Vanza (2013) reveal the effect of sample scale on certain engineering parameters. These parameters include shear strength, modulus of elasticity and stress-strain relationship, which were investigated using the Triaxial test. Dirgeliene et al. (2007) proposed a reduction in the standard D/H ratio in the Triaxial test from 2 to 1 to eliminate friction, while Grisso et al. (1984) showed that the D/H ratio of a Triaxial soil sample has little effect on the compacted soil as compared to a smaller D/H ratio. On the other hand, during Triaxial testing, it was observed that at constant cell pressure, the modulus of elasticity decreases with an increase in the D/H ratio (Kotiya and Vanza, 2013). However, the effect of D/H ratio on the compressibility parameters is lacking. This study benefits from a series of analyses in comparison with the recommended values, and their correlation with compressible parameters are investigated.

1.2.5 Effect of initial moisture content on c_v

Foundation settlements are associated with the design of structures and the changes in initial moisture content (Foundation Support Works, 2014). Excess moisture content saturates the foundation, which then leads to soft soils or weak clay soil. As a result, the foundation will not be able to sustain the loads resulting from foundation settlement (Foundation Support Works, 2014).

The settlement of a structure founded on fine-grained soil such as clay consists of immediate and consolidation settlement. The parameters influencing consolidation settlement are: degree of saturation (S_r %) or initial moisture content (w%), void ratio (e) and amount of overburden pressure (σ_pkPa) (Phanikumar and Amrutha, 2014). Laszlo et al. (2010)

investigated the effect of varying moisture content on the cohesion and internal friction of loam soils. These parameters (cohesion and internal friction) were determined using the Triaxial tests. The initial moisture content (14.37% to 25%) was obtained in the laboratory using the gravimetric method, which is described in the literature. The findings showed that the internal friction increases as the initial moisture content increases (Laszlo et al., 2010). On the other hand, Lei et al.'s (2014) investigation was based on a series of consolidation tests on remoulded dredged soft soil in Tianjin under different initial moisture contents. The outcome showed that, under similar loading conditions, the value of c_v was found to increase with an increase in initial moisture content.

1.2.6 Effect of sample scale on the compression index (c_c) and coefficient of volume compressibility (m_v)

Compression index (c_c) is used for the direct calculation of settlement of structures from the relationship of pressure and void ratio, and is generally used because its value does not change with change in confining pressure for normally consolidated clays (Abbasi et al., 2012 and Singh and Noor, 2012a). The coefficient of volume compressibility (m_v) is also the most suitable compressibility parameter for direct settlement calculation. However, its variability with confining pressure makes it less useful when correlating with some engineering properties (Singh and Noor, 2012a).

Some investigations on compressibility parameters have been previously reviewed by Terzaghi and Peck (1996), Sridharan and Prakash (2000), Cerato (2001), Di Maio et al. (2004), Park and Koumoto (2004) and Singh and Noor (2012a). c_c was previously investigated by numerous researchers to develop its correlation with liquid limit (LL), specific gravity (G_s), natural moisture content (w), initial void ratio (e_o) and plasticity index (PI) (Singh and Noor, 2012a). Terzaghi and Peck (1996) provided an equation correlating c_c with LL of soils. Di Maio et al. (2004) conducted a one-dimensional test on bentonite and kaolin and found a good correlation between c_c and the void ratio (e) at LL of soils. Singh and Noor (2012a) proposed a model to correlate c_c with LL and PI. Sridharan and Prakash (2000) and Cerato (2001) show that c_c correlates better with the shrinkage limit (SL) of soils when compared to either LL or PI. Park and Koumoto (2004) show a linear relationship between c_c and c_c/n (where 'n' is the porosity of the soil). Aksoy and Kaya's (2013) findings were validated by those of Sridharan and Prakash (2000), Cerato (2001) and Park and

Koumoto (2004), and they found that there is a truly strong correlation between SL and c_c. These findings did not account for sample scale effect on the consolidation settlement.

Retnamony and Mether (1998) investigated the effect of clay mineralogy on compressibility parameters (m_v). The investigation was based on one-dimensional consolidation tests where soil samples (montmorillonite, kaolinite, illite and powder quartz) were prepared at moisture content 1.1 times the soil LL. The soil's minerals, except for powder quartz, were mixed with carbon tetrachloride (CCl_4) to control the effect of the exchangeable ions on the compressibility characteristics of clay minerals (Retnamony and Mether, 1998). The findings revealed that m_v increases by 30% for Kaolinite soils, decreases by 33% for illite and 20% for montmorillonite soils as the pore fluid changes to CCl_4, while power quartz exhibited no significant change in m_v. The above response of the compressibility parameters on clay minerals is governed by the mechanical and physicochemical factors (i.e. mechanical such as strength of soil and physicochemical such as the interaction between soil particles). These factors are explained in more detail in the literature.

1.3 Aims and objectives

1.3.1 Aims of research

The effect of sample scale while obtaining engineering parameters in the laboratory poses a challenge which does not correspond to that in the field. There have been various studies of the effect of sample scale on the compressibility parameter (coefficient of consolidation (c_v)) and a limited number of the remaining parameters such as compression index (c_c) and coefficient of volume of compressibility (m_v). The current study aimed at providing additional information to fill in the gap in the existing knowledge of this behaviour using Kaolin clay. The investigation will benefit from both physical and numerical analysis. Kaolin clay was chosen because it is easily obtained, and there have been numerous laboratory investigations conducted on this soil previously. It thus facilitates comparison of data achieved with that in the literature. To achieve the main aim of this study, a set of objectives were outlined.

1.3.2 Research Objectives

The goals of this research are, therefore, to evaluate the following factors:

1.3.2.1 Influence of sample scale in deriving the coefficient of consolidation c_v

This was achieved by using different methods in obtaining c_v. These methods include the Casagrande method, Taylor's method (these are widely used methods) and the Inflection method. These methods are described in detail in Chapter 2. A comparison between these methods with previous work, in terms of sample scale, was conducted.

1.3.2.2 Influence of sample scale on the compressibility parameters

Various sample scale such as: sample height, diameter and diameter to height (D/H) ratio scale were used. Thorough physical and numerical investigations were conducted and compared with those from previous researchers and the research question answered.

1.3.2.3 The effect of initial moisture content on the compressibility parameters

Due to the shrink/swell behaviour occurring in compressible soils (fine-grained soils) which occurs because of the variation in moisture content, this investigation is aimed at contributing to the existing knowledge.

1.4 Research limitations

The principal limitations of this research have been identified as:

1. The initial data were collected manually (using a dial gauge) due to the lack of computerised system connected to a series of consolidation tests. However, this was modified at a later stage in the research (using an LVDT). For accuracy, all the equipment was calibrated and percentage errors implemented.

2. Due to lack of functionality of the equipment, the coefficient of permeability was not measured but was calculated using a previously derived equation within the literature. PLAXIS 2D provides an estimated coefficient of permeability which was employed in the comparison process.

3. Sample diameters were limited to 100mm, 150mm and 250mm. However, this was compared to previous work, where different diameters were used to show a trend in data.

1.5 Thesis Outline

A brief review of the thesis chapters is outlined below:

Chapter 2 – Literature review

A review is provided in this chapter on the main features of fine-grained soils, experimental techniques for testing them and previous work on the effect of sample scale on compressibility parameters. This chapter provides the necessary background for the subsequent chapters.

Chapter 3 – Experimental programme

In this chapter, the physical properties of the material studied and the experimental tests performed in this research are presented. Sample preparation methods, design, calibration of the apparatus and procedures that were adopted are presented.

Chapter 4 – Effect of sample scale on the compressibility behaviour of fine-grained soils

This chapter contains a series of experimental test results on the impact of sample scale on the compressibility parameters. The data was divided in terms of the effect of c_v using different test methods, specimen diameters, height and D/H ratio scales and the impact of initial moisture content on the compressibility parameters.

Chapter 5 – Numerical modelling

Background information on the finite element method used and its application to sample scale is described. Brief information on previous work in the area is also presented and discussed. A description of an attempt at the application of the finite difference method to this study is also presented.

Chapter 6 – Comparison between the experimental and modelling work

Both the experimental and numerical modelling are presented. The validity of the work is shown and compared.

Chapter 7 – Discussion of findings

This chapter presents the discussion of both the experimental and analytical observations and their practical implications.

Chapter 8 – Conclusion and Recommendations

This chapter summarises the conclusions drawn from various parts of the thesis. Recommendations for future investigations in this area are given.

CHAPTER 2

LITERATURE REVIEW

2.1 Overview

This chapter presents a detailed evaluation of previous study into the research area. A review of clay mineralogy, saturated soil mechanics, laboratory data analysis and detailed study on previous work is presented. Summaries of the engineering parameters are presented in Appendix A.

2.2 Basic properties of fine-grained soil fractions

Fine-grained soils are practically impermeable (slow water drainage), and change volume and strength due to variation in moisture conditions (Budhu, 2000). Their engineering properties are controlled mainly by the soil mineralogy, water content and surface area factors rather than particle size. As a result, the inter-particle attraction creates cohesion that is independent of the external force, which explains the term 'cohesive soils' (Budhu, 2000). Fine-grained soils particle sizes are usually less than 0.075mm which is finer than silt, gravel and sand (Smith, 2006).

2.2.1 Clay mineralogy

Clay minerals are those members of the layer-lattice group commonly encountered in the weathering products of rocks containing feldspars and micas (Whitlow, 2001). Four main groups of clay minerals may be identified, depending on the soil particle arrangement and the ions present that provide bonding between layers. These groups are kaolinite, illite, montmorillonite and vermiculite.

2.2.1.1 Kaolinite group

These are the main constituents of china clay derived from weathering feldspar which is an essential mineral of granite (Powrie, 2004). There are large deposits of china clay in Cornwall and Devon. According to the British Geological Survey, the resources of china clay in Britain are confined to the granite areas of South West England, mainly in the central and western part of the St Austell granite region (Scrivener et al., 1997). It is also found in

the USA and Brazil (Cornwall Council, 2013). Kaolinite (Figure 2.1a) consists of layers of one tetrahedral (silica (Si)) sheet and one octahedral (Aluminium (Al)) sheet (Yong et al., 2012). Because of the stacking of the layers of each of the two sheets, kaolinite is referred to as 1:1 clay minerals. The two sheets are stacked together in such a way that the tip of the Si sheet and one Al sheet is about 0.72nm thick (Yong et al., 2012).

2.2.1.2 Illite group

Illite group refers to the degradation of micas under marine conditions resulting in a group of structurally similar minerals (Whitlow, 2001). This group forms the principal minerals in marine clays and shales, such as London and Oxford clay. The bonding between illite group minerals is weaker than in the kaolinite group, which results in thinner and smaller particles (Craig, 2004). Illite has a 2:1 structure similar to montmorillonite but the interlayers are bonded together with potassium ions, as shown in Figure 2.1b (Powrie, 2004).

2.2.1.3 Montmorillonite group

This group occurs due to the further degradation of illite and is formed by the weathering of feldspar in volcanic ash deposits (Craig, 2004). They are also known as smectites and are the main constituents of bentonite. The structural form is similar to that of illite, but also to the substitution of aluminium (Al^{3+}) for silicon (Si^{4+}) in the tetrahedral units, as shown in Figure 2.1c (Powrie, 2004). The ions present, apart from potassium, provide weak bonding between layers. Consequently, water is easily admitted between the soil layers, causing high shrinkage/swelling capacity (Powrie, 2004).

2.2.1.4 Vermiculite group

This consists of weathering products such as biotite and chlorite. The structure is similar to that of montmorillonite (with 2:1 minerals). The main action providing bonding between particles is exchangeable cations such as calcium (Ca^{2+}) and magnesium (Mg^{2+}) as shown in Figure 2.1d (Lambe and Whitman, 1979). The octahedral sheet in Figure 2.1d is brucite (B). As a result, the shrinkage/swelling capacity is similar to montmorillonite but less severe (Whitlow, 2001).

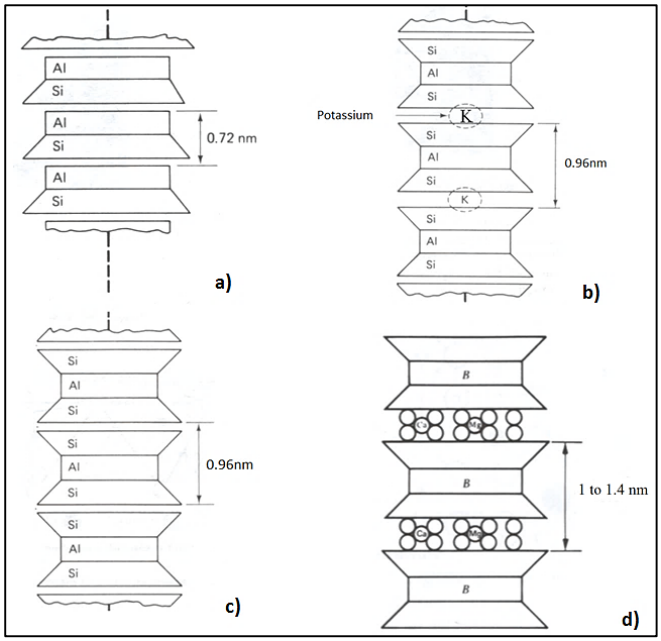

Figure 2-1: Schematic diagram of clay mineral group a) kaolinite group, b) illite group, c) montmorillonite group and d) vermiculite group (Lambe and Whitman, 1979)

2.2.2 Clay structure

The way soil particles interact with each other will determine the characteristics and properties of the soil. Soil composition is a fundamental feature that has a considerable impact on the structure (i.e. macro-structure), physical and physicochemical properties of the soil (Yong et al., 2012). Hence, clay structure is divided into two categories: macro-structure and micro-structure. Macro-structure refers to the visible features of clay deposits and includes fissures, bedding patterns, silt and sand seams or lenses (Smith, 2006). The study of macro-structure is necessary as it usually has an effect on soil behaviour (Smith, 2006).

2.2.2.1 Macro-structure

Clay deposits that exhibit no visible change in structure are said to have no macro-structure or to be uniform (Powrie, 2004). However, many clay soils are layered or stratified, and the individual layers are relatively thin and parallel with one another and are said to be laminated (Nagaraj and Srinivasa, 1994). Clay deposits formed in glacial tilt exhibit a unique type of laminated clay structure called Varved clay (Powrie, 2004). Varved clay occurs due to seasonal variation in the glacial tilt and the deposit consists of silt or fine sand (deposited

rapidly over the summer period) and clay (usually dark in colour, deposited over the remaining seasonal period) (Powrie, 2004).

2.2.2.2 Micro-structure

Micro-structure refers to the microscopic or micro-fabric structural arrangement of clay particles. Nagaraj and Srinivasa (1994) stated that the microstructure of a compacted or slurry clay soils affects the permeability parameter and volume of voids due to the size, arrangement and distribution of the voids. Micro-structure experimental interpretation was conducted by Nagaraj and Srinivasa (1994). It was concluded that the micro-structure of fine-grained soils at their liquid limit was of the same pattern, and the change in micro-void volume with stress is proportional to its initial state. When clay minerals are in suspension in water, they may experience a mutual attraction caused by the Van Der Waal forces. The attraction occurs between the soil and water cations (Berry and Reid, 1987). The environment exerts a major influence on the micro-structure of clay deposits. For example: deposition through salt water would produce marine clays showing a flocculated structure, as in Figure 2.2a, and deposition through fresh water would produce lacustrine or alluvial clays with a dispersed structure, as depicted in Figure 2.2b (Berry and Reid, 1987). On the other hand, the micro-structure of natural clay, as seen using a scanning electron microscope (SEM) has a complex structure as compared to alluvial and marine clays (Berry and Reid, 1987). The complex micro-structure arrangement that commonly occurs in natural clays is shown in Figure 2.2c. From Figure 2.2c, aggregations that are commonly found in natural clay, sometimes act as a connector between the silt or sand particles (Berry and Reid, 1987).

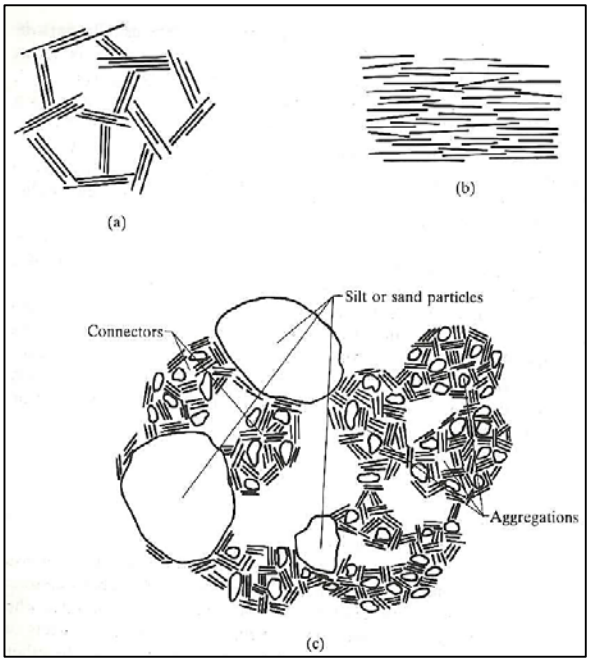

Figure 2-2: Micro-structure representation of clay structures; a) Flocculated structure, b) dispersed structure and c) natural clay structure (Berry and Reid, 1987)

2.3 Soil physics related to saturated soils

Less than 1% of the earth's water occurs as liquid fresh water associated with land masses, and the rest is either saline water in the oceans and seas or water vapour in the atmosphere (McLaren and Cameron, 2005). Land-based water arrives as a result of rainfall and subsequently percolates under the influence of gravity into the soil. Thus, saturated soils occur throughout the world and are found below the ground water table. The ground water table refers to the water level within a soil profile. The depth of penetration of water into the soil depends on the soil's permeability. Figure 2.3 shows a fully saturated soil profile below the water table, where all the voids spaces are filled with water.

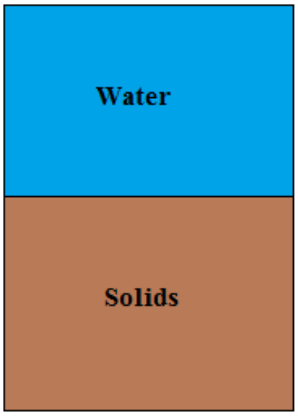

Figure 2-3: Fully saturated soil

When a saturated soil is loaded, the excess pore water pressures are set in the soil mass. Since water cannot sustain shear stress, these excess pore water pressures are allowed to dissipate out of the soil mass. The rate at which water flows is primarily controlled by the permeability of the soil mass. Therefore, the outflow dissipation of the excess pore water pressure from the soil mass is referred to as consolidation (Berry and Reid, 1987). As the pore water pressure is squeezed out of the soil mass, there is a reduction in volume of voids, which leads to a decrease in the total soil mass; and the effective stresses in the soil increase with an increase in shear strength. Thus, consolidation and shear strength processes can be linked (Berry and Reid, 1987).

2.4 Theory of consolidation

The theory of consolidation was first introduced by Terzaghi (1925) in the study of the deformation of soils matrix, due to the expulsion of water from the pores in a material of low permeability. This study was carried out under compressive loading and with the assumption of Darcy's law being valid. The distortion of the soil is caused by the effective stress (defined as the difference between the total stress and excess pore water pressure). The excess pore water pressure is generated due to the initial load transfer applied to the soil matrix (Cavalcanti and Telles, 2003). Terzaghi's theory was later generalised to a three-dimensional version by Biot (1941), and has been implemented in a large variety of practical problems. Moreover, a three-dimensional generalisation of Terzaghi's theory was also proposed by Rendulic (1936). This generalisation led to a two-dimensional diffuse equation where the total stress was assumed to be constant throughout consolidation (Meijer, 1985).

2.4.1 Terzaghi's theory

Terzaghi's vertical consolidation theory refers to the one-dimensional process used on soft clays when subjected to increased loading. Terzaghi (1943) suggested that compression within the soil sample was as a result of the dissipation of water from the void space. One-dimensional compression, in which deformation takes place in the direction of loading, has a particular significance in soil mechanics and foundation engineering (Powrie, 2004). In practice, one-dimensional consolidation tests are used to estimate the compressibility parameters of soils. The conventional Oedometer tests as outlined by Terzaghi's benefits from the following assumptions:

1. The soil is homogeneous
2. Fully saturated soil
3. Validity of Darcy's Law
4. Linear relationship for small strains only
5. Pore fluids incompressible
6. Soil solid incompressible
7. Certain soil properties constant with time (i.e. permeability)
8. Secondary consolidation is ignored (Calabria, 1996).

These assumptions are valid for fine-grained soils with some limitations. These limitations are:

1. The permeability and m_v are assumed to be constant. However, during consolidation, the void ratio (e) decreases, which results in a reduction in permeability. Thus, permeability is not constant. m_v changes with the stress level, resulting in a different value of the coefficient of consolidation
2. The water flow is assumed to be 1D, but in reality it is three dimensional
3. The application of load is assumed to produce excess water pressure on the entire soil stratum, but in some cases the excess water pressure does not develop over the whole clay stratum (Whitlow, 2001)

During consolidation, two types of drainage conditions could occur single and double drainage. Under single drainage conditions, the soil profile is resting on an impermeable base with drainage occurring from the top face. Thus, the distribution of the degree of consolidation with depth for various values of the time factor is represented by the upper

half of Figure 2.4a. For a soil resting on a permeable boundary with drainage taking place both at the top and bottom face, it is referred to as double drainage. In this case, the consolidation of the lower half of the soil layer is a mirror image of the upper half (Berry and Reid, 1987). This consolidation drainage behaviour is represented in Figure 2.4b. As a result of this drainage phenomenon, the excess pore pressure will occur at the centre and bottom of the soil under double and single drainage respectively.

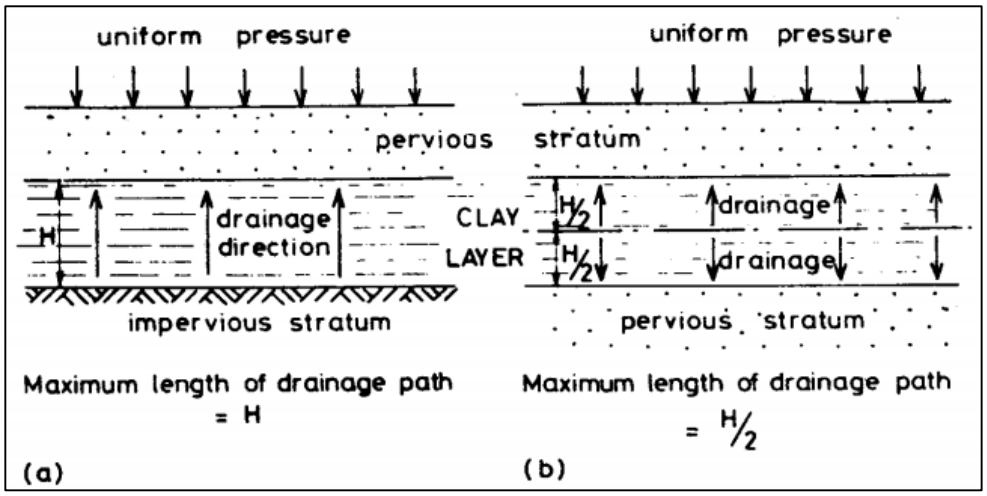

Figure 2-4: Drainage condition of a soil at a) single drainage and b) double drainage (Head, 1998)

2.4.2 Biot's theory

Terzaghi's theory considers the simple one-dimensional problem, while Biot introduced the development of a more general treatment of the quasi-stationary behaviour of saturated soil (Meijer, 1985). In this section, the general three-dimensional consolidation is considered for the case of compressible fluids and particles (Biot, 1941). Biot did not use the concept of effective stress, but the intrinsic compressibility of the soil grains was recognised. The analytical solution on Biot's theory is known for the simple initial boundary value problems (Meijer, 1985).

2.5 Consolidation drainage theory

One of the most common issues in construction is the need to control subsurface water encountered during the building sequence and the subsurface water after construction. When a saturated clay soil is subjected to a stress increase, the dissipation of the excess pore pressure will occur extremely slowly, due to the low permeability of clay soils. Settlement

caused by the drainage of water from the voids will therefore take place over a longer period (McCarthy, 2002). In a consolidation test, there are several drainage scenarios, as depicted in Figure 2.5. From Figure 2.5, any of the drainage and loading conditions can be used during the consolidation analysis. The arrows in Figure 2.5 show the direction of drainage, where upward is for single drainage, upward and downward represent double drainage and outward and/or inward are for radial drainage conditions. There have been numerous studies with the drainage scenarios presented in Figure 2.5, including Seah and Juirnarongrit (2003), Imai and Nawagamuwa (2005), Armstrong (2006), Geng (2008), Wang et al. (2011) and Rosine and Sabbagh (2015). The Oedometer cell with radial consolidation is occasionally used to acquire the horizontal coefficient of consolidation (c_h), since water can flow radially under vertical loading, which simulates field conditions (Seah and Juirnarongrit, 2003).

Radial consolidation is a system where both vertical and radial drainage is under surcharge load. It is used to accelerate consolidation by shortening the drainage path in one of the most popular methods of soft soil ground improvement (Indraratna et al., 2005). Its mathematical formulation is based on the small strain theory and for a given stress range where; a constant m_v and a constant horizontal permeability (k_h) are assumed. Jamiolkowski et al. (1983) stated that for most soft soil deposits, the horizontal permeability (k_h) is greater than the vertical permeability (k_v), leading to rapid radial consolidation (Indraratna et al., 2005). The system has been successfully used to improve foundation soils for embankments, airports and highways (Indraratna and Redana (2000) and Li and Rowe (2001)).

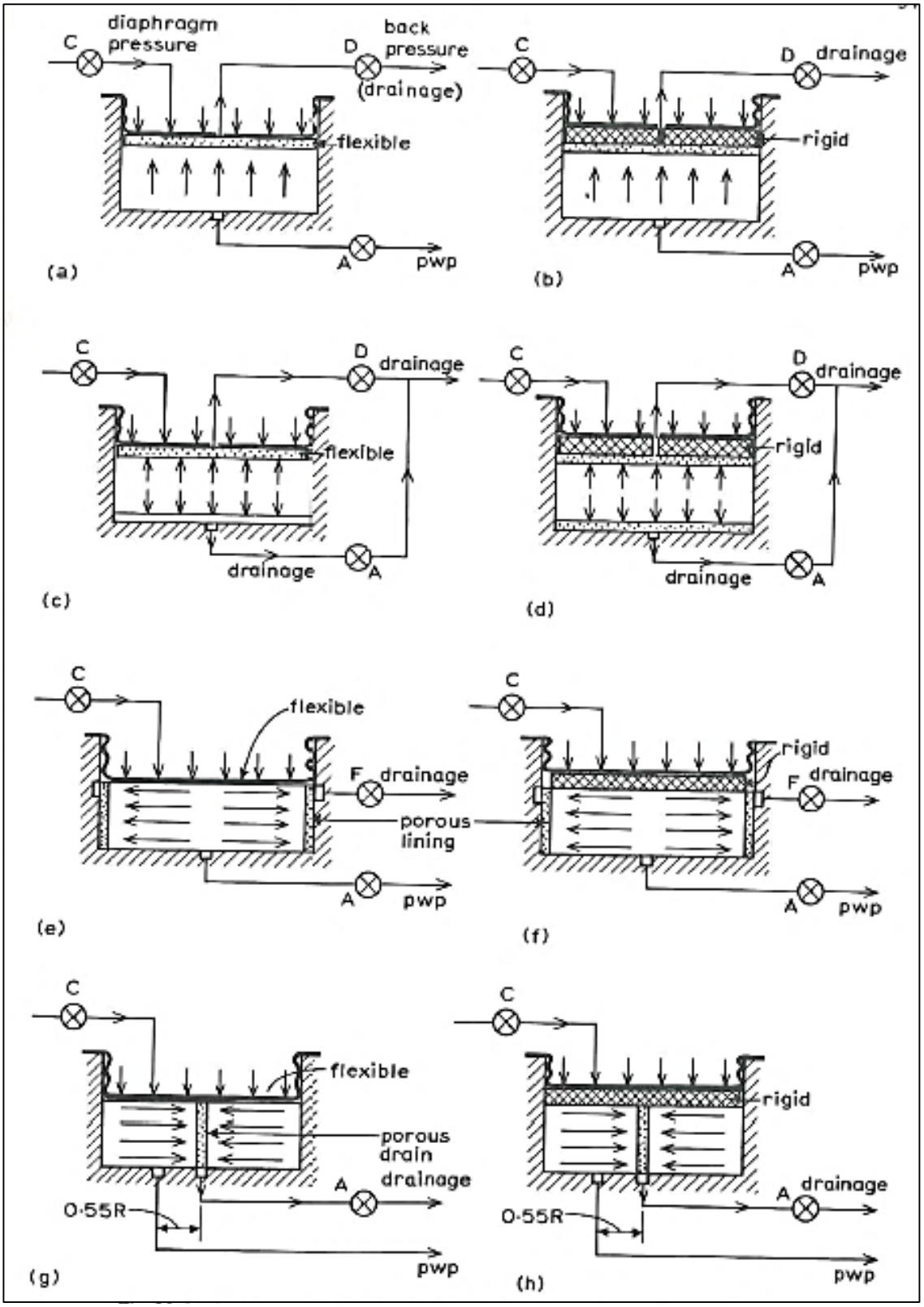

Figure 2-5: Drainage and loading conditions for consolidation in an Oedometer apparatus: a), c), e), g) with free strain loading, b), d), f), h) with equal strain loading (Head, 1998)

2.5.1 Vertical and horizontal drainage theory

The basic theory of radial consolidation around a vertical sand drain is an extension of Terzaghi's one-dimensional theory (Walker and Indraratna, 2006). The coefficient of consolidation in the horizontal direction (c_h) is known to be higher than the coefficient of consolidation in the vertical direction (c_v). The vertical drains reduce the drainage path noticeably in the radial direction, and it benefits in accelerating consolidation and improving the soil strength (Terzaghi, 1948). Indraratna et al. (2005) mentioned that Barron (1948) presented a comprehensive solution to the problem of radial consolidation by drain wells. Barron (1948) investigation was based on two distinct hypotheses: free strain and equal strain. The former hypothesis assumes that the load is uniform over a circular zone of influence for each vertical drain. The differential settlements occurring over this zone have no effect of redistribution of stress (Indraratna et al., 2005). The latter hypothesis assumes arching occurs in the upper layer during the consolidation process without any differential settlements in the clay layer (Indraratna et al., 2005). Practically, both free and equal strain produce nearly identical results, and equal strain is commonly used in most radial consolidation analysis (Indraratna et al., 2005).

The conventional equal strain hypothesis assumptions follows by Hansbo (1981) are as follows:

1. Soil is fully saturated and homogeneous
2. Laminar flow through the soil is adopted (Darcy's law)
3. Soil strain is uniform at the upper boundary of the unit cell. The small strain theory is valid

Head (1998) stated that in practice, not all combinations of the drainage scenarios presented in Figure 2.5 are used. Wang et al. (2011) mentioned that Rendulic (1935) analytical solution did not account for radial drainage. As a result, Barron (1948) presented an analytical solution that combined both vertical and horizontal drainage. This was achieved by first decoupling the radial and vertical drainage, and then obtaining the result from the radial and vertical drainage (Wang et al., 2011). Based on Barron's solutions, various analytical and numerical solutions for soil consolidation with both vertical and horizontal drainage conditions have been gained (Hansbo, 1981; Hawlader et al., 2002; Nogami and Li, 2003; Leo, 2004 and Geng, 2008).

2.6 Consolidation (Oedometer) test

The conventional consolidation apparatus used by the British standard utilises soil samples of sizes: 75mm diameter and 20mm thick (giving a diameter to height (D/H) ratio of 4). The apparatus consists of filter papers, sintered bronze porous stone, consolidation cell, loading cap, two drainage valves for double drainage and dial gauge for displacement measurements. The apparatus is as shown in Figure 2.6. The sintered porous stone is used to spread the load over the sample and helps to facilitate drainage to occur. The porous stone also prevents any soil particles from passing through which could block the drainage valve, and only allows water to pass through. The loading cap is used to apply pressure to the soil sample during consolidation.

Test samples are prepared from a slurry state from which a pre-consolidation pressure is applied to allow the excess water to be dissipated. According to the American Standard D2435 (ASTM, 1996), the minimum specimen D/H ratio should be 2.5. To minimise friction between the specimen and the ring, a D/H ratio greater than 4 is preferable.

When the load is applied, the process of plastic deformation and void ratio reduction takes place over a longer period due to the particle size. Consolidation tests then take place over a 24 hour period to allow for maximum consolidation (i.e. fine-grained soils). However, some soils, such as peat, will require more than 24 hours to allow for complete consolidation.

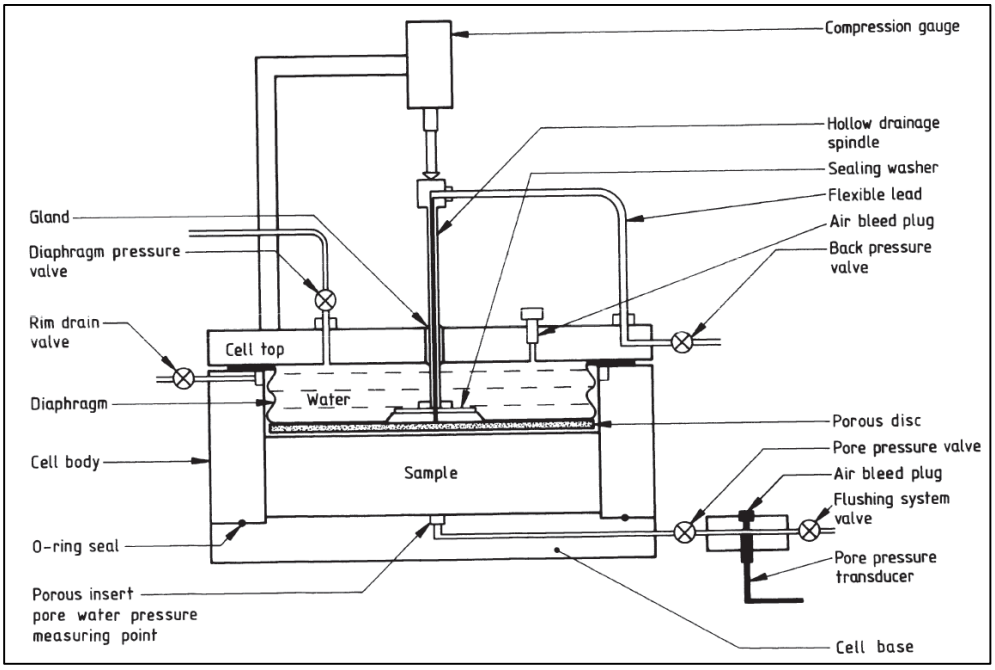

Figure 2-6: Oedometer apparatus from British Standard BS1377 Part 6 (BS, 1990)

2.6.1 Incremental Loading

The American Standard D2435 (ASTM, 2003) suggested the load increment should consist of doubling the pressure on the soil to obtain approximate values of 12kPa, 25kPa, 50kPa, 100kPa, 200kPa, and so forth. The loading device should be able to maintain the pressure applied to the soil sample for an extended period with precision of ±0.5% of the applied pressure and should permit quick application of a given load increment without significant impact (ASTM, 2003). Prior to the consolidation taking place, seating pressure (pre-consolidation pressure) of 5kPa is applied to the specimen (ASTM, 2003). Loading is applied with the aid of a hydraulic system within the Oedometer apparatus, whose magnitude is controlled by a pressure regulator. During the consolidation test, the height change is recorded using the dial gauge reading at time intervals as specified by the American Standard D2435 (ASTM, 2003): 0.1, 0.25, 0.5, 1, 2, 4, 8, 15 and 30minutes and 1, 2, 4, 8 and 24hrs. It should be noted that, from the Terzaghi theory, the first reading taken at 0.1 minute for fine-grained soils, showing c_v at 31.5, 12.6, 3.1, 1.3 and 0.3 m^2/yr corresponds to 31, 19, 10, 6 and 3% consolidation respectively (Feng and Lee, 2001). Hence, it is necessary to increase the number of data points before 1 minute for fine-grained soil to have a c_v value greater than 12.6 m^2/yr (Feng and Lee, 2001).

According to the British Standard BS1377 Part 6 (BS, 1990), a pressure increment of 1 is proposed. This pressure should be maintained to obtain the consistent value of c_v. During investigation by Siddique and Safiullah (1995), a load ratio of 2 was used: 47.9kPa, 95.8kPa, 191.6kPa, 383.2kPa, 766.4kPa and 1532.8kPa for a duration of 24 hours per load increment. Berry and Reid (1987) and Sridharan and Nagaraj (2012) used a load ratio double that required by the American Standard. Thus, different researchers used different loading conditions as compared to BS (1990) and ASTM (2003) and obtained a value of c_v within the range presented in Table A.9 (Appendix A).

The standards recommended each loading cycle to last 24 hours for soft soil and longer for highly compressible soils such as peat. The duration of the load during consolidation has been previously found to impact significantly the value of c_v (Ortega, 1996 and Feng, 2010). Sridharan and Nagaraj (1999) developed a new method to speed up the consolidation process. This was achieved by applying the next load increment as soon as the necessary time required to identify the percent consolidation was attained. This process reduces the consolidation time from the conventional 1 to 2 weeks to 4 to 5 hours. c_v was obtained using

the rectangular hyperbola method within a short load duration. This testing method was also found to yield similar results to the conventional method, thus save time and effort while maintaining a reasonable degree of accuracy (Sridharan and Nagaraj, 1999).

2.6.2 Single Oedometer test

According to the American Standard D2435 (ASTM, 2003), the single Oedometer test involves incremental loading of a soil sample that was incrementally loaded to its natural water content until the desired stress value is reached. The unitary oedometer test, as conducted by Jennings and Knight (1975), consisted of double the stress applied to the sample every half an hour until less than 0.1% of compression occurs in an hour. There is a continuous increase in stress at increments of every half an hour until the stress on the soil sample is equal to, or greater than, the stress that is expected to arise in the field (Houston and Spadola, 1988).

2.6.3 Double Oedometer test

The double Oedometer test comprises the preparation of two identical undisturbed samples which are loaded to a pressure of 200kPa. At this pressure, the sample in the consolidation ring is flooded with water and left for 24 hours, after which the test is carried out to the next maximum loading limit (Haghighi, 2011). One of the samples is initially saturated under loading and allowed to fail and loaded at standard incremental loading. The other sample is tested at initial water content using standard incremental loading (Haghighi, 2011).

2.7 Factors affecting data analysis

2.7.1 The effect of the coefficient of consolidation (c_v) using different test methods

The value of c_v was found by various researchers to vary depending on different methods. For example, Robinson (1999) stated that the value of c_v obtained using Taylor's method tended to be higher than that achieved by the Casagrande method for clayey soils (Al-Zoubi, 2013). The value of c_v obtained by the Inflection method is quite similar to that of the Casagrande method (Mesri et al., 1999). Mesri et al. (1999) findings were based on 18 specimens of undisturbed soft clay and shale deposits with a moisture content ranging from 23-340% and 11.5-30.5% respectively. The value of $c_{v,}$ obtained from the velocity method on clay soils, was found to be close to Taylor's method (Parkin and Lun, 1984). These

variations in c_v value are due to the initial compression or the influence of the secondary compression or both, according to Mesri et al. (1999) and Feng and Lee (2001). Since these methods compute c_v at different stages of consolidation, the value of c_v is affected by the initial and secondary compression (Al-Zoubi, 2013).

Cortellazzo (2002) used Taylor's method in comparison with other methods of obtaining the value of c_v. The investigation was based on 10 Oedometer tests performed on clay samples obtained from a site where the value of c_v gained in the laboratory and in situ were compared. The in situ c_v value was obtained using borehole extensometers (Cortellazzo, 2002). It was found that Taylor's method tended to produce higher c_v values as compared to log (H_D^2/t) – U method. This observation was due to the initial compression and some secondary compression being present, as shown in Figure B.2. If a clear trend is provided in the initial compression part of the curve (Figure B.2), Taylor's method will usually provide a good estimate of c_v (McNulty et al., 1978, Sridharan et al. 1995 and Mesri et al., 1999). However, if a considerable amount of secondary compression is present when U is 90%, the determined deflection reading at this point will yield inaccurate readings of c_v (McNulty et al., 1978, Robinson and Allam, 1996). As a result, Feng and Lee (2001) proposed a simplified version of the Taylor's method, by simply drawing a straight line passing through the linear portion of the square root time consolidation curve (Figure 2.7). The point where the consolidation curve deviates from the straight line represents 60% consolidation with a time factor (T_v) value of 0.286 (Feng and Lee, 2001). Feng and Lee (2001) method is only applicable if the experimental consolidation curves match Terzaghi's theoretical curve. Feng and Lee (2001) investigation was based on 10 natural soft clays with liquid limits ranging from 40 to 152% obtained from field sampling. Robinson and Allam (2002) revised Feng and Lee's method of obtaining the linear segment of the √t consolidation curve and then used it to plot the second straight line that intersects the √t consolidation curve at 45%. c_v can then be computed using the equation by Reeves et al. (2006) in Table A.8, where T_{45} is 0.145 (Muntohar, 2009).

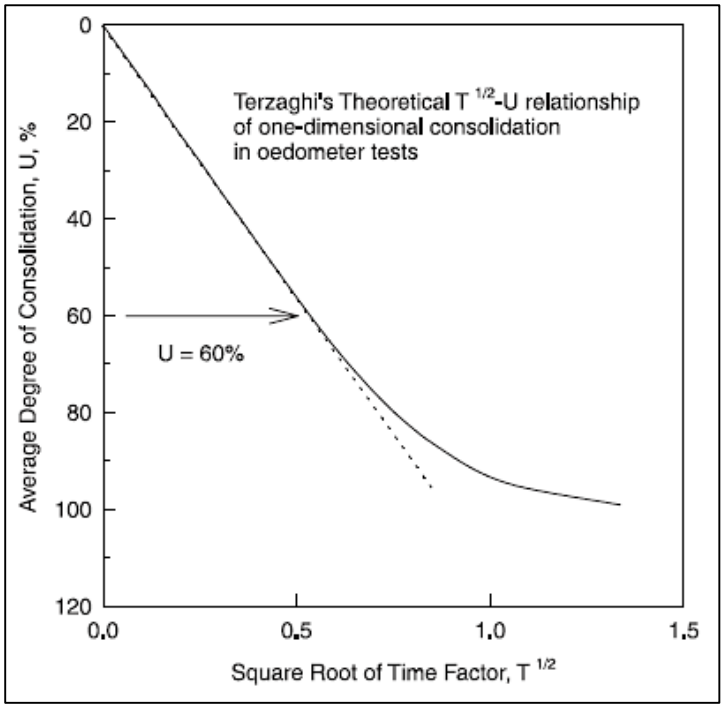

Figure 2-7: Terzhagi's square root time method as proposed by Feng and Lee (2001)

The c_v value obtained using the Casagrande method takes into account the lower section of the consolidation curve and thus the effect of secondary consolidation could have some impact on the value of c_v. Prakash et al. (2011) examined the value of c_v on compacted soft soil and found that the Casagrande and inflection methods show a remarkably close correlation. However, the inflection method is found to produce a higher value of c_v (as it does not identify the primary and secondary part of the curve but the inflection point of the curve as shown in Figure B.2). This correlation was also observed by Mesri et al. (1999), Muntohar (2009) and Al-Zoubi (2013).

The values of c_v obtained using various methods outlined in the literature were also found to decrease with an increase in pressure (Robinson and Allam, 1996 and Muntohar, 2009). For montmorillonite with water as pore fluid, the compression is governed by physicochemical factors (signifying interaction between soil particles, especially through diffuse double layers) and c_v, will decrease with an increase in pressure (Robinson and Allam, 1996). Muntohar (2009) conducted a series of consolidation tests on an undisturbed soil sample (which consisted of: 33% clay, 51% silt, 16% sand and LL 59%) taken from a selected site. The outcome revealed that there was a considerable variability in c_v value using the Casagrande and early stage method. This variation was due to the secondary consolidation segment part of the curve being insufficient, as it did not replicate the

theoretical curve. As a result, the Casagrande and early stage methods were shown to be inadequate to evaluate c_v since the primary and secondary consolidation curve are not clearly distinguished (Feng, 2001).

2.7.2 Effect of sample diameter on the value of c_v

Various studies have been carried out to investigate the effect of sample diameter on soil behaviour (such as bearing capacity and compressibility parameters): Healy and Ramanjaneya (1970), Cerato and Lutenegger (2007), Cerato et al. (2009), Al-Khuzaie (2011) and Dixit and Patil (2013).

Healy and Ramanjaneya (1970) tested a series of Oedometer tests (Oedometer apparatus ranging from 97mm to 147mm) on Varved clay where drainage was allowed both vertically and radially. Radial drainage was conducted by the addition of sand drains within the soil samples, and the consolidation test was carried out as explained in the literature. Shields and Rowe (1965) stated that when using a sand drain during radial drainage to obtain the horizontal coefficient of consolidation (c_h), the ratio of the Oedometer apparatus to sand drain is 20. Healy and Ramanjaneya (1970) varied this ratio from 12.5 to 18.9 with sand drain diameter 7.7mm. The central hole for the sand drain was cut into the sample by an ordinary cork borer, which was centered by means of a template fitting over the consolidation ring (hole diameter 7.7mm) (Healy and Ramanjaneya, 1970). This hole was connected to the side of the base plate, where a stopcock was provided.

c_v and c_h were obtained using Taylor and Casagrande method. The findings showed that c_h is independent of sample scale (the investigation did not account for sample diameter scale). It was also observed that c_h gained in the laboratory was higher than that obtained in situ (in the field) (Healy and Ramanjaneya (1970) and Kwong et al. (2001)). This disparity occured because the laboratory samples were smaller as compared to in situ; samples and to a certain extent drainage was both vertical and radial giving a high c_h value (Healy and Ramanjaneya, 1970). In the field, the distance between the sand drains was greater than the thickness of the Varved clay. Hence, water was allowed to flow radially except around the sand drains where it was both radial and vertical (Healy and Ramanjaneya, 1970). Nevertheless, Kwong et al. (2001) showed that the soil depth influences c_v for Hong Kong marine clay. Their c_v value obtained in the field was found to be greater than that in the laboratory and, the discrepancy was due to the inaccurate estimate of the longest drainage path in the field (Kwong et al., 2001).

Similarly, Cleomence (2005), Miller and Cleomence (2007) and Cerato et al. (2009) showed that for fine-grained soils, the size of the Oedometer sample did not cause differences in the one-dimensional behaviour. However, sample preparation techniques and the difference in soil structures (field and laboratory) seemed to affect the compacted soil behaviour in some cases. The outcome was based on both compacted laboratory and field samples, using a 60mm and 560mm Oedometer ring respectively.

2.7.3 Effect of sample height on the value of c_v

There are numerous studies on the effect of sample thickness on the coefficient of consolidation. The thickness of the soil sample is also important in the secondary consolidation process. Its importance is due to thick and thin soil samples, where there is more primary consolidation and less secondary consolidation in thick soil samples than in thin specimens (Taylor, 1942). This variation is not totally valid, as some secondary consolidation occasionally takes places within primary consolidation (Healy and Ramanjaneya, 1970).

Newland and Allely's (1960) investigation was based on a series of consolidation tests on undisturbed and remoulded clay where the thickness varied from 8.89 mm to 37.6 mm. The findings show that c_v is dependent on the soil thickness but sample thickness has little effect on the relationship of void ratio against stress, as also observed by Healy and Ramanjaneya (1970), Lun and Parkin (1985), Berry and Reid (1987) and Ortega (1996). Newland and Allely's (1960) data were limited to only two soil thicknesses, where the value of c_v was found to be dependent on thickness, as compared to Healy and Ramanjaneya (1970) and Berry and Reid (1987). The increase in c_v for Newland and Allely (1960) was insignificant, as the height was changed compared to Healy and Ramanjaneya (1970) and Berry and Reid (1987). As mentioned by Sivrikaya and Togrol (2006), Yin and Graham (1996) investigated the effect of sample thickness on the total settlement, pore pressure, strain and stress and found that the relationship between strain and effective stress at the end of primary consolidation is not unique but depends on the thickness of the clay layer.

Khan et al. (2012) investigated the effect of sample thickness on the time factor and the degree of dissipation of pore water pressure with time. The investigation was carried out using the finite difference method, and the result was compared with that of conventional linear consolidation theory. The findings revealed that the variation in the degree of settlement with time is relatively large, while the variation in the degree of pore water

pressure dissipation with time is relatively small for thick clays as compared to thin clay layers.

2.7.4 Effect of Diameter to height (D/H) ratio on c_v

The diameter to height (D/H) ratio is used to reduce friction between the soil and the apparatus. The American Standard D2435 (ASTM, 2003) suggested a minimum value of 2.5, with a value greater than 4 considered most suitable; while the British Standard BS1377 Part 5 (BS, 1990) proposed a value of 4 with a cell diameter of 75mm and height 20mm. No available data were found to validate the D/H ratio proposed by the Standards. Morris and Lockington (2002) conducted a self-weight consolidation test on fine-grained marine, riverine and lacustrine soils with a D/H ratio ranging from 1.9 to 4.1. The findings show that the final void ratios were relatively similar; and the similarity was due to the sample particle sizes. The effect of D/H ratio from the self-weight consolidation test, where the possibility of excessive friction is present on the Oedometer wall, was neglected in Morris and Lockington's investigation. Taylor (1942) investigated the effect of side friction in consolidation tests and showed that the frictional force varies from 12-22% of the applied pressure for remoulded clay and 10-15% for undisturbed clay. Therefore, the thinner the sample the less side friction, due to the small lateral surface area in contact with the wall of the Oedometer apparatus.

Figure 2.8 shows the distribution of pore pressure, stress and friction with depth. Figure 2.8a displays the Oedometer apparatus with soil sample of thickness (H), diameter (D) and applied stress (p). When friction between the soil and ring is reduced or not present, p is uniform with depth, as shown in Figure 2.8b. However, as H increases, friction is more pronounced and p decreases to q with depth (see Figure 2.8b) (Sivrikaya and Togrol, 2006). The outcome obtained by Sivrikaya and Togrol (2006) revealed that the frictional stress (τ) does not remain constant during the test. As time decreases, τ increases for Δp of 200, 400 and 800kPa for a soil thickness of 60mm and diameter 75mm. Friction was found to be most significant at low stresses where the clay soil is still overconsolidated (Sivrikaya and Togrol, 2006). The frictional stress (τ) can also be obtained using the following formula, as depicted by Sivrikaya and Togrol (2006) shown in equation 2.6.

$$\tau = \frac{T}{\pi DH} \qquad (2\text{-}1)$$

Wher:
D is ring diameter (mm); H is soil height (mm), and T is the load transmitted to the ring (N).

Taylor (1942) equation to obtained frictional stress (τ) is as shown below:

$$\tau = p(1 - \lambda) \qquad (2\text{-}2)$$

Where;
p is applied stress (kPa), and λ is reduction factor.

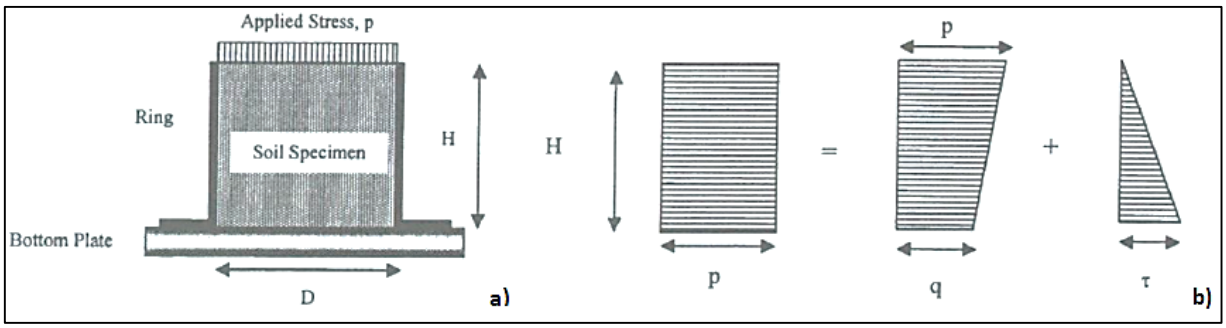

Figure 2-8: Distribution of pore pressure, mean vertical stress (p) and friction stress (τ) with depth in consolidation test (Sivrikaya and Togrol, 2006)

On the other hand, numerous investigations have been conducted on the effect of D/H ratio on strength parameters of soils. The investigations focus on its impact on the shear strength of soil, as in Dirgeliene et al. (2007). Dirgeliene et al. (2007) studied D/H ratio to reduce friction between the soil and the Triaxial end plates. The D/H ratio during Dirgeliene et al.'s investigation was reduced from the standard value 2 to 1 for clay soil. Theoretically, the shear strength parameters were found to be dependent on the D/H ratio if H is less than D (Dirgeliene et al., 2007). It was observed that the elimination of friction (D/H 1) causes a more uniform stress-strain distribution, but it does not decrease friction (Dirgeliene et al., 2007). However, Kotiya and Vanza (2013) found that higher stress values are obtained for lower D/H ratios with higher cell pressure and vice versa for clayey soils

2.7.5 Effect of initial moisture content on compressibility parameters

Structures built on clay soils are susceptible to immediate and consolidation settlement. Consolidation settlement on normally loaded clay layers is affected by the change in degree of saturation or moisture content, void ratio and overburden stress (Hong et al., 2010, Sudjianto et al., 2011, Lei et al., 2014 and Phanikumar and Amrutha, 2014). Phanikumar and Amrutha (2014) conducted a series of consolidation tests on clay soil samples under different initial moisture contents (40%, 30%, 20% and 10%) with corresponding initial degree of saturation (S_r) (100%, 75%, 50% and 25% respectively). The investigation was

conducted using an Oedometer apparatus of 60mm diameter and 20mm height under three loading conditions (25kPa, 50kPa and 100kPa). The findings, as shown in Figure 2.9, reveal that as the initial degree of saturation increases, the amount of compression also increases. This outcome occurs because, as the sample becomes softer (high degree of saturation), it is thus more prone to volume reduction for a given incremental loading (Phanikumar and Amrutha, 2014). The amount of compression obtained was 0.34mm, 0.49mm, 0.52mm and 0.58mm respectively for S_r values of 25%, 50%, 75% and 100%, as depicted in Figure 2.16 (Phanikumar and Amrutha, 2014).

As the initial S_r increases, a_v, m_v and c_c increases, until S_r is 75% and then decreases as S_r rises to 100% (Phanikumar and Amrutha, 2014). This outcome is represented in Figure 2.10, which shows a high compressibility as the value of m_v increases with an increase in S_r at a given loading. Dafalla (2013) explained that the change in moisture content has an influence on the shear strength of soils such as clay-sand mixtures and pure clay or sand. It was observed by Dafalla (2013) that for pure clay, there is a drop in the internal angle of friction by 14% when moisture content increased from 30% to 40%.

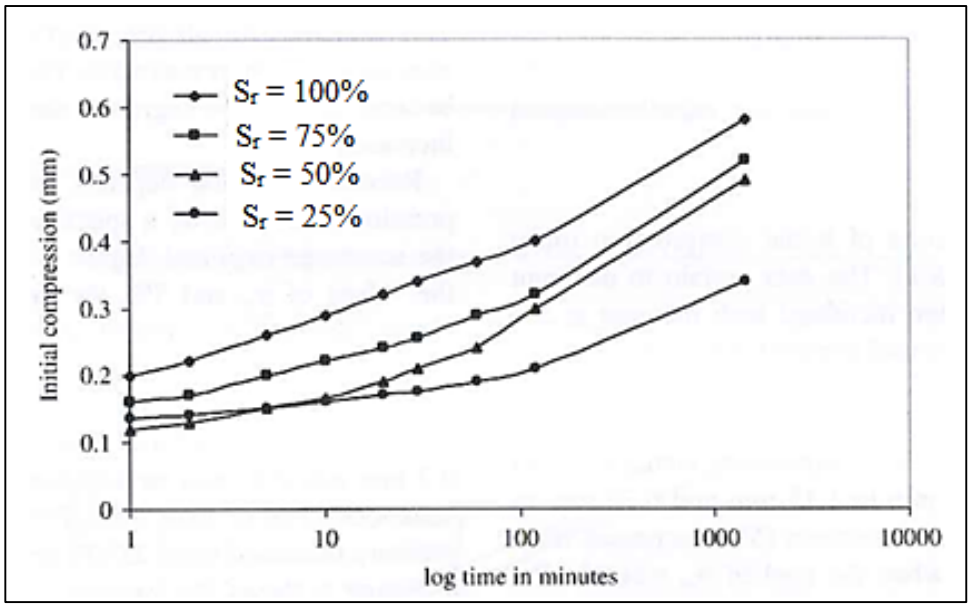

Figure 2-9: Rate of initial compression at different degree of saturation (S_r) at a pressure of 25kPa (Phanikumar and Amrutha, 2014)

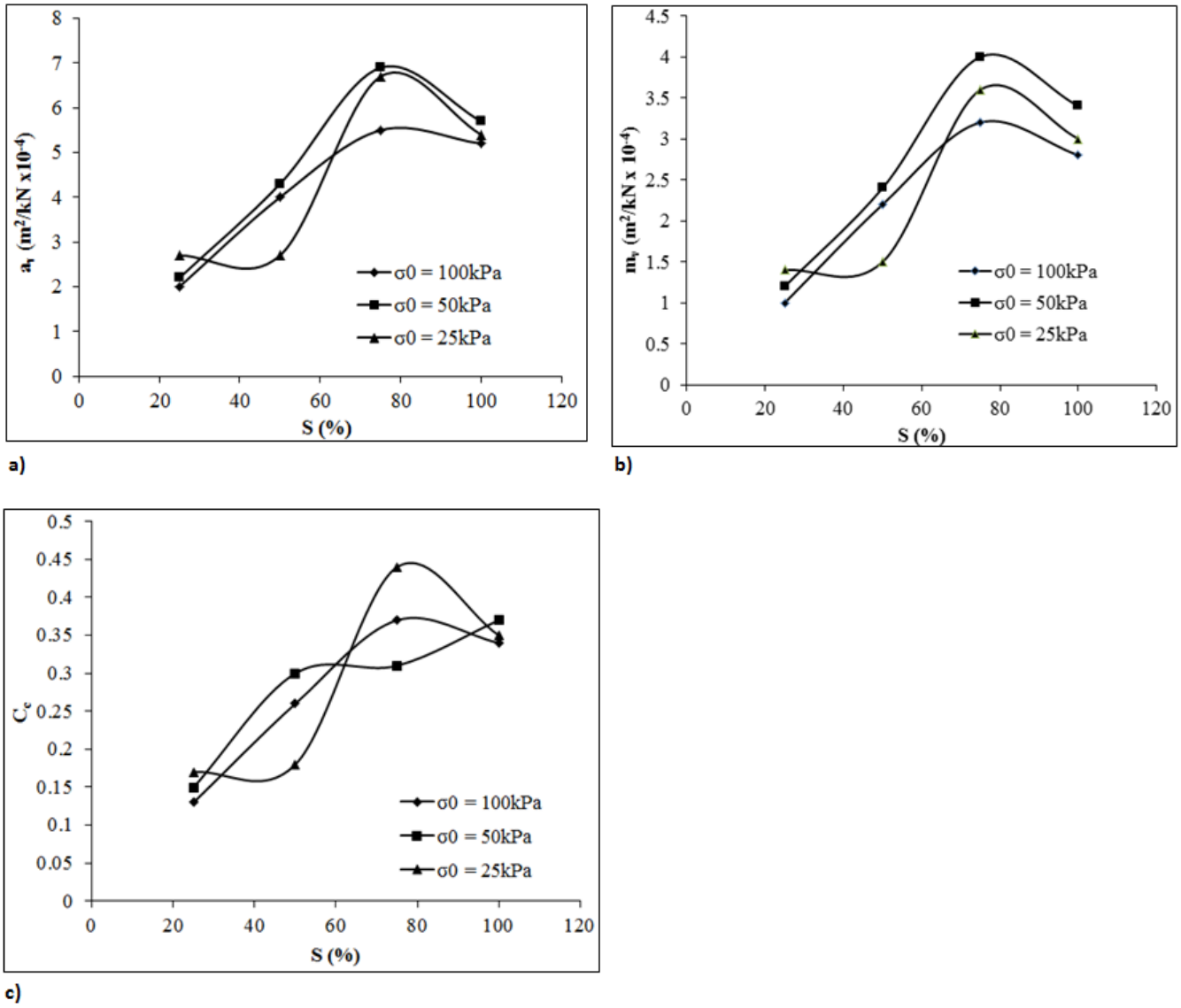

Figure 2-10: Variation in the compressibility parameters with change in degree of saturation as presented by Phanikumar and Amrutha (2014)

2.7.6 Effect of sample scale on the compression index (c_c) and volume compressibility (m_v)

The effect of sample scale on c_c and m_v has not been previously investigated. c_c value does not change with a change in confining pressure for normally consolidated clays (Abbasi et al., 2012 and Singh and Noor, 2012a). On the other hand, m_v variability with confining pressure makes it less useful when correlating with some engineering properties (Singh and Noor, 2012a). These parameters have been studied to obtain a relationship with some engineering properties such as: internal friction angle, recompression index (c_r), moisture content, liquid limit (LL) and specific gravity (G_s).

Abbasi et al. (2012) conducted a series of consolidation tests on twenty-six fine-grained soils collected from a site. The consolidation test was conducted on an Oedometer apparatus 75mm diameter and 20mm height. The soil was saturated for 24 hours and prepared at initial moisture content 0.5, 0.8 and 1.2 times the LL. The specimen with an initial moisture content of 1.2LL was in a slurry state (Abbasi et al., 2012). The outcome of the correlation between c_c and some engineering parameters was calculated using the statistical analytical software SPSS as follows: correlation factor of 0.5 was found when correlated with G_s and the Atterberg limits and 0.92 for void ratio and moisture content (Abbasi et al., 2012). Thus the findings by Abbasi et al. (2012) show that the relationship between c_c and LL is not significant.

Retnamony and Mether's (1998) investigation revealed that m_v decreases with an increase in pressure by 30% for kaolinite soils and 20% for montmorillonite soils (Figure 2.11). The compressibility of the material is governed by the mechanical and physicochemical properties of the soil grains and by the viscosity of the pore fluids (Retnamony and Mether, 1998). The mechanical properties are controlled by the strength of the soil and surface friction (Retnamony and Mether, 1998). Physicochemical properties are assessed by the interactions between soil particles, in particular for the diffuse double layer. Diffuse double layer (DDL) is an ionic structure that describes the variation of electric potential near a charged surface such as clay minerals, as outlined in section 2.2.1 (Powrie, 2004).

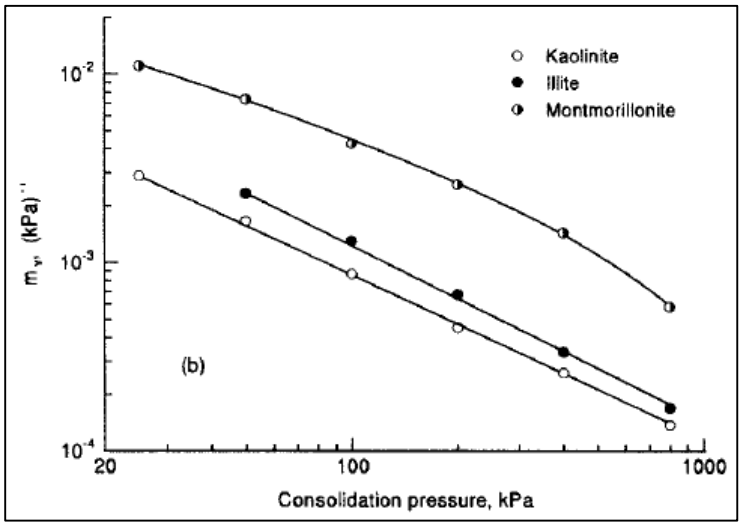

Figure 2-11: Variation of m_v with consolidation pressure at different clay mineralogy (Retnamony and Mether, 1998)

2.8 Chapter Summary

A review of the subject area was presented. Engineering properties of fine-grained soils are given in Appendix A to provide the basic understanding of the soil used in this study. A detailed discussion of previous work was presented. In addition to Terzaghi's consolidation theory, which is widely used, a brief description of Biot's consolidation theory was also presented.

There have been various studies conducted over the past few decades on the effect of sample scale on the coefficient of consolidation (c_v), most especially under sample height scale. The outcome of the investigation revealed that c_v is dependent on the soil sample thickness. Partial work has been conducted on the effect of sample scale on the remaining compressibility parameters.

It was also presented that under the D/H ratio scale, the American standard proposed a minimum value of 2.5 with a value of greater than 4 considered more suitable to minimise friction between the soil and apparatus. However, the British standard proposed a standard Oedometer apparatus size (cell diameter of 75mm and height 20mm) without referring to the D/H ratio. Hence, knowledge of the effect of D/H ratio on the compressibility parameters is limited. Nevertheless, D/H ratio effect on shear strength and friction in Triaxial tests was previously investigated and it was found that D/H has an impact on internal friction and strength of soil.

Other compressibility parameters such as m_v and c_c were previously investigated; however, not in terms of sample scale. m_v was found to decrease with an increase in pressure, whereas c_c was found to correlate well with LL. There have been numerous studies using radial consolidation on soil behaviour, without accounting for sample scale except for the study by Healy and Ramanjaneya (1970). Radial drainage was investigated using vertical and horizontal drainage, but limited to the combined drainage effect on sample scale.

The effect of initial moisture content on c_v, m_v and c_c was previously investigated. The findings reveal that, as the moisture content increases, c_v also increases. This outcome was also valid for m_v and c_c. However, c_v increases with an initial moisture content of 30% and then decreases as moisture increases to 40%. Healy and Ramanjaneya's (1970) investigation using radial drainage on Varved clay did not account for diameter scale, but sample height scale was used with D/H 3 being constant. The findings showed no significant difference in c_v.

CHAPTER 3

EXPERIMENTAL SETUP

3.1 Introduction

To study the effect of sample scale on the compressibility behaviour of fine-grained soil, a series of one-dimensional consolidation test were conducted under controlled conditions. This chapter presents the physical characteristics of the material under study and describes experimental tests performed in this research. The sample preparation methods, experimental techniques and calibration procedures that were adopted are presented. To carry out the test at different sample scales, different Oedometer apparatus diameters ranging from 100mm to 250mm were used.

3.2 Characteristics of material

The fine-grained soil used in this study was Kaolin clay, with a series of properties shown in Table 3.1, and a summary of the average values in the properties is indicated in Table 3.2. Cornwall Council, England supplied the Kaolin clay. The soil sample was passed through a 850μm sieve to obtain the liquid and plastic limit, following the procedure described by American Standard D4318 (ASTM, 2010) and British Standard BS1377: part 2 (BS, 1990). The Casagrande method was used to obtain the liquid limit (LL). The moisture content of the soil obtained during the Casagrande method is shown in Table 3.1. The values in Table 3.1 were used to obtain the LL of Kaolin clay at 25 blows with the average value shown in Table 3.2 and Figure 3.1. The specific gravity of the clay was obtained as 2.6 using test methods in accordance with the British Standard BS1377: part 2 (BS, 1990) and American Standard D854 (ASTM, 2010), as explained in Section 2.4.4. The initial moisture content of the material at each test conducted was obtained using test methods described in the American Standard D2216 (ASTM, 2010), as depicted in section 2.4.1.

Table 3-1: Detail soil properties

	Casagrande method moisture contents			Moisture content used to obtain the average PL			G_s		
China clay	50.8	56.3	69.2	31.3	33.7	32.3	2.6	2.58	2.6
Number of blows	373	55	14	N/A			N/A		

Where;
PL = Plastic limit and PI = Plasticity index

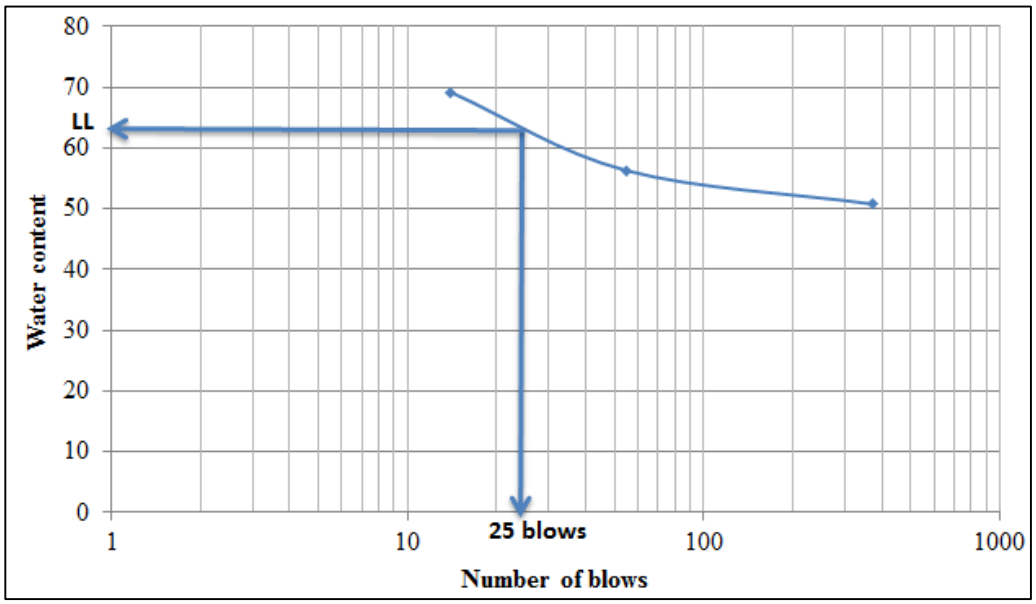

Figure 3-1: Casagrande method liquid limit derivation

Table 3-2: Soil Properties summary

	LL	PL	PI	G_s
China clay	63%	32.4%	30.6%	2.6

The clay mineralogy compositions of the soil used are presented in Table 3.3. The mineralogy analyses were carried out by Salford Analytical Services (SAS) enterprise, Salford University, UK. The sample primarily contained Kaolinite and Quartz in various proportions. Table 3.3 shows the percentages of clay minerals obtained using X-ray diffraction (XRD). The soil particle arrangement was also obtained using a scanning electron microscope (SEM). The equipment used for qualitative characterization of the mineralogy composition of the material was a Siemens D5000 X-Ray diffractometer and for the particle image arrangement was the FEI Quata 250 ESEM. A powder sample of Kaolin clay was used for the XRD and SEM.

Table 3-3: Mineralogy of the fine-grained soil studied

Soil Sample	Minerals	%
Kaolin Clay	Kaolinite	98
	Quartz	2

The X-ray diffraction patterns consist of a series of peaks with different intensities and are shown in Figure A.1 in the appendix. Clay minerals are too small to be seen by the naked eye, so their arrangements are referred to as micro-structure or micro-fabric (Barnes, 2010). The micro-structure of the kaolin clay minerals is shown in Figure A.2 in the appendix. From Figure A.2, it can be seen that the soil particles are close together as the load is applied, giving a denser soil sample. This phenomenon is observed in consolidation tests: as the loading increases, the thickness of the soil sample decreases, thus providing a denser sample.

3.3 Experimental test programme

The University of Salford provided three Oedometer cells: 100mm, 150mm and 250mm in diameter. The key features of the cells are a bottom plate with two ports (one for water pressure readings or applying the back pressure to the sample and the other for the second drainage). The second component is the cell body composed of sintered bronze porous stone, drainage plates, soil sample and acrylic loading jacket (made from Bellofram membrane) (Calabria, 1996). The Porous stone was saturated with tap water for approximately 5 minutes to prevent absorption of water from the soil sample. The Oedometer cell assembly is shown in Figure 2.8. Drainage is accomplished through the top and bottom channels, and two ports are provided in the upper blind flange, one for pressure application and the other for first drainage point. A pressure regulator is used to set up the pressure to be exerted on the soil sample. A scale was used to measure the mass of the soil and cells; and values are accurate to the nearest 0.1g. The equipment used is calibrated according to the British Standard BS1377 Part 6 (BS, 1990) and American Standard D2435 (ASTM, 2003).

3.3.1 Sample preparation

The sample preparation technique for the consolidation analysis was as per the British standard BS1377 Part 6. This was consistent through the various sample scales used. Details of the preparation as the moisture varied are presented below.

3.3.1.1 One-dimensional test sample

The sample preparation for the consolidation test was prepared as per the standard method mentioned above. A sample of kaolin clay (in powder form) was mixed with tap water using a soil mixer. The powder clay (1000g) was added to 1200cm^3 of water, and this was repeated accordingly. The soil sample was mixed in the mixer for approximately five minutes. Vaseline was applied to the Oedometer ring to reduce friction between the soil sample and the ring. The soil mixture was then poured into the Oedometer apparatus. Due to the variability of the sample scale used, a pre-consolidation pressure of 27kPa was applied for four hours to allow for excess water to be dissipated. This was done by allowing the soil to drain both ways i.e. from the top and bottom. After four hours, the apparatus was dismantled, and the soil trimmed to the required height. The initial moisture contents were obtained from the trimmings. Before the consolidation test began, equilibrium was attained at each loading, which was indicated by the nearly constant reading of the dial gauge.

3.3.1.2 Vane test sample

The vane shear test was used to obtain the undrained shear strength of the kaolin clay used. A sample of Kaolin clay weighing 720g was mixed with 62% of tap water, which brought the soil to a slurry state. A maximum value of 62% was selected because this is near the liquid limit (LL) of the soil. This means that the soil is fully saturated. In a slurry state, the soil mixture was left in the mould to set for an hour, before the undrained shear strength was obtained. The vane was inserted into the soil at a depth of 10mm, and the value of c_u was determined to be 12kN/m^2. Prior to commencing the vane test, the torsion springs were calibrated according to the American Standard D2571 (ASTM, 2001). A total number of 4 springs were calibrated, as presented in Figure 3.2. The weakest spring (spring 1) was used, as its general descriptive term of strength is very soft according to the British standard BS1377 part 2.

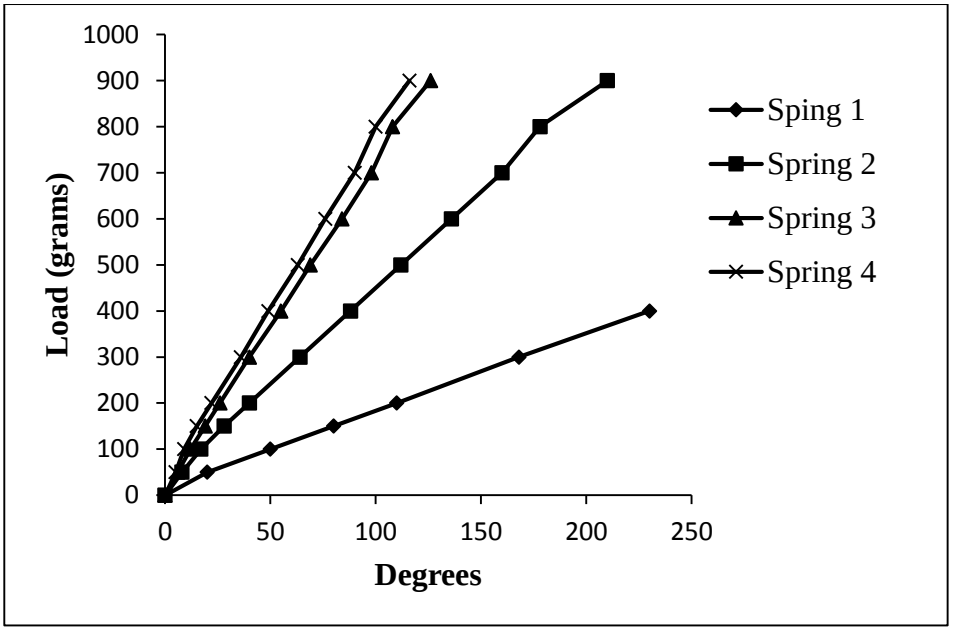

Figure 3-2: Torque spring calibration

3.3.2 Loading Increments

After the sample was prepared in the Oedometer apparatus, a load increment was applied using the standard test method, as described in the American Standard D4318 (ASTM, 2010) and British Standard BS1377: part 2 (BS, 1990). The load increment was applied in double until the maximum load that each cell could sustain was achieved. However, when the 100mm cell was used at a soil thickness of 23mm, a different load increment was used. This was because when a similar loading pattern to the remaining Oedometer cell was applied, the apparatus was damaged due to exceeding the maximum load limit of the cell. Therefore, for the 100mm cell with soil height 23mm (D/H 4), the load was applied at an increment of 28kPa to a maximum pressure of 138kPa, as shown in Table 3.4.

Table 3-4: Summary of maximum pressure for each Oedometer cell

Cell	Height	Cell material	Maximum pressure (kPa)
100mm	< 30mm	Plastic	138
100mm	30 < H < 200	Plastic	276
150mm	Any	Plastic	276
150mm	Any	Steel	276
250mm	Any	Steel	276

3.3.3 Dial gauge calibration

Dial gauges were initially used to measure the soil deformation under loading and were replaced at a later stage with LVDTs. LVDTs were calibrated to the nearest 0.1% accuracy. Each dial gauge used had a maximum travel length of 20mm, after which it was reset to zero in the data collection. The dial gauge was calibrated against a Coventry Gauge Limited (CGL) grade 1 (Figure 3.3a). The Coventry Gauge Limited (CGL) grade 1 comprised a series of steel plates with thicknesses ranging from 0.01mm to 50mm. The dial gauge was mounted on a stand, as shown in Figures 3.3b and c. Using one of the CGLs of thickness 20mm, the dial gauge was set to zero. A CGL of any thickness was placed beneath the dial gauge, and the reading of the dial gauge was noted. Ideally the dial gauge reading should reflect the thickness of the CGL used and any discrepancy is the percentage error. This process was repeated at various CGL thicknesses, and the difference between the true value (CGL thickness) and the dial gauge reading was taken as a 0.3% error.

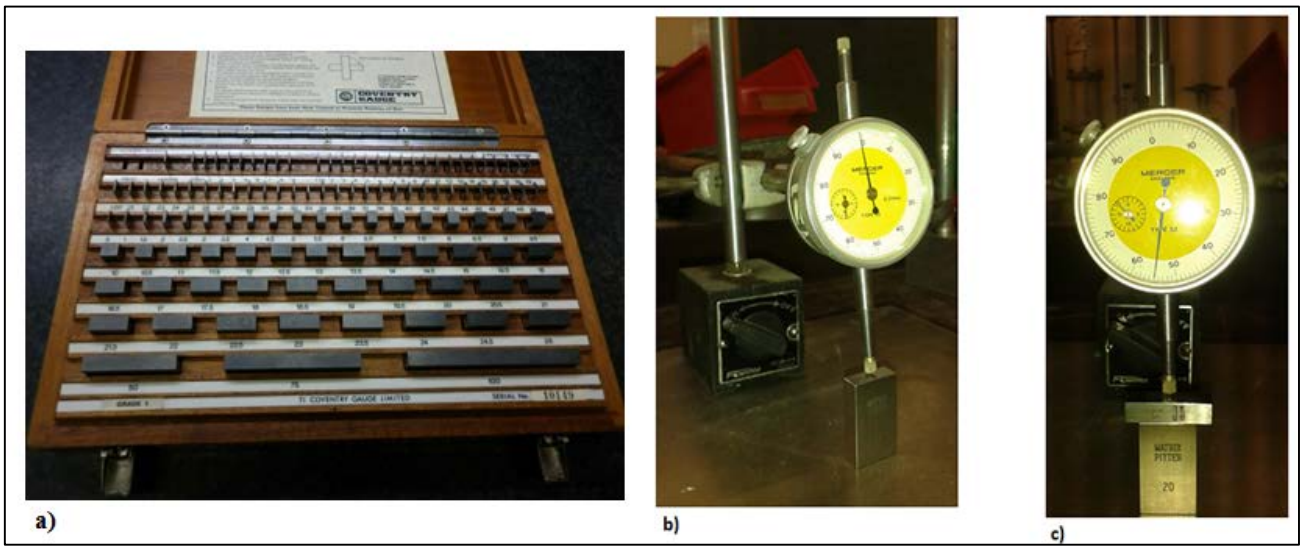

Figure 3-3: Dial gauge calibration; a) Coventry Gauge Limited Grade 1, b) Dial indicator set at zero with 20mm Coventry Gauge limited and c) Gauge moved 7.5mm corresponding to the thickness of Coventry Gauge Limited

3.3.4 Cell Calibration

The Oedometer cell was calibrated according to the British Standard BS1377 Part 6 (BS, 1990) and American Standard D2435 (ASTM, 2003) to ensure accuracy in the functionality of the apparatus. According to the British Standard, the equipment and accessories were

measured with a scale and Venier callipers to the nearest 0.1g. The measured values of the cells used in this study with their calibrations are shown in Table 3.5.

Table 3-5: Cell measured valued

Cell internal diameter (mm)	100	150	250
Area (mm^2)	7850	17671.4	49087.4
Overall height of cell body	390mm	399mm	680mm
Internal Depth from top edge of cell to the base	101mm	57mm	125mm
Thickness of porous stone (top)	-	3mm	4.3mm
Thickness of porous stone (bottom)	-	3mm	5mm
Mass of cell body with normal attachment	4268.7g	21250g	57000g
Mass of dry porous stone (top)	-	289.1g	1067g
Mass of porous stone (bottom)	-	270.9g	1132.8g
Mass of dry filter paper + filter material (top and bottom)	2g	9.8g	18.5g
Mass of wet porous stone (top)	-	302.8g	1092.6g
Mass of wet porous stone (bottom)	-	283.5g	1170.1g
Mass of wet filter paper + filter material (top and bottom)	7.7g	42.4g	69.1g
Thickness of diaphragm	95mm	148mm	250mm
Maximum projection length of the diaphragm	20mm	40mm	60mm

3.3.5 Pressure regulator Calibration

Pressure cells for each Oedometer cell were calibrated to obtain the accuracy of the pressure being set up. The calibration consisted of using a calibrated transducer to obtain an accurate measure of the pressure being supplied by the pressure regulator. The calibration setup consisted of calibrated transducer, pressure regulator and computerised system.

One end of the transducer pressure cell was connected to the pressurised water outlet of the regulator. The other end of the transducer pressure cell was connected to the pressure gauge line (to read the pressure being set out by the regulator manually). The air inlet was connected to a pressure cell of the regulator. The transducer was then connected to a computerised system (CATMAN) from which the actual pressure reading from the regulator pressure was observed. Once the setup was completed, the pressure was applied using the pressure regulator. The applied pressure was read from the pressure gauge and the actual pressure being applied to the pressure regulator was read out from a computerised system. This was manually conducted for a series of pressures. The actual pressure obtained through

the transducer is accurate to the nearest 1% (this is because the transducer was calibrated to the nearest 1%). The average pressure calibration error was found to be 3.7kPa. The difference between these pressures ($\pm$3.7kPa) is the error in the applied pressure. The significance of the pressure difference is as shown in Figure 3.4. From Figure 3.4, the best fit line has a correlation factor of 0.99, which shows there is no significant difference between the applied and actual pressure. Hence, the error of $\pm$3.7kPa is not substantial.

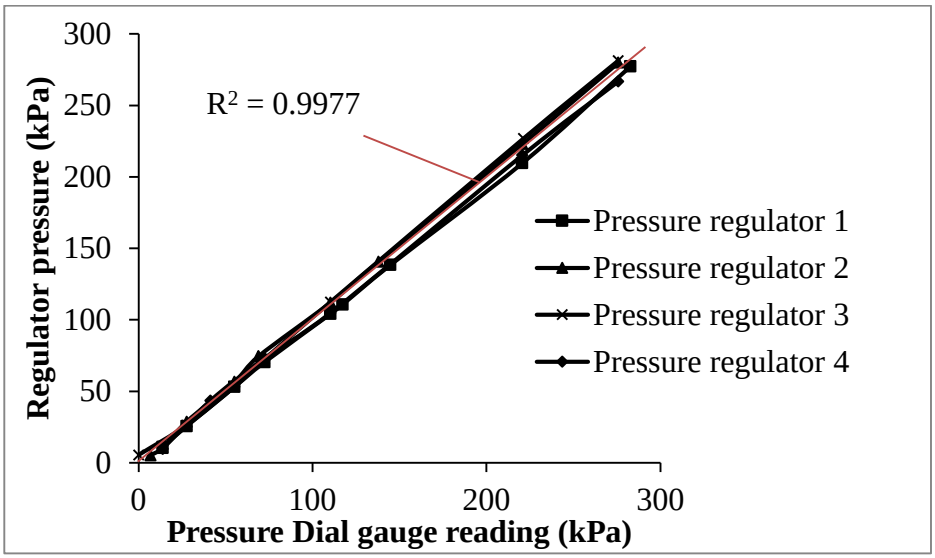

Figure 3-4: Relationship between actual and applied pressure at various pressure regulators

3.3.6 Bellofram membrane calibration

The bellofram membrane, one of the essential components of the Oedometer cell, was calibrated as per the British Standard BS1377 Part 6 (BS, 1990). The membrane is used for the load application onto the sample during consolidation. The force exerted by the bellofram membrane on a rigid top plate may be less than that calculated from the hydraulic pressure and cross-sectional area of the cell, owing to the diaphragm stiffness and side friction (BS, 1990). The difference between the actual and the calculated force is determined, and it has a more significant influence in a small cell than in a large one (BS, 1990). It can vary with both the applied pressure and diaphragm extension and values are greatest at low pressures (BS, 1990).

The applied force by the diaphragm was measured by the following method, as described by the British Standard BS1377 Part 6 (BS, 1990). An applied pressure is applied to

pressurise the water within the diaphragm. The following equation gives the actual pressure P (kPa) applied to the area of cross section of the cell:

$$P = \frac{F+9.81m}{A} \text{ x } 1000 \qquad (3\text{-}1)$$

Where:
F is the measured force (N), m is the mass of the porous stone (g) shown in Table 3.5 for each cell, and A is the area of the cell (mm^2)

The relationship between the diaphragm pressure (P_d) and the pressure correction to be applied δp (where $\delta p = P_d - P$) was plotted for a load-unload cycle to the maximum working pressure. Table 3.6 shows a summary of the pressure being applied to the bellofram membrane with its correction factor. From Table 3.6, the value of P was obtained for cell 100mm by assuming m to be equal to the filter paper mass because no porous stone was used with this cell. Therefore, the pressure being exerted on the specimen in this study is on average accurate to 0.1%.

Table 3-6: Summary of the bellofram membrane (Diaphragm) pressure calibration with the respective loading use in this study for each Oedometer cell

Cell (mm)	Diaphragm applied pressure (P_d) (kPa) $\pm$3.7kPa	Actual pressure (P) (kPa)	Pressure correction (δp) (kPa)
100	55	55.002	0.002
	82	82.002	0.002
	110	110.002	0.002
	138	138.002	0.002
	276	276.002	0.002
150	55	55.16	0.160
	110	110.16	0.160
	220	220.16	0.160
	276	276.16	0.160
250	55	55.21	0.213
	110	55.21	0.213
	220	55.21	0.213
	276	55.21	0.213

3.4 Sample Scale Terminology

Tables 3.7 to 3.10 show different sample scales used in this study. The scales are presented in three categories as follows:

1. **Diameter scale:** This refers to a situation where the diameter of the sample varies while the soil thickness is kept constant. This benefits three diameters: 100mm, 150mm and 250mm from the Oedometer apparatus provided by the University of Salford.
2. **Height scale:** This discusses a state where various thicknesses are used, but the diameter of the soil sample is kept constant. Heights used are 23mm, 30mm, 80mm, 130mm and 200mm.
3. **Diameter to Height ratio scale:** This stage will evaluate the results in terms of diameter to height (D/H) ratio standard value 2.5 according to the American Standard D2435 (ASTM, 2003). This study benefits from D/H ratio of less than 2.5 and greater than 2.5 such as 0.5, 1, 1.5, 2, 3, 4, 5, 6.5 and 11.

Table 3-7: Sample scale ranges for single Oedometer test run over 24hours (Diameter scale)

Scale	**Diameter**								
Diameter (mm)	100	150	250	250	100	150	250	150	250
Height (mm)	23	23	23	200	200	130	130	80	80
Tests	T1			T2		T3		T4	
Moisture content	67.5%			73%		64.5%		60%	
Sample	China clay								

Table 3-8: Sample scale ranges for single Oedometer test run over 24hours (Height scale)

Scale	**Height**							
Diameter (mm)	150	150	150	150	250	250	250	250
Height (mm)	23	30	80	130	23	80	130	200
Test	T5				T6			
Moisture content	67.1%				55%			
Sample	China clay							

Table 3-9: Diameter to Height ratio scale tests

D/H	0.5	1	1.2	2 (a)	2 (b)	3	4	5	6.5	11
Diameter	100	150	250	150	250	250	100	150	150	250
Height (mm)	200	130	200	80	130	80	23	30	23	23
Test	T7	T8	T9	T10	T11	T12	T13	T14	T15	T16
Initial moisture	91%	74%	55%	65%	55%	55%	80%	60%	59%	64%
Average moisture	66%									

Table 3-10: Double Oedometer test

D/H	6.5		6.5		2		0.5		2			
Diameter (mm)	150	150	150	150	150	150	100	100	250	250	250	250
Height (mm)	23	23	23	23	80	80	200	200	130	130	130	130
Tests	T17		T18		T19		T20		T21			
Moisture content	67.5				65		91		55	68	74	105
Sample	China clay											
Test Duration	24 hours		24 hours	7days	24 hours		24 hours	7 days	24 hours			

3.4.1 Sample scale Range Oedometer Test

3.4.1.1 Single Oedometer test

A single Oedometer test occurs when a sample is tested at a certain pressure, recording the change in height of the sample during consolidation. The test procedure is as stated in the American Standard D2435 (ASTM, 2003), where the sample is loaded at different load increments at approximate time intervals of up to 24 hours to ensure primary consolidation has been achieved. However, at some sample scales, a period of 24 hours has been shown not to produce an accurate value of c_v due to the end of primary consolidation (EOP) not being complete. As a result, tests at some sample scales were conducted for a duration of 7 days to ensure the end of primary consolidation (EOP) was fully attained. Tables 3.11 and 3.12 show a summary of the series of consolidation tests conducted.

Table 3-11: Series of consolidation testing programmes at different sample scales using samples of China Clay

Tests	Diameter (mm)			Height (mm)					
	100	150	250	23	30	180	130	80	200
1	X	X	X	X					
2	X		X						X
3		X	X				X		
4		X	X					X	
5		X		X	X		X	X	
6			X	X			X	X	X

3.4.1.2 Double Oedometer test

The double Oedometer tests at different stress levels and the deformation differences on soil samples at various sample scales and moisture contents were determined. The sample scales used for this test are as shown in Table 3.12. As described in the literature, this test requires identical samples to be prepared in two identical Oedometer cells. One specimen is maintained at its initial moisture content and/or void ratio, while the moisture content and/or void ratio is changed in the other specimen. However, for the purpose of this research, the double Oedometer test refers to the following:

1. Identical samples with identical initial moisture content tested on the identical sample scale. This is to produce identical results and any discrepancy in results was due to soil mineralogy.
2. Two soil samples of similar initial moisture content and sample scale but run over different time periods (24 hours and 7 days)
3. Identical soil at identical sample scale but different moisture content. This is aimed at investigating the importance of initial moisture content on the compressibility parameters.

Table 3-12: Series of consolidation testing programmes at different sample scales - double Oedometer test on China clay

Tests	Diameter (mm)			Height (mm)				
	100	150	250	23	40	80	130	200
17		X		X				
		X		X				
18		X		X				
		X		X				
19		X				X		
		X				X		
20	X							X
	X							X
21			X				X	
							X	
							X	
							X	

3.5 Variability and uncertainty of data

Uncertainty is extensive in all engineering fields including geotechnical engineering (Dasaka, 2005). Natural soils are heterogeneous and exhibit anisotropy and physical properties due to their composition and depositional process (Dasaka, 2005). The uncertainty in geotechnical engineering is mainly attributed to characteristic variability, a limited number of samples, testing and measurement errors (Dasaka, 2005). Ding et al. (2014) calculated the uncertainty and variability of consolidation parameters obtained in the laboratory using soft and stiff clay with that obtained in practice. This was achieved with a series of one dimensional consolidation test on samples collected on respective sites. Ding et al. (2014) found that the variability and uncertainty in the consolidation parameters achieved in the laboratory were less than that in practice for soft soils. However, for stiff soil, both variability and uncertainty in the laboratory and in practice was similar (Ding et al., 2014). The terminology applied by Ding et al. (2014) was implemented in the current study to evaluate the variability and uncertainty of data.

Therefore, uncertainties observed in the current study were in the following aspects: functionality of the equipment, pressure regulator system, dial gauge readout and data analysis and variability in the coefficient of consolidation (c_v). Calibration and repeating the

tests twice was used to resolve the first three points. Once calibrated, percentage error or percentage accuracy was found to describe the degree of precision of the data obtained. At a later stage, a computerised system was implemented, where the deformation of the specimen was measured using an LVDT instead of a dial gauge, which then reduced human error. The latter aspect forms one of the major effects in the values of c_v. As described in the literature, methods used in obtaining c_v are based on the curve-fitting method. This is appropriately used when the experimental curve matches the theoretical curve. However, due to sample scale and duration of each load increment during the consolidation test, the experimental curve did not match the theoretical curve. This presented some uncertainties where human judgement was relied on to identify the end of primary consolidation (EOP). This was mainly affected when using the Casagrande and Inflection method. Hence, results obtained from different sample scales were compared to draw a conclusion regarding the variability and uncertainty associated with the consolidation parameters.

3.6 Chapter Summary

In summary, the methodology of the series of consolidation tests carried out in this study has been presented. The Oedometer apparatus with its components were calibrated to provide a level of accuracy on the data obtained. Some degree of uncertainties in the data acquisitions was explained. During the data analysis, which will be presented in Chapter 4, the reliability and uncertainty of results were presented at each sample scale. The percentage error of the calibrated equipment was presented, and this showed the accuracy (0.3% and 3.7kPa) in the results obtained in the laboratory. A series of consolidation tests at their respective sample scales were presented. Data obtained at different sample scales were compared with previous work presented in the literature. Emphasis was placed on the diameter to height ratio, as little is known in this area.

CHAPTER 4

EFFECT OF SAMPLE SCALE ON THE COMPRESSIBILITY BEHAVIOUR OF FINE-GRAINED SOILS

4.1 Introduction

In this chapter, the experimental results of the impact of sample scale on the compressibility behaviour of fine-grained soil are presented in terms of change in initial moisture content, void ratio and compressibility parameters. A series of single and double Oedometer tests were conducted on samples prepared from slurry at various initial moisture contents. The double Oedometer test was conducted to validate the reproducibility/variability of the data while the single Oedometer test was mainly for scale variation purposes. The values of the compressibility parameters obtained were compared with standard values presented in Tables A.7 to A.9.

4.2 Scales at University of Salford

The University of Salford provided a series of Oedometer apparatus (Figure 4.1), and the investigation was conducted in the following stages.

1. First stage: single Oedometer test on kaolin clay at different initial moisture contents
2. Second stage: Double Oedometer test on identical samples at identical scale and initial moisture content.

The purpose of the above stages was to elaborate a pattern/trend in the compressibility parameters with sample scale due to material consistency, initial moisture content and void ratio. Figure 4.1 shows the variability of the Oedometer apparatus, using different materials from plastic to steel. The variation in cell material affected the one dimensional consolidation tests where the maximum pressure the cell could sustain was proportional to the soil sample scale. This variability in pressure is depicted in Table 3.4.

Figure 4-1: Various Oedometer cell sizes at the University of Salford

4.3 Statistical analysis

Correlation and validation of the data were conducted using Pearson correlation in IBM SPSS (Statistical Package for the Social Sciences) software to define the significance (p) of the data obtained. The correlation coefficient is a measure of the association between two variables and ranges between -1 and 1 (Laerd Statistics, 2013). The sign indicates that the variables are positively or negatively related; a value of zero implies that there is no correlation. Table 4.1 is used to describe the correlation factor achieved during the analysis.

Table 4-1: Magnitude of Pearson correlation coefficient as provided by Cohen (1988) (Laerd Statistics, 2013)

Coefficient value	Strength of Association
$0.1 < r < 0.3$	Small correlation
$0.3 < r < 0.5$	Moderate correlation
$r > 0.5$	Strong correlation

The analysis was conducted for the following relationships:

1. **Normality of c_v values obtained using different test methods**

Three different methods: Casagrande, Taylor's and Inflection were used to derive the value of c_v. Its significance and normality were investigated in SPSS using one-way Analysis of Variance (ANOVA) and Normality respectively.

2. Effect of sample thickness on coefficient of consolidation (c_v)

Each c_v values was correlated with different soil thicknesses while the soil diameter was kept constant. This procedure was done using Pearson correlation in SPSS.

3. Effect of sample diameter on the coefficient of consolidation (c_v)

This was conducted as explained in no.2 above but at different diameters. c_v values obtained using various methods were correlated with the respective diameter used.

4. Effect of sample scale on the compression index (c_c) and coefficient of volume of compressibility (m_v)

This was conducted using the principles outlined in nos. 2 and 3 above.

5. Effect of diameter to height (D/H) ratio on the value of c_v, c_c and m_v

A series of D/H ratios were correlated with the compressibility parameters under different loading conditions. They were correlated for each method used to obtain c_v. Procedure outlined in nos. 1 to 5 was adopted during the analysis of the effect of initial moisture content on the compressibility parameters and time factor on c_v.

4.4 Results

The results obtained from the series of consolidation tests are presented. Graphical representation of the relationship between void ratio and time, time deformation characteristics and tabular results of data obtained for both single and double Oedometer tests are illustrated. The loading applied is written with a pressure error of $\pm$3.7kPa and deformation reading has a percentage error of 0.3%, as discussed in sections 3.3.5 and 3.3.3 respectively. Only one representative test series (D/H = 0.5 at 110kPa$\pm$3.7kPa) of the ten tests connected in the series was selected for illustration purposes. The remaining curves are presented in Appendix B.

4.4.1 Void ratio versus stress

The relationship between the void ratio against time for the entire range of the consolidation process is provided in the Appendix (Figures B.1 to B.18). The figures show that as the load increases, the void ratio decreases and the process is continuous depending on the previous load applied. This was observed through the ten consolidation tests. The void ratio was obtained from the relationship between the specific gravity and moisture content, as

presented in equation A.3. Figure 4.2 shows a trend in the void ratio relationship with stress at various scales (diameter, height and D/H ratio sample scales). The general trend shows a decrease in the void ratio with an increase in stress. At a constant soil thickness of 23mm (Figure 4.2a), as the diameter of the soil increases, the initial void ratio decreases, due to the rearrangement of the soil particles with sample scale. However, at a constant soil thickness of 200mm, as the diameter increases there is an increase in initial void ratio, whereas, at constant soil diameter of 250mm, as the soil height increases, the initial void ratio increases as well. At diameter 150mm, a fluctuation in the initial void ratio is observed as the soil thickness increases (Figure 4.2b). This variation in initial void ratio is mainly due to the soil diameter to height ratio effect (Figure 4.2c).

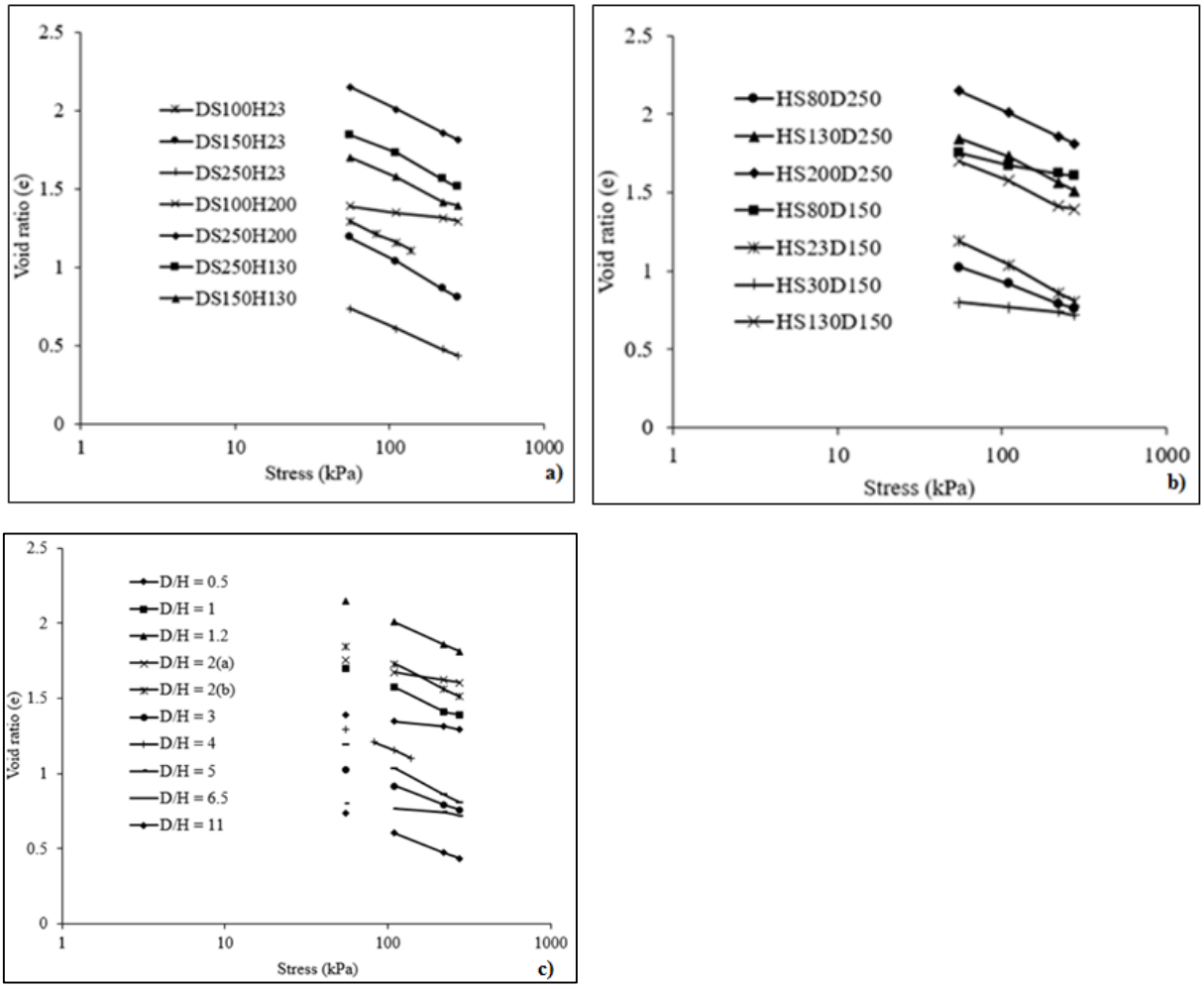

Figure 4-2: Relationship of void ratio against stress at loading 55kPa at a) Diameter scale, b) Height Scale and c) D/H ratio scale (Rosine and Sabbagh, 2015)

4.4.2 Time-deformation characteristics

The time – deformation curves obtained for D/H = 0.5 under 24 hours' load duration is presented in Figures 4.3 to 4.5 for illustration purposes. These curves are used to derive the value of c_v. The graphs plotted demonstrate how the values of the coefficient of consolidation shown in Table 4.2, and Tables C.1 – C.15 in Appendix C, were obtained.

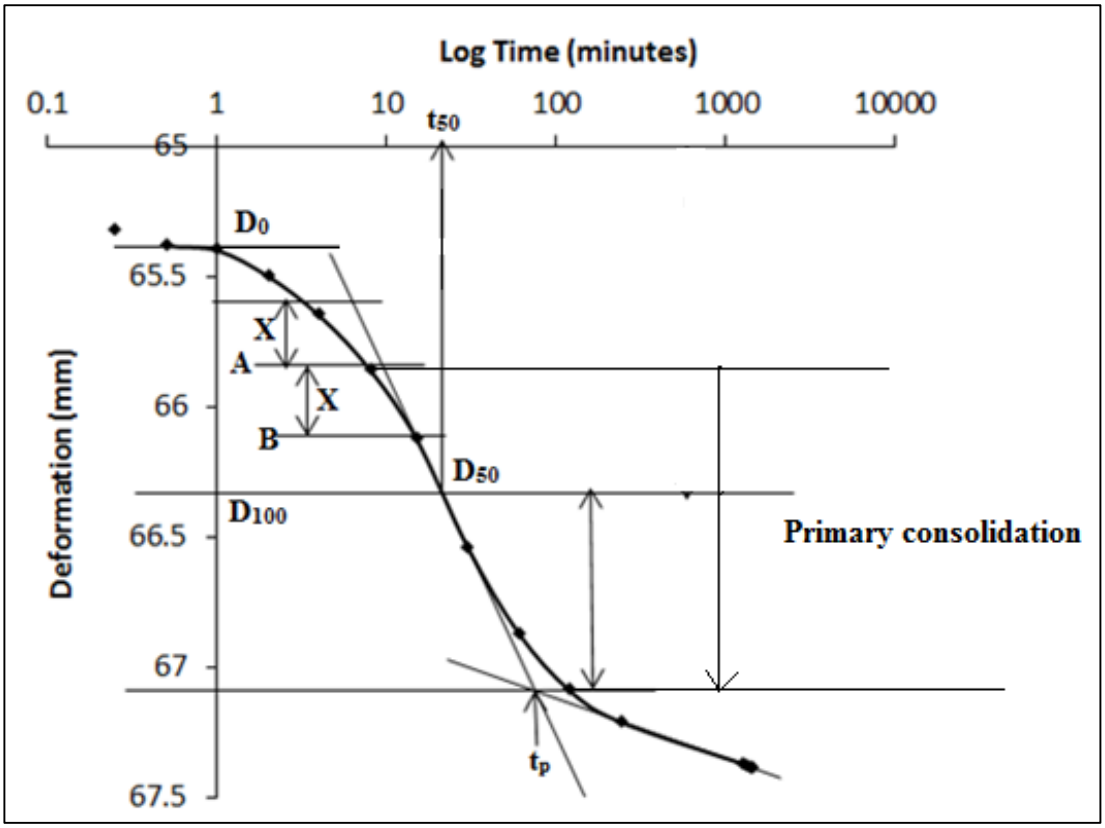

Figure 4-3: Casagrande method 110kPa±3.7kPa

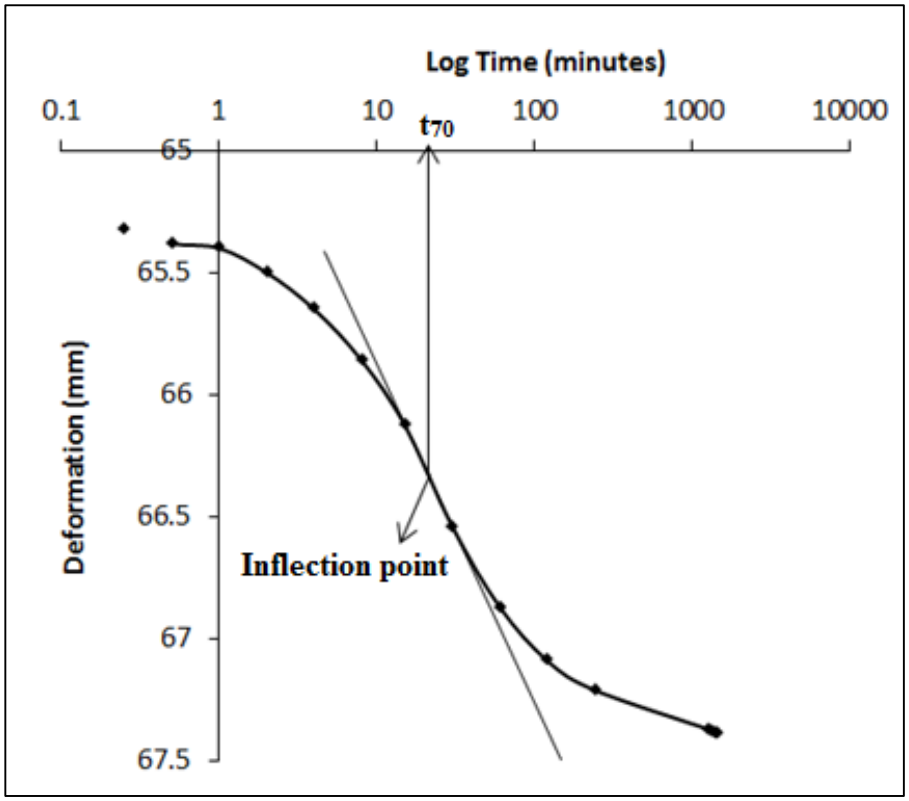

Figure 4-4: Inflection method at 110kPa±3.7kPa

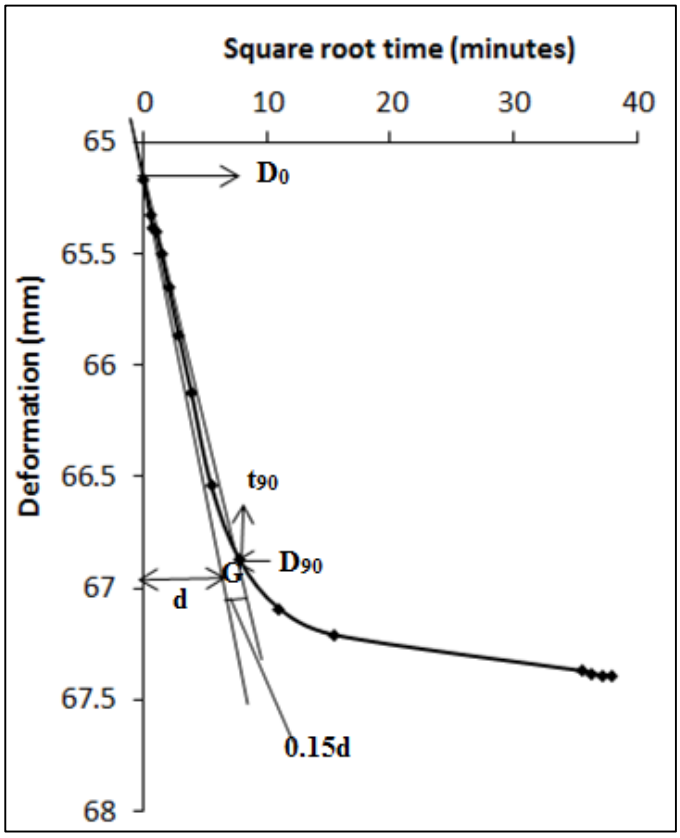

Figure 4-5: Taylor's method at 110kPa±3.7kPa

4.4.3 Series of single Oedometer tests

The data obtained on china clay prepared from slurry at various moisture contents are presented in Appendix C. The data are displayed in two categories: 24-hour duration and 7-day duration. Different load incremental durations were measured from observations made on the time-deformation curve obtained at 24 hours' loading. This showed that at some sample scales, 100% EOP was not reached, which led to the conclusion that a longer testing period was required.

Table 4.2 shows an illustration of the effect on height scale on the value of c_v and also the importance of the time deformation curve. It can be observed that irrespective of the method used, as the soil height increases, c_v increases. The logarithm scale was not clearly represented at a soil thickness of 200mm, which resulted in a high c_v value (35.50 m^2/yr). This could be due to two factors: time factor (time taken for consolidation at each loading) and initial moisture content (due to the soil not being fully saturated, there could be the presence of air within the soil sample, which could have affected the result). The latter was examined by investigating the effect of initial moisture content on c_v.

Table 4-2: Test 3 – Effect of sample height scale on c_v at 55kPa

Load (±3.7kPa)	**Load Inc (±3.7kPa)**	**Diameter (mm)**	**Height (mm)**	**c_v (m^2/yr)**		
				C	T	I
0	0			0	0	0
55kPa	55kPa	250	80	4.12	5.04	5.68
		250	130	14.52	5.22	14.99
		250	200	20.61	22.75	35.50

Where;
C = Casagrande method, T = Taylor's method, I = Inflection method, inc = Increment, c_v = coefficient of consolidation

4.5 Evaluation of Findings

4.5.1 Normality and significance of the c_v values using different methods

The aim of this analysis was to examine the influence of various methods used in obtaining c_v. This was done by evaluating the c_v values obtained for all sample scales (Tests 1 to 21) with initial moisture content that varied from 55% to 105%. The significance of the value of c_v obtained using different methods was evaluated using one-way ANOVA in SPSS. One

way ANOVA is typically used to investigate differences in the mean between two groups (either Casagrande and Taylor's method or Taylor and inflection method or Casagrande and Inflection method) with the independent variable c_v. Thus the analysis shows the statistical significance of the value of c_v obtained using different methods. During the analysis, the statistical significance and magnitude difference in c_v value were observed.

A one-way ANOVA was conducted on a total of 15, 21, 30 and 12 data points for diameter, height, D/H ratio and time scale for kaolin clay respectively. There was an outlier as assessed by boxplot during sample diameter scale analysis, where it was observed that c_v obtained using Taylor's method was normally distributed, as compared to Casagrande and Inflection methods. There was homogeneity invariance (c_v) as assessed by Levene's tests in SPSS, and there was no statistically significant difference in c_v obtained using the various method at the diameter scale. Similar observations were made on the sample height scale; however, c_v was normally distributed under the Casagrande and Inflection method as compared to Taylor's method. At D/H ratio scale, the data were homogenous with no statistical significance in c_v, but not normally distributed across the different test methods. Under the time scale (tests 17 and 19), data were normally distributed using the Casagrande and Inflection method, but by Taylor's method, there was homogeneity in the data and no significant difference in c_v. Data are presented as the mean $\pm$ standard deviation in Table 4.3. The significant difference in c_v between the test methods is 0.01 for the sample scales; thus insignificant.

The statistical analysis presented shows that c_v values obtained using either test method are not significantly different, and the general difference in the value was found to be 0.01; thus not significant. A general observation was also made from Table 4.3, where Taylor's method has the highest c_v mean value except in the time scale. The observation achieved in this study was also observed by previous researchers, such as Cortellazzo (2002), McNulty et al. (1978), Mesri et al. (1999) and Sridharan et al. (1995). Casagrande and Inflection methods were also found not to be significantly different from previous research, and this was also observed in this study.

Table 4-3: Output of Normality and Significance of c_v values obtained using Casagrande, Taylor's and Inflection methods

Sample scale	Casagrande	Taylor	Inflection
Diameter	5.5±6.6	9.8±7.8	9.1±10.3
Height	6.1±4.5	7.6±6.3	8.9±6.7
D/H ratio	5.8±5.4	7.6±6.2	8.6±7.9
Timescale	6.6±7.5	7.4±8.8	10.3±11.9

4.5.2 Effect of sample thickness on the coefficient of consolidation (c_v)

Tests 5 and 6 (shown in Table 3.8) were used for the correlation between sample height and c_v using Pearson correlation in SPSS. Both tests are analysed separately due to variation in height and moisture employed in each test.

Test 5 showed a strong correlation in c_v with sample thickness with a positive correlation factor of 0.641. The correlation value is statistically significant at a 0.01 level. Similarly, Test 6 also showed a strong correlation, with a correlation factor of 0.589 significant to 0.01. The data thus revealed that, as the thickness increases, c_v increases at each load increment. This finding validates previous work by researchers such as Healy and Ramanjaneya (1970) and Ortega (1996). Figure 4.6 shows a summary of data obtained in this study, together with that of Berry and Reid (1987). Load 55kPa±3.7kPa for both Tests 5 and 6 were plotted for representation purposes. It can be observed that soil thickness has a significant influence on the value of c_v, the higher the thickness, the greater the value of c_v. Test 6 and Berry and Reid's test data present similar curve patterns that are due to the identical loading scenario. However, test 5 at 110kPa and Berry and Reid's curve scenario do not follow identical trends with the remaining curves. c_v decreases at 79mm and then increases to 238mm, which could be due to the drainage path length, duration of loading and soil mineralogy.

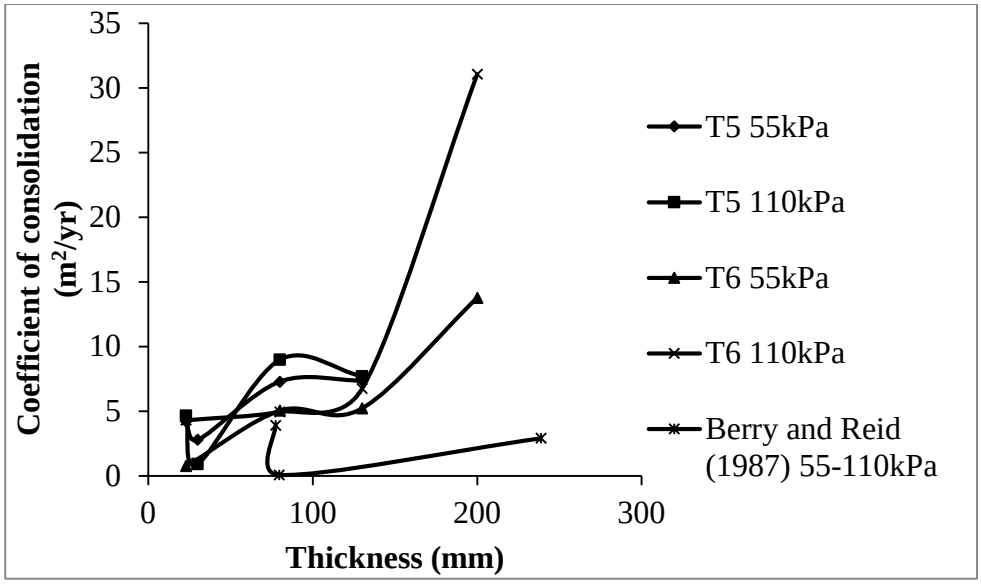

Figure 4-6: Summary of current study and previous work on the effect of soil sample thickness on the coefficient of consolidation (c_v) (using Taylor's method)

4.5.3 Effect of sample diameter on the coefficient of consolidation (c_v)

Test 1 to 4 were conducted on kaolin clay from slurry and tested in an Oedometer apparatus with diameters of 100mm, 150mm and 250mm and thickness kept constant. The value of c_v obtained was correlated with the various diameters used and was found to have a positive low correlation factor of 0.027. The low correlation shows that diameter scale is dependent on c_v. As the diameter increases, there is a reduction in the rate of consolidation only at soil thickness of 23mm, whereas at soil thickness between 80mm and 130mm, there is a fluctuation in the rate of consolidation as the load increases (refer to Figure 4.7). Hence c_v is significantly influenced by the soil sample diameter where the water flow was taken to be one-dimensional (vertical only). Previous investigation by researchers such as Healy and Ramanjaneya (1970) was based on radial consolidation over Varved clay without taking into account the effect of diameter scale. Due to the difference in soil mineralogy and permeability, the rate of drainage and length of drainage was affected by sample scale. Since the experimental study is on one-dimensional consolidation drainage, further investigation into this conclusion using finite element analysis is presented in the following chapters. From Figure 4.7, as the specimen diameter increases, there is a reduction in the rate of consolidation where the D/H is less than 2.

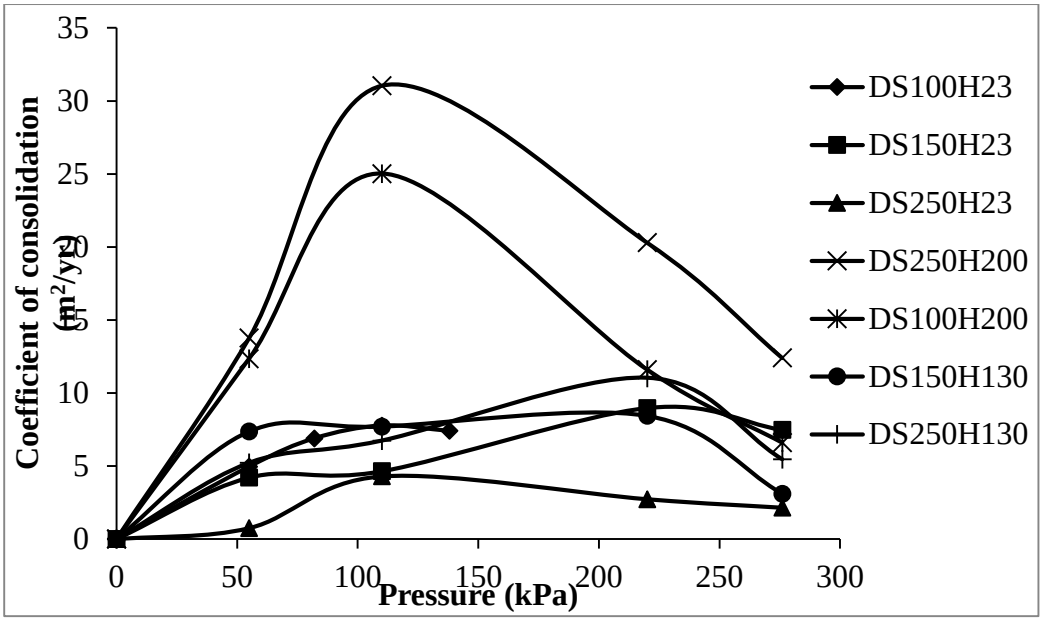

Figure 4-7: Effect of diameter scale of the coefficient of consolidation (c_v)

4.5.4 Effect of sample scale on the compression index (c_c) and coefficient of volume compressibility (m_v)

The compressibility parameters c_c and m_v are important in the calculation of settlement of structures. c_c is used to determine the primary consolidation settlement of the normally consolidated soil. Normally consolidated soils are a type of soil whose present effective overburden pressure is the maximum pressure that the soil was subjected to in the past (Budhu, 2000). Thus, the soil in this study is termed normally consolidated. A high c_c value indicates higher compressibility and higher consolidation settlements (Table 2.5).

The effect of diameter scale (Test 1 to 4) showed a low negative correlation of -0.161 and -0.172 for c_c and m_v respectively; height scale (Test 5 and 6) on c_c and m_v also showed a low negative correlation of -0.006 and -0.045 respectively. At the D/H ratio, c_c and m_v had a positive correlation of 0.052 and 0.090 respectively (Figure 4.8). It was thus observed that when the height and/or diameter increase, c_c has the tendency to decrease. A fluctuation in c_c value was also noticed with a rise in pressure to a maximum pressure of 276kPa$\pm$3.7kPa, where c_c was constant (Figure 4.8a).

Similarly, m_v was observed to fluctuate as the height and/diameter increases and pressure increases. This was mostly seen in the sample height scale. Diameter scale showed a sharp rise in m_v from 0 – 110kPa$\pm$3.7kPa and a steady decrease from 220kPa$\pm$3.7kPa to 276kPa$\pm$3.7kPa. This contradicts findings by Retnamony and Mether (1998), where m_v was

found to increase with an increase in pressure for kaolinite soil. The current study showed that m_v fluctuates with an increase in sample scale and pressure, up to a pressure of 220kPa$\pm$3.7kPa, where the value decreases. This trend was observed with the remaining sample scale, where m_v was found to decrease with an increase in pressure. Test 21 showed that, as the initial moisture content increases, m_v increases at load 55kPa$\pm$3.7kPa, and 220kPa$\pm$3.7kPa with the increase being less significant. A similar pattern to that shown in Figure 4.8 was also noticed using sample height and diameter scale.

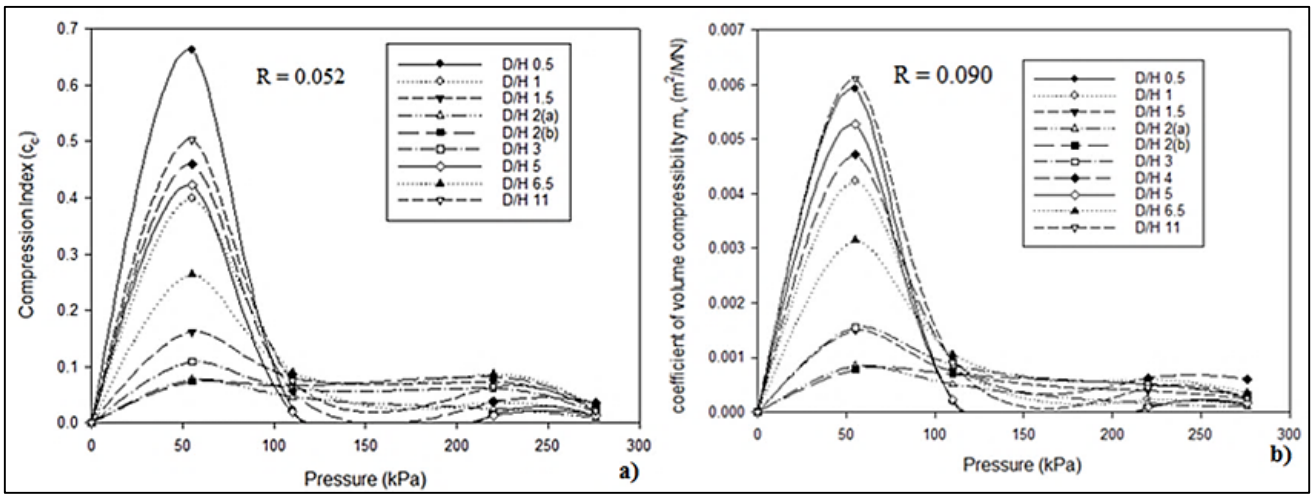

Figure 4-8: Effect of sample scale (D/H ratio) on some compressibility parameters: a) c_c and b) m_v (Rosine and Sabbagh, 2015)

4.5.5 Effect of diameter to height (D/H) ratio on c_v

Prior to the analysis, the significance of c_v value obtained was verified to ensure normality in the data obtained. The data obtained for Tests 7 to 16 were normal, and there was no significant difference in c_v values obtained using either the Casagrande, Taylor's or Inflection method. The importance of D/H ratio is to minimize friction between the Oedometer cell and the soil sample. Some recommended values were presented in the American Standard and British Standard, as stated in the literature in section 2.10.4. The friction in the current study was minimized by applying Vaseline on the Oedometer cell wall.

According to Healy and Ramanjaneya (1970), side friction is a function of pressure, and the e-log p graph is expected to become flatter with an increase in side friction, thereby producing a small value of the compression index. In the current study (Figure 4.2), the e – log p curve obtained contradicts the statement by Healy and Ramanjaneya (1970) except at

D/H 0.5 and 5 where friction was reduced. Sivrikaya and Togrol (2006) derived an expression to obtain the frictional stress (τ_s), as shown in equation 4.1.

$$\tau_s = \frac{T}{\pi DH} \qquad (4\text{-}1)$$

Where;
D is soil diameter (mm); H is soil height (mm), and T is the load transmitted to the ring (N).

Figure 4.9 shows the application of equation 4.1 in the current study. It was observed that at a pressure less than 150kPa, there is no significance difference in frictional stress. The observation was at all sample scales except at D/H 4, 5 and 6.5, with D/H = 4 being greatly influenced. Figure 4.9 is contradictory to Sivrikaya and Togrol (2006), where it is observed that the friction stress is most significant at high stresses for normally consolidated soils under primary consolidation. The difference in findings is due to D/H 1.25 used by Sivrikaya and Togrol (2006) on overconsolidated soils and 10 D/H ratios utilised in this study on normally consolidated soils. Hence, it was proven that friction was reduced on average by 35% at all sample scales except at D/H 4 during the analysis using Sivrikaya and Togrol's (2006) derivation. This is because the Sivrikaya derivation is directly proportional to the stress and inversely proportional to sample scale. As shown in Table 3.4, the applied pressure is dependent on the sample scale.

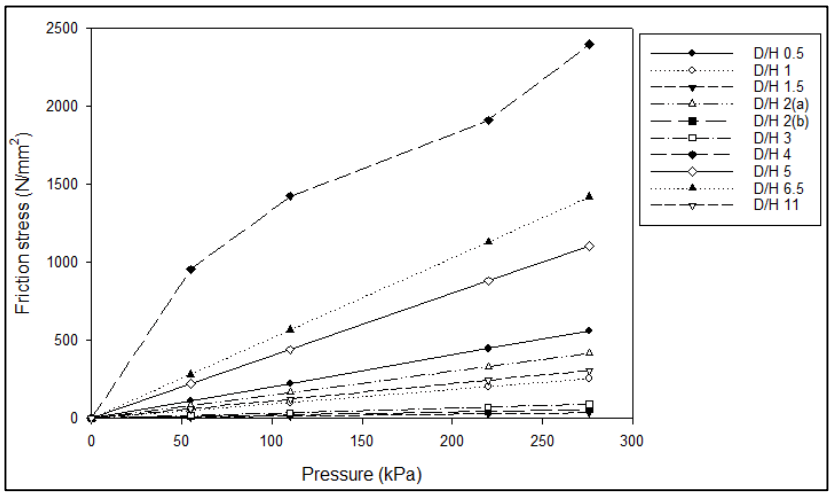

Figure 4-9: Frictional stresses at various D/H ratios (Rosine and Sabbagh, 2015)

A Pearson correlation was undertaken to assess the effect of the D/H ratio on c_v on Tests 7 to 16. Data was analysed in SPSS and showed a strong positive correlation between the D/H ratio and c_v with a correlation factor of 0.711. In this current study, the highest c_v value was observed at D/H 0.5 (Figure 4.10c) and the lowest at D/H 11, as shown in Figures 4.10a, b and c. Thus the value proposed by the American and British Standard is validated in this

study, where a D/H greater than 2 was found to yield a lower c_v value as compared to a D/H less than 2.

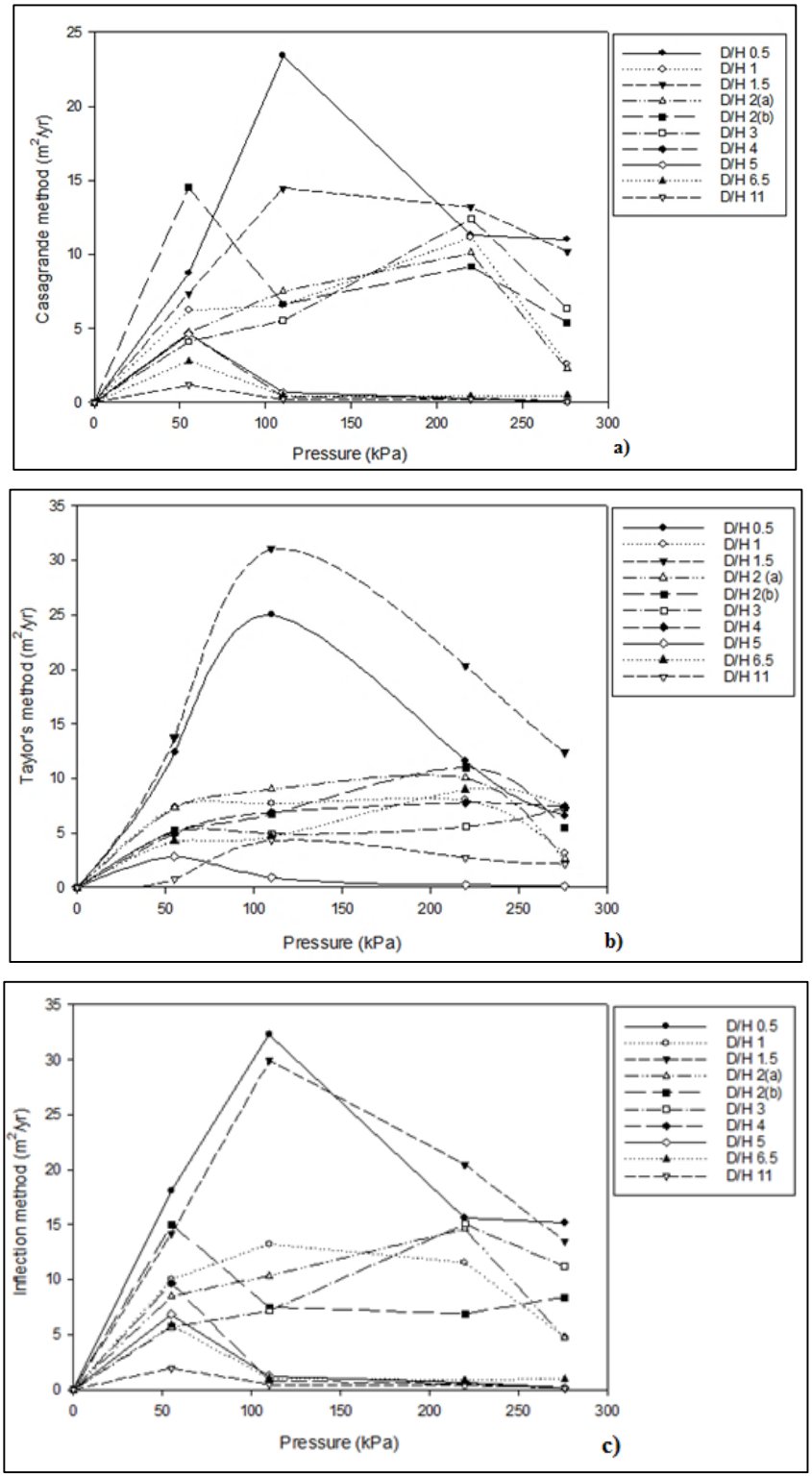

Figure 4-10: c_v relationship with applied pressure obtained at a) Casagrande method, b) Taylor's method and c) Inflection method (Rosine and Sabbagh, 2015)

4.5.6 Effect of initial moisture content on the compressibility parameters

The aim of this test was to evaluate the behaviour of the soil sample over a range of initial moisture contents. The series of tests and initial moisture contents are as shown in Test 21 from Table 3.10. Under Test 21, the initial moisture contents were 55%, 68%, 74% and 105%, which were prepared using the sample preparation procedure outlined in section 3.3.1.1. This analysis reflects the effect of the compressibility parameters in regions where moisture deficiency varies with the change in climate and roads, and the foundation drainage system failed. Thus, road and foundation moisture varies with the environment.

c_v values obtained were normally distributed, and there were no outliers. There was homogeneity in c_v value obtained between each method to a significance value of 0.01. Thus there was no significant difference in c_v values obtained from the three methods used with an important difference of 0.05. Using Pearson correlation, the initial moisture content and c_v had a moderate positive correlation of 0.546 at a significance level of 0.01. Figure 4.11 shows the relationship between the initial moisture content and c_v under load conditions ranging from 0 – 276kPa$\pm$3.7kPa. It was observed that at initial moisture content 105%, c_v increased steadily to a pressure of 220kPa$\pm$3.7kPa and gradually decreased at 276kPa$\pm$3.7kPa (Figure 4.11a). The opposite pattern behaviour occurred under Casagrande and Inflection methods, where a gradual increase was observed at initial moisture content 105% (Figure 4.11b and c). A reverse pattern was observed from 55% to 74% initial moisture content. This pattern is due to the rearrangement of the soil particles as the load increases.

Similarly, there was a small positive correlation between initial moisture content and compression index (c_c) and coefficient of volume compressibility (m_v) with correlation factors of 0.162 and 0.026 respectively. Thus, the findings showed that the effect of initial moisture content has a significant influence on c_c and m_v as compared to c_v. This results in a quick settlement after the application of the structured load. As the initial moisture content increases, m_v and c_c increase to 55kPa$\pm$3.7kPa and then gradually decrease (Figure 4.12). However, at 105%, there is a fluctuation with a rise at 55kPa$\pm$3.7kPa and 220kPa$\pm$3.7kPa and a reduction at 110kPa$\pm$3.7kPa and 276kPa$\pm$3.7kPa (Figures 4.12a and b). This shows a high compressibility as the value of m_v increases with an increase in initial moisture content at a given loading (Figure 4.12b). Also, the behaviour of the soils shows that the

more saturated the soils, the more prone the soil is to volume reduction for a particular incremental loading.

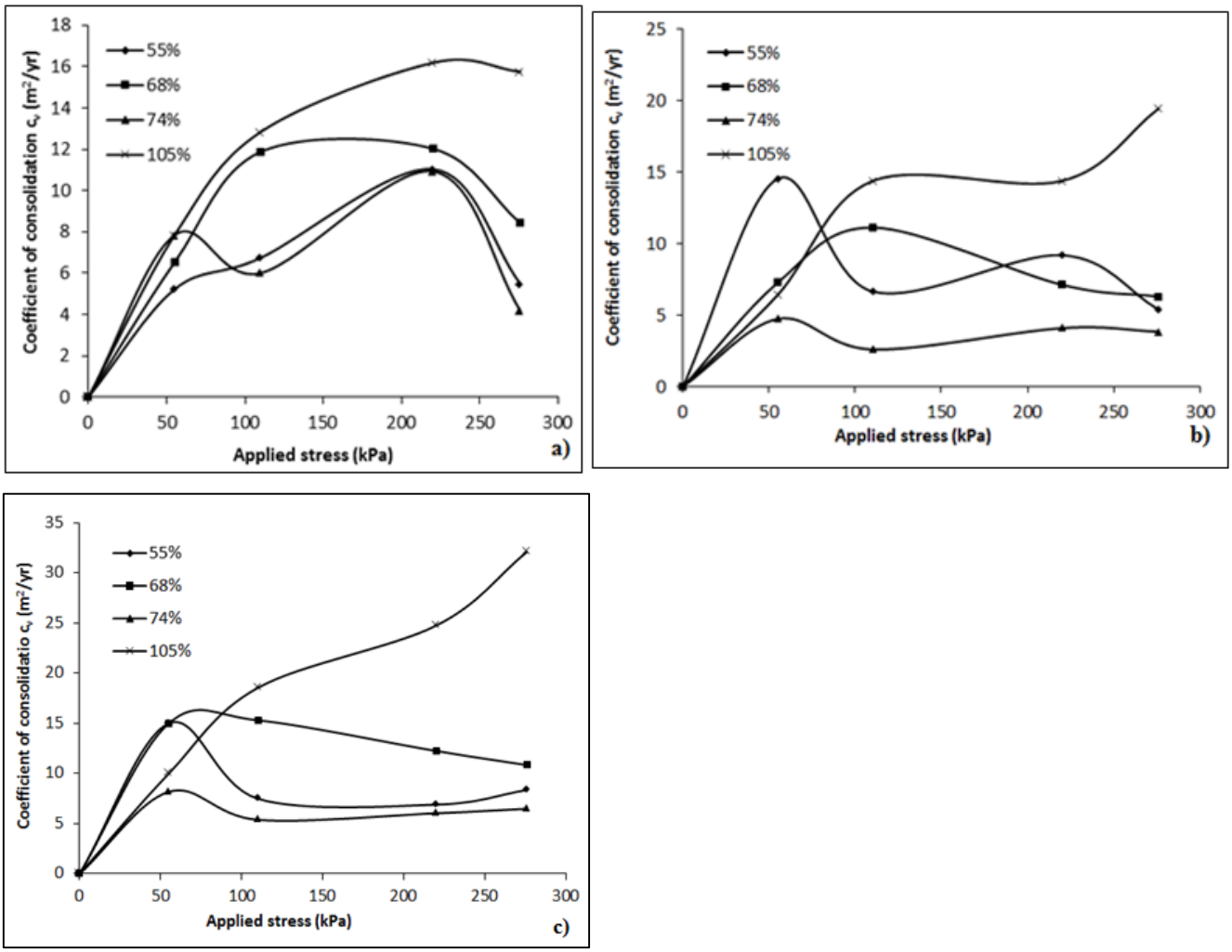

Figure 4-11: Effect of moisture content on c_v: a) Taylor's method, b) Casagrande and c) Inflection method

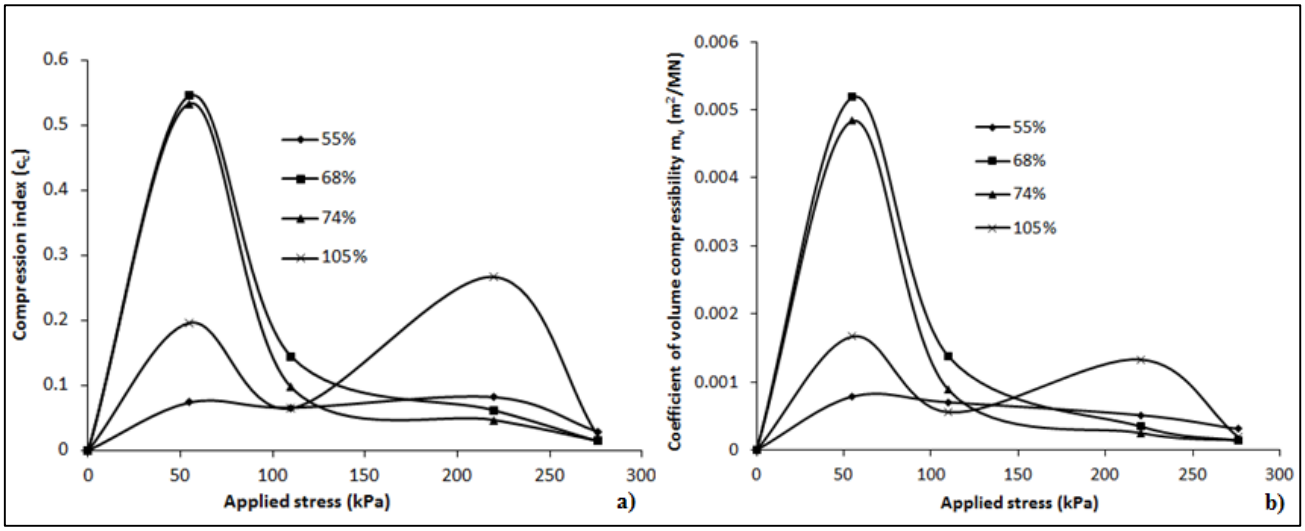

Figure 4-12: Effect of initial moisture content on a) c_c and b) m_v

4.5.7 Effect of time factor on c_v with sample scale

During the data analysis, uncertainty in obtaining c_v using the curve-fitting procedure was one of the main issues encountered. This uncertainty was due to the variety of the sample scale used for the scope of this study. It was mainly observed in Tests 18 and 20. The conventional consolidation test as described in the literature is conducted for 24 hours whereas a longer test is used on soil like peat. Ortega (1996), Conte and Troncone (2006) and Feng (2010) showed that the duration of the tests has an impact on the value of c_v. This finding was also observed in this study where comparable data were presented for soil tested under different time increments.

Tests 18 and 20 were established using identical soil samples and identical preparation methods, but one was tested over 7 days and a second sample over 24 hours at each load increment, using the relevant code of practice. As per section 4.5.1, it was observed that c_v was normally distributed, and there was no significant difference with load duration. There was a negative correlation between the loading time and the value of c_v with a correlation value of -0.309 (Figure 4.13). Thus, loading duration has a significant difference on c_v, which validates observations by Sridharan et al. (1994), Ortega (1996) and Feng (2010). Figure 4.13a at DS150H23 shows a maximum difference in c_v value of 95%; whereas in Figure 4.13b and 4.13c, similar c_v values were observed. On the other hand, at DS100H200, the trend in behaviour is similar in Figures 4.13a, b and c, with the highest value observed in Figure 4.13c. These observations were also noticed in section 4.5.1; and the discrepancy with Table 4.3 is due to sample scale.

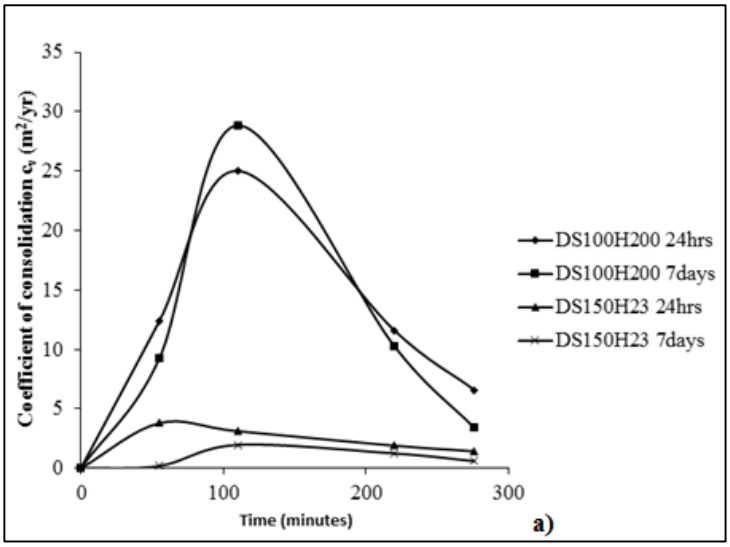

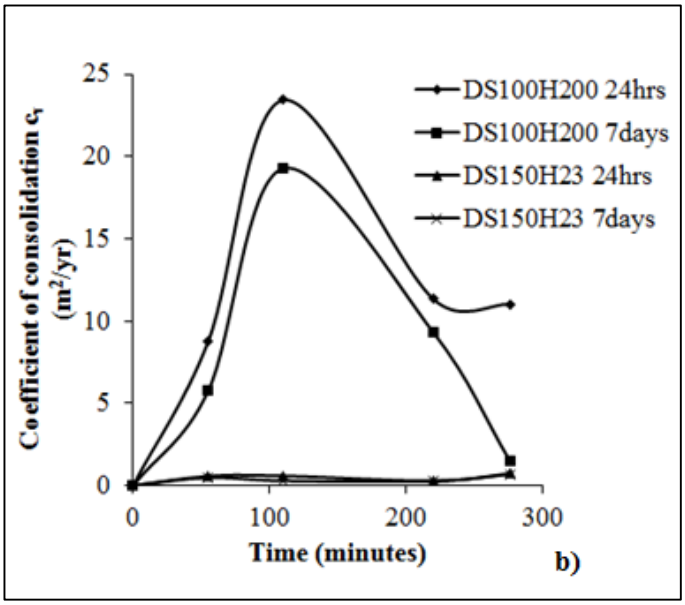

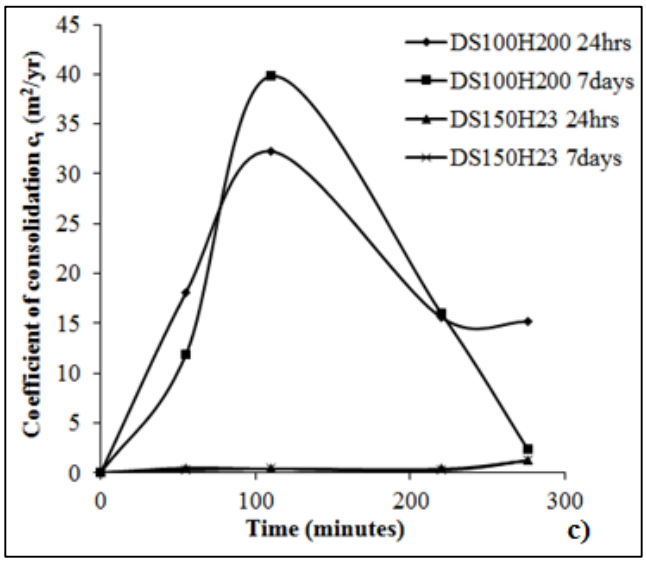

Figure 4-13: Effect of time factor of the coefficient of consolidation c_v; a) Taylor's method, b) Casagrande method and c) Inflection method

4.6 Chapter Summary

In this chapter, a series of single and double Oedometer tests were conducted on samples with different sample sizes, mineralogy, void ratios and initial moisture contents. From the compression curve, the influence of sample scale and initial moisture content on the compressibility parameters was observed. c_v values obtained using either the Casagrande, Taylor's or Inflection methods were found not to be significantly different. Thus, c_v values obtained using any of these methods are reliable. However, due to sample scale and incremental load duration, some experimental curves did not match the theoretical curve. This was mainly an issue when using the Casagrande and Inflection methods. Taylor's method was not greatly affected by sample scale and time factor.

The results also showed that c_v is dependent on soil thickness, which validates observations by previous researchers. In the current study, the effect of sample diameter was investigated on saturated clay without any sand drain (thus vertical drainage only experimentally); the result showed that sample diameter significantly influenced c_v. However, the outcome observed with the soil sample diameter on c_v is inconclusive, and further validation using finite element analysis is presented in the following chapters.

c_c and m_v were also found to be significantly influenced by sample scale, with a negative correlation of -0.161 and -0.172 under sample diameter scale, -0.006 and -0.045 under height scale, and 0.052 and 0.090 at sample D/H ratio. m_v was proven in the laboratory to fluctuate with an increase in pressure, which contradicted previous work where it was found to increase with a rise in pressure.

It was also observed experimentally that, as the initial moisture content increases, m_v and c_c both increase with a pressure of $55\text{kPa} \pm 3.7\text{kPa}$ and then decrease gradually. A similar trend in behaviour was observed by previous researchers such as Retnamony and Mether (1998), using different soil sample and preparation techniques.

The findings attained were expected, especially under the sample diameter scale. It is envisaged that, as the diameter scale increases, drainage should occur more horizontally than vertically. As a result, further analyses are required numerically under various drainage conditions to finalise the findings at this sample scale.

CHAPTER 5

NUMERICAL MODELLING

5.1 Introduction

The use of the modelling method is becoming common practice in geotechnical engineering when it is not practical or possible to use analytical solutions or develop new ones (Platt, 2013). The two most common numerical methods used in geotechnical engineerings are finite difference and finite element method. The finite element method (FEM) is usually more complex than the finite difference method and requires computer programmes to solve the matrices (Lenk, 2009). On the other hand, the finite difference method (FDM) is easy to implement and can be solved with a spreadsheet programme. The finite element method is used in this study to validate experimental data. This is carried out using PLAXIS 2D. An attempt at the application of the finite difference method is also presented.

5.2 Background

Since the development of the consolidation theory by Terzaghi (1943), numerous attempts have been made to derive solutions for the consolidation problem (Lekha et al., 2003). As mentioned in Lekha et al. (2003), Davis and Raymond (1965) obtained a solution for vertical consolidation assuming small strain and constant coefficient of consolidation and permeability. However, during consolidation, the coefficient of consolidation (c_v) varies as the coefficient of volume compressibility (m_v) and coefficient of permeability (k) change (Abbasi et al., 2007). Mesri and Rokhsar (1974) and Mesri and Choi (1985) solved governing differential equations numerically taking into account the effect of variable compressibility and permeability (Ying-Chun et al., 2005).

In addition to the numerical studies, the finite element method (FEM) has also been widely used in the analysis of soil behaviour. Lenk (2009) conducted a series of one-dimensional consolidation tests using the Oedometer apparatus to investigate time-dependent settlement in high-rise buildings for fully saturated clay. The investigation consisted of validating the experimental findings with the FEM. The FEM used was ANSYS 3D, modelled from a 4-node plane with 13 elements. Both the experimental data and the numerical modelling were

found to correlate well. Popa and Batali (2010) presented a finite element model for an embedded retaining wall and compared the results with the numerical analysis and experimental data. The finite element model was conducted using linear elastic, two nonlinear elastic-hardening models and a Mohr-Coulomb model. Each model was compared, and this revealed that the finite element model can lead to false results due to model complexity and a large number of parameters. It was also observed that the difference between the numerical and experimental results was reduced, and the Mohr-Coulomb model was less sensitive compared to the elasticity modulus. On the other hand, the hardening model showed a good correlation with the experimental data. PLAXIS 2D has been used by various researchers such as Aissa and Abdeldjalil (2013) and Wong (2013) in modelling soil behaviour. Aissa and Abdeldjalil (2013) modelled the behaviour of retaining walls stuck in the sand by subgrade reaction method. Both the experimental and numerical methods were compared and were found to correlate well. Wong (2013) modelled a single drainage line element under radial consolidation both with PLAXIS 2D and 3D and found that PLAXIS 3D yields comparably accurate results to 2D. The current study aimed at using PLAXIS 2D as the primary tool for the validation of the experimental data presented in the preceding chapters.

5.3 Finite Difference Method

It is necessary to adapt the two-dimensional consolidation theory to improve the one-dimensional consolidation theory (Tandjiria, 1999). Tandjiria (1999) presented the governing equation of the two dimension consolidation theory by Rendulic (1937) as follows:

$$\frac{du}{dt} = c_h \frac{\partial^2 u}{\partial r^2} + c_v \frac{\partial^2 u}{\partial z^2} \qquad (5\text{-}1)$$

Where:
u = Pore water pressure (kPa)
c_h = Coefficient of horizontal consolidation (m^2/yr)
c_v = Coefficient of consolidation (m^2/yr)
r = Radial distance to the centre of a drain well (mm)
z = Depth of soil (mm)

Equation 5.1 can be used to calculate the one-dimensional strain in conjunction with the dissipation of the excess pore water pressure (Tandjiria, 1999). c_h and c_v are obtained in the laboratory from the one-dimensional consolidation tests using either Taylor's, Casagrande or Inflection method, as depicted in chapter 4.

Assuming an element shown in Figure 5.1 having dimensions dx, dy and dz within a clay layer with thickness 2d, an element of total stress $\Delta\sigma$ is applied to the element (Naser, 2013). The flow velocity is given by Darcy's law as:

$$v_t = ki_t = -k\frac{\partial h}{\partial z} \quad (5\text{-}2)$$

Where:
k is the coefficient of permeability (m/s), ∂z is the change in soil depth (mm) and ∂h is the change in soil thickness (mm).

The rate of volume change can be expressed in terms of m_v as follows:

$$\frac{dV}{dt} = m_v \frac{\partial \sigma'}{\partial t} dxdydz \quad (5\text{-}3)$$

Where:
m_v is the coefficient of volume compressibility (m^2/MN) and σ' is the effective stress (kPa).

As the excess pore water pressure decreases, the total stress increment results in a gradual increase in effective stress (Naser, 2013). Thus, the rate of volume change can be expressed as:

$$\frac{dv}{dt} = -m_v \frac{\partial u}{\partial t} dxdydz \quad (5\text{-}4)$$

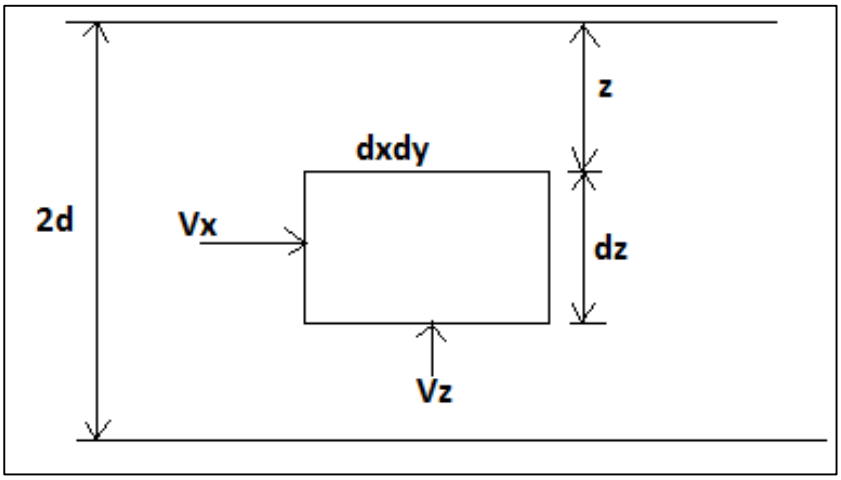

Figure 5-1: Element within a clay layer (Naser, 2013)

5.3.1 Theoretical application

The finite difference method (FDM) has been applied to several geotechnical problems (Tandjiria, 1999; Lai, 2004; Naser, 2013 and Ndiaye et al., 2014). This method has been proven accurate enough as long as the model meets the standard requirement of the consolidation process as presented in section 2.6. There are several ways to simplify a differential equation: forward, backward, central difference approximation and the fundamental difference approximation is the Taylor series (Tandjiria, 1999). Considering Figure 5.2, the corresponding node point's coordinate of the grids to the right is: x_i+h, x_i+2h, y_i+k, y_i+2k, y_i+nk and x_i+nh and to the left is: x_i-h, x_i-2h, y_i-k, y_i-2k, x_i-nh and y_i-nk (Lai, 2004). For convenience, the space between the node points along the x-axis is taken as uniform and equal to h, and along the y-axis is equal to k.

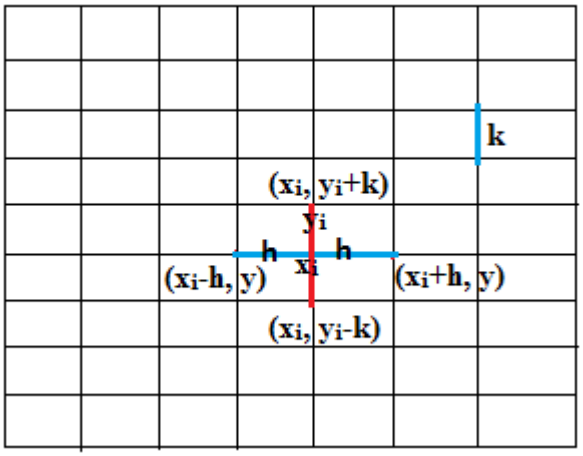

Figure 5-2: Point numbering on finite difference grid (Tandjiria, 1999)

5.3.1.1 Taylor's series

Taylor's series is an expansion of a function into a series of infinite terms. This function is used in the FDM analysis.

$$y_{i+1} = y_i + y_i'h + \frac{y_i''h^2}{2!} + \frac{y_i'''h^3}{3!} + O(h^4) \qquad (5\text{-}5)$$

5.3.1.2 Forward difference approximation

Within the forward difference approximation method, the symbol Δ is used to indicate the forward difference (Lai, 2004). By definition, the forward difference is defined as:

$$\Delta y_i = y_{i+1} - y_i \quad (5\text{-}6)$$

Equation 5.6 can be expressed as follows using the Taylor series solution:

$$\Delta y_i = \frac{h}{1!} y_i' + \frac{h^2}{2!} y_i'' + \ldots \quad (5\text{-}7)$$

Where; y_i' is $(\frac{dy_i}{dx})$ and y_i'' is $(\frac{d^2y_i}{dx})$.

Thus, from Equation 5.7, the first forward equation is written as:

$$y_i' = \frac{dy_i}{dx} = \frac{\Delta y_i}{h} = \frac{y_{i+1} - y_i}{h} \quad (5\text{-}8)$$

5.3.1.3 Backward difference approximation

The procedure used in obtaining the first forward difference approximation is used. The expression for the backward difference approximation is:

$$y_i' = \frac{y_i - (y_i - 1)}{h} \quad (5\text{-}9)$$

5.3.1.4 Central difference approximation

The central difference approximation method is generally used as it provide more accurate data with an accuracy of $O(h^3)$ (where $O(h^3)$ is a symbolic statement that the error involved is of the order h^3) (Lai, 2004). Thus, the first order central approximation equation is written as:

$$y_i' = \frac{y_i + 1 - y_i - 1}{2h} \quad (5\text{-}10)$$

Differentiating Equation 5.10, the second order central difference approximation equation is as follows:

$$y_i'' = \frac{y_i + 1 - 2y_i + y_i - 1}{h^2} \quad (5\text{-}11)$$

5.3.2 Finite difference method for one-dimensional consolidation tests under loading in double drainage conditions

The finite difference method (FDM) can be used to solve ordinary and partial differential equations by replacing the derivatives in an equation with their finite difference approximation (Platt, 2013). This process is used for one-dimensional consolidation tests, where the excess pore water pressure (u in kPa) depends on the elapsed time (t in secs) at the soil depth (z in mm). The assumptions made in deriving Terzaghi's theory are assumed to be valid. The differential equation to be solved is:

$$\frac{\partial u}{\partial t} = c_v \frac{\partial^2 u}{\partial z^2} \qquad (5\text{-}12)$$

Where;
c_v is the coefficient of consolidation (m^2/yr).

The rate of change of excess pore water pressure is approximated using the first forward difference equation (Equation 5.8) and the second partial derivative of the excess pore water pressure with respect to depth is approximated using the second central differential equation (Equation 5.11) (Lai, 2004). Therefore, Equation 5.12 can then be written as:

$$\frac{u_{z,t+\Delta t} - u_{z,t}}{\Delta t} = c_v \frac{u_{z+\Delta z,t} - 2u_{z,t} + u_{z-\Delta z,t}}{(\Delta z)^2} \qquad (5\text{-}13)$$

$$\frac{u_{i,j+1} - u_{i,j}}{\Delta t} = c_v \frac{u_{i+1,j} - 2u_{i.j} + u_{i-1,j}}{(\Delta z)^2} \qquad (5\text{-}14)$$

Where;
Δt is the time step (secs), and Δz is the depth increment (mm)

Equation 5.13 is used for hand calculation; while Equation 5.14 is used for solutions obtained using a digital computer (Lai, 2004). Equation 5.15 is obtained when solving the term $u_{z,t+\Delta t}$ from equation 5.13.

$$u_{z,t+\Delta t} = u_{z,t} + \frac{c_v \Delta t}{(\Delta z)^2} (u_{z-\Delta z,t} - 2u_{z,t} + u_{z+\Delta z,t}) \qquad (5\text{-}15)$$

The term $c_v \Delta t/(\Delta z)^2$ is usually replaced by α to simplify both writing and discussion. Platt (2013) stated that, according to Andersland and Al-Khafaji (1992), previous research showed that α needs to be less than 0.5 for Equation 5.14 to be numerically stable and the

most accurate results are obtained when α is equal to 1/6. According to Equation 5.15, if the pore water pressure is known at time t and point z, and just below and above z, then the pore water pressure can be calculated at point z at a time Δt (Platt, 2013). Thus, Equation 5.15 is term the forward-central equation. In order to derive the central equation for more accurate values, both the first and second order of Equation 5.12 is substituted using the first and second order of the central approximation equation. Hence, Equation 5.12 can be rewritten as:

$$\frac{u_{i,j+1}-u_{i,j-1}}{2t} = c_v \frac{u_{i+1,j}-2u_{i.j}+u_{i-1,j}}{(\Delta z)^2} \quad (5\text{-}16)$$

$$\frac{u_{z,t+\Delta t}-u_{z,t-\Delta t}}{2t} = c_v \frac{u_{z+\Delta z,t}-2u_{z,t}+u_{z-\Delta z,t}}{(\Delta z)^2} \quad (5\text{-}17)$$

Solving for $u_{i,j+1}$ from Equation 5.16 gives the following:

$$u_{i,j+1} = 2\left(\frac{tc_v}{z^2}\right)[u_{i+1,j} - 2_{i,j} + u_{i-1,j}] + u_{i,j-1} \quad (5\text{-}18)$$

Where:
tc_v/z^2 is replaced by α with a value ranging from 0 to 0.5 for accuracy.

5.3.3 Finite difference solution

Equation 5.12 was applied in the current study using the central approximation method (Equation 5.18), and forward-central difference method (Equation 5.15). It was found by Lai (2004) that successive application of Equation 5.15 soon leads to a divergence in excess pore pressure if α exceeds 0.5. During the analysis of the FDM, c_v was assumed to be constant, and α was taken to be 0.25. The excess pore pressure at the interior node (Figure 5.3) is calculated using Equations 5.15 and 5.18, which are shown in Tables 5.1 and 5.2 respectively. The calculated values from Tables 5.1 and 5.2 are plotted in Figures 5.4a and b. Under the top and bottom boundary conditions, excess pore pressure is zero where drainage is allowed. Figure 5.3 displays the node points used in the calculation. At time zero, the excess pore pressure was taken to be 55kPa with an average initial excess pore pressure of 27.5kPa (these values are taken from the experimental loading derivations in Chapter 4). Δz was taken to be 0.2 to simplify the hand calculation. Therefore, $\Delta T = \alpha \Delta z^2 = 0.01$, as shown in Tables 5.1 and 5.2.

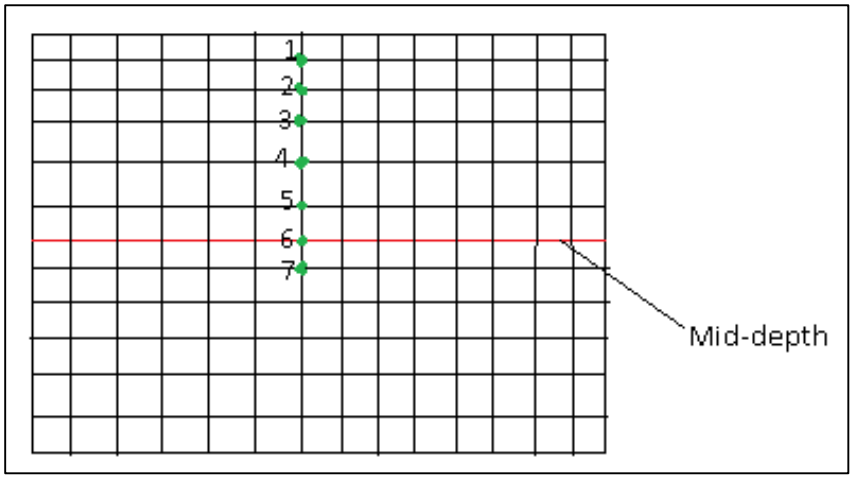

Figure 5-3: Node points used in the FDM calculations

Table 5-1: Forward Central approximation pore pressure hand calculation

T	**0**	**0.01**	**0.02**	**0.03**	**0.04**	**0.05**	**0.06**	**0.07**	**0.08**	**0.09**	**0.1**
$\Delta T/\Delta z^2$	0	0.25	0.5	0.75	1.00	1.25	1.50	1.75	2.00	2.25	2.50
Node 1	27.5	0.0	0.0	0.0	0.0	0.0	0.0	0.0	0.0	0.0	0.0
2	55.0	48.1	36.0	22.5	11.2	4.2	1.0	0.1	0.0	0.0	0.0
3	55.0	55.0	41.2	25.7	12.8	4.8	1.2	0.1	0.0	0.0	0.0
4	55.0	55.0	55.0	34.3	17.1	6.4	1.6	0.2	0.0	0.0	0.0
5	55.0	55.0	55.0	55.0	55.0	20.6	5.1	0.6	0.0	0.0	0.0
6	55.0	55.0	55.0	55.0	55.0	55.0	55.0	6.8	0.0	0.0	0.0
7	55.0	55.0	55.0	55.0	55.0	20.6	5.1	0.6	0.0	0.0	0.0

Table 5-2: Central approximation pore pressure hand calculation

T	**0**	**0.01**	**0.02**	**0.03**	**0.04**	**0.05**	**0.06**	**0.07**	**0.08**	**0.09**	**0.1**
$\Delta T/\Delta z^2$	0	0.25	0.50	0.75	1.00	1.25	1.50	1.75	2.00	2.25	2.50
Node 1	27.5	0.0	0.0	0.0	0.0	0.0	0.0	0.0	0.0	0.0	0.0
2	55.0	41.2	20.6	5.1	0.0	0.0	0.0	0.0	0.0	0.0	0.0
3	55.0	55.0	27.5	6.8	0.0	0.0	0.0	0.0	0.0	0.0	0.0
4	55.0	55.0	55.0	13.7	0.0	0.0	0.0	0.0	0.0	0.0	0.0
5	55.0	55.0	55.0	55.0	55.0	-13.7	6.8	-5.1	5.1	-6.4	9.6
6	55.0	55.0	55.0	55.0	55.0	55.0	55.0	-41.2	41.2	-51.5	77.3
7	55.0	55.0	55.0	55.0	55.0	-13.7	6.8	-5.1	5.1	-6.4	9.6

From Tables 5.1 and 5.2, at time zero the excess pore pressure is 55kPa excess at the boundaries, where it is concurrently 55 and 0kPa. When the pore pressure is increased to 110kPa, 220kPa and 276kPa, similar patterns were observed. From Table 5.1, Figure 5.4a is taken, which presents real trends to the theoretical curve as expected. Figure 5.4a demonstrates the applicability of the forward-central approximation in one-dimensional consolidation test. This outcome was also depicted in Lai (2004).

In the case of double drainage, the excess pore pressure takes place at the soil mid-depth. Below the mid-depth, the soil behaviour is symmetrical to that above the mid-depth. From Figure 5.3, node 6 represents the centre of the soil where the maximum excess pore pressure is expected. It was noticed that nodes 5 and 7 produce identical results, which confirms the symmetrical behaviour of the soils after the mid-depth. Therefore, the excess pore pressure was only calculated up to node 7. The maximum excess pore pressure was observed as 55kPa using the forward-central approximation equation (Figure 5.4a) while the central approximation equation was at 65kPa (Figure 5.4b). Hence, the forward-central equation for excess pore pressure is identical to the applied external load that was expected. Theoretically, as the load is applied this is equal to the excess pore pressure. As time goes by, the excess pore pressure decreases, with an increase in effective stress. The excess pore pressure is then transferred, to become the effective stress. However, the central approximation produced shows a 15% increase in excess pore pressure (Figure 5.4b). The central approximation equation also shows variability in the excess pore pressure approaching the soil mid-depth. The negative excess pore pressure shows that the soil is swelling, which is a reverse process of the consolidation taking place in the current study. Thus, Equations 5.15 and 5.18 are not applicable to this study.

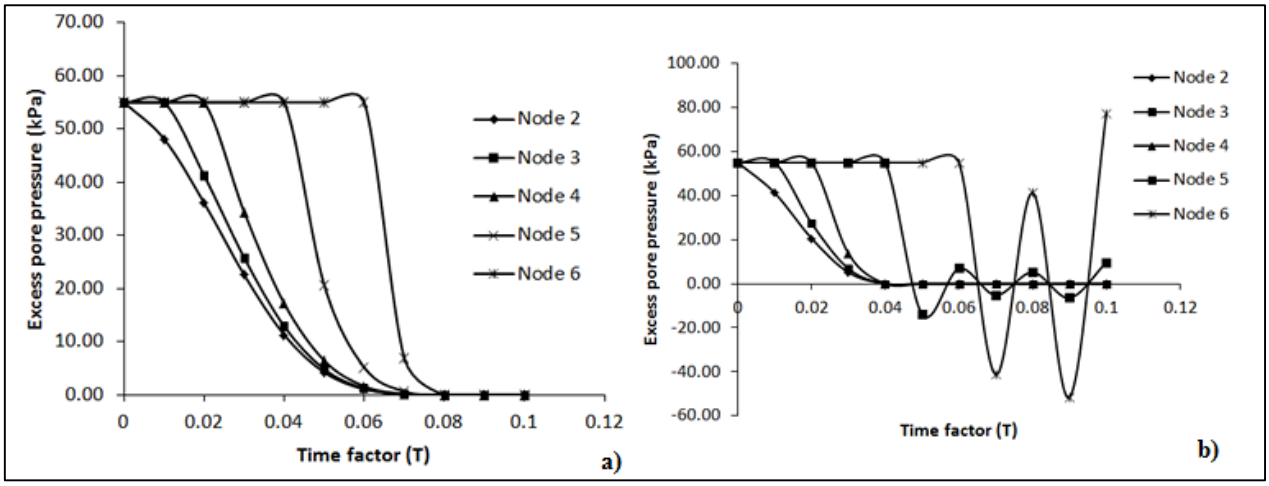

Figure 5-4: FDM hand calculated excess pore pressure using; a) Forward central approximation and b) central approximation

5.4 Finite Element Method

The proficiency in predicting the excess pore pressure is important in evaluating the behaviour of structures, especially those founded on fine-grained soils at various scales. The FDM used has been shown not to be appropriate, due to the negative excess pore pressure observed, as explained in Section 5.3.3. Consequently, the finite element method (FEM) was employed using PLAXIS 2D. PLAXIS 2D was used to validate the experimental data obtained from the Oedometer apparatus. The validation was achieved by employing the Mohr-Coulomb model. According to Brinkgreve (2013), validation is the process of determining the degree to which a model (including the parameters selected for that model) is an accurate representation of the actual model (Nafems and ASME, 2009). The validation process involved using parameters obtained in the laboratory, with some parameters such as the Young's Modulus of elasticity (E) and coefficient of permeability (k) being assumed.

Consolidation tests in PLAXIS are modelled primarily by using the coefficient of permeability (k). Therefore, it is vital that the correct value be assumed and/or calculated. The FEM was conducted using the following steps:

1. The estimated coefficient of permeability (k_e): while inputting the measured parameters such as the void ratio, PLAXIS 2D generated a default coefficient of permeability that was labelled as k_e. This value was constant through all the sample scales, and the soil behaviour was modelled and analysed in terms of the excess pore pressure (u_{excess}).

2. Calculated coefficients of permeability (k_c): These were calculated using Equations 2.9 and 2.10 and were labelled k_c^1 and k_c^2 respectively. The outcome of the model was then compared with that obtained using k_e. This was calculated instead of being measured, due to lack of equipment in the laboratory. However, the values obtained fell within the range of values for fine-grained soils shown in Table A.5 in appendix A.

3. The sample diameter scale was modelled in different drainage scenarios using both k_c and k_e values. One of the advantages of using k_c was that it benefitted from the measured c_v, void ratio (e) and particle grain size (d_{10}).

4. The FEM was compared with the experimental data.

Steps 1 to 4 are presented in Chapter 6.

5.4.1 Basic Mohr-Coulomb model

The Mohr-Coulomb model is an elastic-perfectly plastic model that is often used to model soil behaviour and serves as a first order model (Ti et al., 2009). In the typical stress state, the model stress-strain behaves linearly in the elastic range with two defining parameters of Hooke's law (Young's modulus, E and Poisson's ratio, ν). The failure criterion is defined by two parameters: the friction angle, φ and cohesion, c; and also a parameter to describe the flow rule, the dilatancy angle, ψ (Ti et al., 2009). The Mohr-Coulomb model has been widely used for the analysis of soil behaviour due to its simplicity. It is also applied to a three-dimensional stress model.

5.4.2 Model uncertainties

Uncertainties and lack of parameters play an influential role in modelling the soil behaviour. The numerical model involves several components that introduce approximations and errors. It is essential that these components be analysed in detail for their role and contribution to the incongruity as a whole. The identification of the possible individual inconsistency will give an understanding and opportunity to improve the model. It also enables the quantification of variation of the design quantities by considering parameters' uncertainties and their possible value ranges. A summary of the main discrepancy in the FEM is given below.

5.4.2.1 Coefficient of permeability

During the analysis, the coefficient of permeability was assumed to be constant. The estimated coefficient of permeability (k_e) employed in PLAXIS had a value of $5.5x10^{-7}$ m/s. The k_e value in PLAXIS was obtained using the inputted initial void ratio. Due to limited equipment availability, the coefficient of permeability was not measured in the laboratory during the consolidation test at each load increment. This provides some degree of uncertainty and discrepancy in the values obtained. Theoretically, the coefficient of permeability (k) is not constant during consolidation and varies at each loading increment. Moreover, k can also be derived using equations A.9, A.10 and A.11. The calculated k_c values are shown in Table 5.3.

Table 5-3: Calculated coefficient of permeability for D/H ratio scale

Scale	D/H 0.5	D/H 1	D/H 1.5	D/H 2(a)	D/H 2(b)	D/H 3	D/H 4	D/H 5	D/H 6.5	D/H 11
k_c^1	1.28	0.61	0.67	0.52	0.60	0.14	0.71	0.29	0.35	0.35
k_c^2	0.023	0.00094	0.00064	0.00019	0.00012	0.00024	0.00072	0.00045	0.00041	0.00014

Where:

k_c^1 is the coefficient of permeability ($x10^{-6}$), and k_c^2 is the coefficient of permeability ($x10^{-9}$)

The k_c values presented in Table 5.3 fall within the range of values for fine-grained soils to vary from 10^{-7} to 10^{-9} m/s, as depicted in Table 2.3.

5.4.2.2 Coefficient of consolidation

The coefficient of consolidation (c_v) is a time-dependent parameter and also dependent on the sample scale as observed experimentally in Chapter 4. The value of c_v was found to vary tremendously at each load increment depending on the sample scale and was assumed to be constant. To facilitate the calculation of k_c^2, an average c_v value was used for Taylor's method. Taylor's method was chosen as it was proven experimentally (in Chapter 4) that it produced consistent results as compared to the Casagrande and inflection methods due to the sample scale factor, as explained in section 4.5.

5.4.2.3 Void ratio

The coefficient of permeability (k) varies with the void ratio (e). The greater the void ratio, the greater the coefficient of permeability (Equation 2.9). In the current study, kaolin clay

was used at an initial moisture content ranging from 55% to 105% and void ratio 1.2 to 2.5. The variation in void ratio was affected by the ratio of the sample scale with the applied pressure. This is because irrespective of the soil water content, the rate at which water flows out of the soil sample will depend on the soil mineralogy, sample scale and the ratio of the load to the sample scale. These factors significantly influence the void ratio resulting after the preconsolidation pressure has been exerted on the soil matrix. As a result, the void ratio obtained during the one-dimensional consolidation test under vertical drainage was assumed as constant during the simulation analysis in PLAXIS under various drainage scenarios (refer to Chapter 6).

5.5 Chapter Summary

Chapter 5 has presented a brief introduction to the numerical modelling and the analytical model used in the study. An attempt at implementing the finite difference method has been shown to be problematic using the central approximation method. The central approximation showed a reverse behaviour when reaching the soil mid-depth that does not represent the experimental investigation. On the other hand, the forward-central approximation was deemed precise, as the curve matches the theoretical curve, most particularly that of the Casagrande and Inflection method. An insight into the finite element method was presented. An uncertainty in the input parameters was explained by the assumptions made.

The expected behaviour of the soil under double drainage was observed using the forward-central approximation where the soil is symmetrical. It was also projected that the maximum excess pore pressure will occur at the mid-depth of the soil matrix. This was not observed using the forward-central equation but was nearly observed with the central approximation equation. The term ‘nearly’ is used because of the fluctuation in the excess pore pressure and negative value discerned. Thus, both equations do not clearly illustrate the exact full behaviour of the soil in the current study. As a result, the finite element method was implemented, as shown in more detail in Chapter 6.

CHAPTER 6

FINITE ELEMENT MODEL AND COMPARISON WITH EXPERIMENTAL STUDY

6.1 Overview

Due to the failure of the finite difference method attempted in Chapter 5, the finite element method was chosen as the validation software. As a result, PLAXIS 2D was selected due to its simplicity and easy applicability to one-dimensional consolidation tests. Hence, this chapter incorporates the ratification of the data presented in Chapter 4 using PLAXIS 2D. Detailed descriptions of the ratification of the experimental results are presented. The illustration is presented in terms of sample height scale, D/H ratio scale and sample diameter scale. The finite element (FE) analysis is shown in terms of the excess pore pressure (u_{excess}) observed, and the numerical trends are compared with that obtained experimentally. During the consolidation modelling aspect in PLAXIS 2D, the coefficient of permeability is a key factor. Therefore, values presented in Table 5.3 are used during the simulation.

The simulation in PLAXIS 2D is achieved in the following manner:

- Modelling strategy
- Excess pore pressure
- Mesh geometry
- Calculation phases
- Calibration of the finite element model
- Sample height scale
- D/H ratio scale
- Sample diameter scale (Vertical drainage only)
- Sample diameter scale (Horizontal drainage)
- Sample diameter scale (Vertical and horizontal drainage)
- Chapter Summary

6.2 Modelling Strategy

It is fundamentally necessary to generate the finite element model that will reasonably capture the performance of the soil behaviour under one-dimensional consolidation. The following steps were followed during the input process in PLAXIS:

1. Finite element model layout: A sample scale model was drawn in PLAXIS using an axisymmetric model with 15 nodes for better accuracy. The model included a single clay layer with thickness varying depending on the sample scale used, and properties were as shown in Tables 6.1 and 6.2.
2. Drainage conditions: Three drainage scenarios were considered; firstly vertical drainage only, secondly horizontal drainage only without the use of sand drains, and thirdly both vertical and horizontal. This was achieved using the sample diameter scale for a broader understanding of the water movement within the soil matrix under loading as the soil diameter increases.
3. Mesh quality: the mesh was generated using a coarse mesh. However, additional observations were also presented using the fine mesh, and the results were compared.
4. Soil parameters: Appropriate selection was taken from laboratory tests and some parameters were estimated such as Young's modulus of elasticity. From the laboratory parameters, the coefficient of permeability was calculated as shown in Table 5.3 and the saturated unit weight was calculated using Equation 6.1. Once the parameters are selected, these were input in PLAXIS 2D, and the model type Mohr-Coulomb (MC) was selected under undrained conditions. The average initial moisture content was used to facilitate a comparison between each sample scale.

$$\gamma_{sat} = \frac{(G_s+e)*\gamma_w}{1+e} \qquad (6\text{-}1)$$

Where:
G_s is the specific gravity, e is void ratio, and γ_w is the unit weight of water (kN/m^3).

5. Construction stages: the construction stages are selected according to the consolidation process and model type used. The running time duration per stages is 24 hours. The initial condition occurs where zero initial stress is generated by using the K0 procedure where ΣMweight (total multiplier of the material weight) is equal to zero. The material weight as specified by the unit weight of the material is specified. At the remaining calculation phase, ΣMweight remains at the default value 1. The distributed load is

activated in a separate phase (phase 1) where the calculation phase is plastic analysis. The ‘reset displacement to zero’ and ‘update mesh’ is selected. One consolidation test with minimum excess pore pressure is performed with a duration of 24hours each. A default value of 0.01 is taken for the tolerated error.

6. Another calculation stage was conducted where there was no plastic analysis, and only two phases were present. The initial condition and consolidation analysis was made with minimum excess pore pressure. Results were compared with those of point 5.

Table 6-1: Sample Height and Diameter scale parameters for the finite element model

Scales/ Parameters	HS80D250	HS130D250	HS200D250	HS80D150	HS23D150	HS30D150	HS130D150	DS100H23	DS150H23	DS250H23	DS100H200	DS250H200	DS250H30	DS150H30
γ_{sat}	17.0	15.4	14.4	15.2	15.7	15.9	15.0	17.3	15.7	15.8	14.2	14.4	15.4	15.0
e_i	1.2	1.9	2.0	1.8	1.6	1.5	1.9	2.0	1.6	1.6	2.5	2.0	1.9	1.9
c_u	12	12	12	12	12	12	12	12	12	12	12	12	12	12
w_i	55	55	55	65	59	60	74	67.5	67.5	67.5	91	55	55	74

Where:

w_i = initial moisture content (%), e_i = initial void ratio, c_u = undrained shear strength (kN/m^2) and γ_{sat} = saturated unit weight (kN/m^3)

Table 6-2: Sample D/H ratio scale properties used in the finite element model (Rosine and Sabbagh, 2015)

Scale	D/H 0.5	D/H 1	D/H 1.5	D/H 2(a)	D/H 2(b)	D/H 3	D/H 4	D/H 5	D/H 6.5	D/H 11
e_i	2.53	2.49	2.43	1.88	1.97	1.20	2.09	1.50	1.65	1.61
c_u	12.00	12.00	12.00	12.00	12.00	12.00	12.00	12.00	12.00	12.00
γ_{sat}	14.33	15.00	14.40	15.20	15.40	17.00	17.30	15.90	15.70	15.8
w_i	91%	74%	55%	65%	55%	55%	80%	60%	59%	64%

Where:

w_i = initial moisture content (%), e_i = initial void ratio, c_u = undrained shear strength (kN/m^2) and γ_{sat} = saturated unit weight (kN/m^3)

6.3 Excess pore pressure

Most consolidation tests deal with the application of external loads. The application of the external load gives a more realistic result as it shows the in-situ behaviour of the soil. As the load is applied, settlement takes place as the excess pore pressure is being dissipated. Data presented from the FEM are shown in terms of the excess pore pressure. The applied pressure is predicted to be similar to the excess pore pressure as depicted in Chapter 5. During the consolidation analysis, the load is applied vertically to the soil matrix producing lesser settlement as the load increases. In PLAXIS, to apply a vertical load, a negative load (Figure 6.1a, b) is used while a positive value represent horizontal loading (Figure 6.1c, d) as shown in Figure 6.1. Thus, the negative excess pore pressure presented henceforth only represents the direction of loading (vertically).

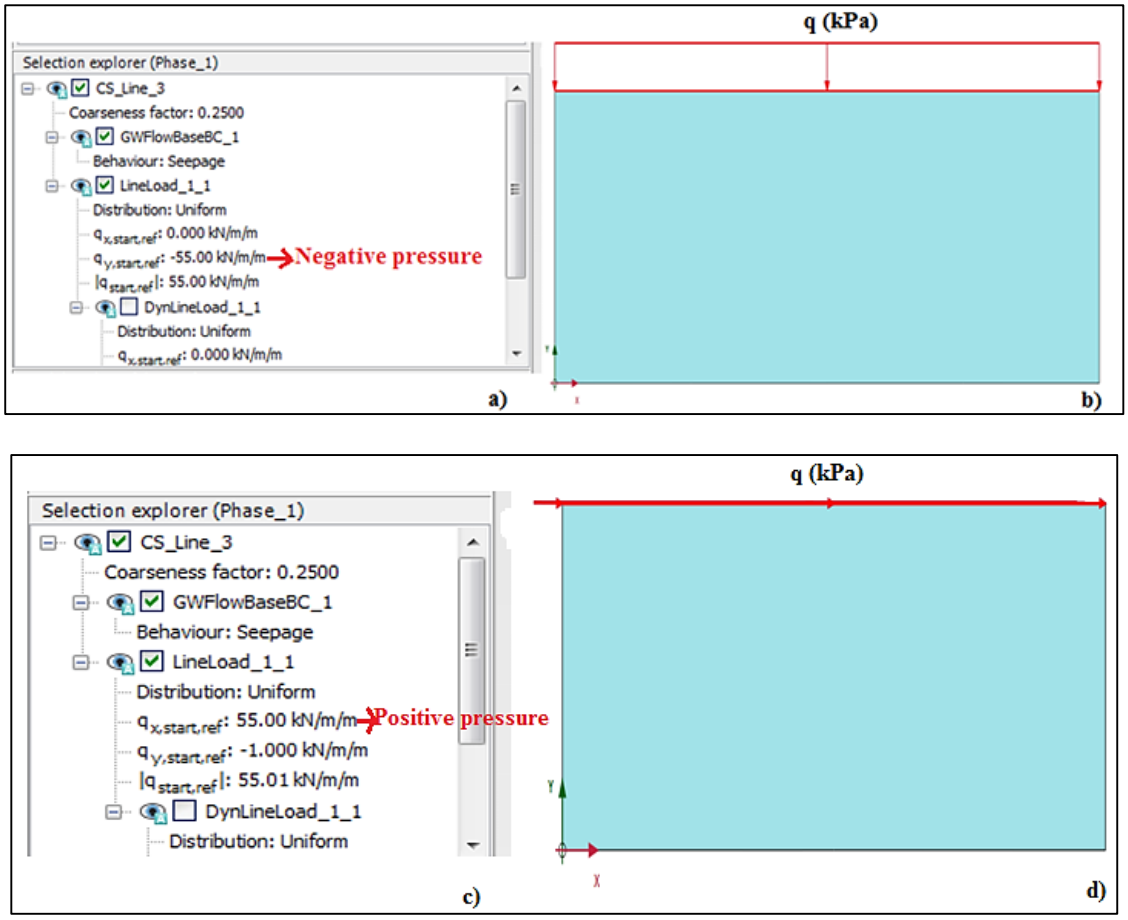

Figure 6-1: PLAXIS screen shot of loading directions; a and b) negative pressure and c and d) positive pressure

6.4 Mesh Geometry

6.4.1 Background

The finite element method (FEM) is a very powerful and versatile analysis tool, but its effectiveness is in the mesh generation, which is time-consuming when done manually (Le, 1988). In some cases, mesh generated automatically are not well-shaped and need to be smoothed. This is achieved using mesh refinement within the computer programme. Mesh refinement involves subdividing some elements into smaller elements while others remain unchanged. In most FEM software, meshes are required to be conforming where adjacent elements share a whole edge or an entire face (as depicted in Figure 5.3). Meshes are mostly composed of triangular or tetrahedral shapes, which are easily conformed and refined. For triangular mesh refinement, a triangle can be divided into two smaller ones by bisecting the longest side (Le, 1988). Various mesh sizes can be generated such as coarse, medium coarse, fine and very fine.

It was previously observed by researchers such as Fonte (2010) and Dey (2011) that coarse meshes do not capture failure mechanics using a complex model as compared to fine meshes which clearly show the failure mechanisms. In the current study, coarse mesh captures the soil failure due to the simplicity of the model. Fine meshes tend to cause the execution time of the model to become very lengthy, compared to coarse mesh whose execution time is rapid (Dey, 2011).

6.4.2 Mesh generation

When the model geometry is completed with all the input parameters, the geometry is then discretised into finite elements. The composition of the finite elements are called “mesh” (PLAXIS, 2011). There are two types of mesh elements: 15-Node triangular elements and the 6-Node triangular elements. In PLAXIS 2D, the generation of the mesh is automatic with options for global and local mesh refinement. This mesh generation is based on a robust triangular procedure and the input geometry model (Dey, 2011). Meshes generated in PLAXIS may not be sufficiently accurate to produce acceptable numerical results. If necessary, meshes could be enhanced by using global and local refinement options. The 15-node elements mesh produces a finer distribution of nodes, and thus more accurate results than the 6-node elements (Figure 6.2). On the other hand, the use of 15-node elements is more time consuming than 6-node elements.

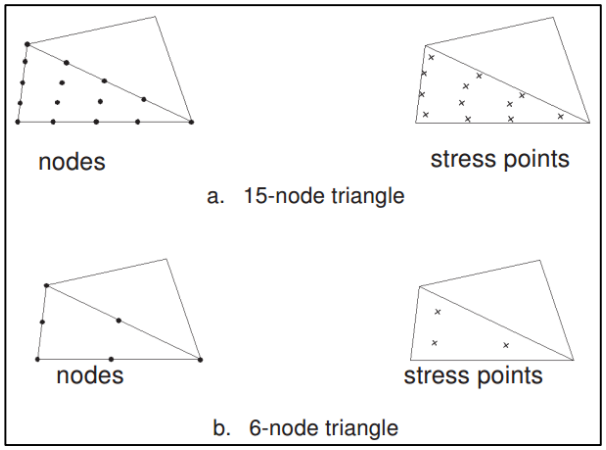

Figure 6-2: Position of nodes and stress points in a soil element (PLAXIS, 2011)

The mesh dependency on sample scale was studied using two meshes: coarse and fine mesh, with their properties shown in Table 6.3. For each mesh, a 15-noded axisymmetric model was used. It was envisaged that due to the simplicity of the current study model, the meshing type would not be of great significance to the soil behaviour. The simulation analysis was

conducted in three calculation phases after the mesh generation. The phases included initial condition, plastic and consolidation conditions at 55kPa external load. Data presented in Figures 6.3 and 6.4 are for sample height and diameter scale, which also correspond to the sample D/H ratio. The average element size varies tremendously with sample scale, especially at DS250H23 under the coarse mesh as compared to DS150H23 and DS100H23. This variation shows the importance of the mesh at sample diameter scale. At the sample height and D/H ratio scale, the variation in mesh element size is insignificant.

Table 6-3: Mesh properties

Sample scales	Coarse			Fine		
	No of element	No of nodes	Average element size	No of element	No of nodes	Average element size
HS80D250	398	3333	7.09m	1287	10591	3.94m
HS130D250	459	3827	8.41m	1721	14075	4.35m
HS200D250	517	4291	9.83m	1986	16201	5.02m
HS80D150	847	6975	3.76m	3206	26045	1.93m
HS23D150	70	637	7.02m	198	1701	4.17m
HS30D150	405	3415	3.33m	1494	12297	1.74m
HS130D150	983	8071	4.45m	3934	31885	2.23m
DS100H23	68	605	5.82m	282	2377	2.85m
DS250H23	24	245	15.48m	102	925	7.51m
DS100H200	434	3613	6.79m	1526	12485	3.62m

Due to the drainage condition being double where the soil is allowed to drain from top and bottom of the soil matrix, the excess pore pressure occurs at the mid-depth of the soil. Thus, Figures 6.3, 6.4 and 6.5 show the relationship between coarse and fine mesh at the soil mid-depth for sample height and diameter scale. Fine mesh produces high volume change as compared to coarse mesh with a percentage difference of 7%, 31%, 7%, 26%, 17%, 2%, 13% and 8% for HS23D250, HS80D250, HS130D250, HS200D250, HS80D150, HS23D150, HS30D150 and HS130D150 respectively. The significant difference in soil behaviour is due to sample scale, where at HS23D250, HS130D250, HS23D150 and HS130D150 no significant difference between the coarse and fine mesh is observed.

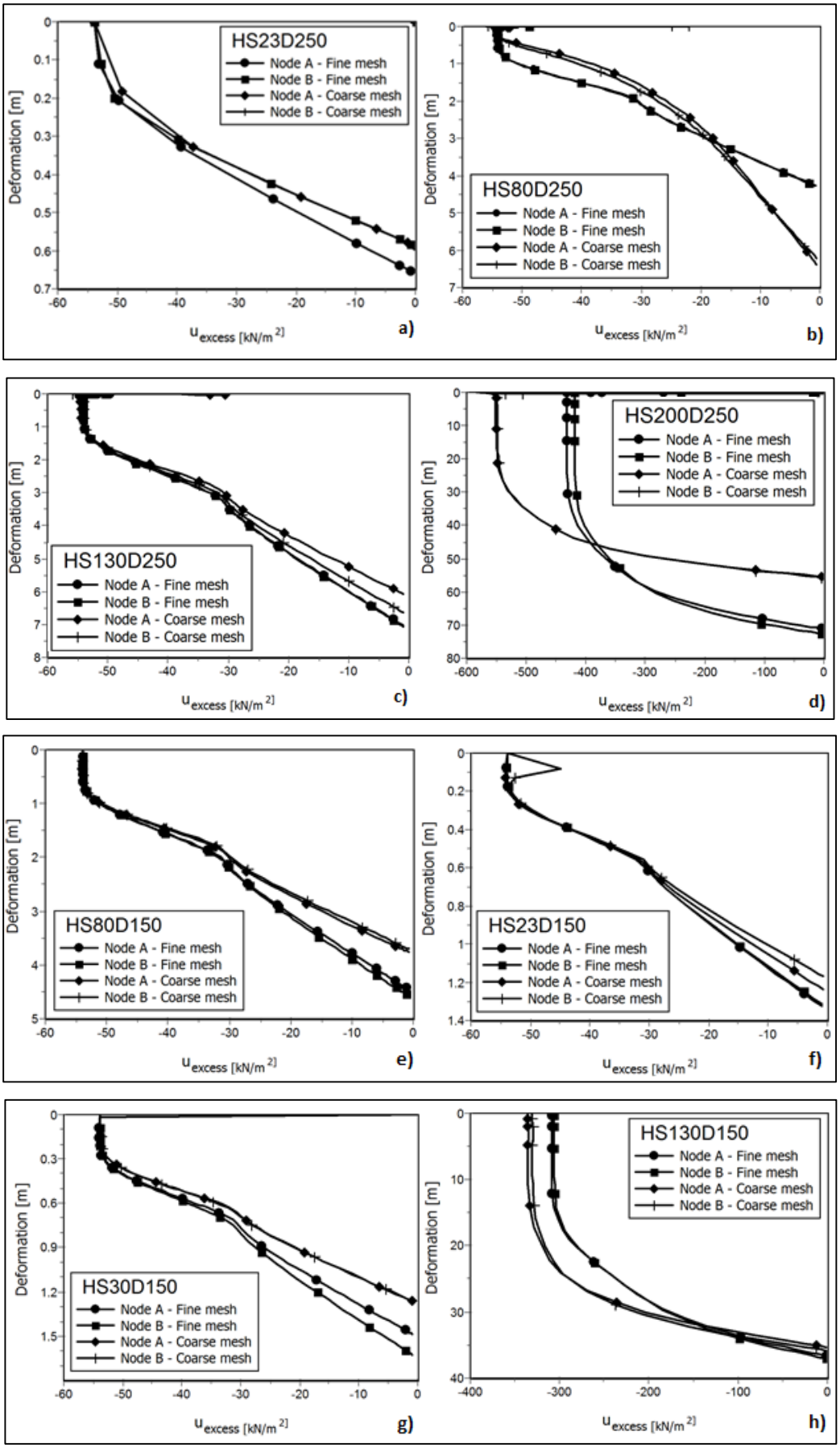

Figure 6-3: Effect of mesh size on sample height scale

Patterns shown in Figures 6.3 to 6.5 are the effect of sample size at various sample scales under double drainage (Vertical drainage only). As the soil diameter increases, the difference between fine and coarse mesh becomes less significant. The computer simulation was fast with the coarse mesh and slow with the fine mesh. The time required for each simulation depends on the density of the mesh, the selection of the parameters to obtain proper convergence, and sample scale. Due to the consistency of the graph trends at both coarse and fine meshes, no time being consumed when using the coarse mesh, and the simplicity of the model, coarse mesh was selected for the soil behaviour analysis in the current study. Figures 6.3, 6.4 and 6.5 show trends similar to the sample D/H ratio scale. From Figures 6.4 and 6.5, there is a maximum difference of 15%, 2%, 7%, 6%, 26%, 7%, 8%, 31% and 17%, which represents that observed in Figure 6.3 except at DS100H23 and DSS100H200. In this case, it can be seen that, as the diameter increases, the difference between the fine and coarse mesh increases, which is associated with the D/H ratio being less than 2. Whereas, at thickness 23mm, as the soil diameter increases, there is a fluctuation in the alteration (sharp decrease and minor increase) between the fine and coarse mesh. There is a significant difference increase from diameter 100mm to 150mm as compared to 150mm to 250mm where the variation is insignificant (D/H ratio greater than 2). Hence, as the D/H ratio increases, there is a minor difference between the fine and coarse mesh.

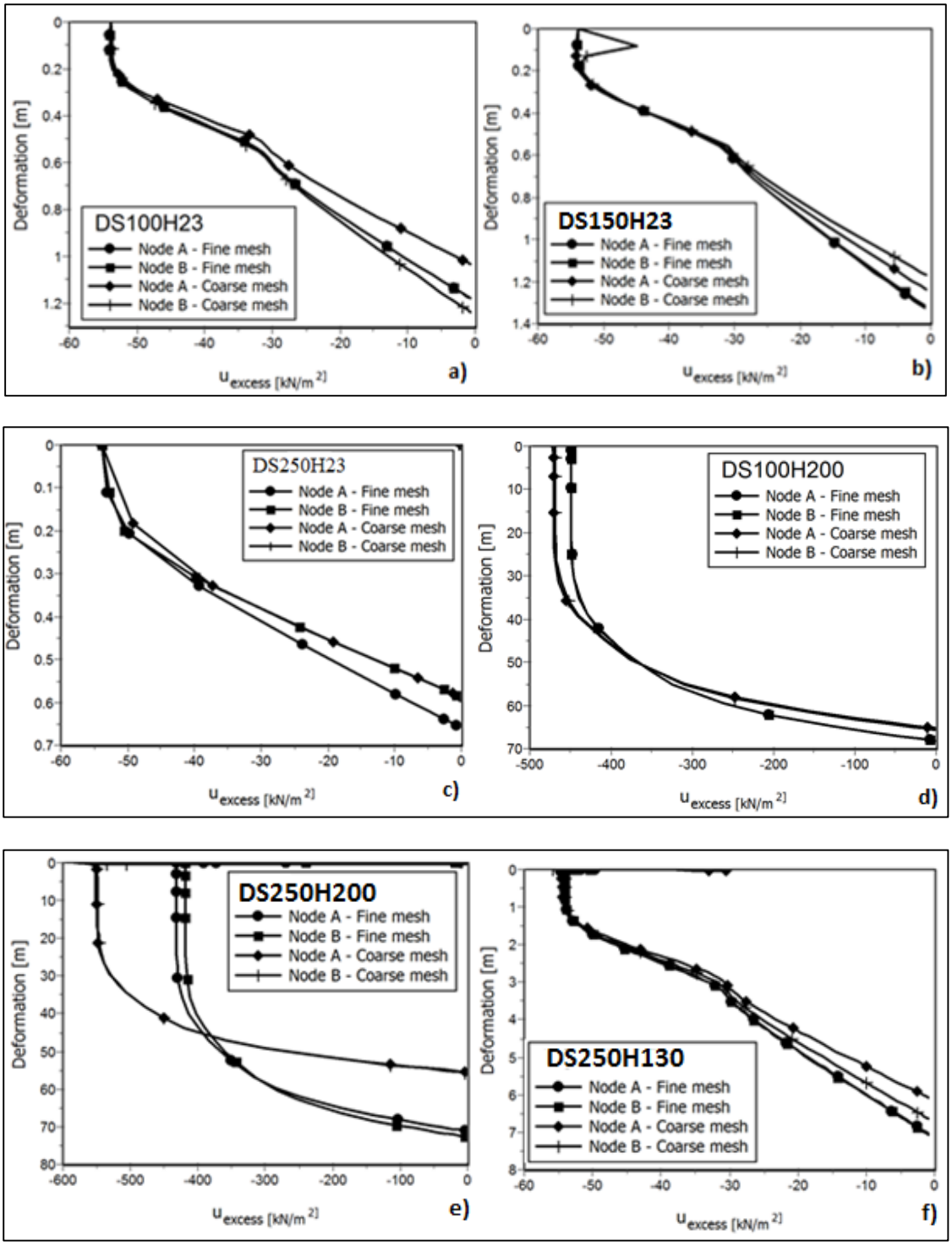

Figure 6-4: Effect of mesh size on sample diameter scale

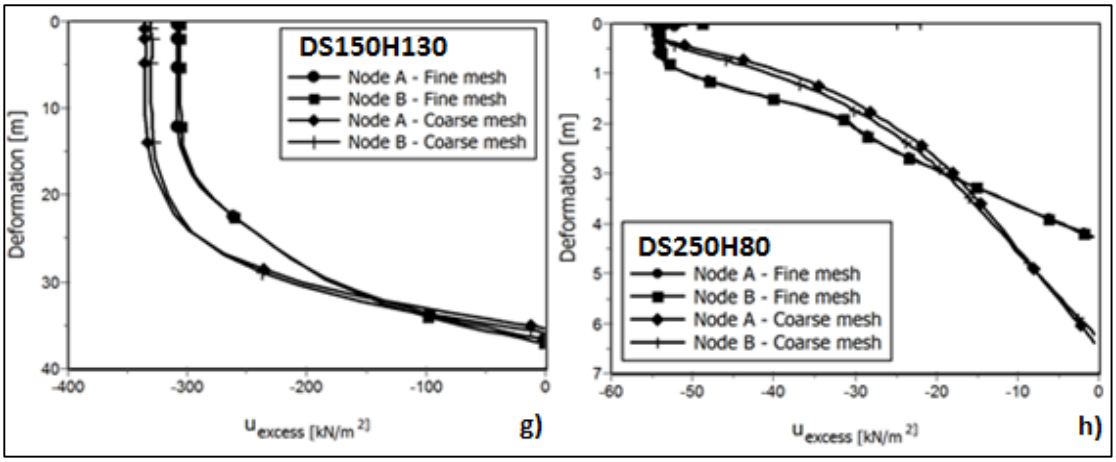

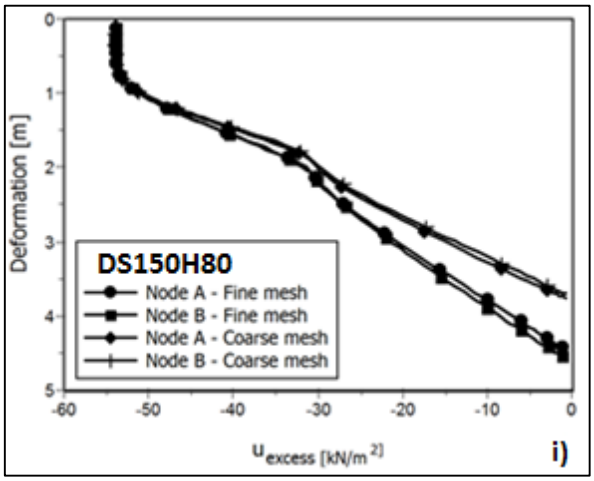

Figure 6-5: Effect of mesh size on sample diameter scale (Figure 6.4 continued)

6.5 Calculation stages

After the mesh had been generated, and the node points (use to plot graphs) selected at the mid-depth of the soil, the calculated phases were conducted. After the initial condition at zero initial stress, the remaining calculation stages were undertaken in two scenarios. During the simulation process, the Mohr Coulomb model was adopted for the analysis of soil behaviour. Once the simulation model had been drawn and the parameters selected, the calculation stages were set. Figure 6.6a shows the calculation phases used in the current study model. The plastic calculation refers to the elastoplastic or undrained analysis (consolidation analysis is not considered at phase 1). Phase 2 consolidation calculation type refers to the time-dependent analysis of the soil deformation and excess pore pressure (soil permeability is required for this analysis). Additional simulations were conducted using calculation phases in Figure 6.6b where the plastic calculation stage was removed. Figure 6.6a is for plastic-consolidation analysis while Figure 6.6b is termed ‘consolidation

analysis'. The excess pore pressure generated in PLAXIS with the Mohr-Coulomb (MC) model has been checked with the laboratory vertical effective stress.

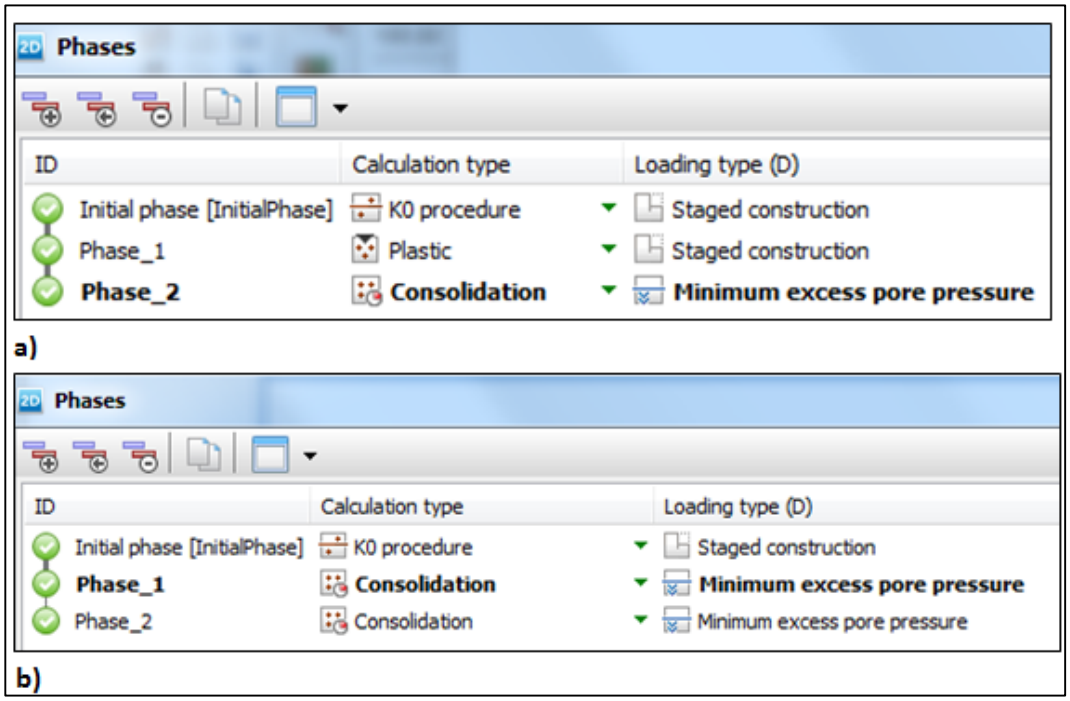

Figure 6-6: PLAXIS phases calculation

6.5.1 Plastic-consolidation analysis

The conventional one-dimensional consolidation analysis developed by Terzaghi treated soil as a linear elastic porous material in which the change in volume is proportional to the change in pressure (Hassan, 2013). Soil is a complex material that behaves in a highly non-linear way, and the modelling of the elasto-plastic behaviour of clay during consolidation is achieved using the FEM. Soil behaviour differs in primary loading, unloading and reloading and also undergoes plastic deformation (Ti et al., 2009). Thus the soil behaviour is divided into two categories: elastic and plastic behaviour. The elastic behaviour is assumed to be isotropic, with parameters such as shear modulus (G) and the bulk modulus (K). The plastic response can be visualised using the Oedometer apparatus. Comparable to Figure 2.5, the Oedometer presents a semi-logarithmic plot between stress and volume change. The section in Figure 2.5 representing c_r of the unload-reload line characterised the elastic volumetric response of the soil, whereas the average slope c_c of the normal compression line characterised the plastic volumetric response (Wood, 2004).

PLAXIS 2D presented an analysis of the one-dimensional problem using a linear elastic model under plastic analysis. The analysis was performed under single drainage, and the

result obtained was in good correlation with PLAXIS 3D and Terzaghi's analytical solution (PLAXIS, 2011). In their analysis, Rosine and Sabbagh (2015) used a similar approach to PLAXIS 2D but using the Mohr-Coulomb model and observed that at D/H greater than 1, adequate results in the excess pore pressure were obtained. D/H 0.5 was shown to be most problematic in obtaining the compressibility parameters, and this was observed numerically where the highest excess pore pressure was noted. These observations were made under the consolidation analysis that followed the plastic analysis.

Under the plastic analysis, there was a linear relationship between the excess pore pressure and the volume change at D/H 1 (DS150H130). At D/H 0.5 (DS100H200), there was no change in excess pore pressure, while a gradual change in volume was noted. As the load increased from 55kPa to 110kPa, the model simulation failed before the calculation phase ended for most consolidation analysis preceding the plastic analysis (Tables 6.4 – 6.6). The failure in the simulation was due to NaN (Not A Number) found in the stiffness matrix element. The failure was triggered when a stress point inside the free field elements violated the Mohr-Coulomb failure criteria and became plastic (PLAXIS, 2011). A summary of this failure found at each sample scale is presented in Tables 6.4 to 6.6.

Table 6-4: Calculation error in PLAXIS using Plastic calculation phase with k_c^1 parameter

Sample scales	Phase 1		Phase 2		Calculation error
	Plastic		Cons (min u_{excess})		
	55kPa	110kPa	55kPa	110kPa	
D/H 0.5	y	y	y	n	NaN found
D/H 1	y	y	n	n	NaN found
D/H 1.2	y	y	y	n	NaN found
D/H 2(a)	y	y	y	y	N/A
D/H 2(b)	y	y	n	n	Soil body collapse and NaN found
D/H 3	y	y	y	n	NaN found
D/H 4	y	y	y	n	NaN found
D/H 5	y	y	y	n	NaN found
D/H 6.5	y	y	y	y	N/A
D/H 11	y	y	y	n	NaN found

Where:

y = yes, n = no, N/A = not applicable, NaN = Not a number, k_c^1 = calculated coefficient of permeability using equation 2.9 (m/s) and Cons (min p_{excess}) = consolidation with minimum excess pore pressure (kPa).

The D/H ratio scale presented in Table 6.4 also relates to the sample diameter and height scale. From Table 6.4, it is seen that at 55kPa, the minimum excess pore pressure was observed at D/H greater than 2 while at D/H less than 2, there was a fluctuation in behaviour especially at D/H 2(b). The 'y' symbol in Table 6.4 shows that simulation was complete while 'n' symbol shows simulation failed. The reason for the failure is depicted under the calculation error column. The simulation error is resolved in section 6.5.3.

Table 6-5: Calculation error using Plastic calculation phase with PLAXIS k_e parameter

Sample scales	Phase 1		Phase 2		Calculation error
	Plastic		Cons (min p_{excess})		
	55kPa	110kPa	55kPa	110kPa	
D/H 0.5	y	y	n	n	NaN found
D/H 1	y	y	y	n	NaN found
D/H 1.2	y	y	n	n	Soil body collapse
D/H 2(a)	y	y	y	n	NaN found
D/H 2(b)	y	y	y	n	NaN found
D/H 3	y	y	y	n	NaN found
D/H 4	y	y	y	n	NaN found
D/H 5	y	y	y	n	NaN found
D/H 6.5	y	y	y	n	NaN found
D/H 11	y	y	y	y	N/A

Where:

y = yes, n = no, N/A = not applicable, NaN = Not a number, k_e = estimated coefficient of permeability (m/s) and Cons (min p_{excess}) = consolidation with minimum excess pore pressure (kPa).

From Table 6.5, the simulation failure found at D/H ratio 1 and 2(b) at 55kPa consolidation analysis in Table 6.4 were eliminated. However, D/H 0.5 and 1.2 were not achieved in Table 6.5. This shows the great importance of the coefficient of permeability during simulation under sample scale. However, at 110kPa, there was a uniformity from D/H = 0.5 to 6.5 consolidation analysis, which could not be completed due to NaN found. A third attempt is presented in Table 6.6, where the calculated coefficient of permeability k_c^2 presented in Table 5.3 was used. Table 6.6 also confirms findings observed in Tables 6.4 and 6.5. An attempt at resolving the simulation failure in presented in Section 6.5.3.

Table 6-6: Calculation error using Plastic calculation phase with PLAXIS k_c^2 parameter

Sample scales	Phase 1		Phase 2		Calculation error
	Plastic		Cons (min p_{excess})		
	55kPa	110kPa	55kPa	110kPa	
D/H 0.5	y	y	y	n	NaN found
D/H 1	y	y	n	n	NaN found
D/H 1.2	y	y	y	n	NaN found
D/H 2(a)	y	y	y	n	NaN found
D/H 2(b)	y	y	y	n	NaN found
D/H 3	y	y	y	n	NaN found
D/H 4	y	y	y	n	NaN found
D/H 5	y	y	n	n	Soil body collapse and NaN found
D/H 6.5	y	y	y	n	NaN found
D/H 11	y	y	y	n	NaN found

Where:

y = yes, n = no, N/A = not applicable, NaN = Not a number, k_c^2 = calculated coefficient of permeability using a equation 2.10 (m/s) and Cons (min p_{excess}) = consolidation with minimum excess pore pressure (kPa).

6.5.2 Consolidation analysis

In addition to the plastic analysis, a consolidation analysis was performed, and a distinct difference in excess pore pressure between the two calculation stages was noted. For illustration purposes, only D/H less than 2 is presented, with the remaining sample scales presented in Appendix D. Excess pore pressure was observed at the mid-depth of the soil, also noticed under the plastic-consolidation analysis which validates theoretical statement (Figures 6.7, 6.8 and 6.9). Figures 6.6 to 6.8 show a 67%, 95% and 56% decrease respectively in excess pore pressure when the calculation phase varied from plastic-consolidation to consolidation analysis. Therefore, from Figures 6.7 to 6.9 the consolidation analysis generates satisfactory results; however, this is far from the true soil behaviour during the consolidation process, as explained in Section 6.5. Plastic-consolidation analysis seems to overestimate the soil behaviour, but it shows the worst case scenario at each scale. The high percentage difference was only observed at D/H less than 2, whereas, at D/H greater than 2, steady nominal variability was observed (as depicted in Appendix D).

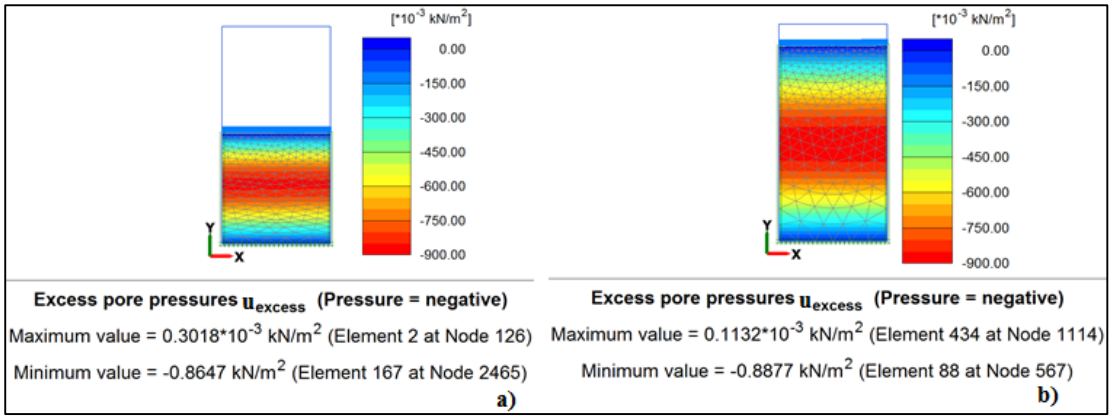

Figure 6-7: Excess pore pressure at 55kPa under D/H = 0.5 estimated coefficient of permeability at a) Plastic-Consolidation analysis and b) Consolidation analysis

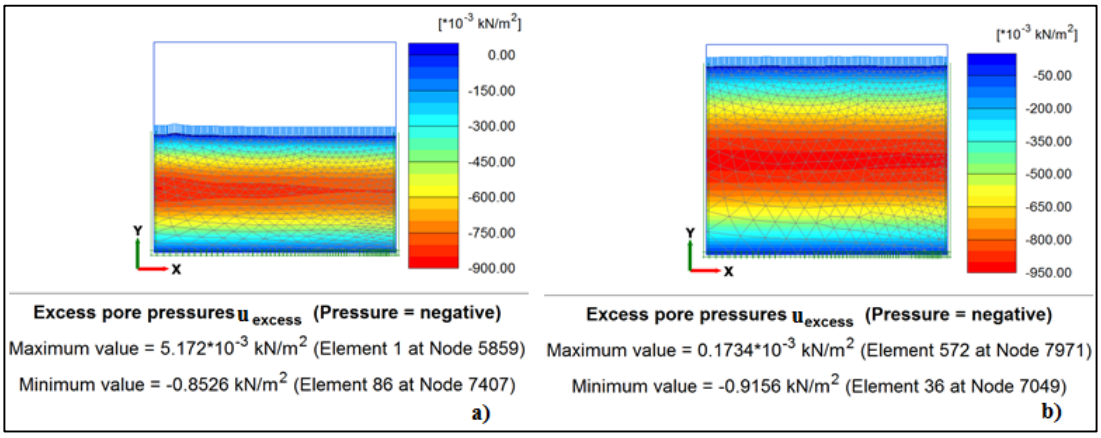

Figure 6-8: Excess pore pressure at 55kPa under D/H = 1 estimated coefficient of permeability at a) Plastic-Consolidation analysis and b) Consolidation analysis

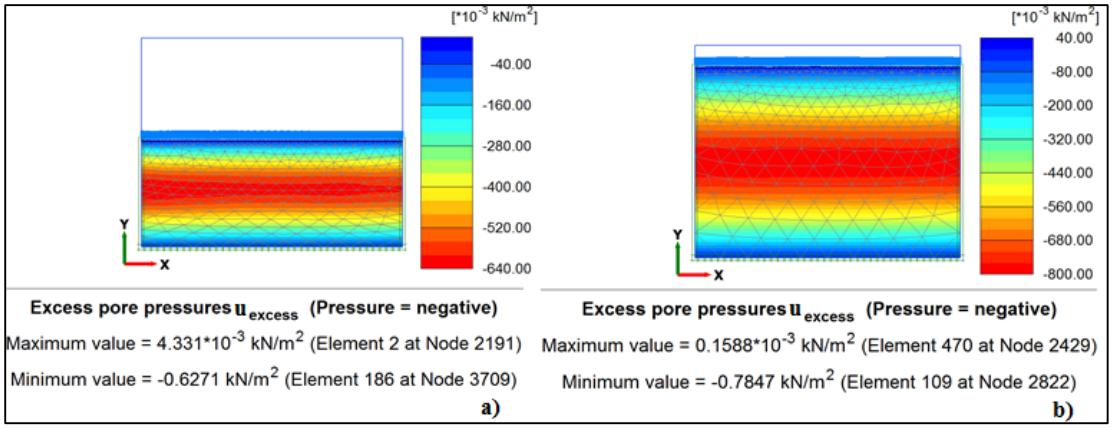

Figure 6-9: Excess pore pressure at 55kPa under D/H = 1.2 estimated coefficient of permeability at a) Plastic-Consolidation analysis and b) Consolidation analysis

It is clear from Table 6.7 that the consolidation analysis was not applicable at all sample scales at 110kPa. This observation was valid for loadings ranging from 110kPa to 276kPa (similar loads to those used experimentally). There is an inconsistency in simulation from Table 6.7 as compared to Tables 6.4 to 6.6, which is due to the elastic to plastic phase occurring as the load increases. It is clearly shown in the consolidation analysis that the elasto-plastic behaviour of the soil is vital at all the sample scales.

Table 6-7: Calculation error in PLAXIS using consolidation analysis phase

Sample scales	Phase 1- k_c^1		Phase 1- k_e		Phase 1- k_c^2		Calculation error
	Cons (min p_{excess})						
	55kPa	110kPa	55kPa	110kPa	55kPa	110kPa	
D/H 0.5	y	n	y	n	y	n	NaN found
D/H 1	y	n	y	n	y	n	NaN found
D/H 1.2	y	n	y	n	y	n	NaN found
D/H 2(a)	y	n	y	n	y	n	Soil body collapse and NaN found
D/H 2(b)	n	n	y	n	y	n	NaN found
D/H 3	y	y	y	n	y	n	NaN found
D/H 4	y	n	y	n	y	n	NaN found
D/H 5	y	n	y	n	n	n	NaN found
D/H 6.5	y	n	y	n	y	n	NaN found
D/H 11	y	n	y	y	y	n	NaN found

Where:
y = yes, n = no, N/A = not applicable, NaN = Not a Number, k_e = estimated coefficient of permeability (m/s), k_c^1 and k_c^2 = calculated coefficient of permeability using a equation 2.9 and 2.10 respectively (m/s) and Cons (min p_{excess}) = consolidation with minimum excess pore pressure (kPa).

6.5.3 Calculation error solution

It is clear from Tables 6.4 to 6.7 that the most common error found during the soil analysis was at 110kPa. This was believed to be due to the NaN found. NaN simply refers to 'Not a Number'. NaN only occurs when the field elements are in a plastic state. As a resolution, the strength of the soil material could be increased, or a linear elastic soil material could be used (PLAXIS, 2011). This is because during consolidation, as the load increases, the soil behaviour changes from elastic to plastic, which is affected by the strength and compressibility characteristics of the soils.

It was concluded that the estimated coefficient of permeability (k_e) from PLAXIS produced consistent results. Hence, the resolution of the simulation error is presented in Table 6.8, which is also applicable to the remaining sample scales. The shear strength used for all the sample scale simulations was 12kN/m^2 obtained using the Vane shear test. During the simulation, 12kN/m^2 was used, which resulted in the simulation error shown in Tables 6.4 to 6.7. Hence, as stated by PLAXIS (2011), to resolve the simulation error 'NAN found' the strength should be increased. The shear strength of kaolin clay was thus increased in increments of 5kN/m^2 to a value of 50kN/m^2 when the simulation was complete. The value of 50kN/m^2 falls within the range of values for kaolin clay previously obtained by researchers such as Sharifounnasab and Ullrich (1985) and Black et al. (2009). The estimated strength of 50kN/m^2 was applied at D/H 0.5 to 6.5 from Table 6.5. The simulation error was corrected using 50kN/m^2 at all sample scales using k_e, except at D/H 1, where it was resolved to a shear strength value of 55kN/m^2 (Table 6.8). The theoretical statement is thus confirmed that as the load increases, the soil tends to become plastic, and it also confirms the sample scale effect on the soil behaviour. Hence, the soil behaviour depends greatly on the sample scale, and the value recommended by the American and British standard is confirmed. In the current study, it is consistently illustrated that at D/H greater than 1, acceptable findings are discerned. The solution presented in Table 6.8 was successfully applied to Tables 6.4 to 6.7. However, at D/H 1, calculation was completed at 50kN/m^2 under k_c^1 (plastic-consolidation and consolidation analysis) and k_c^2 consolidation analysis only. No successful correction was found at D/H 1 k_c^2 plastic-consolidation analysis, where various strength values from 0.28 to 100kN/m^2 were used. An elastic model was also used for the correction at D/H 1, but this was unsuccessful. Thus, data are only presented using the estimated coefficient of permeability under plastic-consolidation analysis that produced accurate results throughout the sample scales used.

Table 6-8: Corrected error within PLAXIS k_e parameter

Sample scales	Phase 1	Phase 2	Corrected shear strength (kN/m^2)
	Plastic	Cons (min p_{excess})	
	110kPa	110kPa	
D/H 0.5	y	y	50
D/H 1	y	y	55
D/H 1.2	y	y	50
D/H 2(a)	y	y	50
D/H 2(b)	y	y	50
D/H 3	y	y	50
D/H 4	y	y	50
D/H 5	y	y	50
D/H 6.5	y	y	50
D/H 11	y	y	N/A

Where:

y = yes, N/A = not applicable, k_e = estimated coefficient of permeability (m/s) and Cons (min p_{excess}) = consolidation with minimum excess pore pressure (kPa).

6.6 Model calibration

The model was first compared with the experimental data under hydraulic loading at different D/H ratios and/or height and diameter sample scales to establish the validity of the FEM. D/H 1 to 2(a) are presented for illustration purposes (Figure 6.10). The properties of the studied fine-grained soil used to calibrate the model are as shown in Table 6.2. During the simulation, the load applied in the laboratory ranged between 55kPa – 276kPa. For representational purposes, load range 55kPa – 110kPa was adopted and compared with that observed in the laboratory (Chapter 4).

Hence, after the application of 55kPa in PLAXIS, the maximum excess pore pressure produced was 54kPa at all sample scales, except at: DS100H23 (D/H 4) where it was 60kPa, DS150H130 (D/H 1) and DS250H200 (D/H 1.2) with 500kPa and DS100H200 (D/H 0.5) with 470kPa. Thus, the maximum excess pore pressure generated in PLAXIS is considered to be representative and in good agreement with that measured by the laboratory tests at D/H greater than 2. This is because there is a 2% difference between the applied load and the excess pore pressure at all sample scales, except at D/H 4 with 9% and D/H < 1 with an overall difference of 89%. Figure 6.8 shows that the FEM can simulate the stress-strain

deformation of the fine-grained soil with good accuracy with a maximum difference of 1.4%, 55% and 23% at D/H 1, 1.2 and 2(a) respectively.

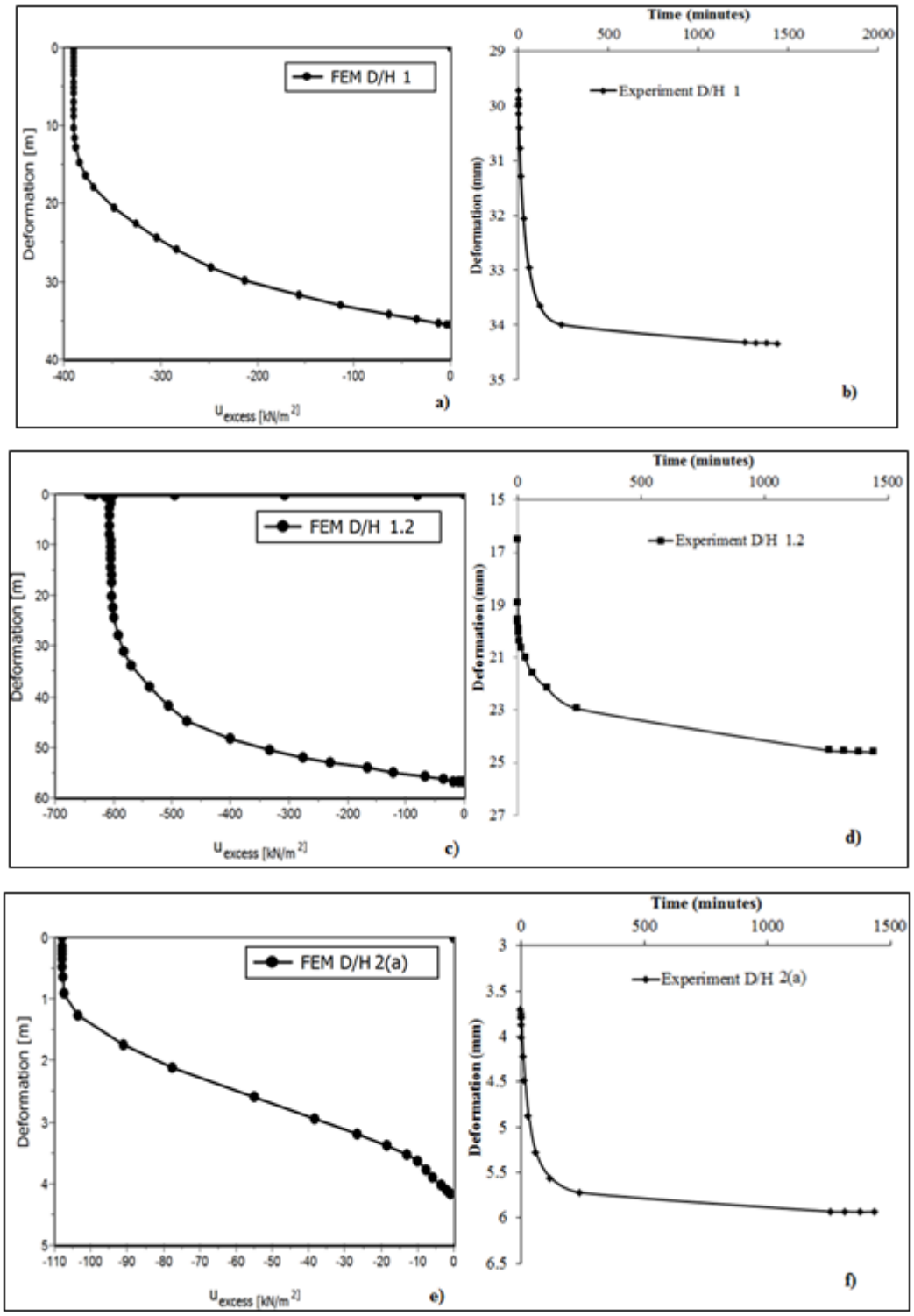

Figure 6-10: Comparison between experimental and numerical model at 110kPa for D/H 1 to 2(a); a, c, e) normalised FEM and b, d, f) experimental model.

Where: u_{excess} is the excess pore pressure, u is pore pressure

6.7 Sample height scale

It has been proven experimentally in Chapter 4 that the sample height scale (HS) had a significant impact on the compressibility parameters with an average correlation factor of 0.6. This was also observed in the literature by Newland and Allely (1960), Healy and Ramanjaneya (1970), Ortega (1996) and Khan et al. (2012). Within PLAXIS, the estimated coefficient of permeability (k_e) was established to produce consistent results at all sample scales. Hence, data presented are using the following variables: k_e, loading between 55-110kPa, coarse mesh and plastic-consolidation analysis. The loading range 55-110kPa was selected for representational purposes.

Figure 6.11 displays the difference in excess pore pressure at mid-depth in the soil matrix. It shows that the excess pore pressure is influenced by the sample HS, which was also observed experimentally and by previous researchers. The trend in behaviour between various sample scales is more or less the same. Figures 6.11 a and c clearly show that HS130D150 (D/H 1) is 90% away from HS80D250 (D/H 3) and HS130D250 (D/H 2(b)) and with the remaining HS. The remaining scales are closely packed together except at HS80D250 and HS200D250 depicted in Figures 6.11b and d. The distinctive variation in behaviour between HS80D250 and HS200D250 is due to the D/H ratio of the soil matrix and strength of the soil. HS200D250 and HS130D150 trends do not relate to the remaining curve, because the D/H is 1, and it was previously illustrated that D/H less than 2 presents inadequate results. When compared with experimental data, there was a maximum difference of 36%, 37%, 43%, 70%, 92%, 93% and 96% at HS80D150, HS130D150, HS130D250, HS23D150, HS30D150, HS80D250 and HS200D250 respectively. The immense differences between the FEM and HS experimental data are due to the shear strength input parameters, D/H ratio and coarse mesh.

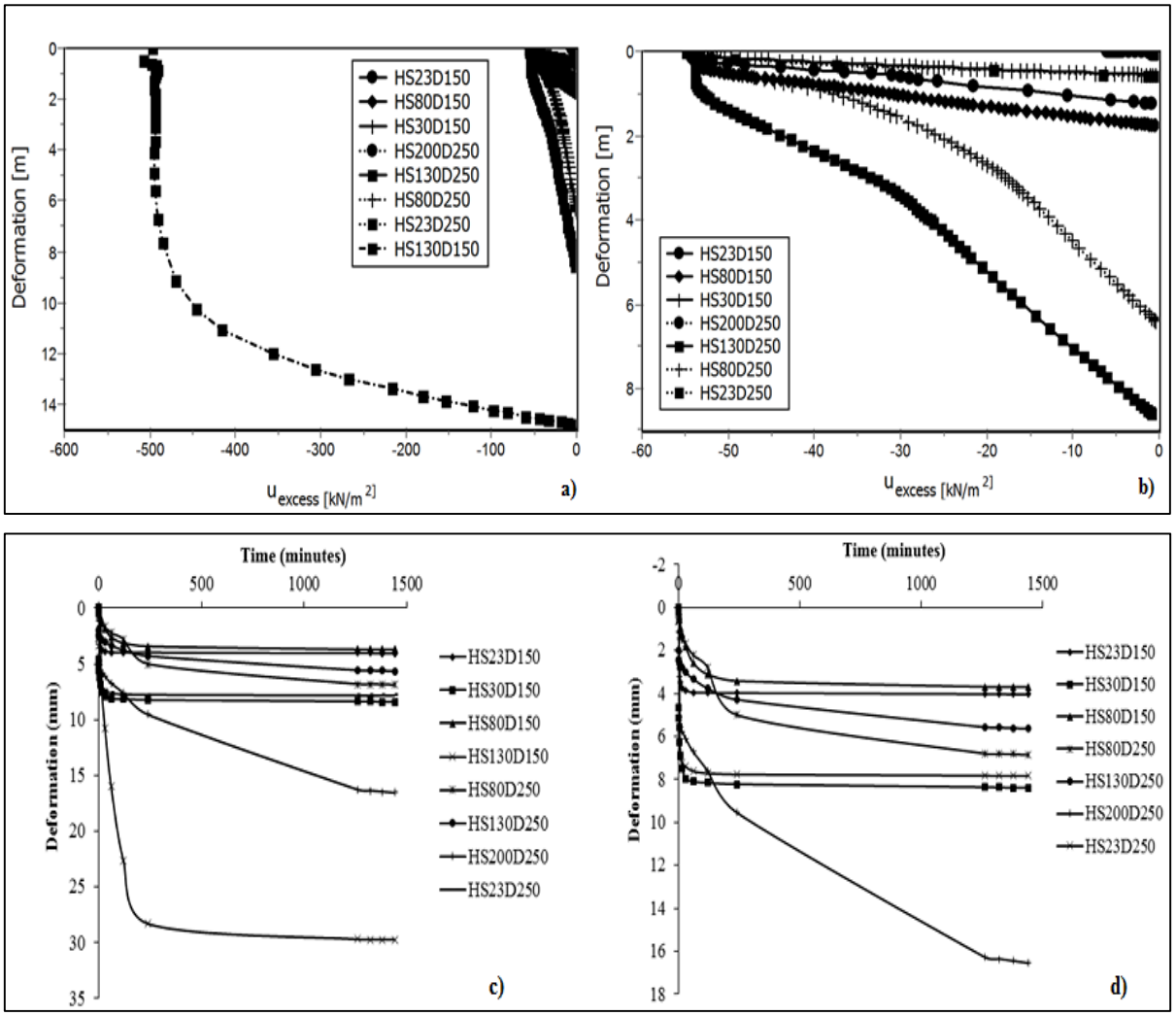

Figure 6-11: Variation of excess pore pressure using external load 55kPa under sample height scale; a and c) general representation, b and d) representation without HS130D150 and c) experimental data

6.8 Sample D/H ratio scale

The purpose of the D/H ratio is to minimise friction between the soil sample and the Oedometer apparatus. The current investigation aimed at validating the Standard recommended value mentioned in the literature. From the experimental study (refer to chapter 4), it was observed that D/H ratio greater than 2 for normally consolidated Kaolin clay is applicable. At D/H ratio less than 2, instability and inconsistent stress-strain and excess pore pressure outcomes were observed (Figure 6.12). There was a significant difference in u_{excess} with the applied load at D/H less than 2, which justifies the recommendation in the American standard value. The British standard did not refer to the D/H ratio but to the sample size. Hence, this aim not only justifies the American standard value but highlights the importance of the D/H ratio in the British standard code of practice.

The data shown in Figure 6.12 were observed under the diameter and height scale. Under the observations presented in Figure 6.11, a common factor 'D/H ratio' was noticed to be one of the main impacts on the soil behaviour. From Figure 6.12, D/H greater than 2 shows a less significant difference in the rate of consolidation. There is an important maximum difference between D/H less than 2 and greater than 2, indicating the importance of selecting the appropriate value for the D/H ratio as per the Standard. Similar patterns were observed at load increments ranging between 110kPa and 276kPa.

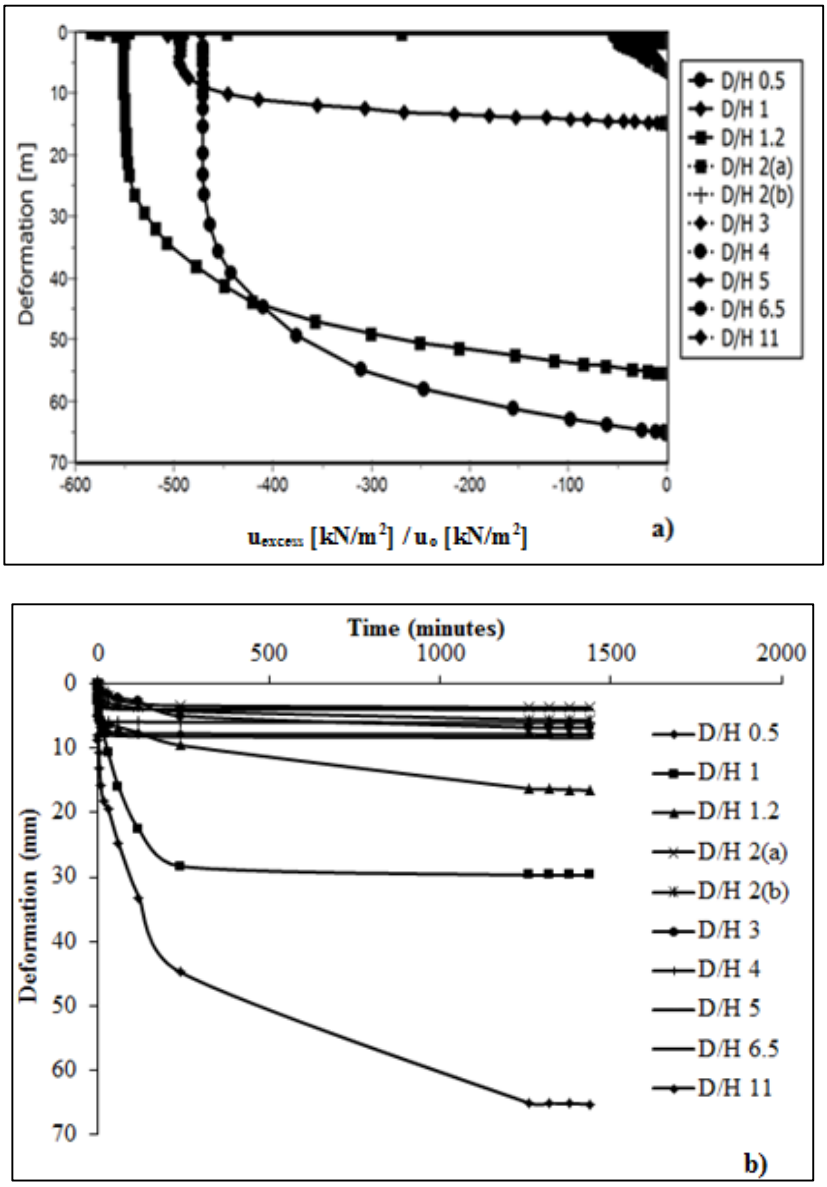

Figure 6-12: D/H ratio results compared with FEM at 55kPa; a) normalised FEM and b) experimental observation ***where: u_o is the initial pore pressure***

6.9 Sample diameter scale

It was proven experimentally in Chapter 4 that the diameter scale (DS) greatly influences the compressibility parameters of fine-grained soils. This was observed under one-dimensional consolidation analysis with vertical drainage. The outcome contradicts observations by Healy and Ramanjaneya (1970), where both radial and vertical drainage were used with the benefit of the sand drain and without reference to DS. Due to the limitations of the currently used equipment at the University of Salford, radial consolidation using sand drain could not be accurately performed. Hence, further analyses were conducted using FEM with radial drainage (without sand drain). This analysis is aimed at providing a broader understanding of the soil behaviour under DS. The FEM model obtained with both vertical and radial drainage is thus compared with experimental data. The radial drainage refers to a scenario where the finite element model is allowed to drain horizontally and both vertically and horizontally without sand drain.

6.9.1 Vertical drainage

Vertical drainage occurs when the soil is allowed to drain from the top and bottom of the soil matrix with the side boundary being impervious. The trends in behaviour between each scale are more or less the same for HS, D/H ratio and DS (Figures 6.11, 6.12 and 6.13). From Figures 6.13a and b, DS150H130 is 81% further away from DS250H23. The remaining scales are closely packed together (Figure 6.12), similarly to HS. Due to the similar pattern to Figure 6.12, descriptions and observations are identical to HS (refer to Section 6.7).

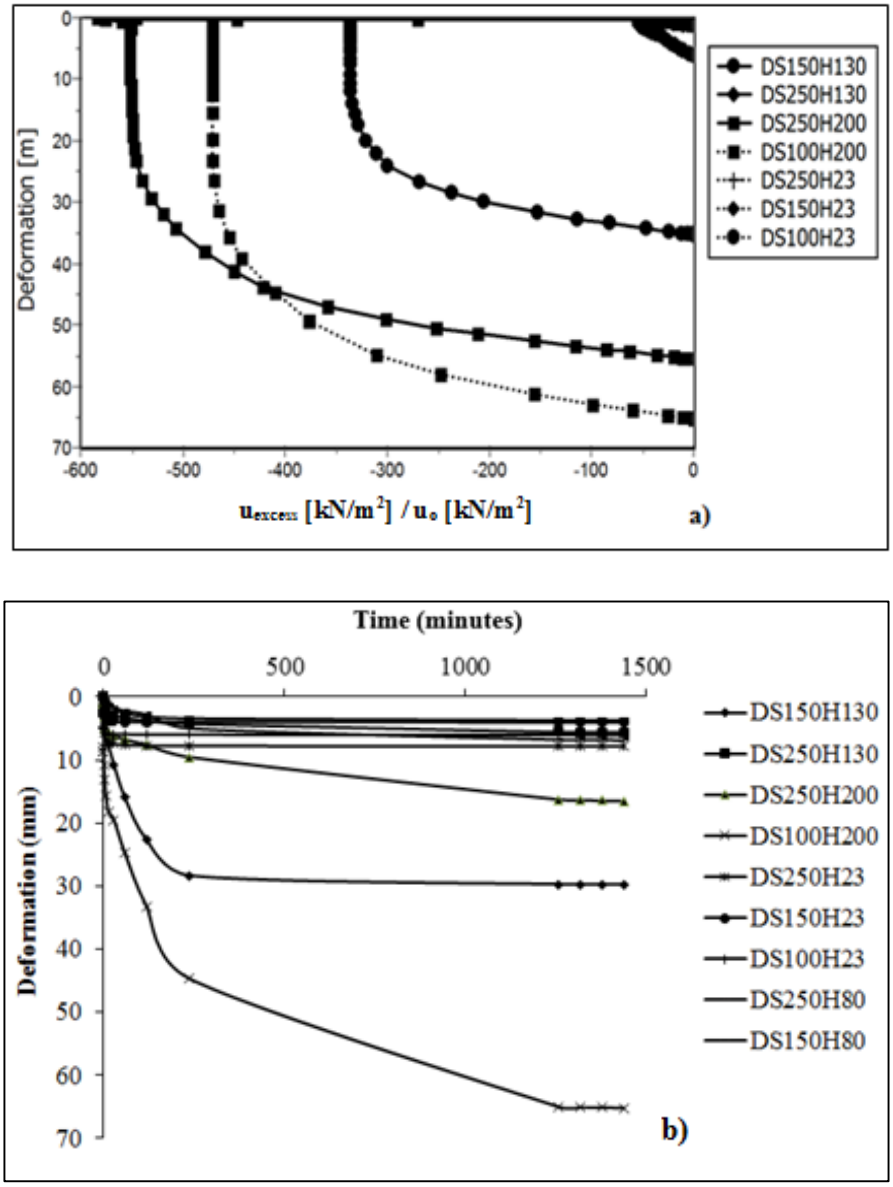

Figure 6-13: Variation of excess pore pressure using external load 55kPa under sample diameter scale; a) Normalised FEM model and b) experimental result ***where: u_o is the initial pore pressure***

6.9.2 Horizontal drainage

Experimental studies were carried out under double drainage where the soil was allowed to drain both at the top and bottom of the soil sample. Head (1998) presented different drainage scenarios that can be taken into consideration during the consolidation analysis (Figure 2.7). Healy and Ramanjaneya (1970) investigation used radial drainage with the implementation of the sand drain and found that there is no significant difference of sample scale on c_v. Healy's findings cannot be directly compared with the outcome in this study due to the different soil sample and drainage conditions used. In addition to DS outcome under vertical

drainage (Section 6.9.1), further analysis is conducted in PLAXIS under different drainage conditions. A schematic drawing of the horizontal drainage condition is shown in Figure 6.14.

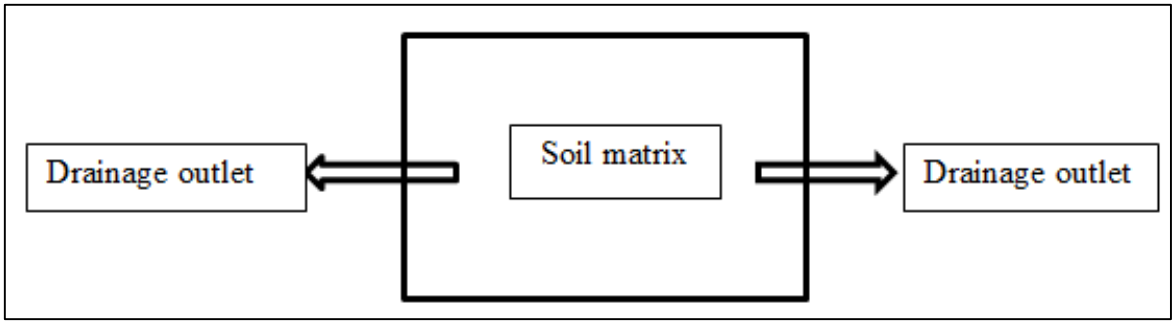

Figure 6-14: Schematic drainage representation of the FEM for DS at horizontal drainage (case 1) (Head, 1998)

From Figure 6.14, the top and bottom of the soil matrix was impervious while the drainage was allowed sideways. As DS increases, the drainage type is more radial than vertical. Data presented in Figure 6.13 are used for the modelling of the drainage scenarios.

During the FEM analysis using k_e under plastic-consolidation, D/H 1 and 1.2 simulations were unsuccessful using the correction depicted in Table 6.8. This was as a result of the soil collapsing before the end of the consolidation stage, and NAN being found in DS250H200. At DS250H200 NaN found was not successfully corrected when using various strength values (in the range shown in Table 2.3 after Sharifounnasab and Ullrich (1985), Burns et al. (2010) and Messerklinger et al. (2011)). The simulation failure explains why case 1 is not represented on Figure 6.15c. From Figure 6.15, there is no significant change in soil behaviour between vertical and horizontal drainage (case 1) except at D/H 1, 1.2 and 0.5 (DS150H130, DS250H200 and DS100H200 respectively). This is due to the inapplicability of the D/H less than 2 to the drainage scenario and the input parameters. At D/H ratio greater than 2, there was a 50% difference between case 1 and the vertical drainage at DS250H130, DS250H23, DS150H23, DS100H23 and DS150H80 and a 7% difference at DS250H80 (as shown in Figures 6.15 and 6.16).

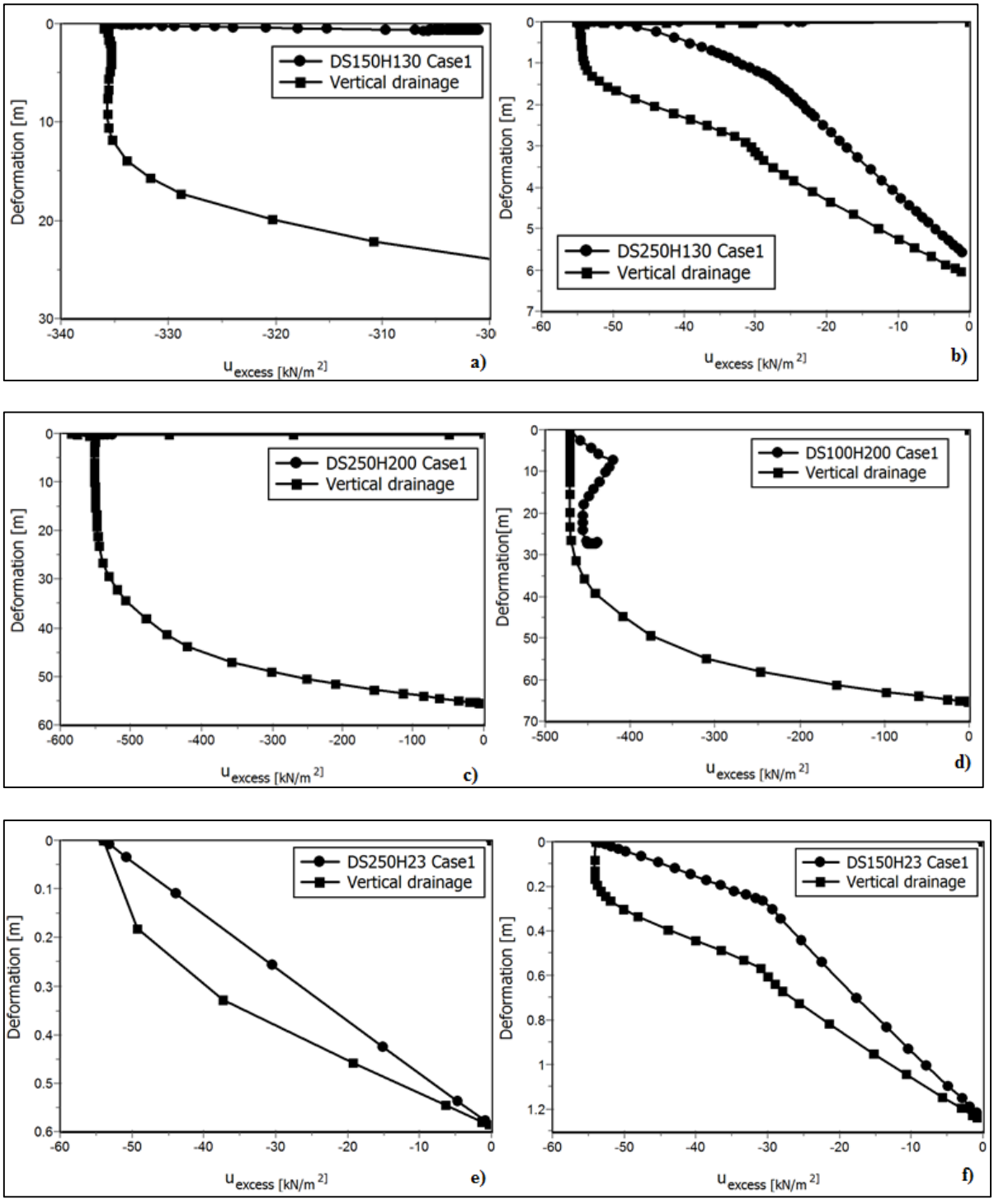

Figure 6-15: Comparison between vertical and case 1 at various sample diameter scales at 55kPa (*Where: case 1 is the horizontal drainage scenario*)

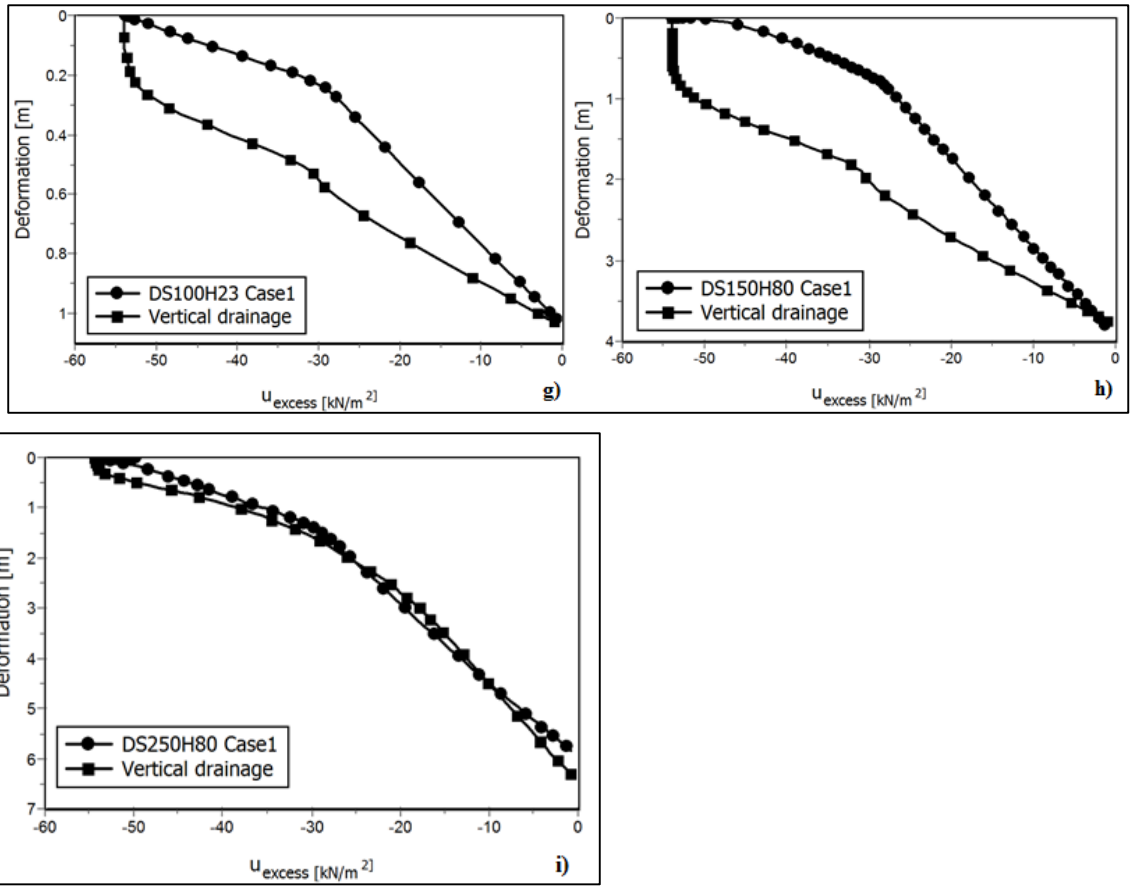

Figure 6-16: Comparison between vertical and case 1 at various sample diameter scales at 55kPa (Figure 6.15 continued)

6.9.3 Vertical and horizontal drainage

Both the combined vertical and horizontal drainage has been previously studied using sand drains. Theoretically, Figure 6.17 is designed with a central sand drain where the soil is allowed to drain horizontally and vertically through the sand drain (Head 1998). However, the current study adopts a different approach in Figure 6.17 without the use of a sand drain. Under case 1 (Figure 6.14), the soil behaviour had a 50% difference with vertical drainage. Theoretically, the rate of consolidation is rapid in Figure 6.17 compared to Figure 6.14. When the soil diameter increases from 150mm to 250mm, there is a confirmed relationship in the excess pore pressure between case 1, case 2 and vertical drainage (Figure 6.15i). However, DS150H130 shows a marginal affiliation between the drainage scenarios and there is a 5% difference between case 1 and 2 at DS150H80 (Figures 6.18a and 6.19h). The variation in behaviour is due to the variation in D/H ratio where D/H is less than 2.5 (the recommended value by the American standard), showing inconsistent results. Figures 6.14 and 6.17 were found to yield similar results under k_e as shown in Figures 6.18 and 6.19. The similarity in drainage scenarios is due to length of drainage and the D/H ratio. Case 1 in

Figure 6.18c calculation phase failed due to similar failure mechanics as described in section 6.9.2 (refer to Figure 6.15c). It was also observed that case 2 and the vertical drainage produced consistent identical excess pore pressures at all sample scales with D/H greater than 2, which could be associated to sample scale and strength of the soil.

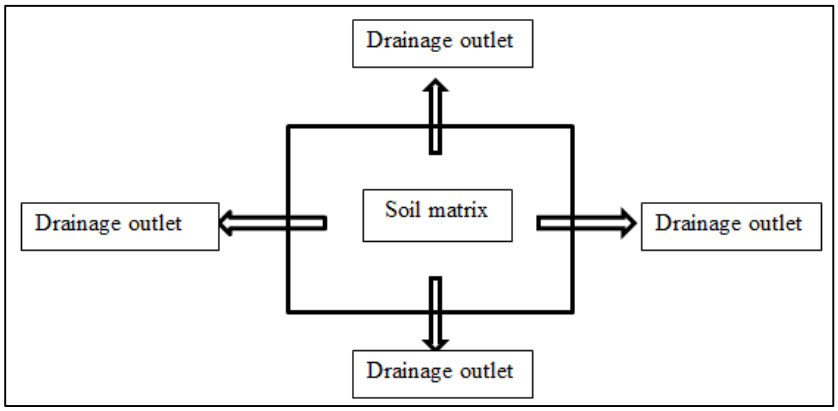

Figure 6-17: Drainage representation of the FEM for DS under vertical and horizontal drainage (case 2)

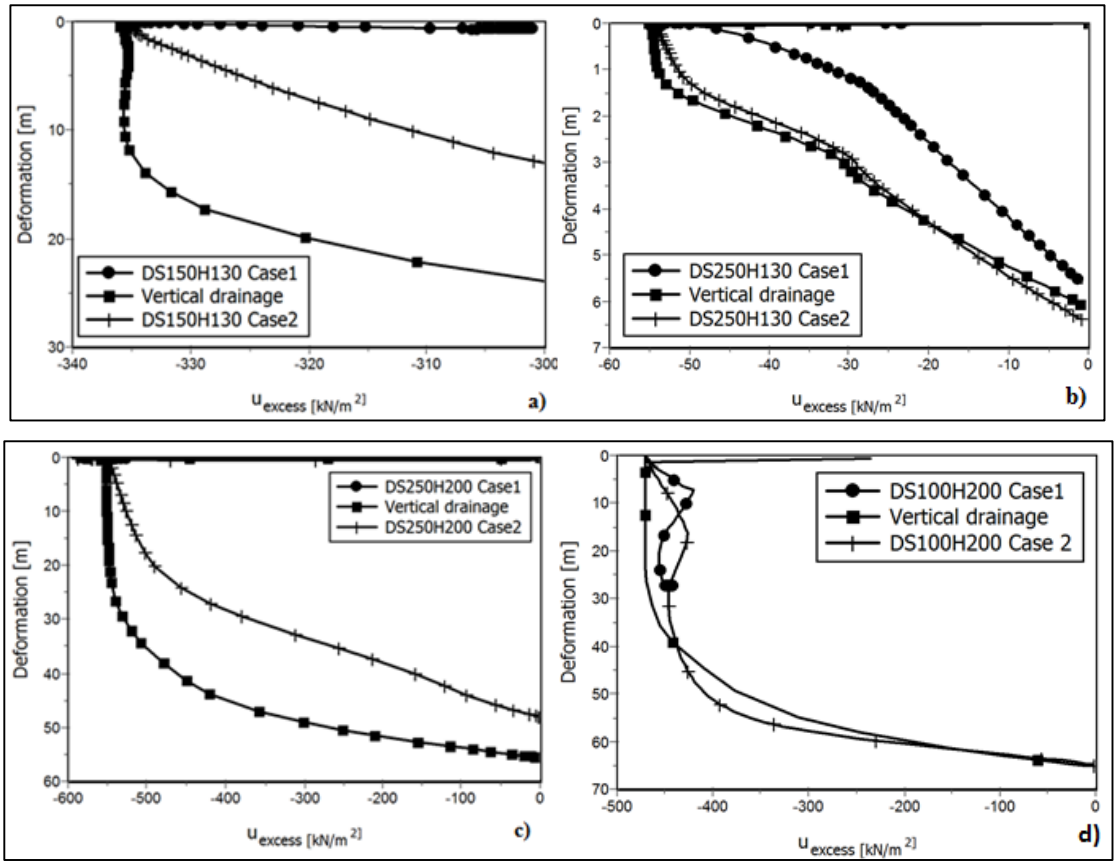

Figure 6-18: Comparison between vertical, case 1 and case 2 at various sample diameter scales at 55kPa (*Where: case 1 is the horizontal drainage scenario and case 2 is combined vertical and horizontal drainage*)

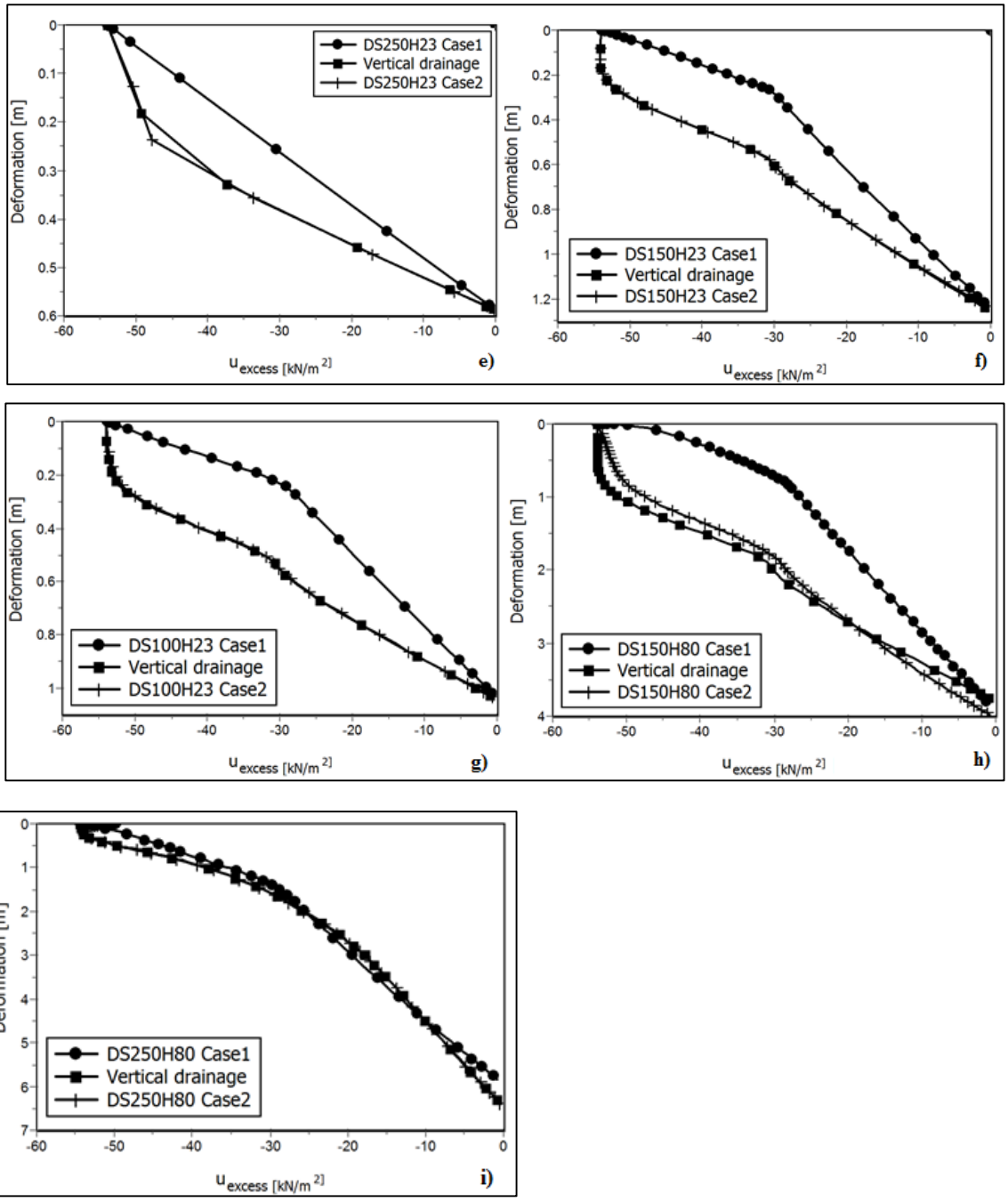

Figure 6-19: Comparison between vertical, case 1 and case 2 at various sample diameter scales at 55kPa (Figure 6.18 continued) (*Where: case 1 is the horizontal drainage scenario and case 2 is combined vertical and horizontal drainage*)

6.9.4 Calculated coefficient of permeability drainage scenarios

Drainage is largely dependent on the permeability of the soil, and can take a considerable amount of time to complete for soils with low permeability, e.g. clays. During the finite element analysis, an undrained analysis should be performed when the permeability is low and the rate of loading is high (PLAXIS, 2011). Undrained analysis is useful when assessing

short term soil behaviour. Kaolin clay has low permeability, as shown in Table 5.3, which falls within the range for fine grained soil. It was noted in Section 6.5 that the estimated coefficient of permeability (k_e) presented identical and consistent results for both drainage scenarios (case 1 and 2) above. However, when the calculated coefficient of permeability (k_c^1) was used during simulation, a drastic change in performance was noted in cases 1 and 2. Figures 6.20 and 6.21 show soil behaviour under the diameter scale (DS) only, as the pattern is similar to the height scale (HS) and D/H ratio. This is because the sample scales used are proportional to the various sample scales employed (DS, HS and D/H ratio scale). DS150H130 (Figure 6.20a) was further corrected using a higher strength value of 150kN/m^2. This was found to be successful only in case 2 when using k_c^1. At DS250H200, the soil collapsed before the consolidation phase calculation was completed in case 1 (depicted in Figure 6.20c) and ended when a strength value of 200kN/m^2 was used in case 2. DS100H200 (Figure 6.20d) strength value of 55kN/m^2 was used in case 2, and case 1 was corrected using 200kN/m^2. The remaining scales were corrected with the values presented in Table 6.8 at all drainage scenarios.

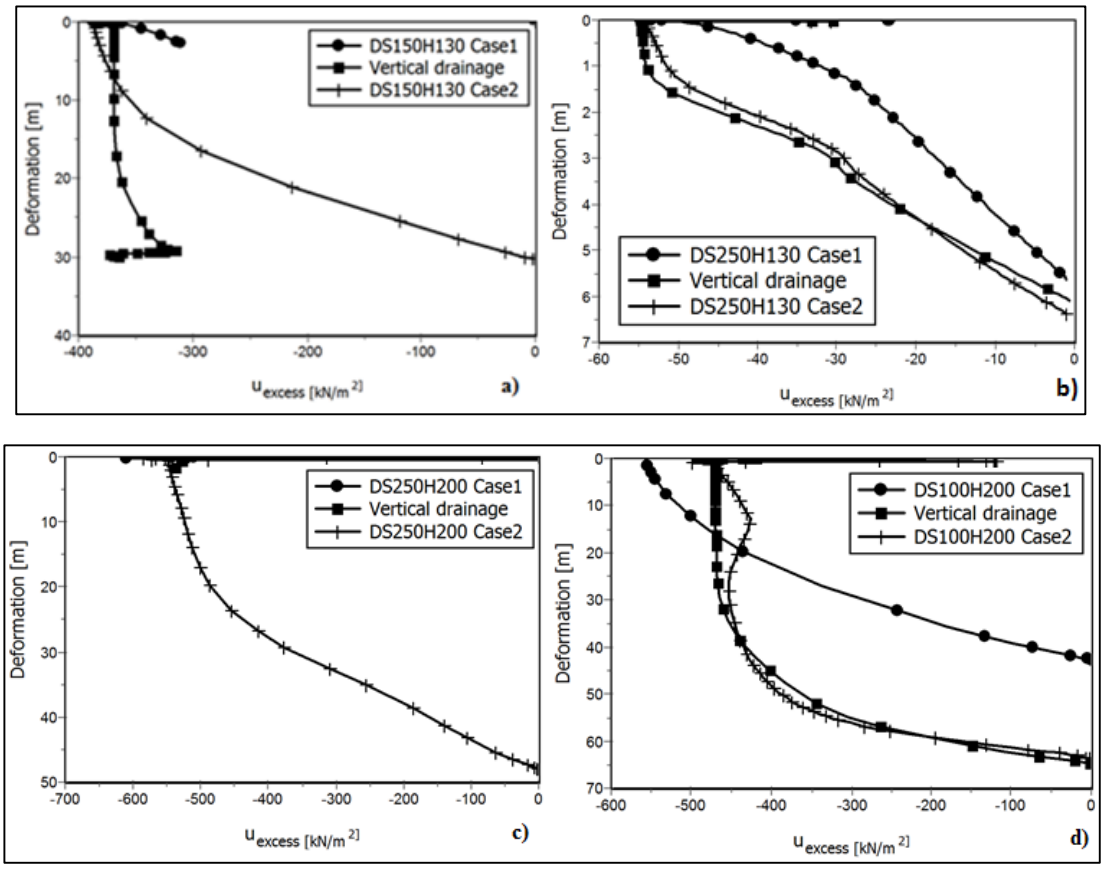

Figure 6-20: Effect of different drainage scenarios under the calculated coefficient of permeability (k_c^1) at 55kPa (*Where: case 1 is the horizontal drainage scenario and case 2 is combined vertical and horizontal drainage*)

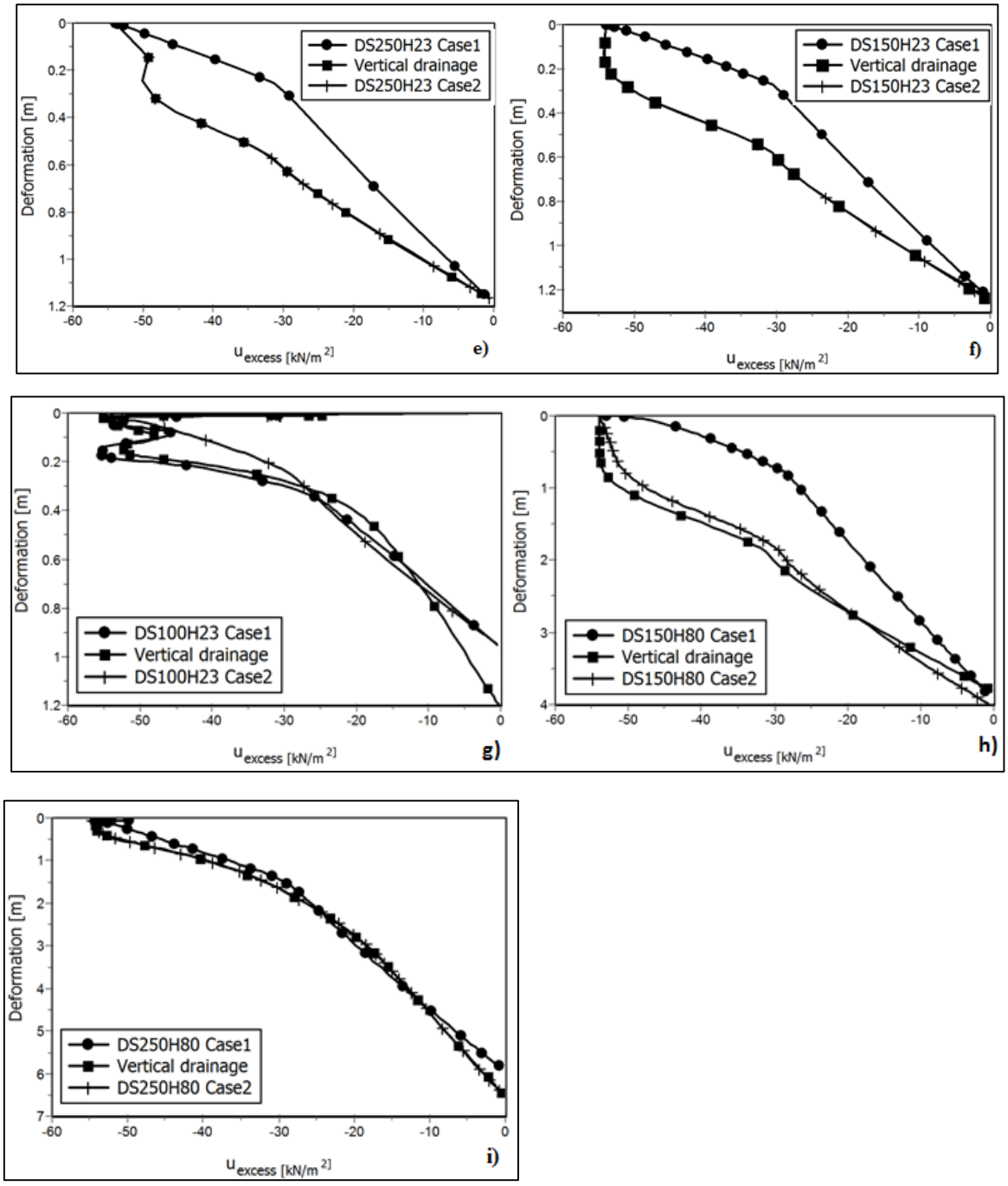

Figure 6-21: Effect of different drainage scenarios under the calculated coefficient of permeability (k_c^1) at 55kPa (Figure 6.20 continued) (*Where: case 1 is the horizontal drainage scenario and case 2 is combined vertical and horizontal drainage*)

Case 2 and vertical drainage were found to produce identical trends at DS250H130, DS250H23, DS150H23, DS150H80 and DS250H80, but DS100H23 has a maximum difference of 18%. On the other hand, DS250H130 and DS100H200 have a maximum difference of 8% and 9% respectively between the vertical drainage and case 2. Case 1 does

not match well with the remaining drainage conditions at all sample diameter scales except at DS100H23 and DS250H80, where the difference is not significant.

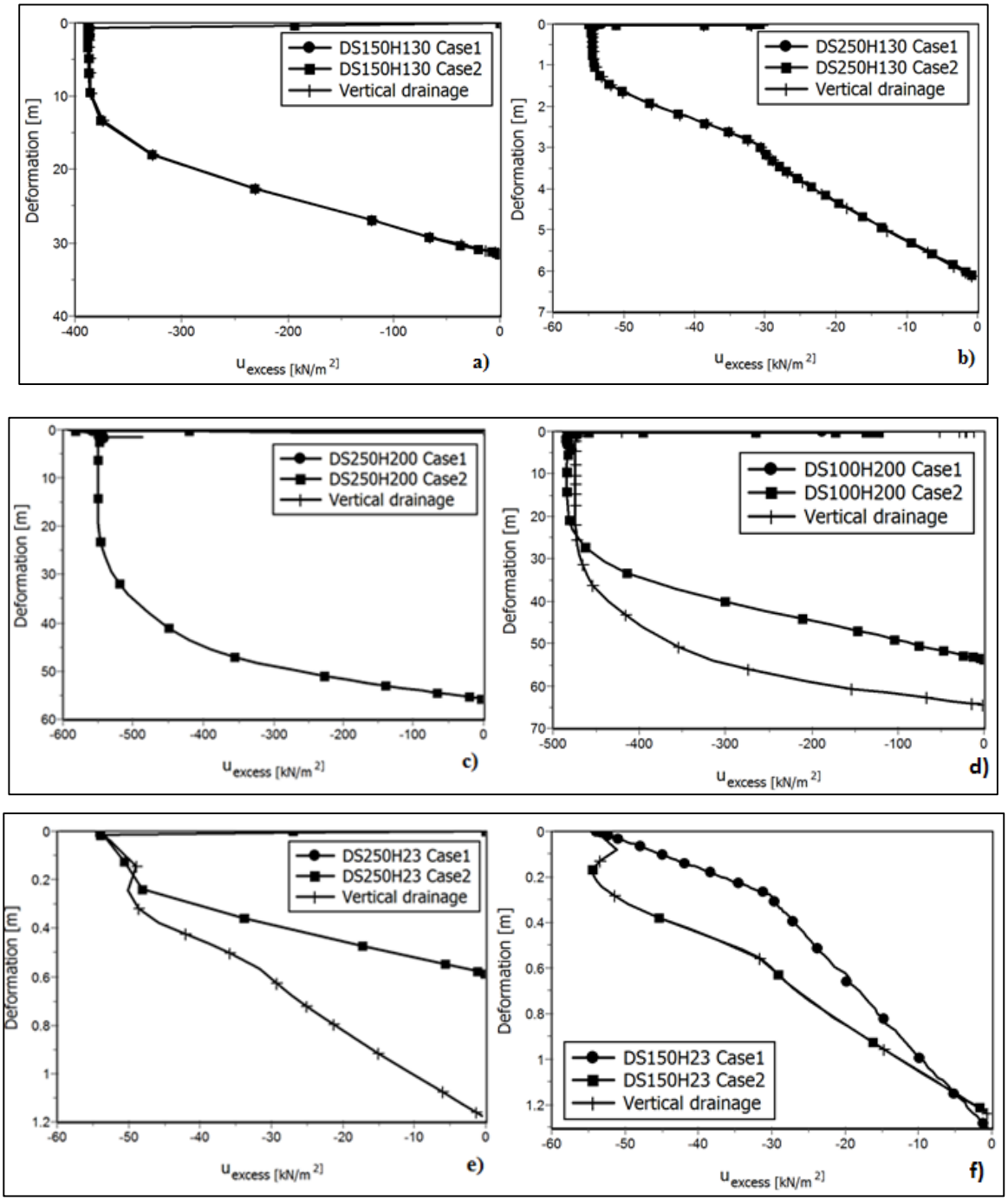

Figure 6-22: Effect of various drainage scenarios under the calculated coefficient of permeability (k_c^2) at 55kPa (*Where: case 1 is the horizontal drainage scenario and case 2 is combined vertical and horizontal drainage*)

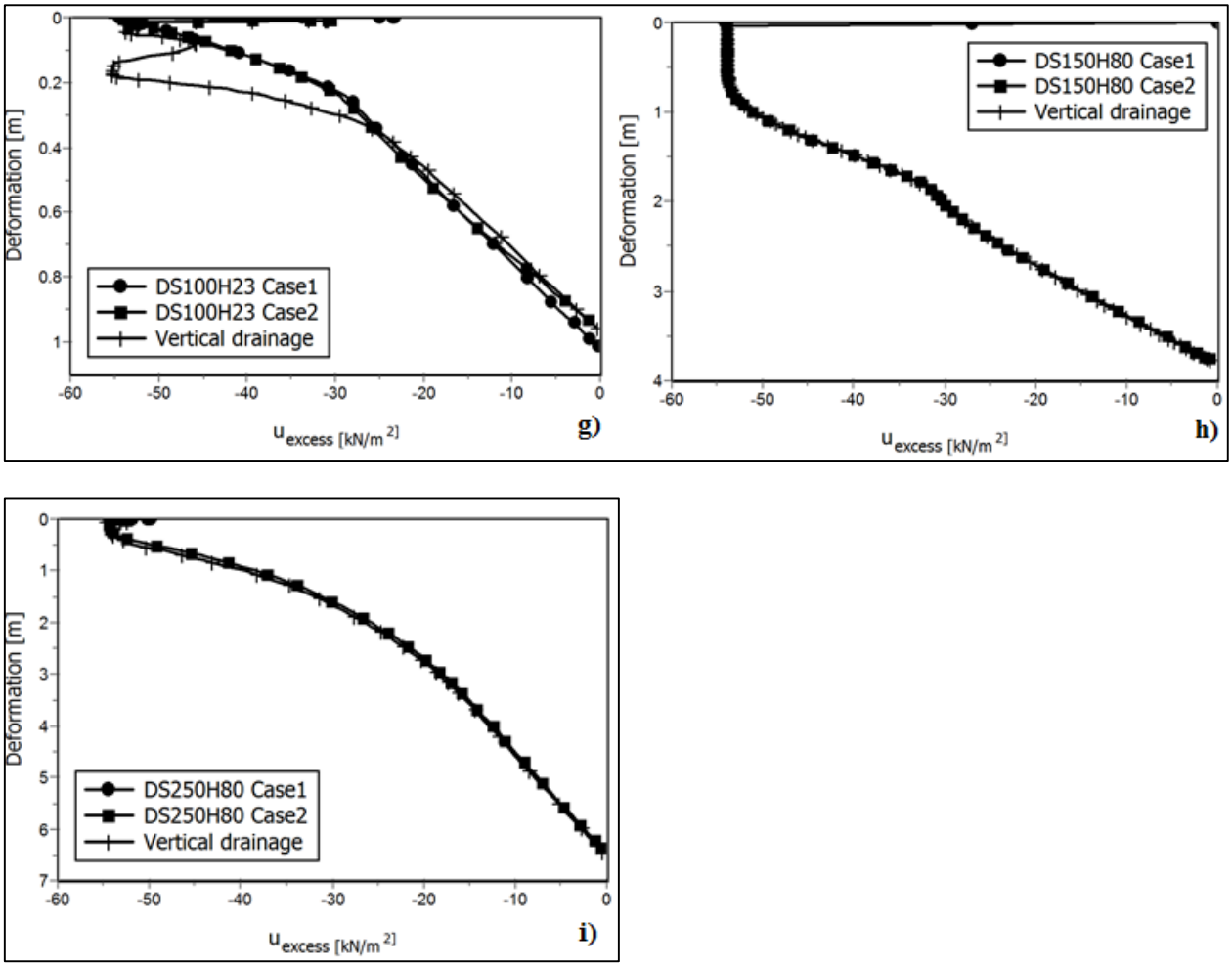

Figure 6-23: Effect of various drainage scenarios under the calculated coefficient of permeability (k_c^2) at 55kPa (Figure 6.22 continued) (*Where: case 1 is the horizontal drainage scenario and case 2 is combined vertical and horizontal drainage*)

Case 1 drainage type was not successfully applied with k_c^2 as shown in Figures 6.21a, b, c, d and e. The simulation failure of case 1 was due to NAN, as mentioned in section 6.9.2. The correction values derived in Table 6.8 were not successfully applied in these scenarios. This is because in PLAXIS, consolidation is modelled using the permeability value. The significant variation between the drainage type in Figures 6.19, 6.20, 6.21 and 6.22 is associated with sample scale and the soil permeability. Hence, these findings show not only the importance of the permeability values but that of the effect of drainage type at several DS.

6.10 Summary

The demonstration of the correlation between the FEM and the experimental study was presented. An evaluation of the selected meshing method used was presented and showed

that fine and coarse mesh presented no significant difference in soil behaviour at various sample scales. The main issue during the simulation process was the correct input parameters such as the coefficient of permeability. A comparison between k_e, k_c^1 and k_c^2 at various DS was presented. Experimentally, DS was found to have the greatest influence on the soil compressibility under vertical drainage. This was later validated using FEM under different drainage scenarios.

Theoretically, there are numerous drainage scenarios with radial drainage (with the implementation of sand drains) being widely used. Due to the limitation of the equipment provided by the University of Salford, an attempt at radial consolidation experimentally was deemed unsuccessful. Thus, DS was further analysed using FEM at vertical, horizontal and the combination of vertical and horizontal drainage. This analysis was performed without sand drains. Reliable and comparable findings were observed between the three different drainage scenarios when modelled with k_e. When varying the coefficient of permeability from k_e to k_c^1 and k_c^2, non-comparable data were obtained under the horizontal drainage especially at k_c^2. k_c^2 which is calculated from the relationship between c_v and m_v obtained experimentally providing a lower k values (10^{-9}) as compared to k_e (10^{-7}) and k_c^1 (10^{-6}) which falls within the range of values indicated in Table 2.5.

Due to the soil exhibiting some plastic behaviour during the consolidation analysis as the load increases, the simulation was performed using a plastic-consolidation analysis (refer to section 6.5). Both the plastic and consolidation analysis were performed under a load duration of 24 hours, and data were assessed for load range of 55-110kPa. During the FEM scrutiny, at some sample scales with an increase in loading, the measured strength parameter used was not applicable, especially at 110kPa. This was not applicable because the simulation failed; hence a solution was performed by increasing the strength values with reference to Table 2.3. The solution was found to apply to all sample scales under k_e; but at k_c^1 and k_c^2 the applicability of the solution was not consistent with all sample scales.

The above observation was not expected using k_c^2, due to the fact that it uses more measured parameters as compared to k_c^1. This is because it was envisaged that k_c^2 would show a realistic behaviour of the experimental study using the measured c_v and m_v that was clearly observed with the vertical drainage and case 2 (refer to section 6.9). The uncertainty was also observed during the solution scenario of the NaN error found during the analysis with k_c^1 and k_c^2 where a maximum strength value of 200kN/m^2 was used. The strength value of 200kN/m^2 is deemed too high for the type of soils used, hence showing the inefficiency of

the calculated k. Under k_e, the correction estimated strength value of 50kN/m^2 was constant at all sample scales under vertical and horizontal drainage. Hence, k_c^2 was found to be applicable only in case 1 and vertical drainage.

CHAPTER 7

DISCUSSION OF FINDINGS

7.1 Overview:

The impact of sample scale on the compressibility parameters was successfully studied experimentally and simulated using the finite element analysis in the current study. Emphasis was based on the D/H ratio and sample diameter scale, as they were found to have a significant influence on the soil behaviour. Moreover, there has been limited research in this area. Chapter 7 complements chapter 4 and 6, and provides valuable arguments on the outcome obtained.

In parallel with investigating the effect of sample scale on the compressibility of fine-grained soils, some scale-dependent factors were noticed. Section 7.2 presents how various curve-fitting methods affect the coefficient of consolidation (c_v) of test specimens. This provides the reader with an understanding of the importance and applicability of the curve-fitting procedure and how scale influences the outcome. Sections 7.3 to 7.5 provide discussions on the sample height, diameter and D/H scale analysis and its effect on compressibility parameters. Section 7.6 presents the effect of the initial moisture content on the compressibility parameters. Due to the above mentioned factors, it was also observed at some sample scales that the experimental time-deformation curve did not match the theoretical curve and that could be due to the duration of the load increment. As a result, Section 7.7 presents the effect of the load increment duration on the coefficient of consolidation (c_v). Further analysis was conducted using the finite element analysis under the diameter scale at various drainage scenarios. During the simulation analysis, the undrained shear strength (c_u) and coefficient of permeability were found to be vital parameters and the variation of the soil behavior was affected by these parameters. Thus, Section 7.4 also discusses the simulation error/limitations and the significances of these parameters in fine-grained soils.

7.2 Effect of different curve-fitting methods on c_v

This research benefits from using three methods to obtain c_v: Casagrande, Taylor's, and Inflection methods. All three methods use the curve-fitting procedure, and it is imperative that the experimental curve matches the theoretical curve for appropriate determination. The

outcome obtained was found to correlate well with that in the literature, where Taylor's method shows the highest c_v value except at the sample time scale (Table 4.3). The observation achieved was also observed by Cortellazzo (2002), McNulty et al. (1978), Mesri et al. (1999) and Sridharan et al. (1995). Casagrande and Inflection methods were also found not to be significantly different in the literature and the same trend was also observed in this study. This observation was at all sample scales. This means that in practice, irrespective of the test method used, there is little or no significant difference in the effect on c_v values. However, where sample scale is an issue, Taylor's method was observed to be more appropriate and reliable, since the experimental curve consistently matched the theoretical curve, especially at D/H values greater than 2.

7.3 Effect of sample height scale on c_v

Sample height scale refers to a situation where the soil thickness varied from 23mm to 200mm, and the soil diameter is kept constant. This is classified in Table 3.8 for Tests no. 5 and no.6. For every test and consolidation phase, it was necessary to obtain the following information:

1. The void ratio was obtained using equations 2.4 and 2.5.
2. Initial moisture content was measured at the end of each pre-consolidation pressure after the soil thickness has been noted. This was conducted using the test method described in the literature (Section 2.4.3).
3. Equilibrium was reached at each load increment. This was needed to remove any air entrapment from the loading device.
4. The compression index (c_c) and coefficient of volume compressibility (m_v) were calculated using the equations by Budhu (2000) and Whitlow (2001) respectively presented in Table 2.6.
5. The experimental results were compared with the finite element model results.

The thickness of the soil is important during the primary and secondary consolidation process. This is due to thick and thin soil samples, where there is more primary consolidation and less secondary consolidation in thick soil samples than in thin soil samples. This variation is not totally valid, as some secondary consolidation occasionally takes place during primary consolidation. As the soil thickness varied from 23mm to 200mm, the variation mentioned above was observed. Figure 4.6 presents the relationship between the soil thickness and c_v values. As mentioned in Chapter 4, as the soil thickness increased to

80mm (under constant sample diameter of 150mm), c_v increased steadily with the highest value of 14.6m^2/yr and dropped to a value of 13.3m^2/yr at 130mm. The variation is due to a decrease in the D/H ratio from 6.5 to 1. However, at diameter 250mm, there was a sharp increase as the height increased to 200mm with a c_v value of 31m^2/yr (high rate of consolidation). Hence, from the Oedometer sizes used, cell 250mm is recommended, provided the D/H is greater than 2. This is because the sample D/H ratio is dependent on the size of the cell. On the other hand, Healy and Ramanjaneya (1970) found a steady rise in c_v values with an increase in soil thickness on Varved Clay, using sample diameters ranging from 97mm to 147mm. Thus, the findings obtained were as expected from the literature, and this means that for pure clay such as Kaolin clay, there is a fluctuation in the soil behaviour at soil thickness alternating from 130mm to 200mm. Less secondary compression was observed at soil thickness 200mm, 30mm and 23mm compared to 80mm and 130mm. This fluctuation, together with that in the literature, is due to three factors: duration of the load increment, D/H ratio and clay minerals.

Moreover, the above findings were inputted in PLAXIS 2D, and the model was compared to the experimental data (refer to Figure 6.10). The experimental patterns were noted using PLAXIS; however, with some conflicting remarks. Prior to the validation process, some of the models were calibrated and had shown a good trend with the experimental data with a maximum overall difference of 26%. When comparing FEM with the laboratory data, it showed that as the soil thickness increased, there was an excessive difference in settlement with a maximum difference of 96%. The incompatibility of the FEM with the experimental data could be due to the input parameters in PLAXIS such as strength and coefficient of permeability. Simulation in PLAXIS was conducted using the coefficient of permeability as detailled in Chapter 6. Despite the maximum difference, the trends observed in the laboratory and FEM showed that HS130D150 and HS200D250 have the greatest influence on the compressibility of the soil matrix as compared to the remaining height scales. The outcome is acceptable as it relates well to the literature and theory. Therefore, soil thickness has an effect on soil behaviour, but is most problematic when the D/H ratio of the soil matrix below a structure is considered.

7.4 Effect of sample diameter scale on c_v

Sample diameter scale is a situation where the diameter of the soil is varied as the soil thickness is kept constant. Limited research has been done in this area as presented in the

literature. As depicted in Section 2.10.2, Healy and Ramanjaneya (1970) found no significant influence on c_v using radial consolidation but did not make reference to the diameter scale. Numerous studies have been carried out using radial consolidation with sand drains, but without taking into account the diameter scale effect or different spatial effects on soil compressibility. The current study provides additional findings to Healy's using fine-grained soil. This is achieved in three scenarios as follows with the relevant limitations explained.

7.4.1 Limitation of tests

Healy's investigation was conducted using three diameters: 97mm, 121mm and 147mm; and the current study used 100mm, 150mm and 250mm. Sample sizes were selected taking into consideration the ratio of the soil diameter and height. Healy's investigation maintained a D/H ratio of 3; and various D/H ratios were used in the current study. Under Healy's study, the sample thickness was one-third of the soil diameter, thus thickness was not constant. The radial consolidation was investigated using sand drains, while these were not employed in the current study. The limitations of both studies are presented and compared:

1. The thickness of the soil was not kept constant in Healy's investigation, but a D/H ratio of 3 was kept constant
2. In the current study, various sample scales were used: height scale, diameter scale and the Diameter to Height ratio scale. The variation in the sample scale was used to obtain soil compressibility parameters.
3. Due to a lack of equipment in the current study, the soil permeability was calculated and estimated using PLAXIS. The estimated value in PLAXIS was obtained using input parameters such as void ratio, Young's modulus, etc.
4. Healy's findings cannot be directly correlated with the present study due to the different sample used and sample diameter scale not being considered.
5. The current study's limitation is in Tests 2 and 3, where only two diameters were used. This is still acceptable as the trend in soil behaviour is noticed.

According to point 3, during the consolidation analysis the coefficient of permeability could not be measured due to the lack of functionality of the equipment. Thus, this was calculated using the equation from the literature and theory (k_c^1 and k_c^2). The calculated values were compared with the estimated constant value in PLAXIS (k_e). As described in Section 6.9.2, 6.9.3 and 6.9.4, k_e (estimated coefficient of permeability) produced consistent behaviour of

the soil at various diameter scales that was also observed with the remaining scales. One pertinent issue observed during the analysis was the shear strength value gained from the Vane shear test. Across each sample scale, as the load increased, the soil became plastic due to the strength value ($12kN/m^2$) being used. To correct this, the strength value was increased to a maximum of $200kN/m^2$ at a load greater than 55kPa. The strengh value of $200kN/m^2$ is considered high for the type of soil used (fine-grained soil) (refer to Table A.3). This means that, as the soils become stiffer, the shear strength value increases to its maximum while, in a slurry state, the shear strength is at its lowest value. This observation was expected and was consistently proven, using k_e as compared to k_c^1 and k_c^2 where the trends fluctuate. Hence, k_e was mainly utilised due to the consistent trend in the results. The consistency in results was due to a similar pattern observed at various sample scales where the D/H ratio exceeds 2, which validates the recommended D/H ratio value by the American Standards.

With regard to point 5, if a diameter of 150mm is added in test 2 and 100mm in test 3, no significant difference in trend will be observed due to the D/H being 0.7. In practice, a structure founded on a soil matrix with scale DS100H200 and DS150H200 will have greater settlement as compared to one built on DS250H200. Hence in the analysis of the results presented by Healy and results in the current study, D/H is isolated to draw conclusive remarks. The limitations in point 5 are acceptable as it provides no significant difference in soil behaviour due to the D/H ratio being in the range of 0.5 – 1.2 for test 2 and test 3 (refer to Figure 4.7).

7.4.2 Vertical drainage

The conventional one-dimensional consolidation test drainage system is vertical only either by single or double drainage. The rate of the drainage depends on the soil permeability. At low permeability, the excess pore pressure is generated slowly, which implies that settlement caused by the drainage of the water from the soil voids space will gradually take place over a longer period. As shown in Section 4.5.3, as the diameter increases, c_v has the tendency to decrease with an increase in pressure, which contradicts Healy and Ramanjaneya's (1970) findings. Due to the difference in soil mineralogy with that of Healy and Ramanjaneya (1970), the rate of drainage was affected by sample scale, especially at DS250H200 and DS100H200 (refer to Figure 4.7). The variation in findings is due to the proportion of the length of drainage to the soil width and the duration of the load increment. It was envisaged that, despite the duration of the load increment, the soil behaviour would not change

significantly due to the D/H and distribution of the stress in the soil matrix during the consolidation stage. The trend observed in the laboratory was also shown on the finite element model (FEM) with an average percentage difference of 15%, as presented in section 6.9.1.

7.4.3 Vertical and Horizontal drainage

In addition to 7.4.1, a further drainage scenario was modelled on PLAXIS 2D. The main aim of this investigation was to show any significant difference in soil behaviour under this drainage scenario as the soil diameter increases. It was predicted that as the diameter increases, drainage occurs more radially as compared to vertically. Within the literature, this was conducted using vertical sand drains, but in the current study was carried out without sand drains. This model was performed using the finite element model only using the experimental model under the vertical drainage. Since it was already observed that the FEM shows the trends in the experimental data with good accuracy, the FEM model was compared with that of the vertical drainage.

As already referred to in Sections 6.9.2 to 6.9.4, vertical and horizontal drainage tests produced identical results, except at DS150H130 under k_e. However, at k_c^1 and k_c^2 there was fluctuation in trends at all sample scales except at DS100H23, DS150H23 and DS250H200. Thus, sample diameter scale has a significant effect on the calculated coefficient of permeability. However, the consistency in soil behaviour trends was mainly observed when the estimated coefficient of permeability k_e was used. A similar observation was also expected using k_c^2 (calculated coefficient of permeability using equation A.10) because it uses more measured data as compared to k_c^1 (calculated coefficient of permeability using equation A.9). The expectation was not met when using k_c^2, and this could be for the following reasons:

1. Sample scale effect. This is related to the D/H ratio and possible friction between the soil and the Oedometer cell.
2. Measured input parameter. This was verified by calibrating the equipment and collecting data to an accuracy of $\pm$0.1% as discussed in Chapter 3
3. Speculated findings

Point 3 refers to the current model obtained under horizontal drainage (Case 1) and combined vertical and horizontal drainage (Case 2). This was speculated using the derived

laboratory measured void ratio value under vertical drainage. It was thus assumed that the void ratio is constant under all drainage conditions, and the only varying variable is the soil sample scale. As results, the findings are comparable with the vertical drainage, as only one variable changed (the direction of drainage) (Figures 6.12 to 6.22). The reason the void ratio was ignored and assumed to be constant was because the length of drainage is proportionate to the soil D/H ratio and the ratio of the load increment to the soil profile. The latter is observed theoretically and within the literature and was envisaged to be similar in cases 1 and 2. The former was consistently observed at all sample scales and elaborated in the following section.

7.5 Effect of sample D/H on c_v

In the literature, the sample D/H ratio recommended by the American Standards and the British Standards did not refer explicitly to the sample size. The D/H ratio effect on the compressibility parameter c_v has not previously been investigated, but its impact on other engineering parameters such as shear strength and bearing capacity was previously studied. It was observed under the sample height and diameter scale that one of the main rationales for the discrepancy in the result was due to the D/H ratio. The American Standards recommended a D/H ratio value of 2.5; whereas, in the current study, it was proven that for fine-grained soils, D/H ratio values greater than 1 are recommendable. This was first analysed by eliminating friction between the cell and the sample using the method described in the literature (Figure 4.9). As mentioned in Section 4.5.5, friction was reduced at all sample scales except at D/H = 4 (DS100H23), where it was greatly influenced by a maximum difference of 75%. Theoretically and from the literature, friction is most likely to be observed on the thicker sample as compared to thinner specimens, and this is always ignored in the Oedometer test. An attempt in the current study to prove friction was eliminated was successful except at D/H = 4. The discrepancy could be due to the calculation, experimental error, or the plastic Oedometer cell used at D/H = 4. The latter was on the 100mm cell only as the remaining cell materials were steel. Due to the cell being plastic, the maximum load it could sustain varied depending on the soil thickness. At thickness 23mm, the maximum load used was 138kPa, while at 200mm it was 276kPa. This explains the friction observed at D/H = 4 which was as a result of the cell's inability to maintain high load thus the lower pressure been applied. Hence, the frictional stress obtained

is directly proportional to the applied load and inversely proportional to the sample scale, as presented in Equation 4.1.

The highest c_v value was observed at D/H = 0.5 and the lowest at a D/H = 11 and 5 (refer to Figures 4.10a, c and Figure 4.10b respectively). As already explained in Section 7.2, Taylor's method was deemed accurate where sample scale is an issue, since it has a negligible fluctuation in the rate of consolidation at D/H greater than 2. Meanwhile at D/H less than 2, there is a substantial variation in c_v where high settlement occurs after immediate application of the load. There is no available data in the literature or theoretically to relate to the D/H ratio scale in the current study as recommended in the American Standards. The current investigation confirms that for fine-grained soils, D/H greater than 2 is valid. The findings gained are acceptable because the validity of the D/H ratio was consistently observed at both sample height and sample diameter scales. These were also positively authenticated using the FEM (refer to Figure 6.11). Overall, the presented outcome shows good agreement with the Standards.

7.6 Effect of initial moisture content on the compressibility parameters

Due to environmental change, any variation in the subsoil moisture will cause the soil to shrink or swell, which may lead to structure failure. This had been previously studied by Hong et al. (2010), Lei et al. (2014) and Phanikumar and Amrutha (2014). Previous analysis showed that, as initial moisture content increases, the amount of compression also increases. However, the coefficient of compressibility (a_v), coefficient of volume compressibility (m_v) and compression index (c_c) increase until an initial moisture content of 30% and then decrease until 40% (Phanikumar and Amrutha, 2014). It was observed that as the initial moisture content increases, m_v and c_c increase to 55kPa$\pm$3.7kPa and then gradually decrease (Figure 4.12). However, a reverse pattern was observed at 105% (Figures 4.12a and b). The fluctuation in behaviour in the current study was also observed by Phanikumar and Amrutha (2014). The outcome observed here confirms that found in the literature.

7.7 Effect of time factor on the compressibility parameters

The time factor was found to be an issue where the experimental curve did not correspond to the theoretical curve, most especially when using the logarithmic scale of the time-deformation curve (Figures 2.10 and 2.11). This was observed in tests 18 and 20, which were repeated at load increment times of 7 days. Using Taylor's method, there was a 10%

and 9% difference in c_v values when the duration of the loading was increased from 24 hrs to 7 days at DS100200 and DS150H23 respectively (Figure 4.13a). However, with the Casagrande and Inflection methods there was a difference of 17% and 0.1% at DS100H200 and DS150H23 respectively. This confirms observations in the literature by previous researchers and in theory. The change in c_v values at different loading durations is not significant because the values obtained fall within the range presented in Table 2.9; thus high compressibility is observed throughout the sample scales presented in tests 18 and 20. Hence, despite the time factor having an impact on the compressibility parameter, this parameter is affected mainly by the sample size and D/H ratio scale being less than 2.

7.8 Summary

An evaluation and explanation of the current study findings are presented in this chapter. This has entailed providing a reasonable significance of the acceptability of the results to expectation and the literature. The evaluations from both sample height and diameter scale have been shown to relate to the sample D/H ratio scale.

The consolidation test is carried out over 24 hours as per Standards using fine-grained soils. Time was then increased from 24 hours to 7 days in order to reach the end of primary consolidation (EOP). Hence, findings obtained are in good agreement with the literature, and the Standard value was confirmed in this study, with a 0.5% difference between standard and the current study.

CHAPTER 8

CONCLUSIONS AND RECOMMENDATIONS

8.1 Conclusions

An experimental and analytical study on the effect of sample scale on the compressibility parameters of fine-grained soil has been carried out. The experimental programme involved measuring the coefficient of consolidation (c_v) using a range of methods, and compression index (c_c) and coefficient of volume of compressibility (m_v) using equations presented in Table A.6. The experimental investigation also included microstructural investigation using the X-ray diffraction (XRD) and scanning electron microscope (SEM) for the soil under investigation. The analytical study on the other hand was based on validating the experimental data using PLAXIS 2D. The validation was achieved using the measured void ratio and coefficient of permeability (calculated and estimated). The void ratio was derived using equation A.3. Based on the analysis of both the experimental and FEM data presented in Chapters 4, 6 and 7, the following conclusions can be drawn.

1. In order to obtain c_v, three methods were used: the Casagrande, Taylor's and Inflection methods. In accordance with the relevant code of practice, to determine c_v, the experimental curve should match the theoretical curve. However, it was shown in the current study that at some sample scales the experimental time-deformation curve did not match the theoretical curve. This is because when the test was run over a period of 24 hours at each loading, the end of primary consolidation (EOP) was not observed. However, for soil thicknesses less than 30mm, uncertainty in the derivation of c_v using the curve-fitting procedure was found using both the Casagrande and Inflection methods. As a result, a judgement was made to identify the EOP. Hence, compared to the Casagrande and Inflection methods, Taylor's method is considered more appropriate in deriving c_v as the uncertainty issue is removed.

2. In addition to point 1, EOP was not observed at sample scales DS100H200 and DS150H23 when the test was run over 24 hours at each loading. The test was hence repeated for a load duration of 7 days at each loading. Previous researchers had found

that load duration had an effect on c_v values, which was also observed in this study. The value of c_v obtained for DS150H23 ranged from 1 – 7m^2/yr and 1 – 35m^2/yr for DS100H200, with c_v ranging from medium to high rate of consolidation as the load duration varied from 24 hours to 7 days (refer to section 4.5.7).

3. The significant differences in the value of c_v obtained using the Casagrande, Taylor's and Inflection methods were analysed in SPSS (Statistical Package for the Social Sciences). This was achieved using the one-way ANOVA method as described in section 4.5.1. The statistical analysis in the current study showed that, irrespective of sample scale, there was an insignificant difference of 0.01 in c_v value between each method.

4. The influence of sample thickness on the coefficient of consolidation (c_v) plays an important role in settlement calculations. The accurate prediction of the rate and amount of settlemet is crucial to engineers. In the current study various soil thicknesses, ranging from 23mm to 200mm, produced a range of c_v values from 1-36m^2/yr. c_v was found to vary significantly with an average correlation factor from both tests 5 and 6 of 0.615.

5. Sample diameter scale was investigated in this study using Oedometer apparatus cell sizes ranging from 100mm – 250mm. A series of consolidation tests have shown that as the soil diameters vary, this has a significant influence on c_v with a correlation factor of 0.027. The low correlation factor shows the dependency of c_v on the diameter scale, which could be affected by the drainage path and the sample diameter to height ratio relationship.

6. In accordance with the American Standards, a D/H ratio of 2.5 is recommended during the consolidation analysis, while the British Standards refer to the Oedometer size with no inclusion of to the D/H ratio (refer to section 2.8.4). To the author's knowledge, this thesis presents for the first time the D/H ratio effect in consolidation tests for the reason mentioned above. During the consolidation analysis, data were analysed under the assumption of a frictionless boundary condition between the soil and the Oedometer apparatus. In practice, some friction still exists. Hence, the D/H ratio recommended by the American Standards was to reduce friction. In the current study, the D/H ratio effect was investigated in two stages.

Firstly, an attempt at deriving the percentage of friction reduction was completed using Sivrikaya and Togrol's (2006) derivation (refer to section 4.5.5). It was observed that friction was reduced on average by 35% at all sample scales except at D/H of 4. This is because Sivrikaya and Togrol's (2006) derivation is directly proportional to the stress and inversely proportional to sample scale. At D/H of 4 (DS100H23), the material of the oedometer apparatus used was plastic, which might have affected the maximum load the cell could sustain at this sample scale (refer to Table 3.4). Hence, Sivrikaya and Togrol's (2006) derivation, which is based on overconsolidated soil, was found not applicable to the current study, due to the inconsistency in friction reduction with D/H ratio effect.

Secondly, a statistical analysis in SPSS on the effect of D/H ratio on c_v was completed with a correlation factor value of 0.711.

7. The influence of sample scale on other compressibility parameters such as compression index (c_c) and coefficient of volume compressibility (m_v) were also investigated. This has not previously been investigated and the current study showed that as the height and/or diameter increases, c_c has the tendency to decrease. Similarly, m_v was observed to fluctuate as the height and/diameter and pressure increase. This contradicts the findings by Retnamony and Mether (1998), where m_v was found to surge with a rise in pressure for kaolinite soil. Statistical analysis showed that at the diameter scale there was a correlation factor of -0.161 and -0.172 for c_c and m_v respectively; height scale -0.006 and -0.045 and D/H ratio 0.052 and 0.090 (refer to section 4.5.4). Hence, sample scale has an effect on c_c and m_v but the effect is not significant except at DS100H200, which yielded a high degree of compressibility of 5.92×10^{-3} m^2/MN. The high compressibility as compared to the theoretical value in the literature is due to D/H being less than 2.

8. The effect of moisture content on compressibility parameter was previously studied by researchers such as Lei et al. (2014) and Phanikumar and Amrutha (2014). In the current study, a series of saturated fine-grained soils at various initial moisture contents was conducted (section 4.5.6). The investigation showed a positive correlation factor between the initial moisture content and c_v of 0.546. Similarly, a correlation factor of 0.162 and 0.026 was noted with c_c and m_v respectively. Hence,

the current study validates findings by previous researchers where moisture content has an effect on the compressibility parameter, especially at c_c and m_v.

9. An attempt on the finite difference method (FDM) on sample scale has been shown to be challenging, due to the fact that the outcome obtained did not complement the current study (refer to section 5.3.3). Hence, due to the ambiguity presented with the FDM, the finite element method (FEM) was used to validate the experimental data using PLAXIS 2D. The numerical analysis was conducted in four stages: input parameter analysis, FEM calibration, FEM comparison with experimental data and new FEM analysis. Below is a concise description of each stage:

   During the FEM, two parameters were crucial: strength and coefficient of permeability. The undrained shear strength was measured using the Vane shear test, and the coefficient of permeability (k) was calculated using Equations 2.9 and 2.10 and was estimated within PLAXIS 2D (refer to section 5.4.2.1 and 6.5.3). The outcome revealed that the estimated coefficient of permeability (k_e) relates well with the experimental solutions and is consistent across all sample scales. However, in the calculated coefficient of permeability values (k_c^1 and k_c^2) there was fluctuation in the behaviour at all sample scales, and these were therefore considered not reliable. Hence, k_e value was maintained at all sample scale simulations (refer to section 7.4). Where simulation was incomplete due to NAN (not a number) found, the strength was increased to a maximum 50kN/m^2 in accordance with previously derived values for Kaolin clay by previous researchers (refer to Table A.3).

   Before the FEM was compared with the experimental data, a calibration was conducted, as presented in section 6.6. The result showed that there is a 2% difference between the applied load (experimental load) and the excess pore pressure (FEM load output) at all sample scales except at D/H 4 with 9% difference and D/H < 1 with a overall difference of 89%.

   Sample scale outcome trends were found to correlate well with the FEM, especially at D/H greater than 2. At D/H ratio less than 2, there was an irregularity in behavioural trends which was due to the D/H being less than the recommended value of 2.5 and observed value of 2 (refer to Figures 6.11 and 6.12). Hence, the experimental findings were positively validated in PLAXIS.

In addition to point 5, one of the issues for the effect of diameter scale on the compressibility behaviour of fine-grained soil was due to the drainage path. Hence a new finite element model was designed within PLAXIS to incorporate different drainage scenarios (refer to section 6.9). The new approach showed that there was an average of 50% difference between the vertical drainage and case 1 (horizontal drainage) when the estimated coefficient of permeability (k_e) was used (Figures 6.15 and 6.16). Case 2 (combined vertical and horizontal drainage) and the vertical drainage produced consistent identical excess pore pressures at all sample scales with D/H greater than 2. The consistency in the simulation could be associated to the sample scale and strength of the soil. However, where the calculated coefficient of permeability was used, there was an inconsistent fluctuation in the model simulation (refer to Figures 6.20 to 6.23). This outcome was noticed to be dependent on the coefficient of permeability used, which was also stated in PLAXIS 2D (2011).

8.2 Recommendations for Future work

1. In this thesis, a D/H ratio greater than 2 was shown to produce a lower settlement and coefficient of consolidation as compared to D/H less than 2. Sample diameter scale was also observed to be crucial, where an increase in diameter leads to a reduction in settlement, which is linked to the D/H ratio and drainage path. Therefore, it needs to be confirmed that the analysis of sample diameter scale with the implementation of horizontal sand drains will not deviate greatly from the current findings.

2. It is recommended to measure the shear strength and coefficient of permeability at each loading stage of the consolidation process to provide a better comparison of the values instead of trends. The excess pore pressure could also be measured using miniature piezometers. A set of miniature piezometers is inserted at various depths within the soil matrix after the preconsolidation pressure is complete. This is because, on a denser soil sample, the miniature piezometer will not change position as the load increases. A hole is drilled into the soil matrix to the required depth to insert the miniature piezometer.

REFERENCES

ABBASI N., RAHIMI H., JAVADI A.A. & FAKHER A. 2007. Finite difference approach for consolidation with variable compressibility and permeability. *Computers and Geotechnics*, 34, Pp.41-52

ABBASI N., JAVADI A.A. & BAHRAMLOO R. 2012. Prediction of Compression Behaviour of Normally Consolidated Fine-grained soils. *World Applied Science Journal*, 18(1), Pp.6-14

ABU-FARSAKH M. 2011. Control of embankment settlement field verification on PCPT prediction methods. *Louisiana Transportation Research Centre*, Report 476, Pp.1-2

AISSA C. & ABDELDJALIL Z. 2013. Modelisation numerique et analyse de comportment d'un ecran de soutenement autostable. *31eme rencontres de L'AUGC*, E.N.S., Cachan, Pp.1-13

AKSOY Y.Y. & KAYA A. 2013. Specific surface area effect on compressibility behaviour of clayey soils. *Proceedings of the Institution of Civil Engineers, Geotechnical Engineering*, 166(GE1), Pp.76-87

AL-KHUZAIE H.M. 2011. Verification of Scale effect of shallow foundation in determination of bearing capacity of sandy soil. *Al-Rafidain Engineering*, 19(2), Pp.1-11

ALMEIDA M.S.S. & MARQUES M.E.S. 2002. The behaviour of Sarapui Soft Clay. *Proceeding international workshop on characterisation and engineering properties of natural soils*, Singapore, Pp.1-30

AL-SHAMRANI M.A. 2005. Applying the Hyperbolic Method and C_α/C_c concept for settlement prediction of complex organic –rich soil formations. *Engineering Geology*, 77, Pp.17-34

ALSHERNAWY A.O.S. 2007. Determination of the Coefficient of Consolidation using different methods and study the effect of applied pressure for different type of soils. *King Saud University, College of Engineering, Research Centre*. PP.1- 75

AL-TABBAA A.W. 1987. Some measurements of the permeability of Kaolin. *Geotechnique,* 37(4), Pp.499-503

AL-ZOUBI M.S 2010. Consolidation analysis using the settlement rate-settlement (SRS) method. *Applied clay science*, (1), Pp.34-40

AL-ZOUBI M.S 2013. Consolidation analysis by the Slope and Settlement Rate – Settlement Methods. *Journal of Civil Engineering*, 7(4), pp. 377-391

AL-ZOUBI M.S. 2008. Consolidation Characteristics Based on a Direct Analytical Solution of the Terzaghi Theory. *Journal of Civil Engineering*, 2(2), pp.91-99

AMERICAN SOCIETY FOR TESTING AND MATERIAL, 'D2435' 2003. Standard test method for one-dimensional consolidation properties of soils

AMERICAN SOCIETY FOR TESTING AND MATERIALS 'D2571' 2001. Standard test method for field vane shear test in cohesive soils.

AMERICAN SOCIETY FOR TESTING AND MATERIALS, 'D2216' 2010. Standard test methods for laboratory determination of water (moisture) content of soil and rock by mass

AMERICAN SOCIETY FOR TESTING AND MATERIALS, 'D2922' 2001. Standard test methods for density of soil and soil-aggregate in place by nuclear methods (Shallow Depth)

AMERICAN SOCIETY FOR TESTING AND MATERIALS, 'D4318' 2010. Standard test method for liquid limit, Plastic limit and plasticity index of soils.

AMERICAN SOCIETY FOR TESTING AND MATERIALS, 'D854' 2010. Standard test methods for specific gravity of soil solids by water pycnometer.

ANDERSLAND O.B. & AL-KHAFAJI A. 1992. Geotechnical engineering and soil testing. *Oxford University Press*

ARMSTRONG D. 2006. Consolidation drainage of fine-grained materials. *International journal of mine water*, Pp.1-14

BARNES G. 2010. Soil mechanics: Principle and practice. *3rd Edition, Palgrave Macmillan*, Pp.10-11

BARRON R.A. 1948. Consolidation of fine-grained soils by drain wells. Transactions ASCE, 113, Pp.718-754

BERRY P.L. & REID D. 1987. An introduction to soil mechanics. *McGraw Hill*, Pp.100-137

BIOT M.A. 1941. General theory of three-dimensional consolidation. *Journal of Applied Physics*, 12, Pp.155-164

BLACK J.A., STANIER S.A. & CLARKE S.D. 2009. Shear wave velocity measurement of kaolin during undrained unconsolidated triaxial compression. *In: Proceedings of the 62nd Canadian Geotechnical Conference*, Halifax, Canada, Pp.1-8

BOLTON M.D., GUI M.W. & PHILLIPS R. 1993. Review of miniature soil probes for model tests. *Eleventh Southeast Asian Geotechnical Conference*, Singapore, Pp.85-90

BRINKGREVE R.B.J. 2013. Validating geotechnical finite element models. *Proceeding of the 3rd International Symposium on Computational Geomechanics (COMGEO III)*, Krakow, Poland, Pp.292-304

BRITISH STANDARD, BS1377: PART 2, 1990. Methods of tests of soils for civil engineering purposes – Classification Tests.

BRITISH STANDARD, BS1377: PART 4, 1990. Methods of tests of soils for civil engineering purposes – Compaction-related tests.

BRITISH STANDARD, BS1377: PART 5, 1990. Methods of tests of soils for civil engineering purposes - Compressibility, permeability and durability tests

BRITISH STANDARD, BS1377: PART 6, 1990. Methods of tests of soils for civil engineering purposes – Consolidation and Permeability tests in hydraulic cells and with pore pressure measurement

BRITISH STANDARD, BS1377: PART 7, 1990. Methods of tests of soils for civil engineering purposes – Shear strength tests (Total stress).

BUDHU M. 2000. Soil Mechanics & Foundations, *John Wiley & Sons*.

BURNS C.A., GAUGLITZ P.A. & RUSSELL R.L. 2010. Shear strength correlations for Kaolin/Water slurries: A comparison of recent measurements with historical data. *U.S. Department of Energy under contract DE-AC05-76RL01830*, Washington, Pp.1-42

CALABRIA C.R. 1996. Series Consolidation of Organic Soils. *PhD thesis, Department of Civil Engineering,* University of Salford, pp. 66 -116

CASAGRANDE A & FADUM R.E 1940. Notes on soil testing for engineering purposes. *Soil Mechanics Series.* Graduate school of Engineering, Harward University, Cambridge, M.A.

CAVALCANTI M.C. & TELLES J.C.F. 2003. Biot's consolidation theory – Application of BEM with time independent fundamental solutions for poro-elastic saturated media. *Engineering analysis with boundary elements*, 27, Pp.145-157

CERATO A.B. 2001. The influence of specific surface area of geotechnical characteristics of fine-grained soils. *MSc thesis*, Massachusetts University, Amherst, MA, USA.

CERATO A.B. & LUTENEGGER A.J. 2007. Scale effects of shallow foundation bearing capacity on granular material. *Journal of geotechnical and geoenvironmental engineering*, 133(10), Pp.1192-1202. DOI: 10.1061/ (ASCE) 1090-0241(2007)133:10(1192)

CERATO A.B., MILLER G.A. & HAJJAT J.A. 2009. Influence of clod-size and structure on wetting-induced volume change of compacted soil. *Journal of geotechnical and geoenvironmental engineering*, Pp.1620-1628. DOI: 10.1061/ (ASCE) GT.1943-5606.0000146

CLEOMENCE E. 2005. Scale and fabric effect on one-dimensional compression behaviour of compacted soils. *MS Thesis*, University of Oklahoma, Norman, Oklahoma

CODUTO D.P. 1999. Geotechnical Engineering: Principles and Practices. *Prentice Hall*, Pp.220-460

COHEN J. 1988. Statistical power analysis for the behavioural sciences. *2nd edition, New Jersey*, Lawrence Erlbaum

CONTE E. & TRONCONE A. 2006. One-dimensional consolidation under general time-dependent loading. *Canadian Geotechnical Journal*, 43, Pp.1107-1116

CORNWALL COUNCIL 2013. China Clay. *Technical paper M1*, Pp.3-22

CORTELLAZZO G. 2002. Comparison between laboratory and in situ values of the coefficient of primary consolidation c_v. *Canadian Geotechnical Journal*, 39, Pp.103-110

COUR F.F. 1971. Inflection point method for computing c_v. *Journal of the soil mechanics and foundation engineering division*, ASCE, 97 (5), Pp. 827-831

CRAIG R.F. 2004. Craig's Soil Mechanics 7th Edition, *Department of Civil Engineering*, Dundee, UK.

DAFALLA M.A. 2013. Effects of clay and moisture content on direct shear tests for Clay-Sand Mixtures. *Advanced in Materials Science and Engineering*, Research Article, Pp.1-8

DARCY H. 1856. Determination des lois d'ecoulement de l'eau a travers le sable. *In: Les fontaines publiques de la ville de Dijon*, Victor Dalmont, Paris, Pp.590 - 594

DASAKA S.M. 2005. Probabilistic site characterization and reliability analysis of shallow foundations and slopes. *PhD thesis, Department of Civil Engineering, Indian Institute of Science,* Bangalore, P. 1

DASGUPTA T. 2013. Geotechnical aspects of light structure on expansive soils. *International journal of scientific engineering and technology,* 2(12), Pp. 1187-1193

DAVIS F.H. & RAYMOND G.P. 1965. A non-linear theory of consolidation. *Geotechnique,* 15(2), Pp.161 - 173

DEY A. 2011. Calibration of a PLAXIS Finite Element Dynamic Model : Effect of Domain Width and Meshing Schemes/AES. *Third Indian Young Geotechnical Engineers Conference,* Indian Geotechnical Society, Pp.127 - 132

DI MAIO C., SANTOLI L., & SCHIAVONE P. 2004. Volume change behaviour of clays: The influence of mineral composition, pore fluid composition and stress state. *Mechanics of Materials,* 36(5-6), Pp.435-451

DING D., LIKOS W.J. & LOEHR E. 2014. Variability and Uncertainty in consolidation and settlement parameters from different sampling and testing methods. *From soil behaviour fundamentals to innovations in Geotechnical Engineering,* Pp.338-351

DIRGELIENE N., JONAS A. & STRAGYS V. 2007. Effects of end conditions on soil shear strength parameters during Triaxial Testing. Pp. 1-6, http://leidykla.vgtu.lt/conferences/MBM_2007/5pdf/Dirgeliene.pdf

DIXIT M.S. & PATIL K.A. 2013. Effect of shape of footing and water table on bearing capacity of soil. *EJGE, BUND.G,* Vol. 18, Pp.1655-1667

DUNCAN M.J. ASCE. 1993. Limitations of conventional analysis of consolidation settlement. *Journal of Geotechnical Engineering,* 119(9), Pp.1333-1359

FANG H.Y & DANIELS J. 2006. Introductory Geotechnical Engineering: An environmental perspective. *Taylor & Francis,* Pp.259-266

FENG T.W. 2001. Using a $\sqrt{t_{60}}$ Method to determine the coefficient of consolidation of two clays. *Proceeding of the eleventh international offshore and polar engineering conference*, Stavanger, Norway, Pp.413-416

FENG TAO-WEI & LEE YI-JIUAN 2001. Coefficient of consolidation from the linear segment of the $t^{1/2}$ curve. *Canadian Geotechnical Journal*, 38, Pp.901-909, DOI: 10.1139/cgj-38-4-901

FENG TAO-WEI 2010. Some observations on the oedometric consolidation strain rate behaviours of saturated clay. *Journal of GeoEngineering*, 5 (1), Pp. 1-7

FOGUET A.P., LEDESMA A. & HUERTA A. 1998. Analysis of the Vane test considering size and time effects. *International Journal for Numerical and Analytical Methods in Geomechanics*, Pp.1-40

FONTE J.B. 2010. Numerical modelling of excavations below the water table. Master thesis, Department of Civil Engineering, Engineering College Harbor University, Pp. 13-15

FOUNDATION SUPPORT WORKS 2014. What causes foundation settlement: Identifying the settlement issues in your home and providing lasting solutions? [Online] Available from http://www.foundationsupportworks.com/foundation-repair/foundation-settlement/what-causes-foundation-settlement.html [Accessed: 28th August 2014]

GENG X. 2008. Non-linear consolidation of soil with vertical and horizontal drainage under time-dependent loading. *International Conference on Advanced Computer Theory and Engineering*, Pp.800-804

GHOSH R. 2013. Effect of soil moisture content in the analysis of undrained shear strength of compacted clayey soil. *Journal of Civil Engineering and Construction Technology*, 4(1), Pp.23-31

GONG Y., CAO. & SUN Z. 2003. The effect of soil bulk density, clay content and temperature on soil water content measurement using time-domain reflectometry. *Hydrological Processes*, 17, Pp.3601-3614 DOI: 10.1002/hyp.1358

GRABOWSKI R.C. 2014. Measuring the shear strength of cohesive sediment in the field. *British Society for Geomorphology*, Geomorphological Techniques, Part 1, Section 3.1, Pp.1-7

GRISSO R.D., JOHNSON C.E., BAILEY A.C. & NICHOLS T.A. 1984. Influences of soil sample geometry on hydrostatic compaction. *American Society of Agricultural Engineers*, DOI: 0001-2351/84/2706-1650$02.00, Pp.1650-1653

GUILI G, DEQUAN S & JINGWEI D. 2012. Review on the methods for measuring the moisture content of green sand. *Proceedings of the international conference on mechanical engineering and material science*. Atlantis Press, Pp. 501-504

HAGHIGHI A. 2011. Thermo-Hydro-Mechanical behaviour of kaolin clay. *Doctor of Philosophy, Heriot-Watt University.*

HANSBO S. 1981. Consolidation of fine-grained soils by prefabricated drains. *In: Proceeding of 10th international conference on soil mechanics and foundation engineering*, Stockholm, Balkema, Rotterdam, 3, Pp.677-682

HASSAN A.M. 2013. Elasto-Plastic Finite Element One-Dimensional Consolidation Analysis. *Minia Journal of Engineering and Technology*, 32(1), Pp.78-82

HAWLADER B.C., IMAI G. & MUHUNTHAN B. 2002. Numerical study of the factors affecting the consolidation of clay with vertical drain. *Geotextiles and Geomembranes*, 20, Pp.213-239

HEAD K.H. 1998. Manual of Soil Laboratory Testing. *Effective stress tests*, 2nd edition, Vol.3, Pp. 340 - 367

HEALY K.A. & RAMANJANEYA G.S. 1970. Consolidation characteristic of a Varved Clay. *Report*, Department of Civil Engineering, University of Connecticut

HILLEL D. 1980. Fundamental of soil physics. *Academic Press*, Pp. 11-19

HOLTZ R.D & KOVACZ W.D 1981. An introduction to geotechnical engineering, *Prentice-Hall, Inc., Englewood Cliffs, New Jersey.*Pp.380-409

HONG Z.S., YIN J. & CUI Y.J. 2010. Compression behaviour of reconstituted soils at high initial water contents. *Geotechnique*, Thomas Telford (ICE Publishing), 60(9), Pp.691-700

HOUSTON S.L, HOUSTON W.N & SPADOLA, D. 1988. Prediction of Field Collapse of Soils Due to Wetting. *Journal of Geotechnical Engineering,* 114**,** Pp.40-58.

IBM SPSS 2009. SPSS statistics since 2009. [Online] Available from http://www-01.ibm.com/software/analytics/spss/products/statistics/downloads.html. [Accessed: 22nd May 2014]

IMAI G. & NAWAGAMUWA U.P. 2005. Consolidation of clayey sub-soils with intermediate permeable layers improved by vertical drains with smear effect. *International Association of Lowland Technology (IALT),* 7(2), Pp.1-11

INDRARATNA B. & REDANA I.W. 2000. Numerical modelling of vertical drains with smear and well resistance installed in soft clay. *Canadian Geotechnical Journal*, 37(1), Pp.133-145

INDRARATNA B., RUJIKITHAMJORN C. & SATHANANTHAN I., 2005. Radial consolidation of clay using compressibility indices and varying horizontal permeability. *University of Wollongong Research Online*, Pp.1-10

JAMIOLKOWSKI M., LANCELLOTTA R. & WOLSKI W. 1983. Precompression and speeding up consolidation. *In Proceeding of the 8th European Conference on Soil Mechanics and Foundation*, Helsinki, Finland, 3, Pp.1201-1206

JENNINGS J.E & KNIGHT K 1975. A guide to construction on or with materials exhibiting additional settlement due to collapse of grain structure. *Proceedings of the 6th Regional Conference for Africa on Soil Mechanics and Foundation Engineering*, Durban, South Africa. Pp.99-105.

KATARZYNA G & ALOJZY S 2010. The analysis of consolidation in organic soils. *Annals of Warsaw University of life Sciences - SGGW,* 42**,** Pp.261 - 411.

KHAN P.A., MADHAV M.R. & REDDY E.S. 2012. Comparative study of linear and non-linear theories one-dimensional consolidation of thick clay layers. *Lowland Technology International,* 14(1), Pp.19-30

KOLEKAR Y.A. & DASAKA S.M. 2013. Variability in the soil properties of laboratory consolidated clay beds. *International Journal of Geotechnical Engineering*, 8(4), Pp.365-371

KOTIYA N.R. & VANZA M.G. 2013. Effect of H/D ratio on stress-strain characteristics of clayey soil in Triaxial Test. *Indian journal of research*, 2(7), ISSN – 2250-1991, Pp.101-103

KWONG A.K.L., LAU C.K., LEE C.F., NG C.W.L., PANG P.L.R., YIN J.H. & YUE Z.Q. 2001. Soft soil engineering. *Published by Francis & Taylor,* P.698

LAERD STATISTICS 2013. Pearson's Product-Moment Correlation Using SPSS. [Online] Available from https://statistics.laerd.com/spss-tutorials/pearsons-product-moment-correlation-using-spss-statistics.php [Accessed: 29th September 2014]

LAI J. 2004. Application of finite difference methods to the solution of consolidation problems. *Department of Construction Engineering Chaoyang University of Technology, Advanced soil mechanics*, Pp.68-92

LAMBE T.W & WHITMAN R.V. 1979. Soil mechanics. *John Wiley and Sons,* Pp.45-51

LASZLO M., GYORGY P. & PETER K. 2010. Effect of varying moisture content and settlement on the internal friction, load capacity and cohesion in loam soils. *FISITA*, Pp.1-5

LE K.H. 1988. Finite element mesh generation methods: a review and classification. *Butterworth and Co (Publishers),* 20(1), Pp.27-38

LEI H., CHEN L., HUANG M., WANG X., & ZHANG W. 2014. Experiment on the consolidation property of dredger soft soil under different moisture contents in Tianjin. *Soil behaviour and Geomechanics Geo-Shanghai*, Pp.110-124

LEKHA K.R., KRISHNASWAMY N.R. & BASAK P. 2003. Consolidation of clays for variable permeability and compressibility. *Journal of Geotechnical Geoenvironmental Engineering*, 129, Pp.1001 - 1009

LENK P. 2009. Modelling of Primary Consolidation, *Slovak Journal of Civil Engineering*, Pp.26-37

LEO C.J. 2004. Equal strain consolidation by vertical drains. *Journal of Geotechnical Geoenvironmental Engineering*, Pp.316-327

LEROUEIL S. 1988. Tenth Canadian Geotechnical colloquim: Recent developments in consolidation of natural clays. *Canadian Geotechnical Journal*, 25(1), Pp.85-107

LI A.L. & ROWE R.K. 2001. Combined effect of reinforcement and prefabricated vertical drains on embankment performance. Canadian Geotechnical Journal, 38, Pp.1266-1282

LIU C. & EVETT J.B. 2005. Soils and Foundations. *SI Edition, Prentice Hall*, Pp.113-196

LOFROTH H. 2008. Undrained shear strength in clay slopes – Influence of stress condition. *PhD thesis, Department of Civil and Environmental Engineering*, Chalmers University of Technology, Sweden, pp. 30 -33

LONG R.P., CAREY P.J. & HOVER W.H. 1980. Determining the Shear strength of Varved clay using Vane shear. *Final Report*, Civil engineering department, School of Engineering, University of Connecticut, Pp.1-19

LUN P.T.W. & PARKIN A.K. 1985. Consolidation behaviour determined by the velocity method. *Canadian Geotechnical Journal*, 22(2), Pp.158-165

MAHMOUD M. 1988. Vane testing in soft soils. *Report of British Geotechnical Society's Informal Discussion*, Pp.36-40

MASCH F.D. & DENNY K.J. 1966. Grain size distribution and its effect on permeability. *Water Resources Research*, 2(4), Pp.665-677

MCCARTHY D.F. 2002. Essentials of Soil Mechanics and Foundations. Basic Geotechnics, 6th edition, Pp.396-419

MCLAREN R.G & Cameron K.C. 2005. *Soil Science:* Sustainable Production and Environmental Protection. Pp.85-91

MCNULTY, E.G., GORMAN C.T. & HOPKINS T.C. 1978. Analysis of Time-Dependent Consolidation Data. *Proceedings of the use of computers in Geotechnical Design and Construction*, American Society of Civil Engineers, P.2

MEIJER K.L. 1985. Computation of stresses and strains in saturated soil. *Thesis*, Pp.4-7

MESRI G. & CHOI Y.K. 1985. Settlement analysis of embankments on soft clays. *Journal of Geotechnical Engineering*, ASCE, 111, Pp.441-464

MESRI G. & ROKHSAR A. 1974. Consolidation of normally consolidated clay. *Journal of soil mechanics and foundation division*, ASCE, 100(GT8), Pp.889-903

MESRI G., FENG T.W. & SHABIEN M. 1999. Coefficient of consolidation by Inflection point method. *Journal of geotechnical and geoenvironmental engineering*, Pp. 716-1212

MESSERKLINGER S., ZUMSTEG R. & PUZRIN A.M. 2011. A new pressurized Vane shear apparatus. *Geotechnical Testing Journal*, 34(2), Pp.1-10

MILLER G.A. & CLEOMENCE E. 2007. Influence of fabric and scale effect on wetting-induced compression behaviour of compacted soils. *Proceeding, GeoDenver: New Peaks in Geotechnics*, ASCE, Pp.1-10

MORRIS P. & LOCKINGTON D. 2002. Geotechnical Compressibility and consolidation parameters and correlations for remoulded fine-grained marine and riverine sediments. *Research Report, CRC for Sustainable Tourism*, P.26

MUNTOHAR A.S. 2009. Reliability of the method for determining the coefficient of consolidation. Pp.1-5

NAFEMS I.C.W. & ASME 2009. What is verification and validation ? Leaflet. *NAFEMS*, UK, www.nafems.org

NAGARAJ T.S. & SRINIVASA B.R. 1994. Analysis and Prediction of Soil Behaviour. *Taylor and Francis*, P.175

NASER A.H. 2013. Finite difference analysis of one-dimensional consolidation of Homogeneous clay layer. *Journal of Babylon University/Engineering Science*, 2.1(5), Pp.1-14

NDIAYE C., FALL M., NDIAYE M., SANGARE D. & TALL A., 2014. A review and update of analytical and numerical solutions of the Terzaghi One-dimensional consolidation equation. *Open Journal of civil engineering*, 4, Pp.274-284

NEWLAND P.L. & ALLELY B.H. 1960. A Study of the consolidation characteristic of clay. *Geotechnique*, 10(2), Pp.62-74

NOGAMI T. & LI M. 2003. Consolidation of clay with a system of vertical and horizontal drains. *Journal of Geotechnical and Geoenvironmental Engineering*, Pp.838-848

ORTEGA A.G. 1996. Variability of the coefficient of consolidation of the Mexico City clayey sediments on Spatial and Time scales. *In: Bulletin of the International Association of Engineering Geology*, 54 (1), Pp.125-135

PARK J.H. & KOUMOTO T. 2004. New compression index equation. *Journal of Geotechnical and Geoenvironmental Engineering*, 30(2), Pp.223-226

PARKIN A.K & LUN P.T.W 1984. Secondary consolidation effects in the application of the velocity method. Geotechnique, 34(1), Pp. 126-128

PARKIN A.K. 1978. Coefficient of consolidation by the velocity method. *Geotechnique*, 28 (4), Pp.472-474

PARKIN A.K. 1981. Consolidation analysis by the velocity method. *Proceedings of the 10th International Conference on Soil Mechanics and Foundation Engineering*, Stockholm, Vol. 1, Pp.723-726

PECK R.B 1974. Foundation Engineering, 2nd edition, New York: Wiley

PHANIKUMAR B.R. & AMRUTHA K. 2014. Effect of overburden pressure and degree of saturation on compressibility characteristics. *Geomechanics and Geoengineering*, 9(1), Pp.52-62

PLATT M.R. 2013. Settlement assessment of highway embankment for SR77/1500 West interchanges in Springville Utah. *Master of Science thesis, Department of Civil and environmental engineering*, P.48

PLAXIS 2D 2011. Reference manual. Essential for geotechnical engineering

POPA H. & BATALI L. 2010. Using finite element method in geotechnical design. Soil Constitutive laws and calibration of the parameters. Retaining wall case study. *WSEAS Transactions on Applied and Theoretical Mechanics*, 5(3), Pp.177-186

POWRIE W. 2004. Soil Mechanics: Concepts and Applications. *2nd Edition, E & FN Spon*, Pp.10-250

PRAKASH K., SRIDHARAN A. & PRASANNA H.S. 2011. On the coefficient of consolidation of compacted soils. *Proceedings of Indian Geotechnical Conference*, No.A-232, Pp.113-116

REEVES G.M., SIMS I. & CRIPPS J.C. 2006. Clay materials used in construction. *Geological Society Engineering Geology Special Publication*, the Geological Society, No.21, P.233

RENDULIC L. 1935. Der hydrodynamische Spannungsangleich in zentral entwasserten Tonzylindren, Wasserwirt. Technology, Pp.269-273

RENDULIC L. 1936. Porenziffer und porenwasserdruck in tonen. *Der Bauingenieur*, 17 (51/52), Pp.559-564

RETNAMONY G.R. & METHER M. ALLAM 1998. Effect of clay mineralogy on coefficient of consolidation. *Clay and minerals*, 46 (5), Pp. 596-600

ROBINSON R.G. & ALLAM M.M. 1996. Determination of the coefficient of consolidation from early stage of log t plot. *Geotechnical Testing Journal*, 19(3), Pp.316-320

ROBINSON R.G. & ALLAM M.M. 2002. Coefficient of consolidation from the linear of the √t curve: Discussion. *Canadian Geotechnical Journal*, 39, Pp.1000-1001

ROBINSON R.G. 1997. Consolidation analysis by an inflection point method. *Geotechnique*, 47(1), Pp.199-200

ROBINSON R.G. 1999. Consolidation analysis with pore water pressure measurements. Geotechnique, 49(1), Pp. 127-132

ROSINE T.N. & SABBAGH T.T. 2015. The impact of the diameter to height ratio on the compressibility parameters of saturated fine-grained soils. *International Journal of Research and Engineering Technology*, 4(5): 8 - 19

RUN L., WANG Y.S., FU Z.L. 2004. Vane shear strength based stability analysis of slopes in unconsolidated soft clay. *Transactions of Tianjin University*, 10(3), Pp.1-6

SCRIVENER R.C., HIGHLEY D.E., CAMERON D.G., LINLEY K.A. & WHITE R. 1997. Mineral resource information for development plans phase one Cornwall: Resources and Constraints. *British Geological Survey*, Techincal report WF/97/11, Pp.1-36

SEAH T.H. & JUIRNARONGRIT T. 2003. Constant rate of strain consolidation with radial drainage. *Geotechnical Testing Journal*, 26(4), Pp.1-12

SEAH T.H., SANGTIAN N. & CHAN I.C. 2004. Vane shear behaviour of soft Bangkok clay. *Geotechnical Testing Journal*, 27(1), Pp.1-10

SEROTA S. & JANGLE A. 1972. Direct-Reading Pocket Shear Vane. Civil Engineering, 42, Pp.73-74

SHARIFOUNNASAB M. & ULLRICH C.R. 1985. Rate of shear effects of Vane shear strength. *Journal of Geotechnical Engineering*, 111(1), Pp.135-139

SHEPHERD R.G. 1989. Correlations of permeability and grain size. *Ground water*, 27 (5), Pp.633-638

SHIELDS D.H. & ROWE P.W. 1965. Radial drainage Oedometer for Laminated clays. *Journal of soil mechanics and foundations division*, ASCE, 91(1), Pp.15-24

SIDDIQUE A. & SAFIULLAH A.M.M. 1995. Permeability characteristics of reconstituted Dhaka Clay. *Journal of the Civil Engineering Division*, The Institute of Bangladesh, CE23 (1), Pp.1-13

SINGH A. & NOOR S. 2012a. Soil Compression Index Prediction Model for Fine-grained soils. *International Journal of Innovations in Engineering and Technology (IJLTET)*, 1(4), Pp.34-37

SINGH A. & NOOR S. 2012b. Estimation of soil permeability using soil index properties. *International Journal of Latest Trends in Engineering and Technology (IJLTET)*, 1(4), Pp.31-33

SIVRIKAYA O. & TOGROL E 2006. Measurement of side Friction between specimen and consolidation Ring with Newly Designed Oedometer Cell. *Geotechnical Testing Journal*, 29 (1), Pp.87-94.

SKEMPTON A.W. 1944. Notes on the compressibility of clays. *Quarterly Journal of the Geological society of London*, 100, Pp.119-135

SMITH I. 2006. Smith's Elements of soil mechanics. 8th *Edition, Blackwell Science*, Pp.5-6

SRIDHARAN A. & NAGARAJ H.B. 2012. Coefficient of consolidation and its correlation with Index properties of remoulded soils. *Geotechnical testing journal*, 27, N.5, Pp.1-6

SRIDHARAN A. & PRAKASH K. 2000. Compressibility behaviour of remoulded, fine-grained soils and correlation with Index properties. *Canadian Geotechnical Journal*, 37(3), Pp.712-722

SRIDHARAN A., MURTHY N.S & PRAKASH K. 1987. Rectangular Hyperbola Method of Consolidation Analysis. *Geotechnique*, 37(3), Pp. 355-368

SRIDHARAN A., PRAKASH K. & ASHA S.R. 1995. Consolidation behaviour of soils. *Geotechnical Testing Journal*, Vol.18 (1), Pp.56-68

SRIDHARAN A., SIVAPULLAIAH P.V. & STALIN V.K. 1994. Effect of short duration of load increment on the compressibility of soils. *Geotechnical testing journal*, 17 (4), Pp.488-496

SRIDHARAN Q., NAGARAJ H.B. & SRINVAS N. 1999. Rapid method of consolidation testing. *Canadian Geotechnical Journal*, 36 (2), Pp. 392-400

SUDJIANTO A.T., SURYOLELONO K.B., RIFA A. & MOCHTAR I.B. 2011. The effect of water content change and variation suction behaviour swelling of expansive soil. *International Journal of Civil & Environmental Engineering, IJCEE-IJENS*, 11(3), Pp.11-17

TAN T.S. 1993. Ultimate settlement by hyperbolic plot for clays with vertical drains. *Journal of Geotechnical Engineering*, ASCE, 119(5), Pp.950-956

TAN T.S. 2003. Characterisation and Engineering Properties of Natural soils. *CRC Press*, Vol. 1, Pp.225-227

TANDJIRIA V. 1999. Development of the finite difference method applied to consolidation analysis of embankments. *Dimensi Teknik Sipil*, 1(2), Pp.73-80

TAYLOR D.W 1942. Research on consolidation of clays. Massachusetts Institute of Technology, Cambridge.

TERZAGHI K & PECK R.B. 1996. Soil mechanics in engineering practice. *John Wiley & Sons*. Pp. 104-111

TERZAGHI K. 1925. Erdbaumechanik auf bodenphysikalischer grundlage. Deuticke, Leipzig

TERZAGHI K. 1943. Theoretical Soil Mechanics. *John Wiley and Sons*, Inc., P.510

TERZAGHI K. 1948. Soil mechanics in engineering practice, Pp.232-233

TI K.S., HUAT B.B.K., NOORZAEI J., JAAFAR M.S. & SEW G.S. 2009. A review of basic soil constitutive models for Geotechnical application. *EJGE*, 14, Pp.1-18

WALKER R. & INDRARATNA B., F.ASCE. 2006. Vertical drain consolidation with parabolic distribution of permeability in smear zone. Journal of Geotechnical and Geoenvironmental Engineering, ASCE, Pp.937-941

WANG Y., XIE K. & ZHU J. 2011. An analytical solution for consolidation of Transversely Isotropic soft ground with double radial drainages and a vertical drainage. *EJGE*, 16, Pp.1489-1504

WHITLOW R. 2001. Basic Soil Mechanics 4th Edition. Pp. 11 – 220

WILUN Z. & STARZEWSKI K. 1975. Soil mechanics in foundation engineering. *Properties of soils and site investigations*, 2nd edition, Vol.1, Pp.68

WONG W.K.J. 2013. Comparison of drainage line elements in PLAXIS 2D and 3D applied in consolidating marine clay deposits. *Soft soil engineering international conference*, Kuching, Sarawak, Malaysia, Pp.1-8

WOOD M.D. 2004. Geotechnical modelling. Cambridge University Press, United State of America

YIN J.H & GRAHAM J. 1996. Elastic Visco-Plastic modelling of one-dimensional consolidation. *Geotechnique,* 46 (46), Pp.515-527

YONG R.N., NAKANO M. & PUSCH R. 2012. Environmental Soil Properties and Behaviour. *CRC Press*, Taylor & Francis Group, Pp.25-33

APPENDICES

A – COLLECTION OF FREQUENTLY USED SOIL PARAMETERS

A - 1 Moisture content

For geotechnical purposes, moisture content (w %) is defined as the ratio of the weight of water to the soil mass as shown in equation A.1. The process for obtaining the moisture content is as illustrated in the American Standard D2216 (ASTM, 2010) where the soil is require to dry at 110±5℃ overnight (16-hour drying period). Gong et al. (2003) used a temperature of 105℃ for 48hours to determine moisture content. The temperature and length of time used to dry soils varies with different soils, i.e., peat 105℃ and sand between 105℃ to 110℃, according to Calabria (1996) and Guili et al. (2012) respectively.

$$w = \frac{M_w}{M_s}\ x\ 100 \qquad \text{(A-1)}$$

Where;
M_w is the mass of water (g), M_s is the mass of dry soil (g), and w is the moisture content expressed in percentage.

A – 2 Degree of saturation

The degree of saturation (S_r) has a significant role in the behaviour of soil. The significance is because S_r has an impact on the engineering properties such as settlement. The higher the value of S_r, the greater the rate of settlement as shown by Phanikumar and Amrutha (2014). S_r is defined as the ratio of the volume of water to the volume of the void as shown in equation A.2 and A.3. In saturated soils, S_r equals to 1 as shown in Table A.1.

$$S_r = \frac{V_w}{V_v} \qquad \text{(A-2)}$$

Where;

V_w = volume of water (m^3) and V_v = volume of voids (m^3).

The degree of saturation can also be obtained using the following equation:

$$S_r = \frac{G_s w}{e} \qquad \text{(A-3)}$$

Table A-1: States of saturation of soils (Wilun and Starzewski, 1975)

Degree of Saturation (S_r)	State of Saturation in the Soil
$0 < S_r \leq 0.4$	Dry to Damp
$0.4 < S_r \leq 0.8$	Moist
$0.8 < S_r \leq 1.0$	Wet

A – 3 Void ratio

The void ratio (e) is the ratio of the volume of voids in a representative elemental volume to the volume of soil solids at that same volume as shown in equation A.4 (Calabria, 1996). The swelling and shrinkage behaviour of fine-grained soil is due to the change in void ratio with a change in moisture content (Calabria, 1996).

$$e = \frac{v_v}{v_s} \qquad \text{(A-4)}$$

Where;
v_v is the volume of voids (m^3), and v_s is the volume of dry soil (m^3).

The void ratio can also be expressed in terms of strain (ε) (equation A.5) and change in soil height (equation A.6) after Budhu (2000).

$$\Delta e = e_0 - 1(1 + e_0)\varepsilon \qquad \text{(A-5)}$$

$$e_0 = \frac{e_f + (\frac{\Delta h}{h_0})}{1 - (\frac{\Delta h}{h_0})} \qquad \text{(A-6)}$$

Where;
e_f is the final void ratio obtained by multiplying moisture content by specific gravity given the degree of saturation (S_r) is 1 for saturated soil, ε is the strain (%), Δe is the change in void ratio, e_0 is the initial void ratio, Δh is the change in height (mm) and h_o initial height (mm).

A – 4 Specific gravity and density

The specific gravity (G_s) is used for the analysis of compaction and consolidation behaviour of soils (equation A.7). It is defined as the ratio of the weight of the soil solids to the weight of water of equal volume (Peck, 1974). Its value for clay soils ranges from 2.68 to 2.72 Mg/m^3 (Reeves et al., 2006). Higher values indicate the presence of heavy metal oxide or other compounds in clay soils. While a lower value suggests the presence of organic matter such as peat or particles containing small cavities such as pumice (Reeves et al., 2006). G_s can be obtained in the laboratory using the standard test method described in British Standard BS1377: Part 2 (BS, 1990) and American Standard D854 (ASTM, 2010).

The soil bulk density (ρ) is the ratio of the dry mass with its bulk volume depending on the soil particle density (equation A.8) and their packing arrangement (Peck, 1974). The bulk density is obtained using British Standard BS 1377 Part 4 (BS, 1990) and American Standard

D2922 (ASTM, 2001). The standard value for the dry density of most soils ranges from 1.1 to 1.6 g/cm^3 (Hillel, 1980).

$$G_s = \frac{W_s}{V_s \gamma_w} \quad \text{(A-7)}$$

Where;
W_s is the weight of solid (N), V_s is the volume of dry soil (m^3), and γ_w is the unit weight of water 9.81 kN/m^3

$$\rho = \frac{M_s}{V} \quad \text{(A-8)}$$

Where;
ρ is bulk density (Mg/m^3), M_s is the mass of dry soil (g), and V is the total soil volume (m^3).

A – 5 Shear strength

The proficiency of a soil to support an imposed loading or support itself is governed by the soil shear strength. The shear strength of a clay deposit is associated with the type of clay minerals and the moisture content but, also affected by the soil stress history (McCarthy, 2002). Over the years, many laboratory-based tests have been developed to enumerate the shear strength of fine-grained soils. These tests methods include direct shear test and Triaxial. The process of obtaining the soil shear strength is as described in the British Standard BS1377: Part 7 1990. The shear strength of fine-grained soils can also be achieved in the laboratory using the Vane shear tests. The Vane test is conducted using the American Standard D2571 and British Standard BS1377: part 7 1990. The effectiveness of the vane test occurs when the following factors are met: dimensions of vane, disturbance of vane due to vane insertion, rest period following vane insertion, rate of vane rotation and the time of failure required to ensure undrained condition apply (Mahmoud, 1988).

Table A-2: Summary of the undrained shear strength formulation using the Vane shear test

Parameters	Equation	Comments	Reference
T	$\tau = \frac{c_u \pi}{2} d_v^2 h_v [1 + (\frac{d_v}{3h_v})]$	Torque at failure	Long et al. (1980)
T	$\tau = \pi d_v^2 (\frac{h}{2} c_{uv} + \frac{d_v}{6} c_{uh})$	Torque at failure related to the horizontal and vertical shear strength	Sharifounnasab and Ullrich (1985)
T	$\tau = c_u (3h_v + d_v) \pi \frac{{d_v}^2}{6}$	Torque at failure	Bolton et al. (1993)
τ_v	$\tau_v = \frac{1}{2} \pi d_v^2 h_v c_u$	Torque in the vertical cylindrical surface	Foguet et al. (1998)
τ_h	$\tau_h = \frac{1}{6} \pi d_v^3 c_u$	Torque in the horizontal cylindrical surface	
c_u	$c_u = \frac{\tau}{\pi[\left(\frac{{d_v}^2 h_v}{2}\right) + \left(\frac{{d_v}^3}{6}\right)]}$	Undrained shear strength	
c_u	$c_u = \frac{\tau}{3.66 {d_v}^3}$	Undrained shear strength when vane height equals to twice its diameter	
T	$\tau = \frac{1}{2} \pi d_v^2 h_v c_{uv} + \frac{1}{6} \pi d_v^3 c_{uh}$	Torque under vertical and horizontal undrained shear strength	Run et al. (2004)
c_u	$c_u = \frac{6\tau}{7 d^3 \pi}$	Undrained shear strength	Messerklinger et al. (2011)

Where;

c_u = undrained shear strength (kN/m^2), τ = torque (kgcm), c_{uv} = undrained vertical shear strength (kN/m^2), c_{uh} = undrained horizontal shear strength (kN/m^2), τ_v = torque in the vertical cylindrical surface (kgcm), d_v = vane diameter (mm) and h_v = vane height (mm).

Table A-3: Undrained shear strength gained by previous researchers

Undrained shear strength (kPa)	Samples	Reference
9.65 – 50.6	Kaolinite	Sharifounnasab and Ullrich (1985)
23.6 – 34.1	Bangkok clay	Seah et al. (2004)
15 – 120	Kaolin Speswhite clay	Black et al. (2009)
0.127 – 0.723	Kaolin clay	Burns et al. (2010)
2 – 10	Kaolinite	Messerklinger et al. (2011)
5.2 – 26.8	Clay	Ghosh (2013)
8 – 22	Marine clay	Kolekar and Dasaka (2013)

A – 6 Atterberg Limit

The Atterberg limit is the basic measurement of fine-grained soils. Depending on the water content of the soils, it may appear in four states: solid, semi-solid, plastic and liquid (Budhu, 2000). In each soil state, the consistency and behaviour of soil are different and thus the engineering properties are different. The Atterberg limit (liquid and plastic limit) is obtained according to the American Standard D4318 (ASTM, 2010) and British Standard BS1377: part 2 1990 and the typical values for different soils types are shown in Table A.4. The plastic limit (PL) is the moisture content below which the soil is plastic; while the liquid limit (LL) is the water content below which the soil behaves as a plastic material.

Table A-4: Typical Atterberg limits for soils (Liu and Evett, 2005)

Soils type	LL (%)	PL (%)	PI (%)
Sand		Non-plastic	
Silt	30 – 40	20 – 25	10 – 15
Clay	40 – 150	25 – 50	15 – 100

A – 7 Permeability

Permeability (which refers to the rate of water flowing through a soil) is an imperative engineering property and it is used in a number of engineering problems such as seepage through and below the earth structures (Al-Tabbaa, 1987). Since water movement within the soil is through void spaces, the larger the void space, the greater the permeability. Thus, coarse-grained soils specifically sand, exhibit higher permeability as compared to the fine-grained soil like clay, which has a lower permeability (Liu and Evett, 2005). Hence, the

permeability of soils depends on particle size, the structure of soil mass, the shape of soil and void ratio, with the major factor being the particle size and void ratio. Table A.5 shows the general permeability coefficient of typical soils.

Over the past few decades, several models were developed to show the relationship between permeability and particle size (Masch and Denny, 1966). Singh and Noor (2012b) developed a new relationship between permeability and grain size using regression analysis as shown in equation A.9:

$$k = (d_{10}^2)*(e^3) \qquad \text{(A-9)}$$

Where;
k is the soil permeability (m/s), d_{10} is the average particle size (mm), to such an extent that 10% of the particles are finer than that size (dimensionless), and e is the void ratio (dimensionless) (Singh nd Noor, 2012b).

Also to equation A.9, the soil permeability can also be obtained using the relationship between c_v, m_v and a_v.

$$k = c_v m_v \gamma_w \qquad \text{(A-10)}$$

$$k = \frac{c_v a_v \gamma_w}{1+e} \qquad \text{(A-11)}$$

Where;
c_v is the coefficient of consolidation (m^2/yr), m_v is coefficient of volume compressibility (m^2/MN), a_v is the coefficient of compressibility, e is the void ratio and γ_w is the unit weight of water (kN/m^3).

Table A-5: Ranges of the coefficient of permeability (Whitlow, 2001)

Coefficient of permeability k (m/s)	Drainage	Typical soil
$10^2 – 10^{-1}$	Very good	Clean gravels
$10^{-2} – 10^{-4}$	Good	Clean sands, gravel-sand mixtures, fissures and weathered clays
$10^{-5} – 10^{-6}$	Poor	Very fine sands and silts and silty sands
$10^{-7} – 10^{-9}$	Practically impervious	Clay silts (>20% clay) and (non) fissured clays

A – 8 Compressibility parameters

Table A-6: Summary of the compressibility parameters with their respective equations and units

Parameters	Descriptions	Equations	Units	References
c_v	Coefficient of consolidation	$c_v = \frac{T_v H_D^2}{t}$	m^2/yr	Reeves et al. (2006)
m_v	Coefficient of volume compressibility	$m_v = \frac{\Delta e}{\Delta \sigma'} x \left(\frac{1}{1+e_0}\right)$	m^2/MN	Witlow (2001)
c_c	Compressibility index	$c_c = 0.009 * (LL - 10)$ $c_c = \frac{-(e_2 - e_1)}{\log(\sigma_2' - \sigma_1')}$	Dimensionless	Skempton (1944) Budhu (2000)
a_v	Coefficient of compressibility	$a_v = \frac{\Delta e}{\Delta \sigma'}$	m^2/KN	Witlow (2001)
c_r	Recompression index at unloading/reloading	$c_r = \frac{-(e_2 - e_1)}{\log(\sigma_2' - \sigma_1')}$	Dimensionless	Budhu (2000)
c_s	Swelling index usually takes place at unloading	$c_s = 0.0463 \left(\frac{LL}{100}\right) G_s$	Dimensionless	Nagaraj and Srinivasa (1994)

Where;
T_v = Time factor (dimensionless), H_D = Drainage path length (mm), t = Consolidation time (minutes), Δe = Change in void ratio, $\Delta\sigma'$ = Change in effective stress (kPa), e_o = initial void ratio, LL = Liquid limit (%), e_1 = Void ratio at σ_1 (dimensionless), e_2 = Void ratio at σ_2 (dimensionless), σ_1' = initial effective stress (kPa), σ_2' = final effective stress (kPa) and G_s = specific gravity (dimensionless).

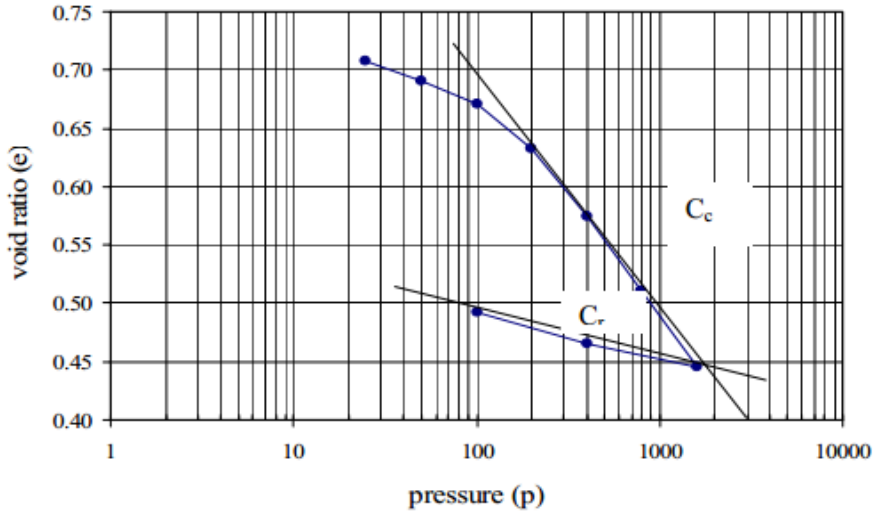

Figure A-1: Typical plot of void ratio against pressure (kPa) logarithmic scale (Holtz and Kovacz, 1981)

Table A-7: Typical value of the compression index for fine-grained soil (Reeves et al., 2006)

Compression index (c_c)	Compressibility behaviour	Clay type
>0.3	Very high	Soft Clay
0.3 – 0.15	High	Clay
0.15 – 0.075	Medium	Silt
<0.075	Low	Sandy clay

Table A-8: Typical values for the coefficient of volume compressibility after Head (1998) in Reeves et al. (2006)

Coefficient of volume compressibility m_v (m^2/MN)	Compressibility	Typical material
<0.05	Very low	Heavily over-consolidated clays and weathered rocks
0.05-0.1	Low	Till (boulder clay)
0.1-0.3	Medium	Fluvio-glacial and lacustrine clays
0.3-1.5	High	Normally consolidated alluvial clays
>1.5	Very high	Organic alluvial clays

Table A-9: Typical values of the coefficient of consolidation (c_v) after Lambe and Whitman (1979) in Reeves et al. (2006)

Coefficient of consolidation c_v (m^2/yr)	Rate of Consolidation	Typical material
<0.01	Very slow	-
0.1-1.0	Low	>25% clay
1-10	Medium	15-25% clay
10-100	High	<15% silt
>100	Very high	-

A – 9 Consolidation settlement

Consolidation settlements are often large and can cause potential damage to structures (Duncan, 1993). The magnitude and progression of settlement can significantly influence the safety and serviceability of structures that are constructed on saturated fine-grained soils that depend on the loading condition (Abu-Farsakh, 2011). Time-dependent volume change may lead to settlement of a structure founded on fine-grained soils. The volume change commonly manifests itself as compression and swelling parameters determined from laboratory tests carried out on representative soil samples (Dasgupta, 2013). Settlement of a structure can be obtained using the general expression shown in equation below.

$$\delta_T = \delta_i + \delta_c + \delta_s \qquad \text{(A-12)}$$

Where;
δ_T = Total ultimate settlement,
δ_i = Immediate settlement resulting from constant volume distortion of the loaded soil mass,
δ_c = consolidation settlement
δ_s = secondary settlement

Settlement of the soil stratum can also be calculated in terms of void ratio:

$$\delta = H \frac{\Delta e}{1+e_0} \qquad \text{(A-13)}$$

Where;

H is the soil height (mm), Δe is the change in void ratio, and e_0 is in the initial void ratio.

$$\delta = \frac{c_c H}{1+e_0} \log \left(\frac{P_0 + \Delta P}{P_0}\right) \qquad \text{(A-14)}$$

Or

$$\delta = Hm_v\Delta_\sigma \qquad \text{(A-15)}$$

Where;
c_c is the compression index, H is the soil height (mm), P_0 is the initial pressure (kPa), ΔP is the change in pressure (kPa), m_v is the coefficient of volume compressibility (m^2/MN), $\Delta\sigma$ is the change in stress (kPa), and e_0 is the initial void ratio.

B – LABORATORY PROCEDURE TO DETERMINE THE COEFFICIENT OF CONSOLIDATION

B.1 Data Analysis

In this section, various methods to obtain c_v is presented. The methods are described in reference to previous researchers.

B.1.1 Primary consolidation

Primary consolidation is the change in volume of fine-grained soil caused by the dissipation of water from the voids and the transfer of load from the excess water pressure on the soil particles (Budhu, 2000). The characteristic of soil due to consolidation are represented by the consolidation parameters described in section 2.5.2. Numerous methods have been developed over the past decades to obtain the value of c_v in the laboratory. These include: Taylor's method (Taylor, 1942), Casagrande's method (Casagrande and Fadum, 1940), the inflection method (Cour, 1971 and Mesri et al., 1999), the velocity method (Parkin 1978, 1981, Lun and Parkin, 1985), the rectangular hyperbola method (Sridharan et al., 1999), early stage log t method (Robinson and Allam, 1996 and Muntohar, 2009), the $\log(H_D^2/t)$ – U_{av} method (Sridharan et al., 1995) where U_{av} is the average degree of consolidation in percentage, H_D is the drainage path length (mm) and t is the consolidation time in minutes, and the slope and settlement rate method (Al-Zoubi, 2013). The first three methods determines c_v at a specified U_{av} value that varies at each methods and computes c_v over a range of U_{av} (Al-Zoubi, 2013). These methods were developed to help facilitate the evaluation of c_v based on Terzaghi's theory, some of which are explained below.

B.1.1.1 Taylor's method

Taylor's method of obtaining c_v by the square root time curve-fitting method is based on the similarity of shapes in experimental and theoretical curves when plotted against the square root of time (Figure B.1). The following standard procedure was recommended:

a) The straight line part of the curve is extended so that it intercedes with the ordinate (t=0) at point D. The intersection of this line and the abscissa is P.
b) Point Q is taken such that OQ = 1.15 OP
c) The intersection of line DQ and the curve is called point G
d) A horizontal line is drawn from G to the ordinate (D_{90}). This position shows the value of$\sqrt{t}90$. The value of T_v corresponds to U_{av} = 90% = 0.848 (where U_{av} is the average degree of consolidation)

e) Therefore, c_v can be calculated using its equation by Reeves et al. (2006) presented in Table A.8 where $T_v = 0.848$

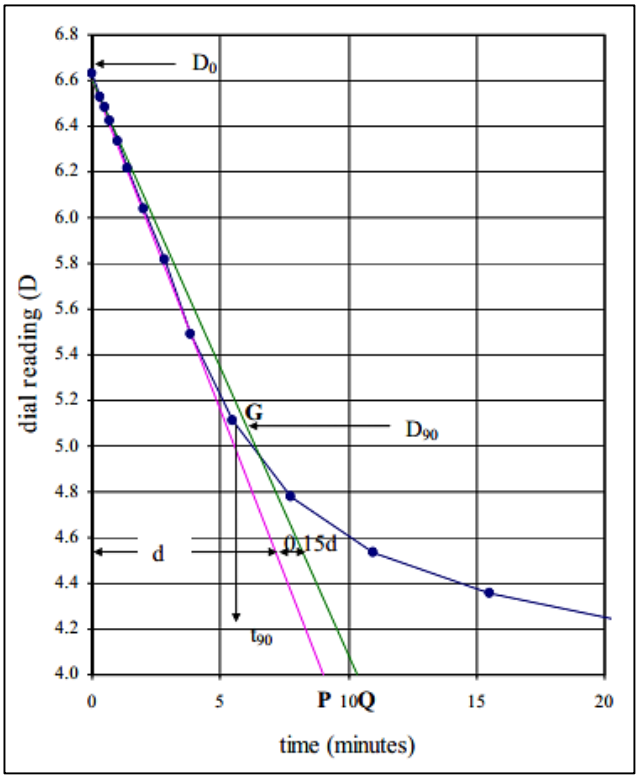

Figure B-1: Determination of c_v using Taylor's method (Taylor, 1942)

B.1.1.2 Casagrande's method

Casagrande's method is based on plotting a graph of the dial reading on the logarithmic scale of time and obtaining the reading at t_{50} which is equivalent to 50% consolidation (Figure B.2). The standard procedure is as follows:

a) A graph of the dial reading against log t is plotted
b) A straight line for the primary and secondary consolidation is produced, and the two lines will meet at point C
c) The ordinate of point C is D_{100} = deformation equivalent to 100% consolidation
d) Time t_1 = point A, $t_2 = 4t_1$ point B and the difference in the dial reading is x
e) D_0 is the deformation at 0% consolidation and may not be equal to initial reading due to air present in the sample
f) The compression between D_0 and D_{100} is primary consolidation
g) U_{av} = 50% is located between D_0 and D_{100} and the value of T_v = 50% = 0.196

h) Therefore, c_v can be calculated using its equation by Reeves et al. (2006) presented in Table A.8 where $T_v = 0.196$

i) The void ratio at t_p is denoted as e_o which is the initial void ratio.

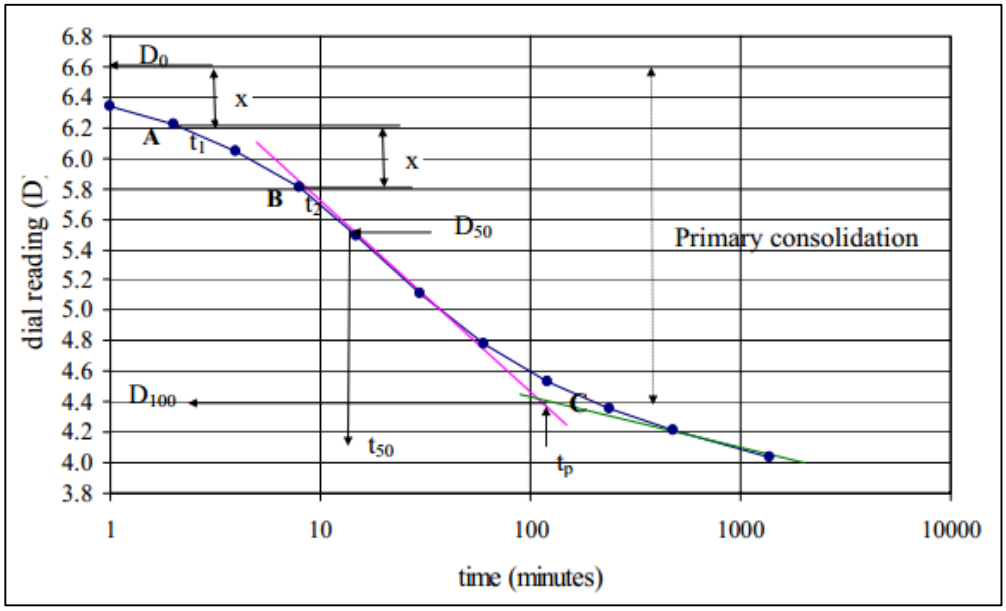

Figure B-2: Determination of c_v by Casagrande's method (Casagrande and Fadum, 1940)

B.1.1.3 Inflection point method

The Taylor and Casagrande method have been used over the past few decades to obtain c_v. There has been some issues with these two methods where the accuracy of c_v is greatly influence by human error. As a result, the inflection point method has been developed by some researchers including Cour (1971) and Robinson (1997). This method has an advantage, as it does not define the beginning and end of the primary consolidation stage as required by Taylor's and Casagrande's method (Figure B.3). It uses the inflection point with an average degree of consolidation of 70% that is within the mid-range of the consolidation curve (Mesri et al., 1999). When the inflection point is carefully identified, the value of c_v is computed using its equation by Reeves et al. (2006) presented in Table A.8 where T_v corresponds to $U_{av} = 70\% = 0.405$.

If the time deformation is plotted, the value of t can be obtained with a reasonable accuracy. However, if the time deformation curve is not plotted or if a more precise inflection point is required, it can be defined as the point at which the absolute value of the tangent to the time curve on a semi-logarithm plot reaches maximum (Fang and Daniels, 2006).

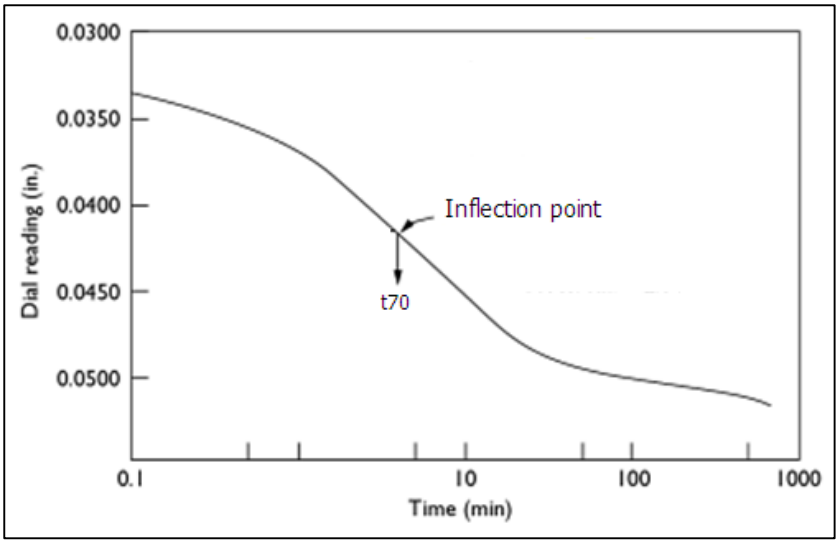

Figure B-3: Determination of c_v by the inflection method (Fang and Daniels, 2006)

B.1.1.4 Rectangular Hyperbola method

The rectangular hyperbola method determines c_v assuming the T_v/U_{av}–T_v curve (where T_v is time factor, and U_{av} is the average degree of consolidation) is linear over a range of $60 \leq U_{av} \leq 90\%$ (Sridharan et al., 1987). This method employs both slope and interception of the corresponding experimental linear segment for obtaining c_v (Al-Zoubi, 2013). Although the hyperbolic curve can provide a reasonable estimate of the total settlement (including secondary compression), data beyond the 90% consolidation is required which renders the hyperbolic method less useful in practice (Al-Shamrani, 2005). The hyperbolic curve is initially concave downward (Figure B.4) but in the range $0.286 \leq T_v \leq 0.848$ which corresponds to $60\% \leq U_{av} \leq 90\%$ (Al-Shamrani, 2005). Al-Shamrani (2005) mentioned that Tan (1993) suggested that the linear segment of the theoretical hyperbolic curve can start from U_{av} at 50% and is described by equation B.1.

$$\frac{T_v}{U_{av}} = \beta + \alpha T_v \qquad \text{(B-1)}$$

Where;
T_v is time factor; U_{av} is the average degree of consolidation, β and α are respectively the intercepts and the slope of the linear portion of the theoretical hyperbolic curve shown in Figure 2.12.

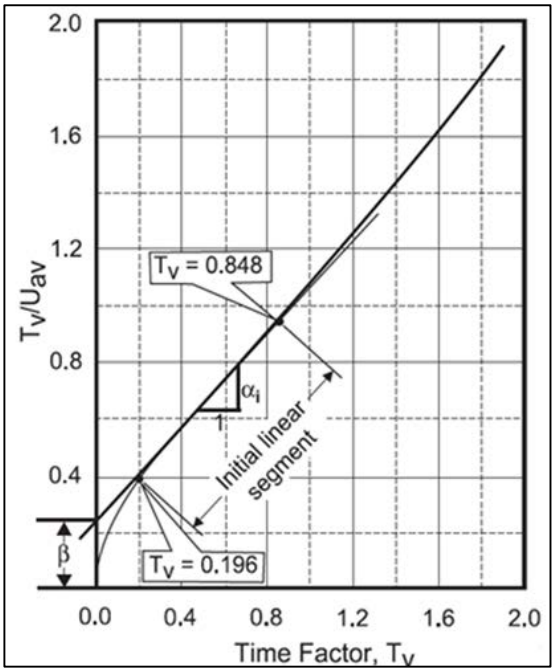

Figure B-4: Terzaghi's theoretical one-dimensional consolidation hyperbolic curve (Al-Shamrani, 2005)

From Figure B.4, the average slope of the initial linear segment is equal to 0.824 ± 0.04 (Sridharan et al., 1987). Beyond U_{av} of 90%, the hyperbolic curve divert slightly upward over a narrow range leading to a slope of 1, except for soils containing organic material where it will divert inward due to the presence of secondary consolidation (Al-Shamrani, 2005).

B.1.1.5 Early stage log t method

This method is an extension of the logarithmic time method that is based on deformation against log of time. Steps 1 to 5 from the Casagrande method also applies to this method. Once d_o is located, a horizontal line DE is drawn through d_o as shown in Figure B.5. A tangent is then drawn through the point of inflection, F which then intercepts DE at G. The time corresponding to G, which is U_{av} = 22.14% is obtained, and the value of c_v is computed using its equation by Reeves et al. (2006) presented in Table A.8 using T_v = 0.0385 (Muntohar, 2009).

The Early Stage log t method produces the highest value of c_v when compared to the Casagrande method that produces the lowest value. This variation is because the early stage method uses the early portion of the consolidation curve while the Casagrande method uses the lower portion of the consolidation curve (Muntohar, 2009).

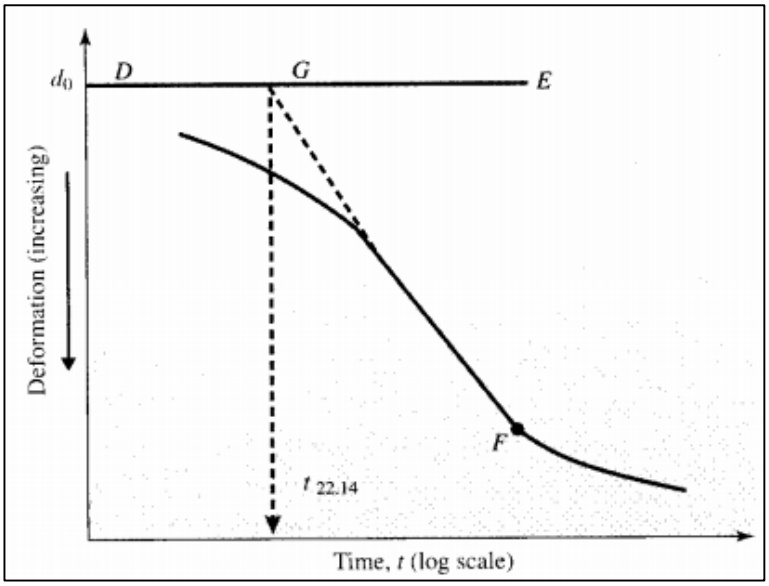

Figure B-5: Early stage log t method (Muntohar, 2009)

B.1.1.6 The slope method

The slope method is based on the fitting procedure in which the slope of the linear segment of δt - √t curve is fitted to the corresponding slope of the Terzaghi U_{av} - $\sqrt{T_v}$ relationship (Al-Zoubi 2010, 2013). According to Terzaghi (1943), the initial linear section of the theoretical U_{av} - $\sqrt{T_v}$ relationship may be 'almost exactly' expressed for $U_{av} \geq 52.6\%$ as shown in equation B.2.

$$U_{av} = M\sqrt{T_v} \qquad \text{(B-2)}$$

Where;
M is the slope of the initial linear segment of the theoretical U_{av} - $\sqrt{T_v}$ relationship; M is constant and equal to 1.128, U_{av} is the average degree of consolidation and T_v is a time factor that is constant (Al-Zoubi, 2013).

Equation by Reeves et al. (2006) in Table A.8 forms the basic equation for the methods mentioned in obtaining c_v. Hence, Taylor's and Casagrande's method are similarly affected by the factors that influence the initial portion of the consolidation curve (Al-Zoubi, 2008). The initial compression that corresponds to 0% consolidation involves obtaining two settlements values from δ - √t curve. The first settlement $\delta_1 = D_1 - D_2$ and second settlement $\delta_2 = D_2 - D_0$ that corresponds to t_1 and t_2 respectively (Al-Zoubi, 2013). The value of D_0 may be obtained using equation B.3 below:

$$D_0 = \frac{D_2 - D_1\sqrt{(\frac{t_2}{t_1})}}{1 - \sqrt{(\frac{t_2}{t_1})}} \quad \text{(B-3)}$$

Where;
D_1 and D_2 are the dial gauge reading at time t_1 and t_2 respectively, and D_0 is initial compression at 0% consolidation (Al-Zoubi, 2013).

B.1.2 Secondary consolidation

During compression, excess water pressure does not cease to dissipate in certain soils, especially those containing organic material, but gradually decreases under constant effective stress (Budhu, 2000). Secondary consolidation is also known as creep, which is the readjustment of clay particles to a more stable state due to structural disturbance caused by a decrease in the void ratio. Previous researchers such as Katarzyna and Alojzy (2010) showed that both primary and secondary consolidation take place simultaneously. Because secondary consolidation occurs after primary consolidation is completed, it is assumed to be negligible during primary consolidation. Secondary consolidation normally occurs at a slower rate following primary consolidation, as illustrated in Figure B.6. From Figure B.6, the rate of secondary consolidation is denoted as $c_{\alpha\varepsilon}$ that represents the slope of the curve. The axial rate of consolidation can be obtained as:

$$c_\alpha = \frac{\Delta e}{\log(\frac{t_s}{t_p})} \quad \text{(B-4)}$$

Where;
Δe is the change in void ratio, t_s and t_p are the time during secondary and primary consolidation respectively (seconds). Therefore, the rate of secondary consolidation (c_α) can be calculated from:

$$c_{\alpha\varepsilon} = \frac{c_\alpha}{1 + e_0} \quad \text{(B-5)}$$

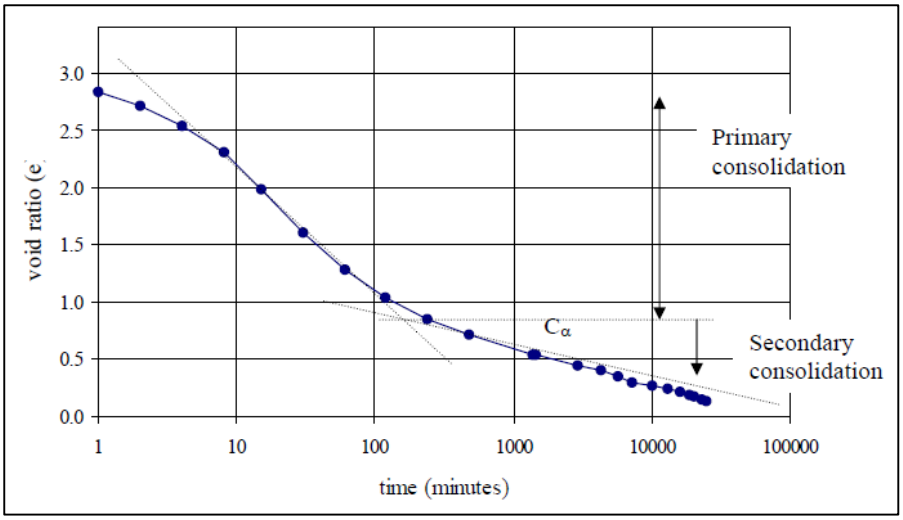

Figure B-6: Determination of the rate of secondary consolidation from consolidation curve after Casagrande (Holtz and Kovacz, 1981)

C - SOIL MINERALOGY

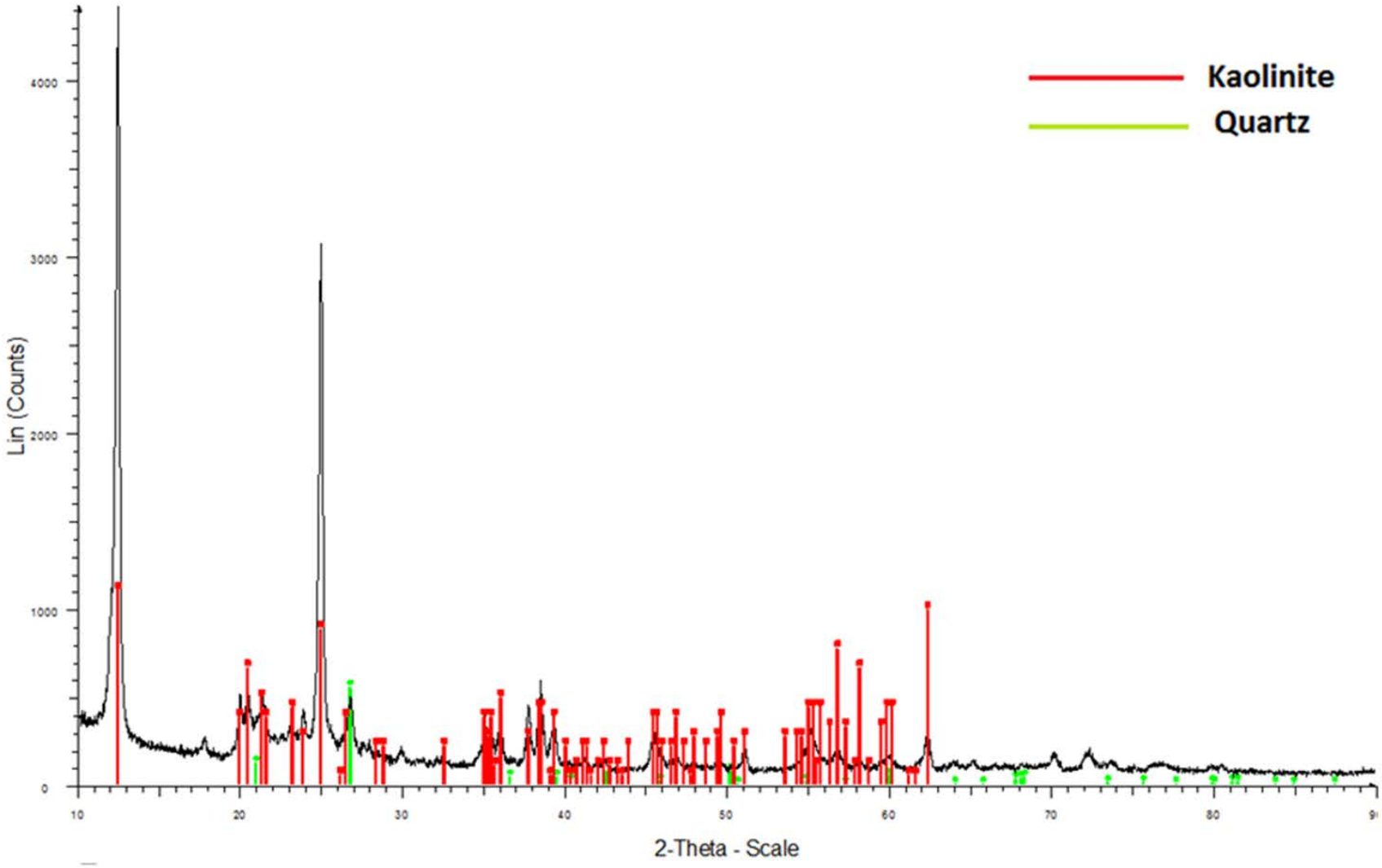

Figure C-1: X-Ray diffraction for Kaolin clay

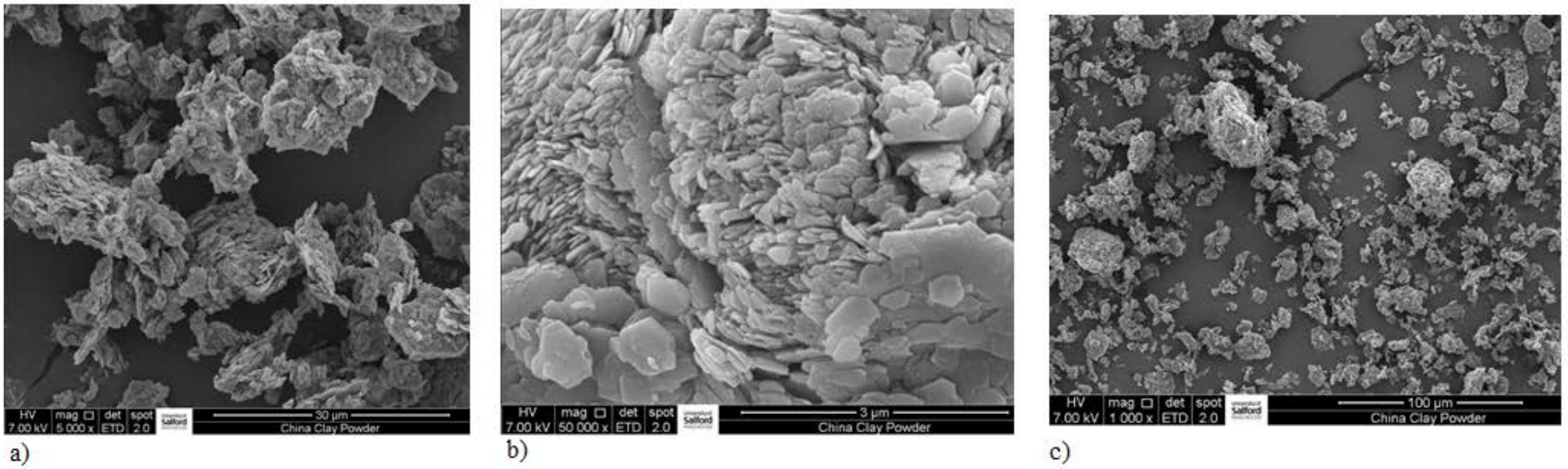

Figure C-2: SEM images of the studied soil sample for Kaolin clay with particle length: a) 30µm, b) 3µm and c) 100µm

D – VOID RATIO CONSOLIDATION CURVES

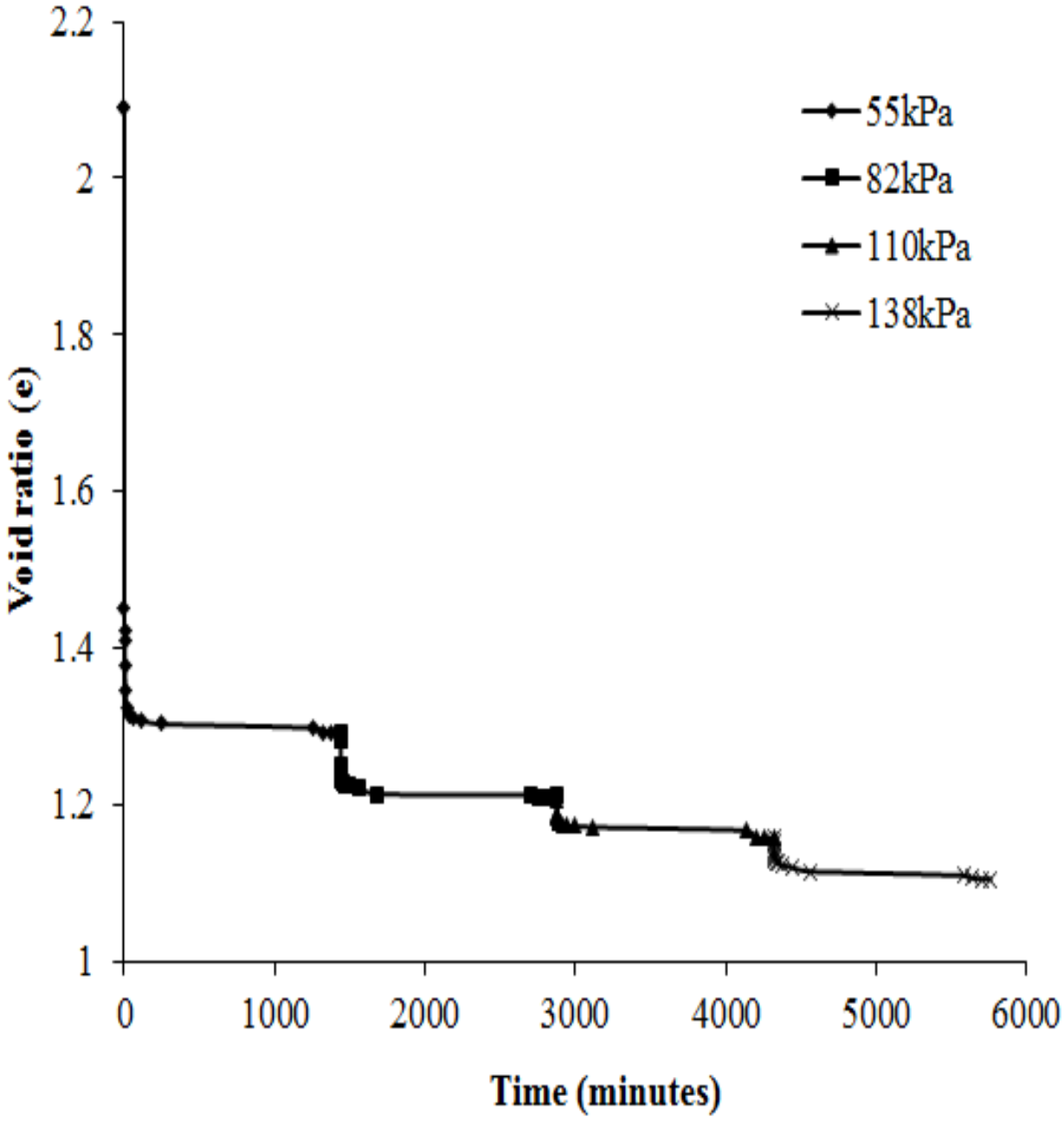

Figure D-1: Change in void ratio at DS100H23 (or D/H 4) (loading is different due to smaller soil sample diameter)

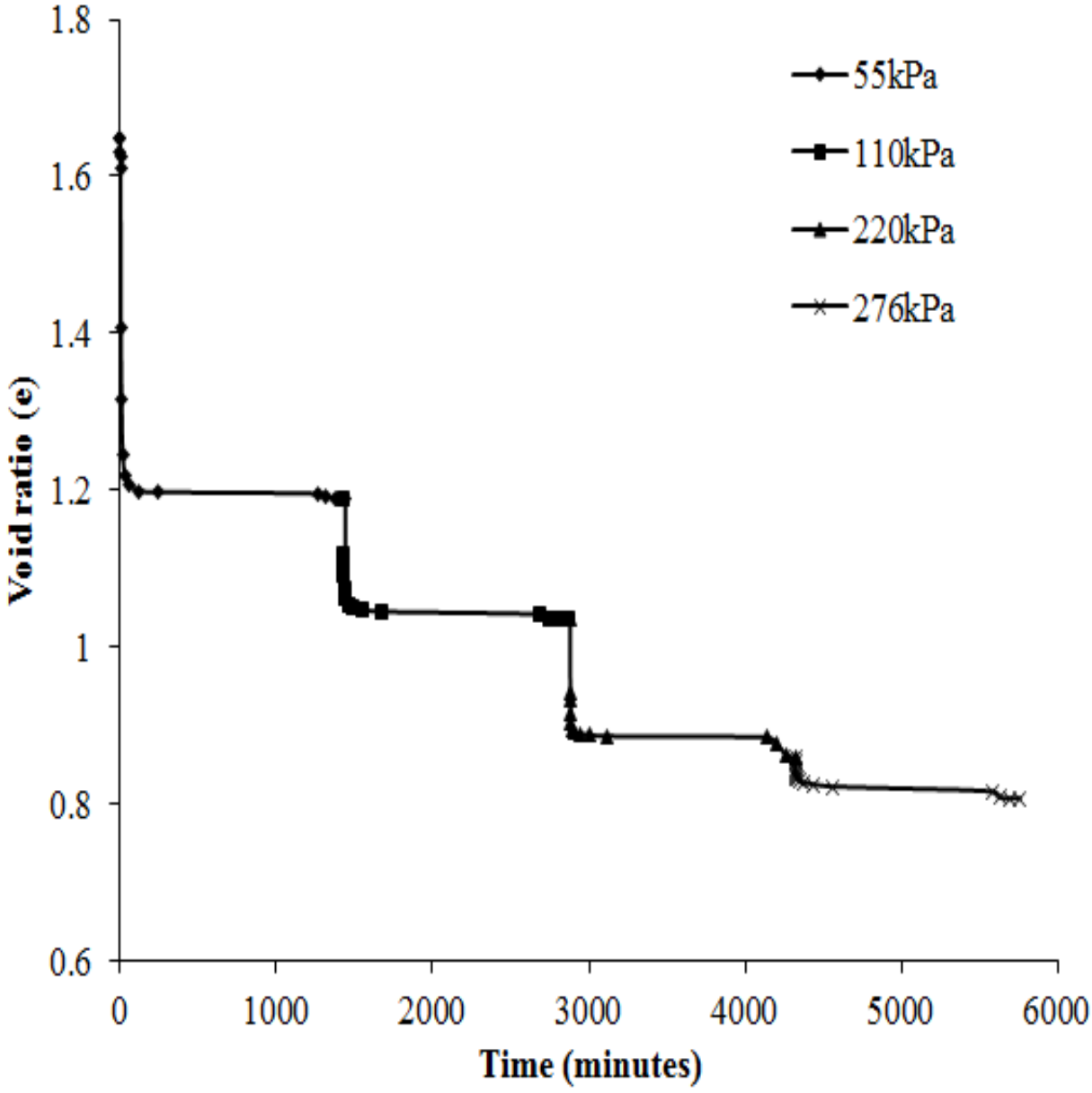

Figure D-2: Change in void ratio at sample scale DS150H23 (or D/H 6.5)

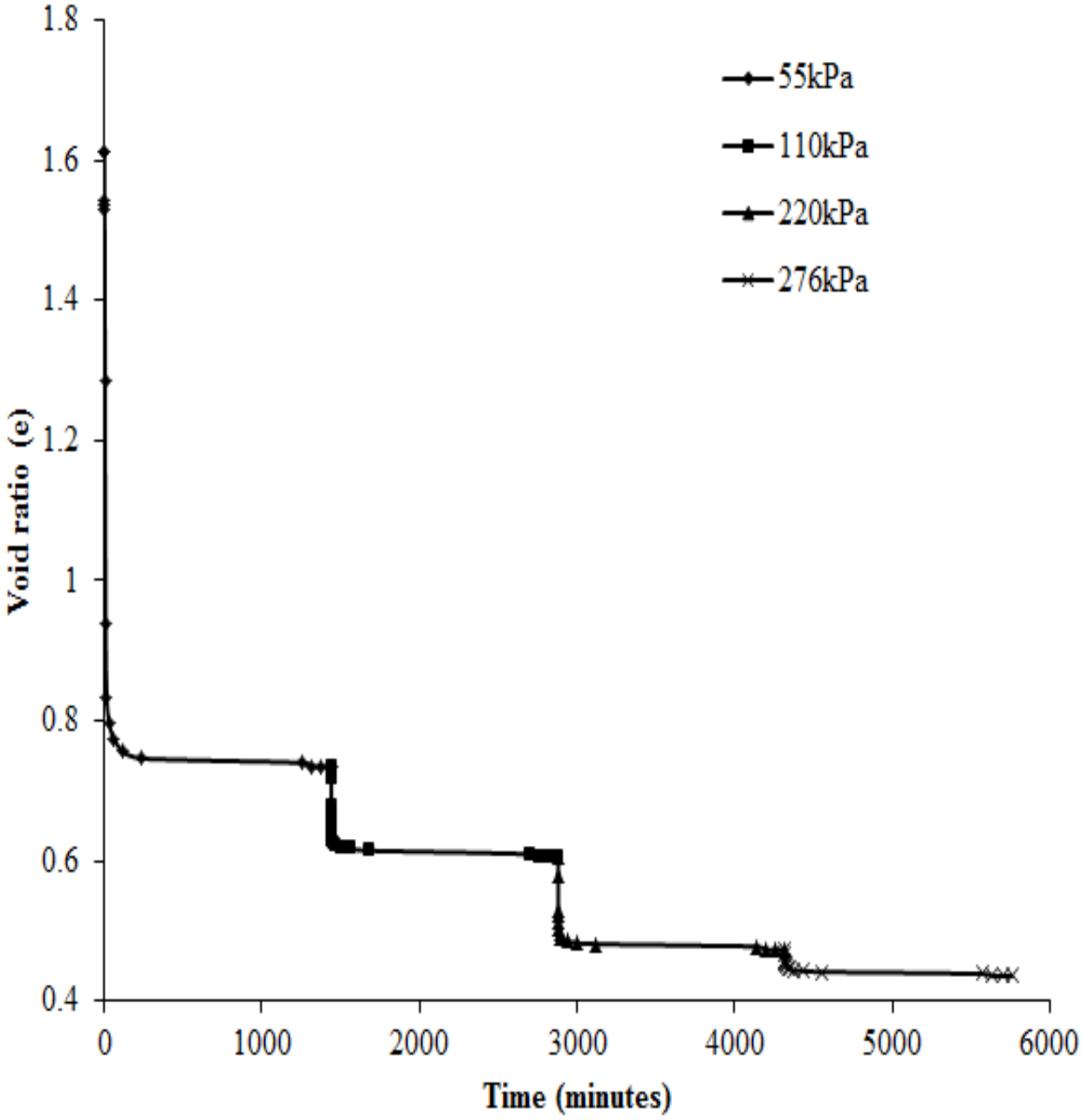

Figure D-3: Change in void ratio at sample scale DS250H23 (or D/H 11)

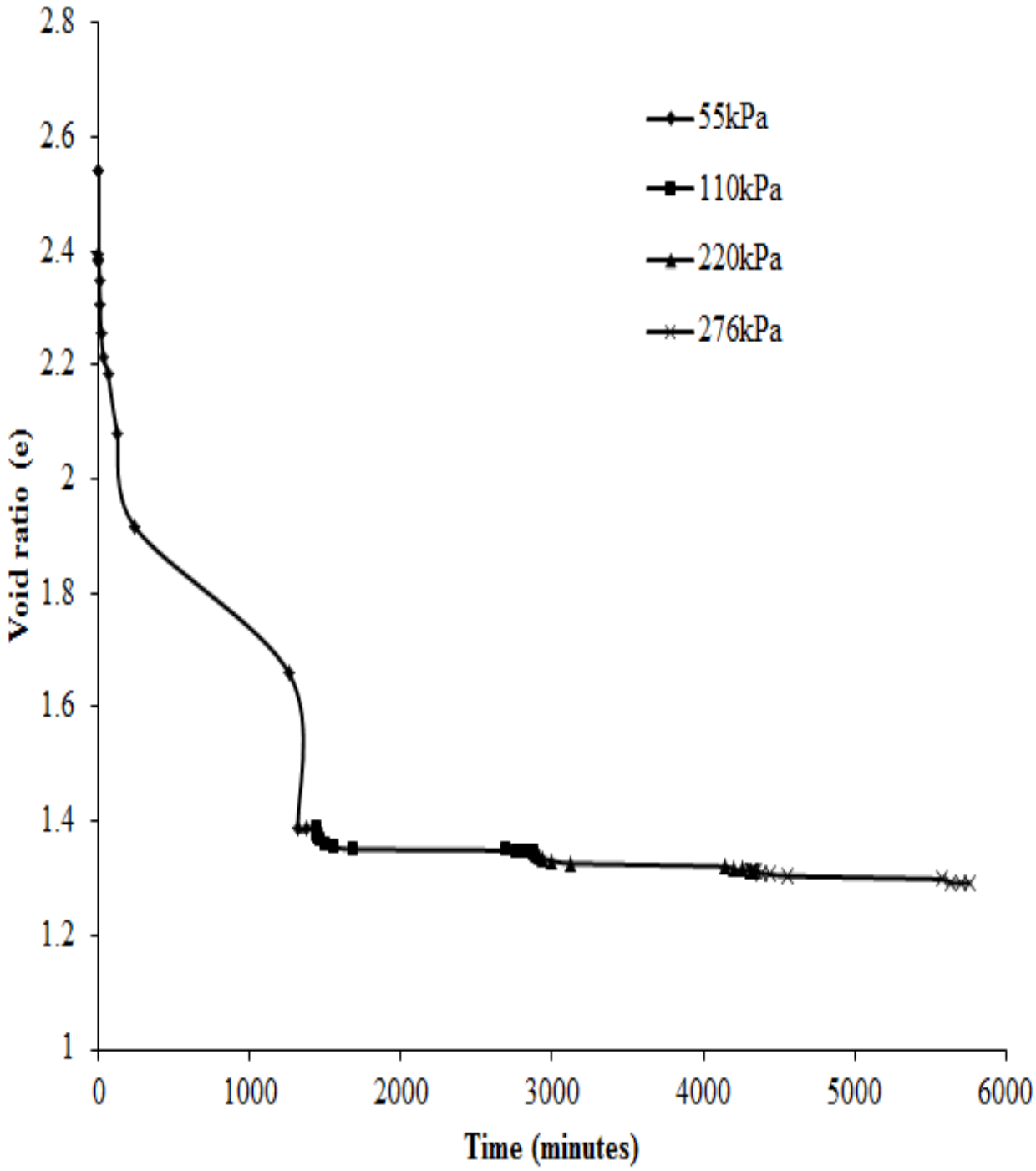

Figure D-4: Change in void ratio at sample scale DS100H200 (or D/H 0.5)

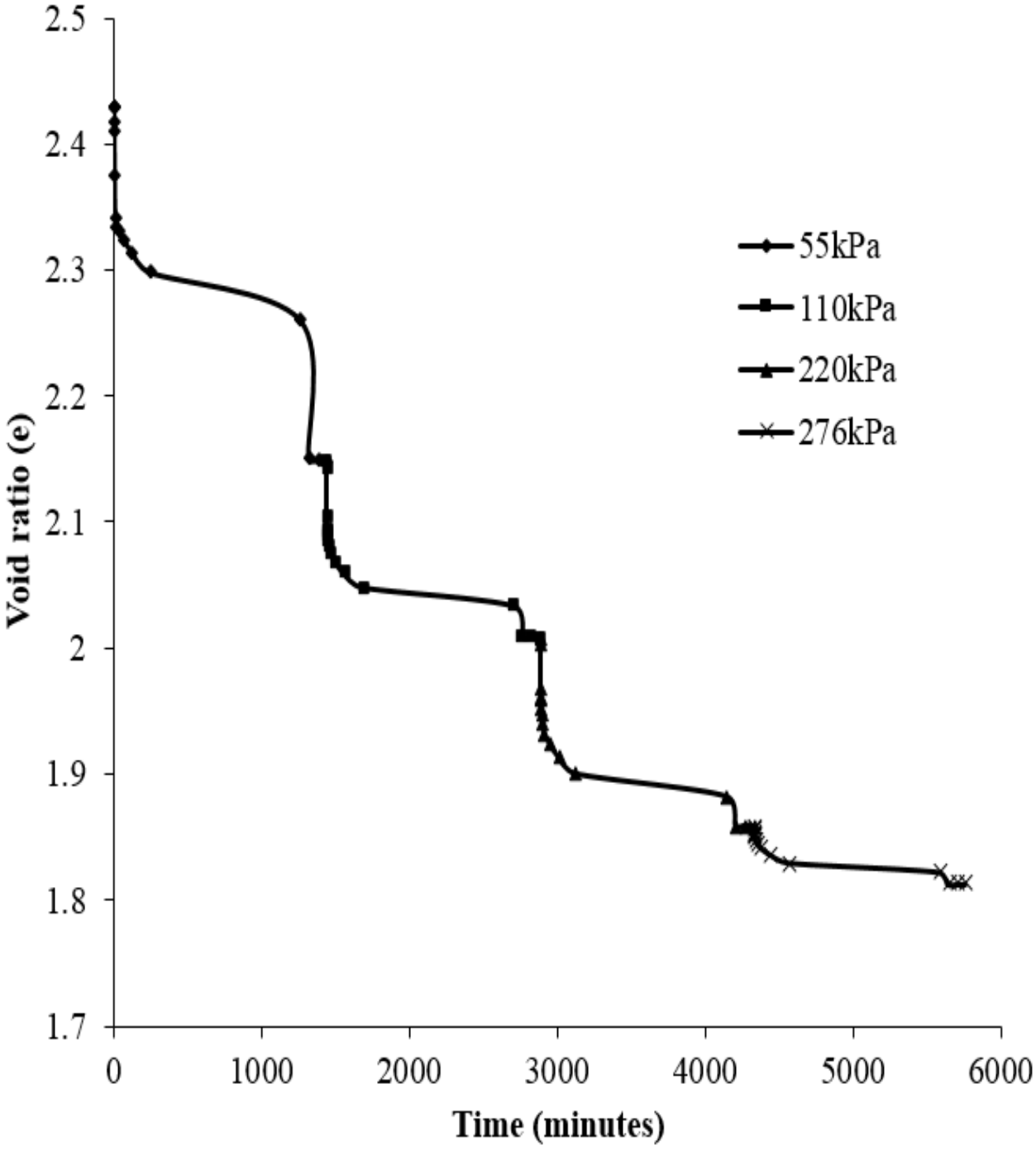

Figure D-5: Change in void ratio at sample scale D250H200 (or D/H 1.2 and HS200D250)

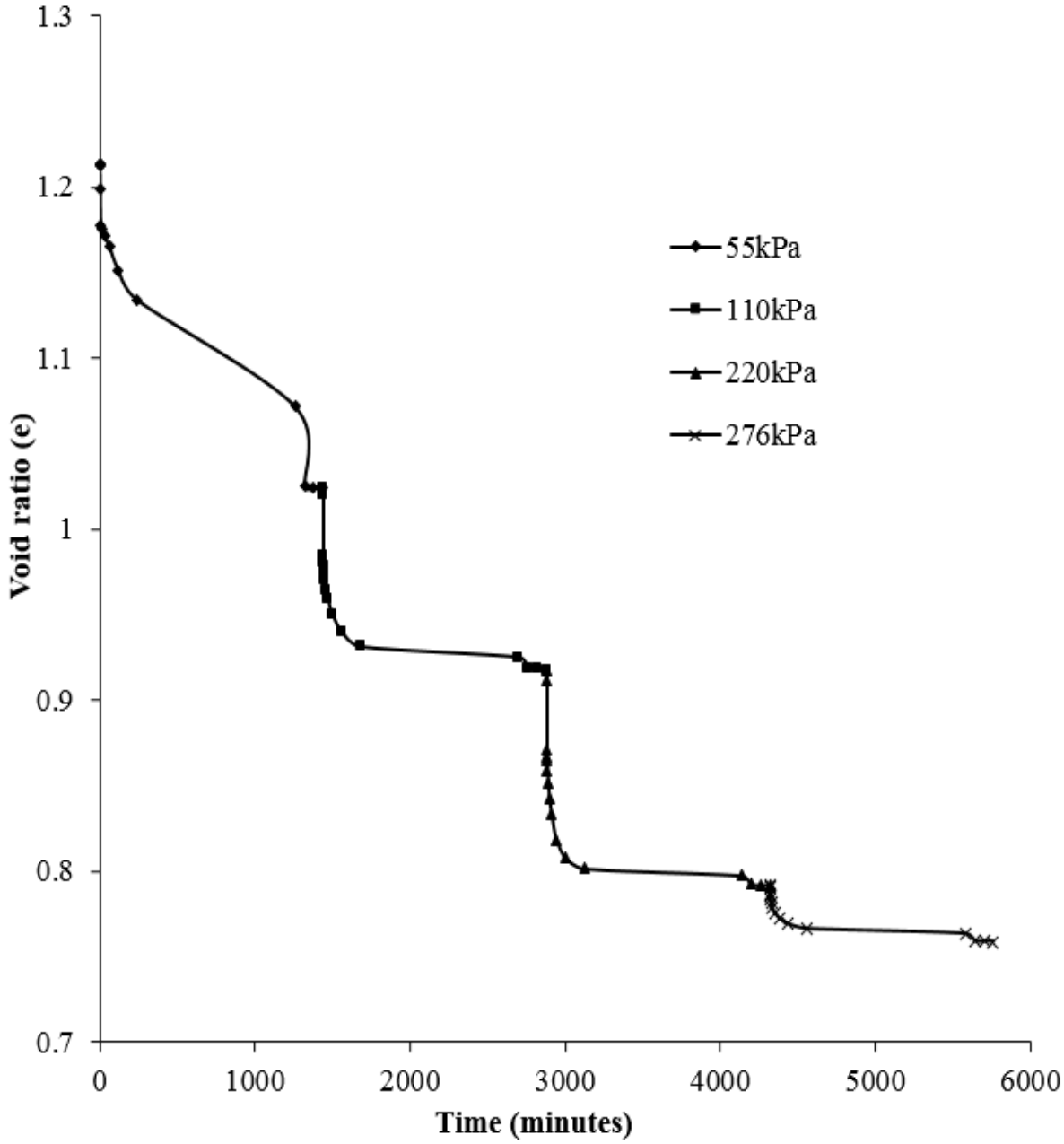

Figure D-6: Change in void ratio at sample scale DS250H80 (or D/H 3 and HS80D250)

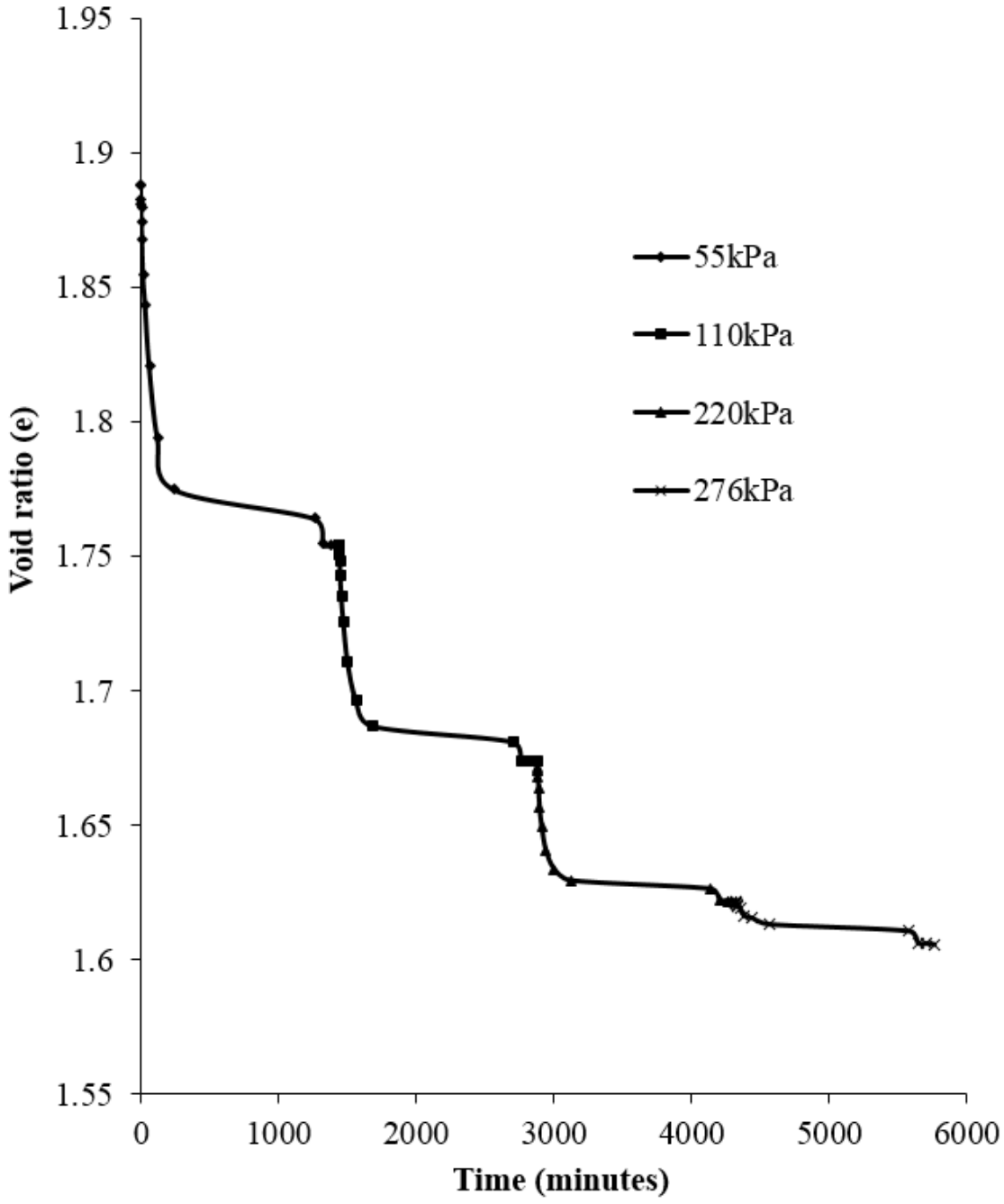

Figure D-7: Change in void ratio at sample scale DS150H80 (or D/H 2(a) and HS80D150)

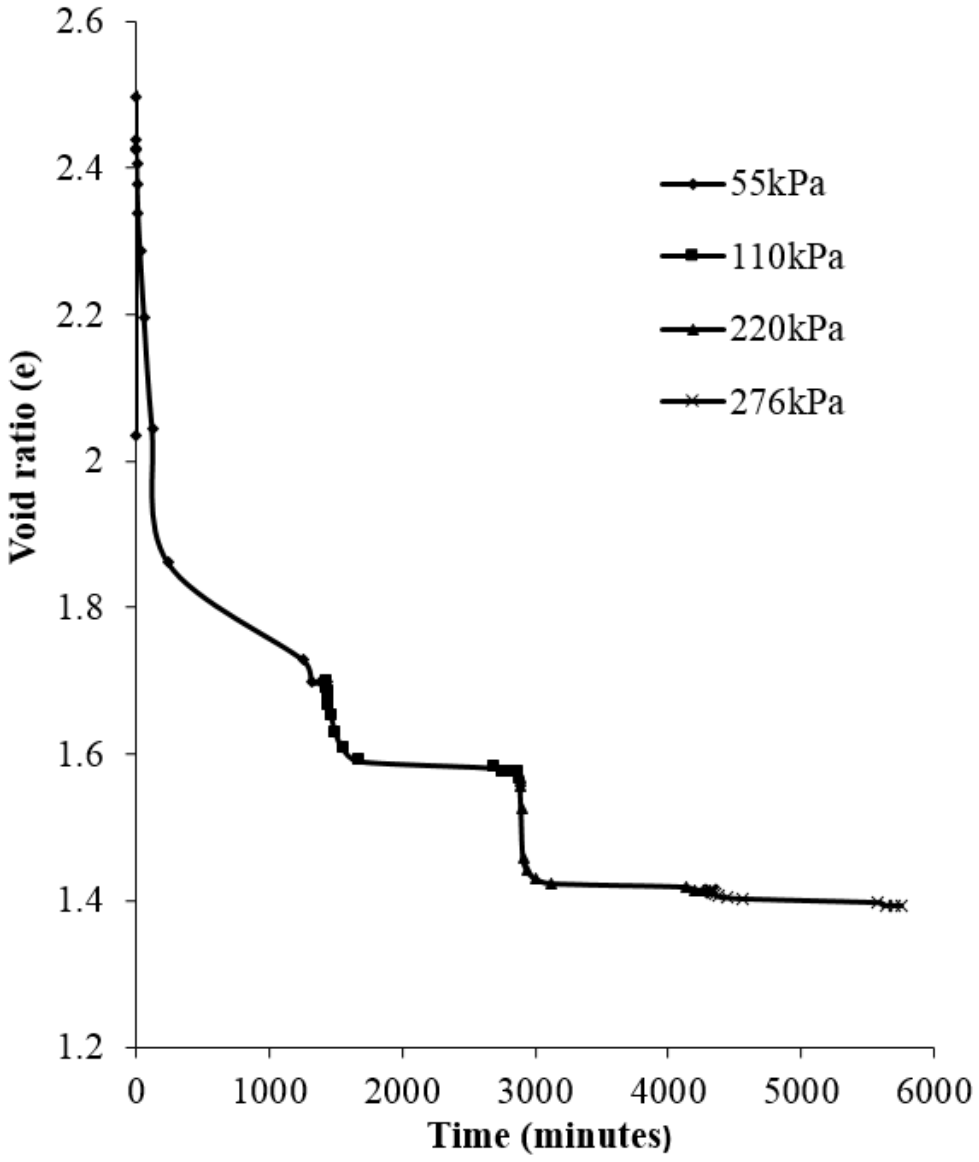

Figure D-8: Change in void ratio at sample scale DS150H130 (or D/H 1 and HS130D150)

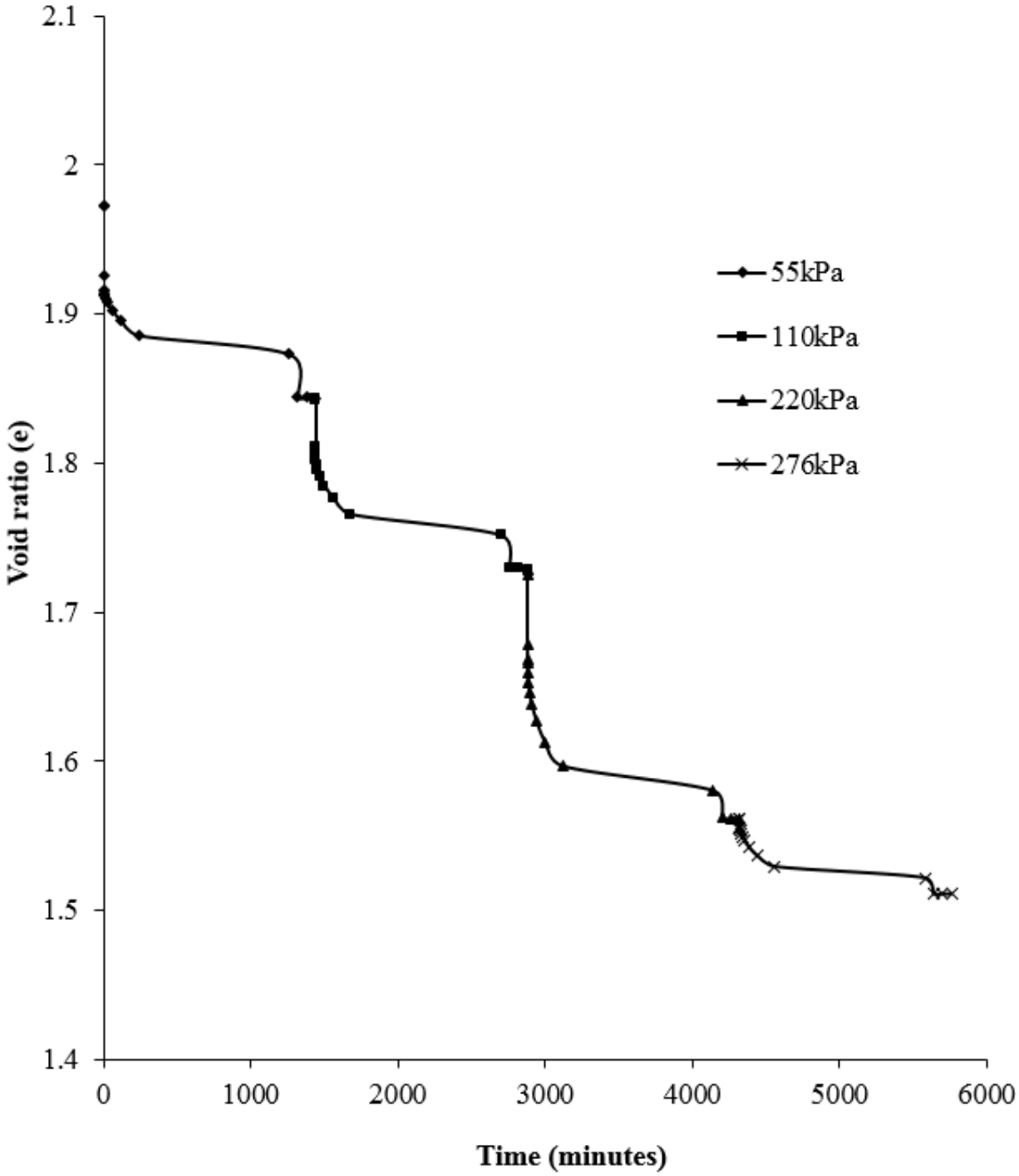

Figure D-9: Change in void ratio at sample scale DS250H130 (or D/H 2(b) and HS130D250)

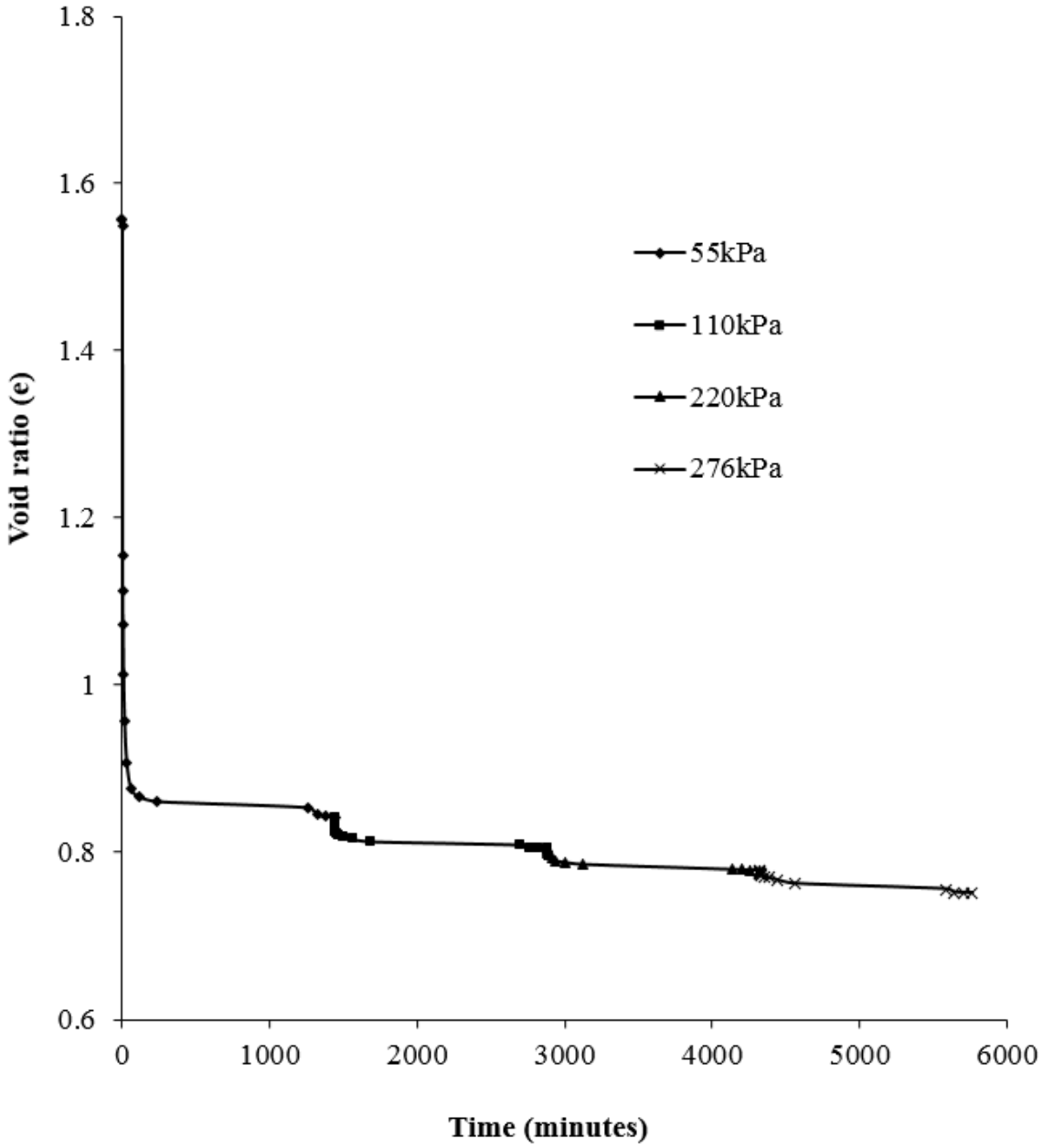

Figure D-10: Change in void ratio at sample scale D/H 5

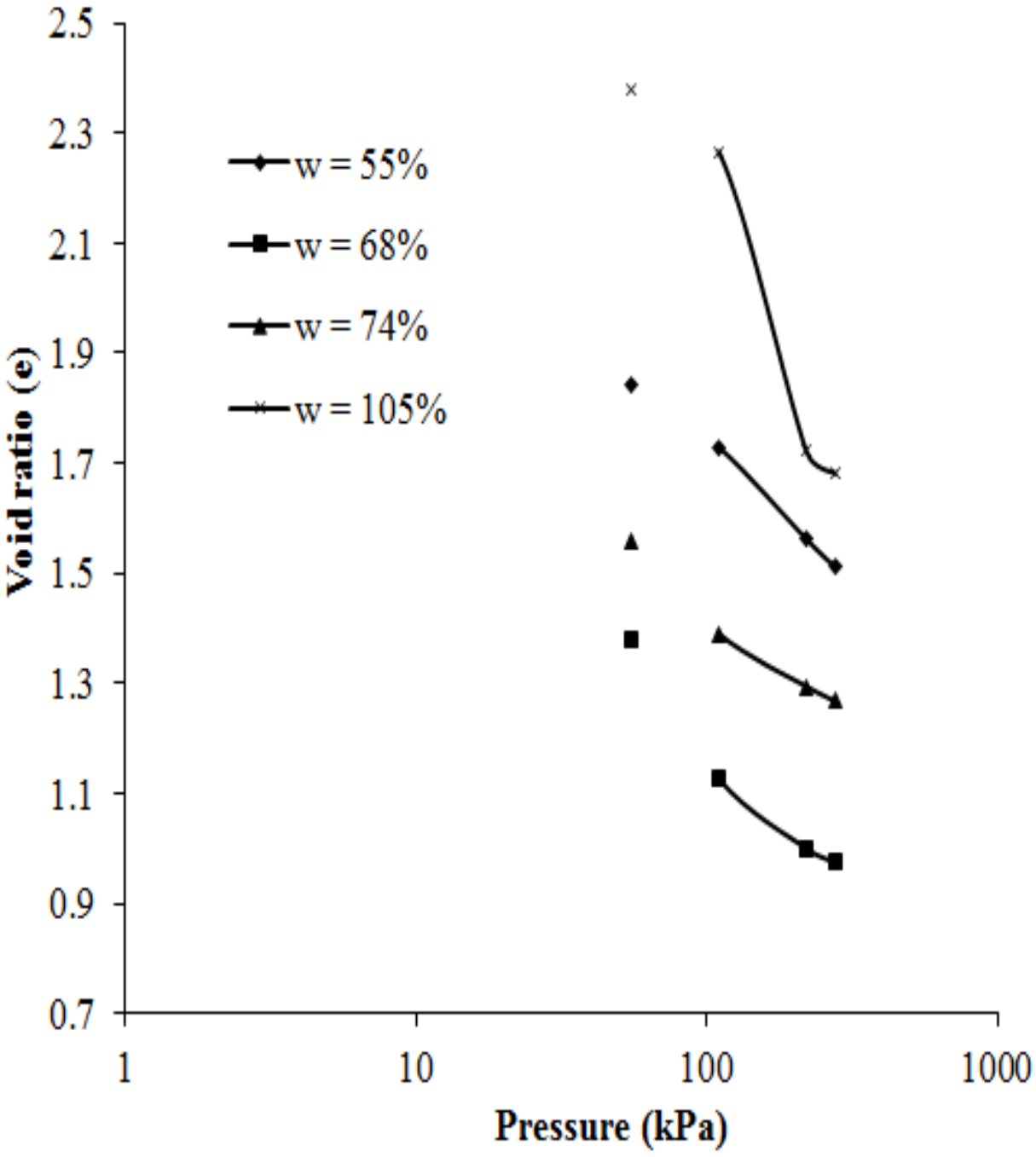

Figure D-11: Logarithm of change in void ratio at various initial moisture content

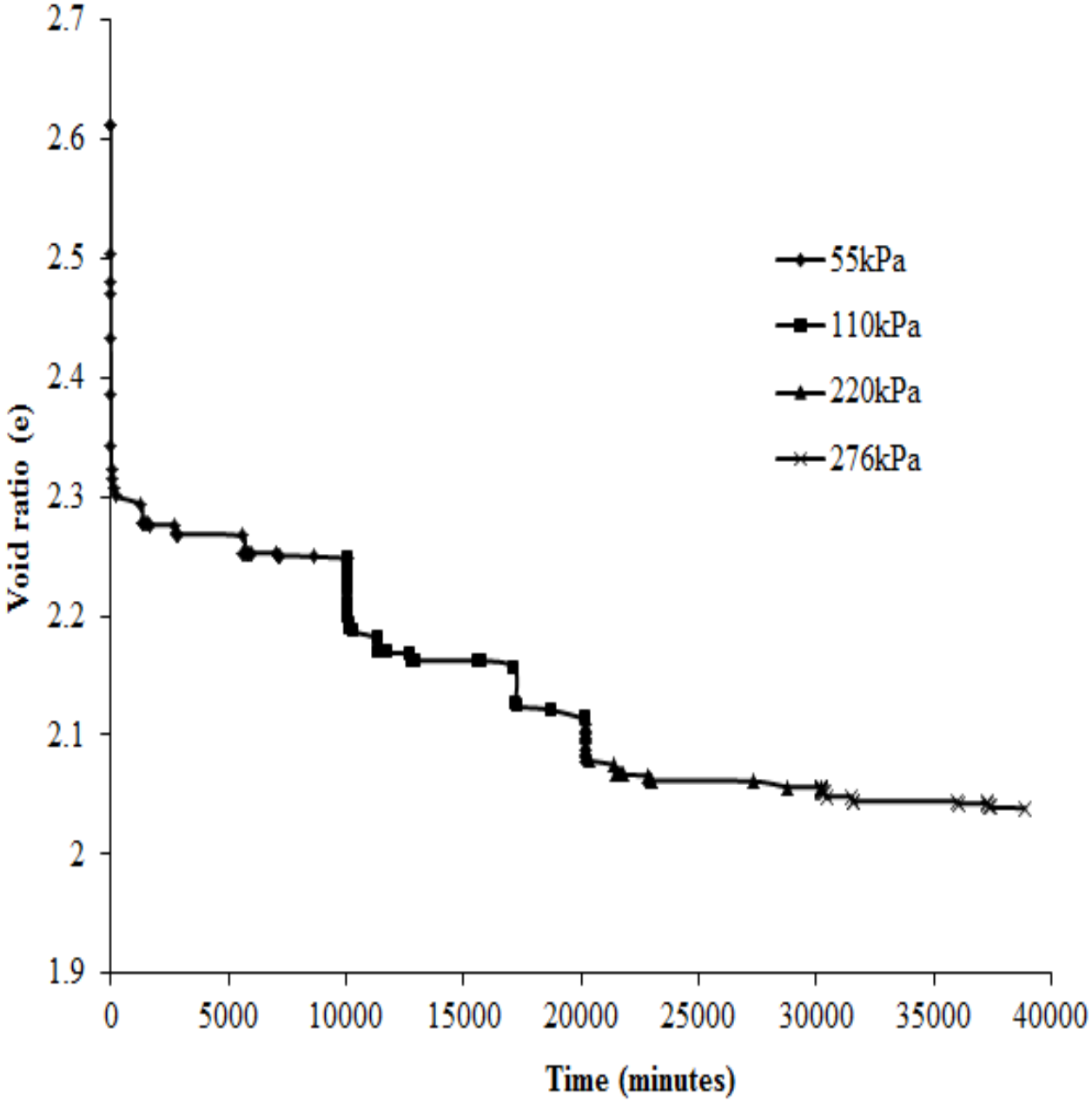

Figure D-12: Effect of time factor on change in void ratio at D/H 6.5 (DS150H23) 7 days loading

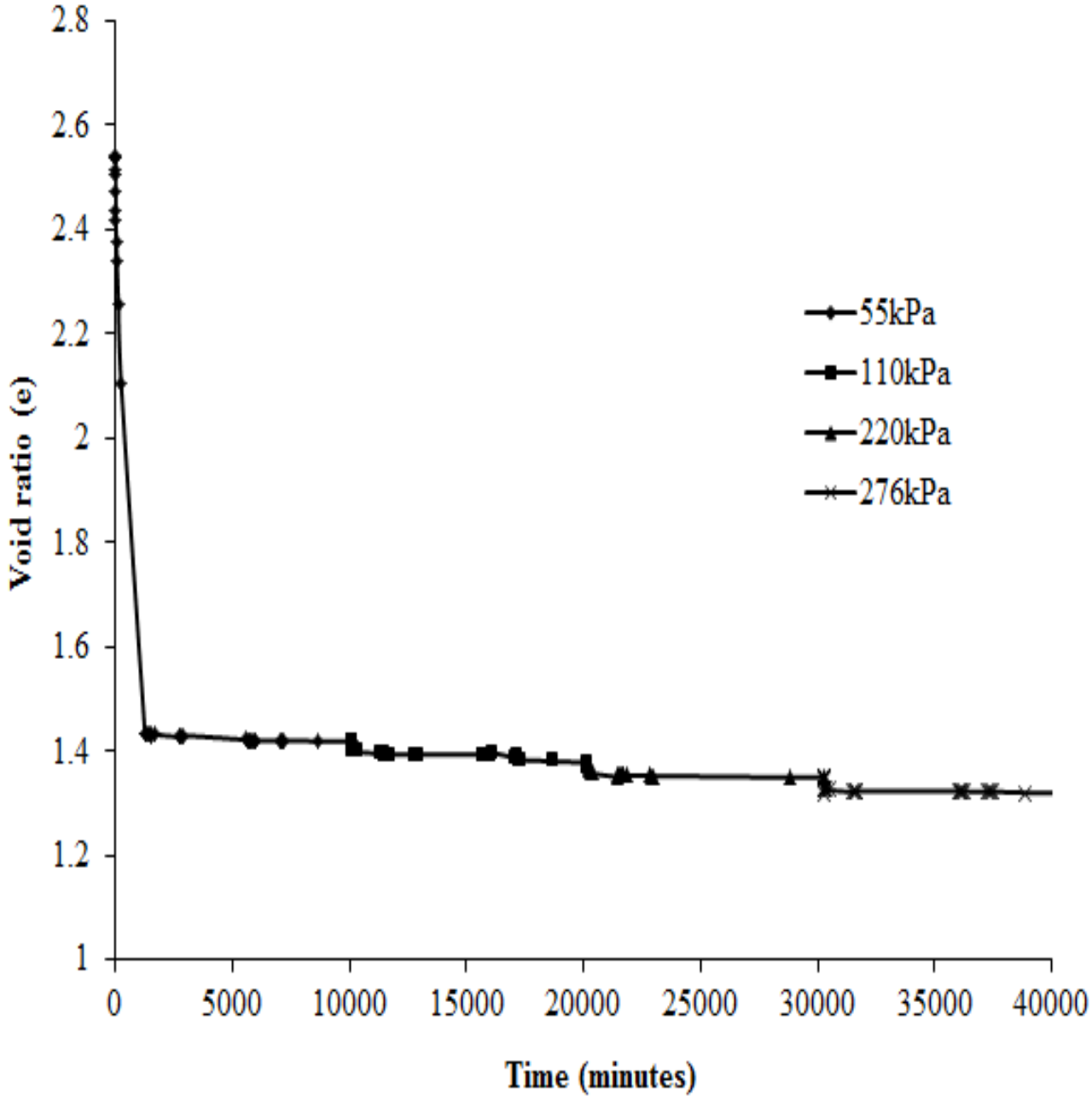

Figure D-13: Effect of time factor on void ratio at D/H 0.5 (DS100H200) 7 days loading

E – TIME-DEFORMATION CHARACTERISTICS

Coefficient of consolidation (c_v) tests on Kaolin Clay (*where; C = Casagrande method, T = Taylor's method, I = Inflection method and inc = Increment*)

Table E-1: Test 1 and 2 – Sample diameter scale (which also corresponds to sample D/H ratio) effect on c_v

Load (±3.7kPa)	Load inc (±3.7kPa)	Diameter (mm)	Height (mm)	c_v (m^2/yr)		
				C	T	I
0	0			0	0	0
55kPa	55kPa	100	23	4.68	4.96	9.67
		150	23	2.81	4.21	5.80
		250	23	1.17	0.75	1.93
		100	200	8.73	12.35	18.05
		250	200	7.36	13.76	14.20
110kPa	55kPa	100	23	0.38	6.89	0.79
		150	23	0.48	4.64	0.99
		250	23	0.20	4.29	0.42
		100	200	23.42	25.02	32.27
		250	200	14.47	31.05	29.90
220kPa	110kPa	100	23	0.28	7.77	0.49
		150	23	0.41	8.97	0.86
		250	23	0.22	2.73	0.36
		100	200	11.33	11.60	15.60
		250	200	13.21	20.29	20.48
276kPa	55kPa	100	23	0.07	7.40	0.10
		150	23	0.46	7.47	0.95
		250	23	0.06	2.15	0.13
		100	200	11.02	6.60	15.18
		250	200	10.22	12.40	13.44

Table E-2: Test 3 and 4 – Sample diameter scale effect (which also corresponds to sample D/H ratio) on c_v

Load (±3.7kPa)	Load inc (±3.7kPa)	Diameter (mm)	Height (mm)	c_v (m^2/yr)		
				C	**T**	**I**
0	0			0	0	0
55kPa	55kPa	150	130	6.22	7.36	9.99
		250	130	14.52	5.22	14.99
		150	80	4.71	7.28	8.52
		250	80	4.12	5.04	5.68
110kPa	55kPa	150	130	6.57	7.70	13.23
		250	130	6.65	6.74	7.49
		150	80	7.50	8.98	10.33
		250	80	5.53	4.94	7.14
220kPa	110kPa	150	130	11.79	8.43	12.18
		250	130	9.18	11.04	6.90
		150	80	10.09	10.05	14.61
		250	80	12.38	5.58	15.06
276kPa	55kPa	150	130	2.59	3.10	4.76
		250	130	5.39	5.47	8.36
		150	80	2.26	2.61	4.68
		250	80	6.36	7.31	11.17

Table E-3: Test 5 – Sample height effect (which also corresponds to sample D/H ratio) on c_v

Load (±3.7kPa)	Load inc (±3.7kPa)	Diameter (mm)	Height (mm)	c_v (m^2/yr)		
				C	**T**	**I**
0				0	0	0
55kPa	55kPa	150	23	2.81	4.21	5.80
		150	30	4.64	2.78	6.84
		150	80	4.71	7.28	8.52
		150	130	6.22	7.36	9.99
110kPa	55kPa	150	23	0.48	4.64	0.99
		150	30	0.67	0.93	1.24
		150	80	7.50	8.98	10.33
		150	130	6.57	7.70	13.23
220kPa	110kPa	150	23	0.41	8.97	0.86
		150	30	0.29	0.25	0.59
		150	80	10.09	10.05	14.61
		150	130	11.79	8.43	12.18
276kPa	55kPa	150	23	0.46	7.47	0.95
		150	30	0.06	0.11	0.14
		150	80	2.26	2.61	4.68
		150	130	2.59	3.10	4.76

Table E-4: Test 6 – Sample height scale effect (which also corresponds to sample D/H ratio) on c_v

Load (±3.7kPa)	Load inc (±3.7kPa)	Diameter (mm)	Height (mm)	c_v (m^2/yr)		
				C	**T**	**I**
0				0	0	0
55kPa	55kPa	250	23	1.17	0.75	1.93
		250	80	4.12	5.04	5.68
		250	130	14.52	5.22	14.99
		250	200	7.36	13.76	14.20
110kPa	55kPa	250	23	0.20	4.29	0.42
		250	80	5.53	4.94	7.14
		250	130	6.65	6.74	7.49
		250	200	14.47	31.05	29.90
220kPa	110kPa	250	23	0.22	2.73	0.36
		250	80	12.38	5.58	15.06
		250	130	9.18	11.04	6.90
		250	200	13.21	20.29	20.48
276kPa	55kPa	250	23	0.06	2.15	0.13
		250	80	6.36	7.31	11.17
		250	130	5.39	5.47	8.36
		250	200	10.22	12.40	13.44

Compression Index (c_c) and coefficient of volume compressibility (m_v) values on Kaolin clay at different sample scale

Table E-5: Test 1 and 2 – Sample diameter effect on the value c_c and m_v

Load (±3.7kPa)	Load inc (±3.7kPa)	Diameter (mm)	Height (mm)	c_c	m_v (x10^{-3})
0	0				
55kPa	55kPa	100	23	0.46	4.7
		150	23	0.26	3.14
		250	23	0.50	6.10
		100	200	0.66	5.92
		250	200	0.16	1.49
110kPa	55kPa	100	23	0.05	0.95
		150	23	0.09	1.06
		250	23	0.07	0.90
		100	200	0.02	0.20
		250	200	0.08	0.74
220kPa	110kPa	100	23	0.04	0.63
		150	23	0.08	0.60
		250	23	0.06	0.46
		100	200	0.01	0.08
		250	200	0.07	0.39
276kPa	55kPa	100	23	0.03	0.59
		150	23	0.03	0.35
		250	23	0.02	0.26
		100	200	0.01	0.11
		250	200	0.02	0.24

Table E-6: Test 3 and 4 – Sample diameter effect of c_c and m_v

Load (±3.7kPa)	Load inc (±3.7kPa)	Diameter (mm)	Height (mm)	c_c	m_v (x10^{-3})
0	0				
55kPa	55kPa	150	130	0.46	4.15
		250	130	0.07	0.78
		150	80	0.07	0.84
		250	80	0.11	1.55
110kPa	55kPa	150	130	0.07	0.64
		250	130	0.06	0.70
		150	80	0.05	0.51
		250	80	0.06	0.87
220kPa	110kPa	150	130	0.08	0.41
		250	130	0.08	0.51
		150	80	0.02	0.16
		250	80	0.06	0.51
276kPa	55kPa	150	130	0.01	0.10
		250	130	0.03	0.31
		150	80	0.01	0.10
		250	80	0.02	0.27

Table E-7: Test 5 – Sample height effect c_c and m_v

Load (±3.7kPa)	Load inc (±3.7kPa)	Diameter (mm)	Height (mm)	c_c	m_v ($x10^{-3}$)
0	0				
55kPa	55kPa	150	23	0.26	3.14
		150	30	0.42	5.3
		150	80	0.07	0.84
		150	130	0.46	4.15
110kPa	55kPa	150	23	0.09	1.06
		150	30	0.02	0.22
		150	80	0.05	0.51
		150	130	0.07	0.64
220kPa	110kPa	150	23	0.08	0.60
		150	30	0.01	0.09
		150	80	0.02	0.16
		150	130	0.08	0.41
276kPa	55kPa	150	23	0.03	0.35
		150	30	0.01	0.16
		150	80	0.01	0.10
		150	130	0.01	0.10

Table E-8: Test 6 – Sample height effect c_c and m_v

Load (±3.7kPa)	Load inc (±3.7kPa)	Diameter (mm)	Height (mm)	c_c	m_v (x10^{-3})
0	0				
55kPa	55kPa	250	23	0.50	6.10
		250	80	0.11	1.55
		250	130	0.07	0.78
		250	200	0.16	1.49
110kPa	55kPa	250	23	0.07	0.90
		250	80	0.06	0.87
		250	130	0.06	0.70
		250	200	0.08	0.74
220kPa	110kPa	250	23	0.06	0.46
		250	80	0.06	0.51
		250	130	0.08	0.51
		250	200	0.07	0.39
276kPa	55kPa	250	23	0.02	0.26
		250	80	0.02	0.27
		250	130	0.03	0.31
		250	200	0.02	0.24

Series of double Oedometer test – Compressibility parameters on Kaolin clay

Table E-9: Test 17 - D/H 6.5 effect on compressibility parameters at initial moisture content 67.5%

Load (±3.7kPa)	Load inc (±3.7kPa)	Diameter (mm)	Height (mm)	c_v (m^2/yr)			c_c	m_v (m^2/MN) ($x10^{-3}$)
				C	T	I		
0	0			0	0	0		
55kPa	55kPa	150	23	2.81	4.21	5.80	0.26	3.14
		150	23	4.68	6.75	7.26	0.22	2.65
110kPa	55kPa	150	23	0.48	4.64	0.99	0.09	1.06
		150	23	1.02	1.23	0.85	0.02	0.22
220kPa	110kPa	150	23	0.41	8.97	0.86	0.08	0.60
		150	23	0.99	2.69	0.68	0.02	0.14
276kPa	55kPa	150	23	0.46	7.47	0.95	0.03	0.35
		150	23	0.14	1.15	0.18	0.01	0.13

Table E-10: Test 18 – D/H 6.5 effect on c_v with moisture content 67.5% at 24 hours and 7 days

Load (±3.7kPa)	Load inc (±3.7kPa)	Diameter (mm)	Height (mm)	Duration	c_v (m^2/yr)			c_c	m_v (m^2/MN) ($x10^{-3}$)
					C	T	I		
0					0	0	0		
55kPa	55kPa	150	23	24 hours	2.81	4.21	5.80	0.26	3.14
		150	23	7 days	0.47	0.18	0.26	0.21	1.8
110kPa	55kPa	150	23	24 hours	0.48	4.64	0.99	0.09	1.06
		150	23	7 days	0.28	1.96	0.39	0.07	0.67
220kPa	110kPa	150	23	24 hours	0.41	8.97	0.86	0.08	0.60
		150	23	7 days	0.26	1.25	0.27	0.03	0.15
276kPa	55kPa	150	23	24 hours	0.46	7.47	0.95	0.03	0.35
		150	23	7 days	0.67	0.60	1.22	0.01	0.08

Table E-11: Test 19 – D/H 2(a) effect on c_v with moisture content 65% at 24 hours

Load (±3.7kPa)	Load inc (±3.7kPa)	Diameter (mm)	Height (mm)	c_v (m^2/yr)			c_c	m_v (m^2/MN) ($x10^{-3}$)
				C	T	I		
0				0	0	0		
55kPa	55kPa	150	80	5.89	8.81	8.52	0.20	2.21
		150	80	4.71	7.28	8.52	0.07	0.84
110kPa	55kPa	150	80	8.48	8.82	8.77	0.06	0.70
		150	80	7.50	8.98	10.33	0.05	0.51
220kPa	110kPa	150	80	12.92	10.27	17.16	0.04	0.27
		150	80	10.09	10.05	14.61	0.02	0.16
276kPa	55kPa	150	80	4.33	7.32	8.95	0.02	0.19
		150	80	2.26	2.61	4.68	0.01	0.10

Table E-12: Test 20 – D/H 0.5 effect on c_v with initial moisture content 91% at 24 hours and 7 days

Load (±3.7kPa)	Load inc (±3.7kPa)	Diameter (mm)	Height (mm)	Duration	c_v (m^2/yr)			c_c	m_v (m^2/MN) ($x10^{-3}$)
					C	T	I		
0					0	0	0		
55kPa	55kPa	100	200	24 hours	8.73	12.35	18.05	0.66	5.92
		100	200	7 days	5.72	9.21	11.83	0.64	5.75
110kPa	55kPa	100	200	24 hours	23.42	25.02	32.27	0.02	0.20
		100	200	7 days	19.26	28.84	39.81	0.02	0.21
220kPa	110kPa	100	200	24 hours	11.33	11.60	15.60	0.01	0.08
		100	200	7 days	9.31	10.28	16.04	0.01	0.07
276kPa	55kPa	100	200	24 hours	11.02	6.60	15.18	0.01	0.11
		100	200	7 days	1.51	3.41	2.35	0.02	0.15

Table E-13: Test 21 – D/H 2 effect on c_v with different moisture content at duration of 24 hours

Load (±3.7kPa)	Load inc (±3.7kPa)	Diameter (mm)	Height (mm)	Moisture content (%)	c_v (m^2/yr)			c_c	m_v (m^2/MN) ($x10^{-3}$)
					C	T	I		
0					0	0	0		
55kPa	55kPa	250	130	55%	14.52	5.22	14.99	0.07	0.78
		250	130	68%	7.26	6.52	14.99	0.54	5.18
		250	130	74%	4.73	7.84	8.18	0.53	4.83
		250	130	105%	6.40	7.84	9.99	0.19	1.67
110kPa	55kPa	250	130	55%	6.64	6.74	7.49	0.06	0.70
		250	130	68%	11.12	11.87	15.31	0.14	1.37
		250	130	74%	2.61	6.01	5.38	0.09	0.88
		250	130	105%	14.36	12.84	18.55	0.06	0.55
220kPa	110kPa	250	130	55%	9.18	11.04	6.90	0.08	0.51
		250	130	68%	7.12	12.03	12.26	0.06	0.34
		250	130	74%	4.09	10.93	6.04	0.05	0.25
		250	130	105%	14.37	16.18	24.75	0.27	1.33
276kPa	55kPa	250	130	55%	5.39	5.47	8.36	0.03	0.31
		250	130	68%	6.29	8.41	10.84	0.01	0.14
		250	130	74%	3.84	4.16	6.49	0.01	0.14
		250	130	105%	19.42	15.75	32.09	0.02	0.19

F – FEM EXCESS PORE PRESSURE

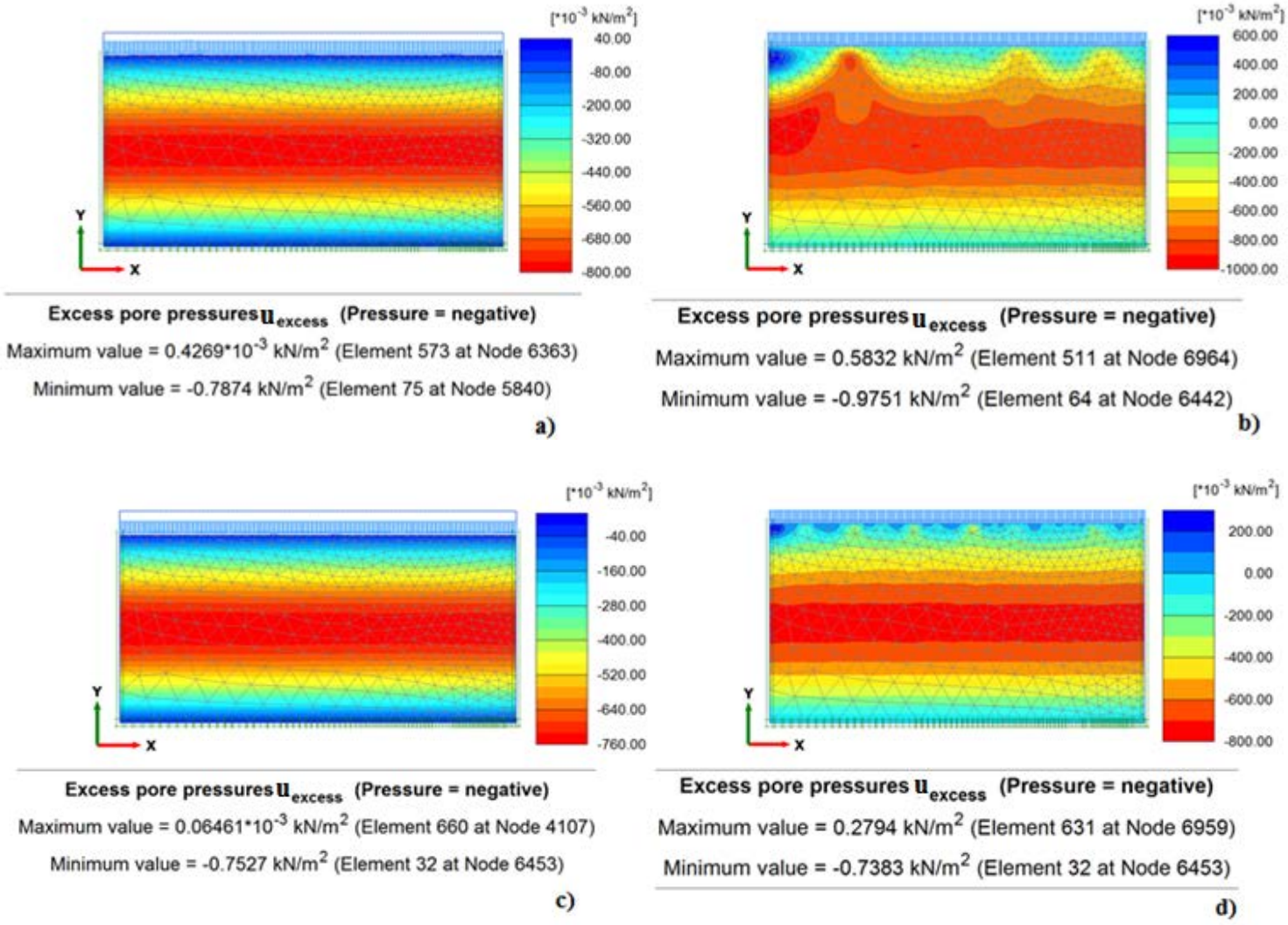

Figure F-1: Excess pore pressure at sample D/H ratio scale 2(a) at; a and c) Plastic-Consolidation simulation model at 55kPa and 110kPa and b and d) Consolidation simulation model at 55kPa and 110kPa respectively

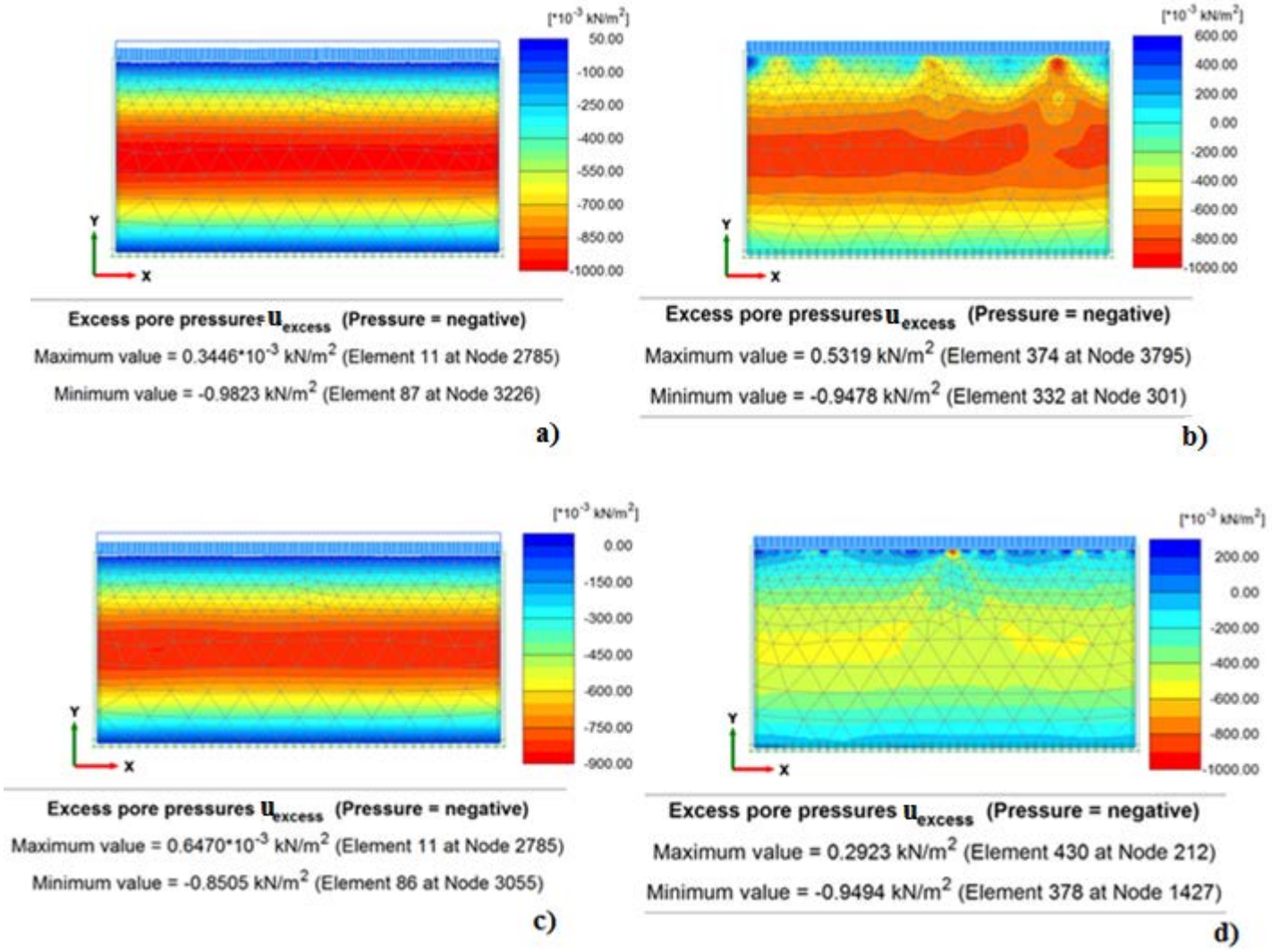

Figure F-2: Excess pore pressure at sample D/H ratio scale 2(b) at; a and c) Plastic-Consolidation simulation model at 55kPa and 110kPa and b and d) Consolidation simulation model at 55kPa and 110kPa respectively

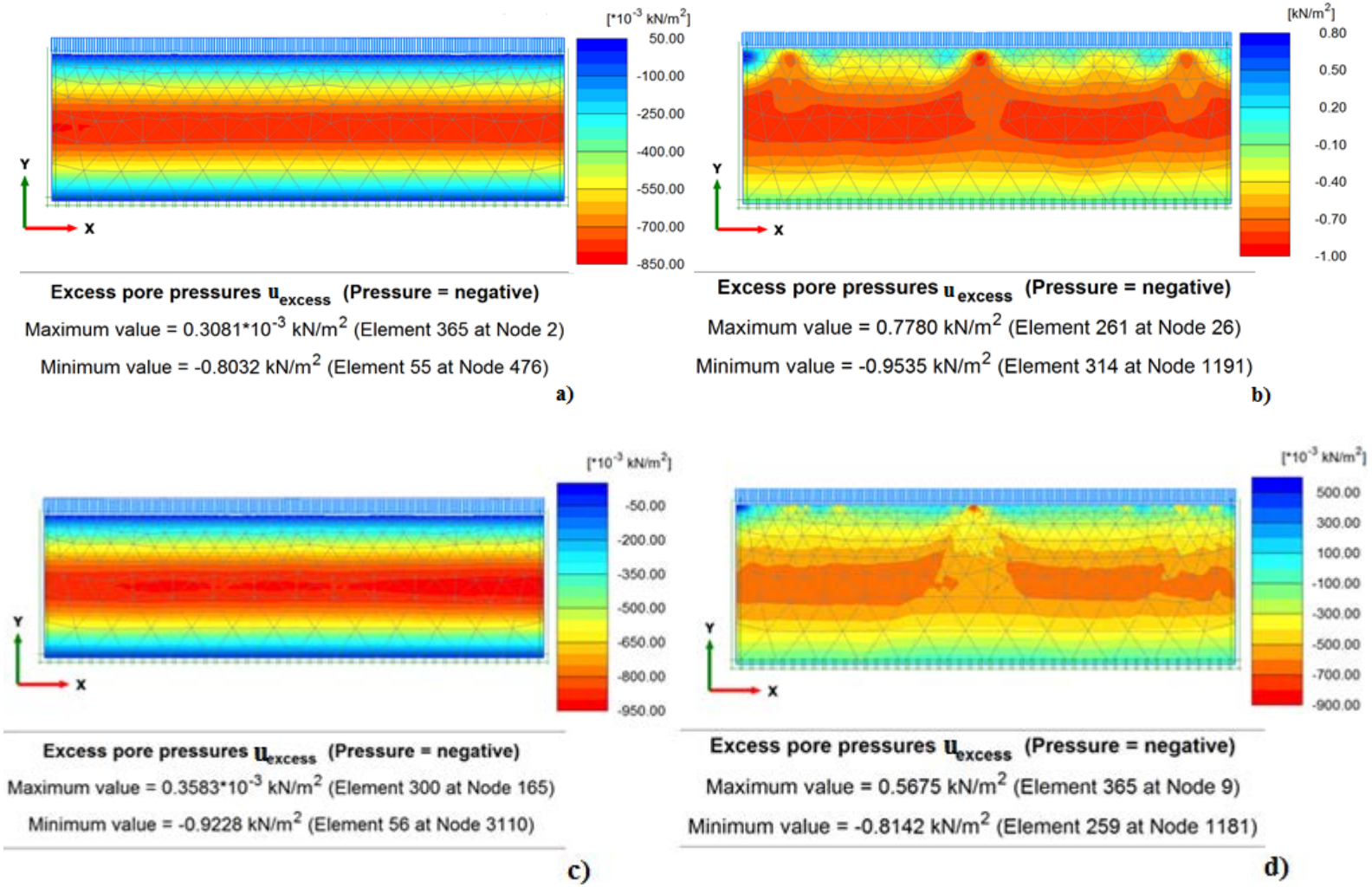

Figure F-3: Excess pore pressure at sample D/H ratio scale 3 at; a and c) Plastic-Consolidation simulation model at 55kPa and 110kPa and b and d) Consolidation simulation model at 55kPa and 110kPa respectively

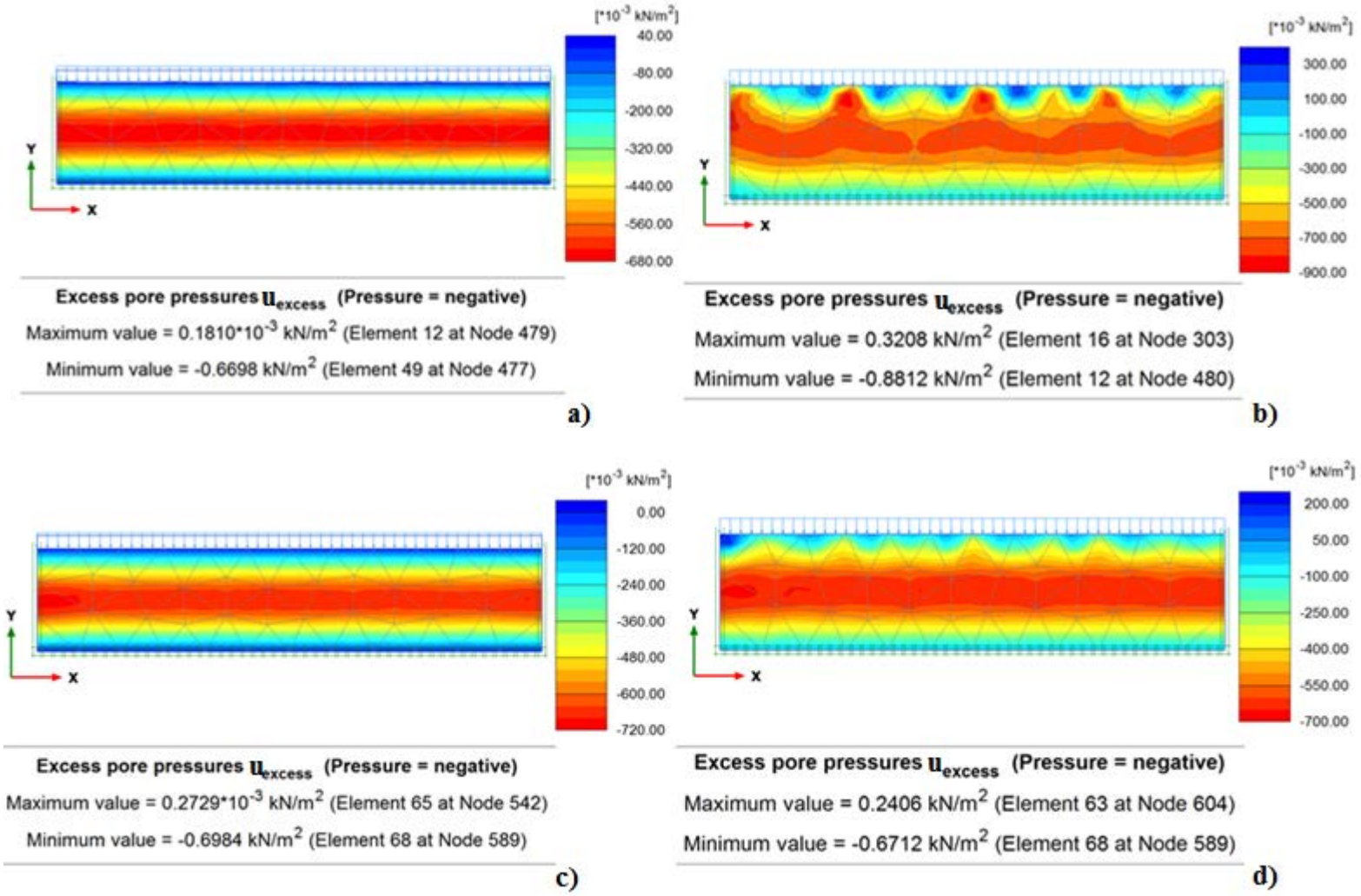

Figure F-4: Excess pore pressure at sample D/H ratio scale 4 at; a and c) Plastic-Consolidation simulation model at 55kPa and 110kPa and b and d) Consolidation simulation model at 55kPa and 110kPa respectively

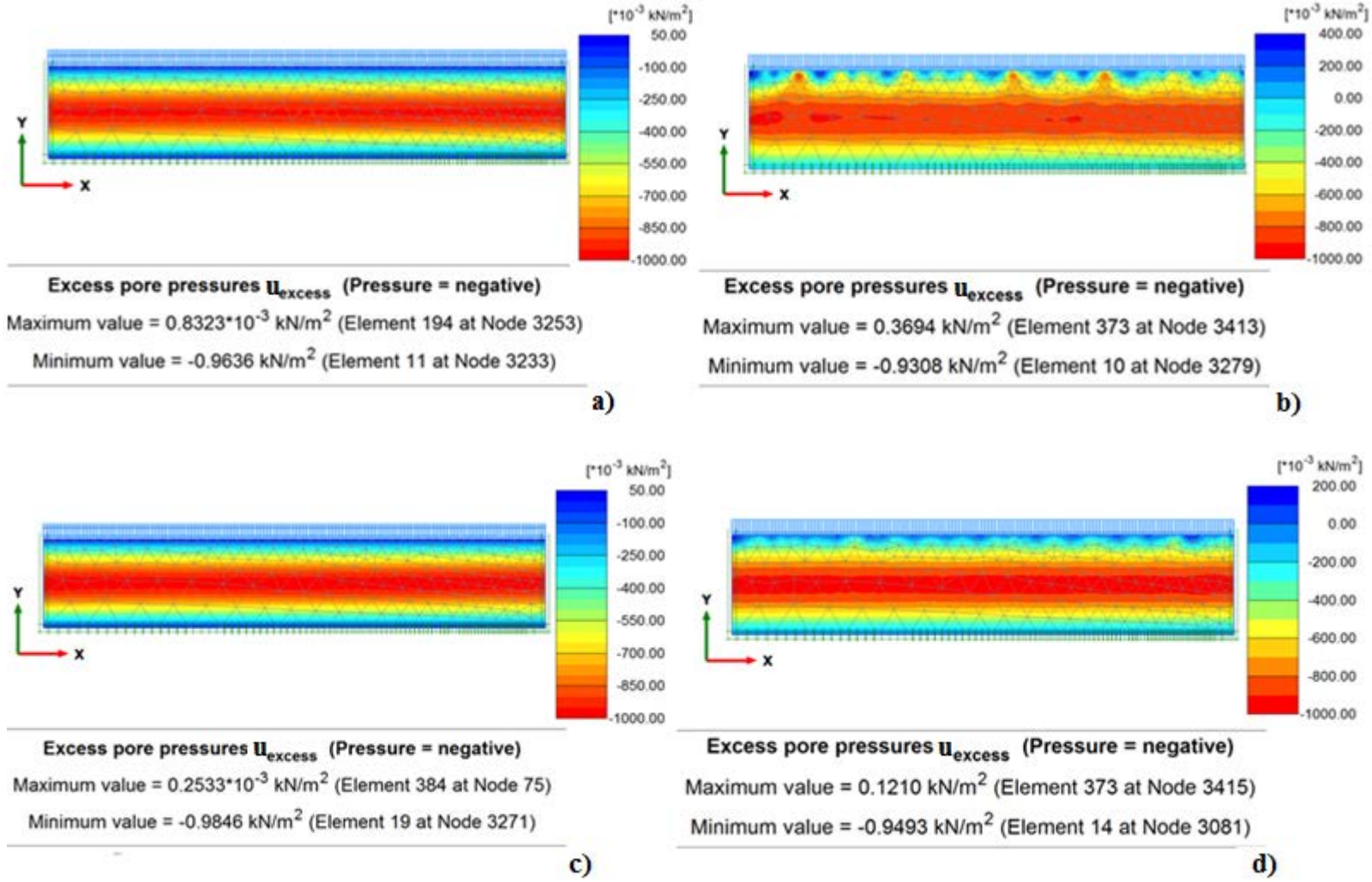

Figure F-5: Excess pore pressure at sample D/H ratio scale 5 at; a and c) Plastic-Consolidation simulation model at 55kPa and 110kPa and b and d) Consolidation simulation model at 55kPa and 110kPa respectively

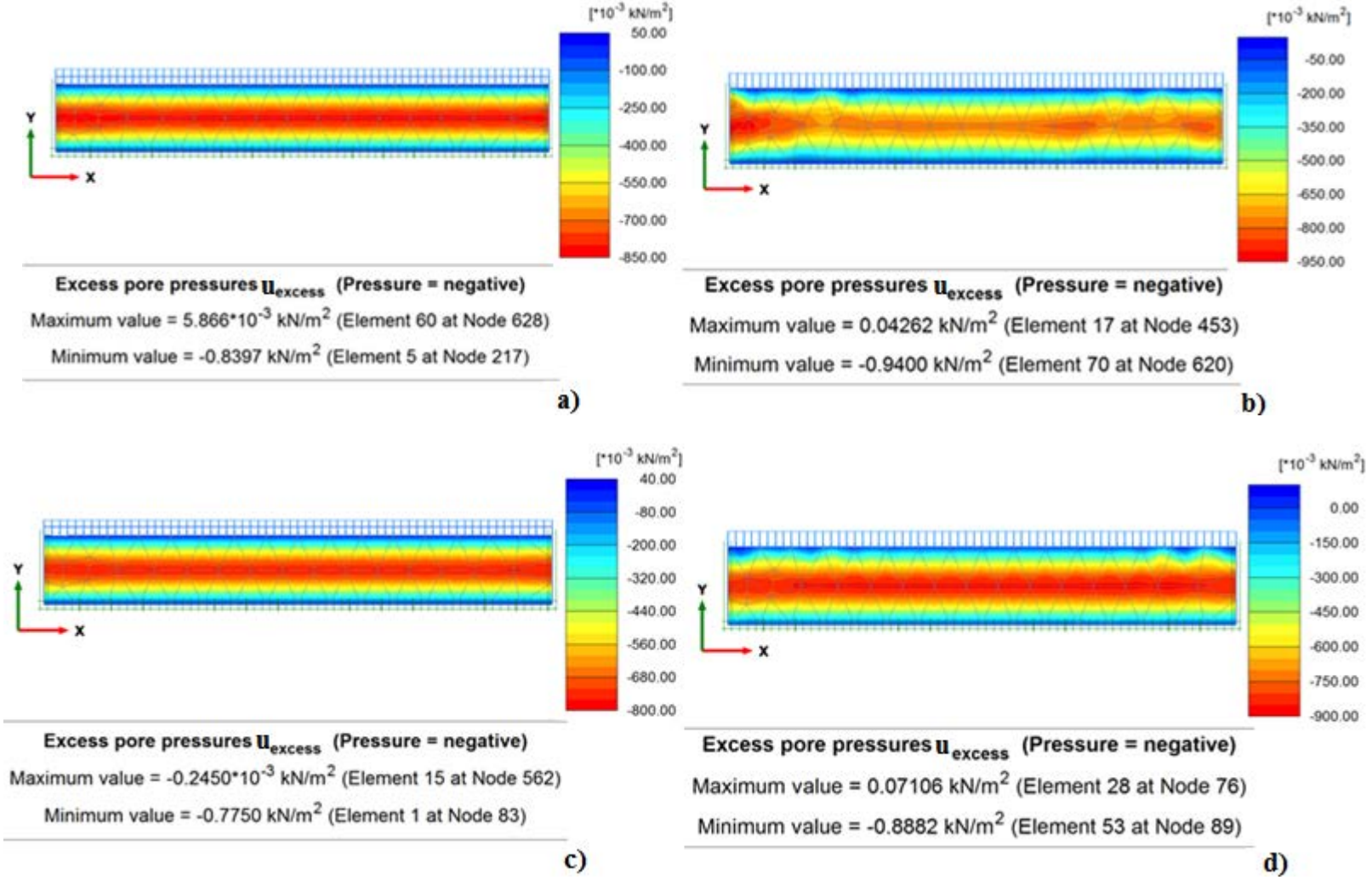

Figure F-6: Excess pore pressure at sample D/H ratio scale 6.5 at; a and c) Plastic-Consolidation simulation model at 55kPa and 110kPa and b and d) Consolidation simulation model at 55kPa and 110kPa respectively

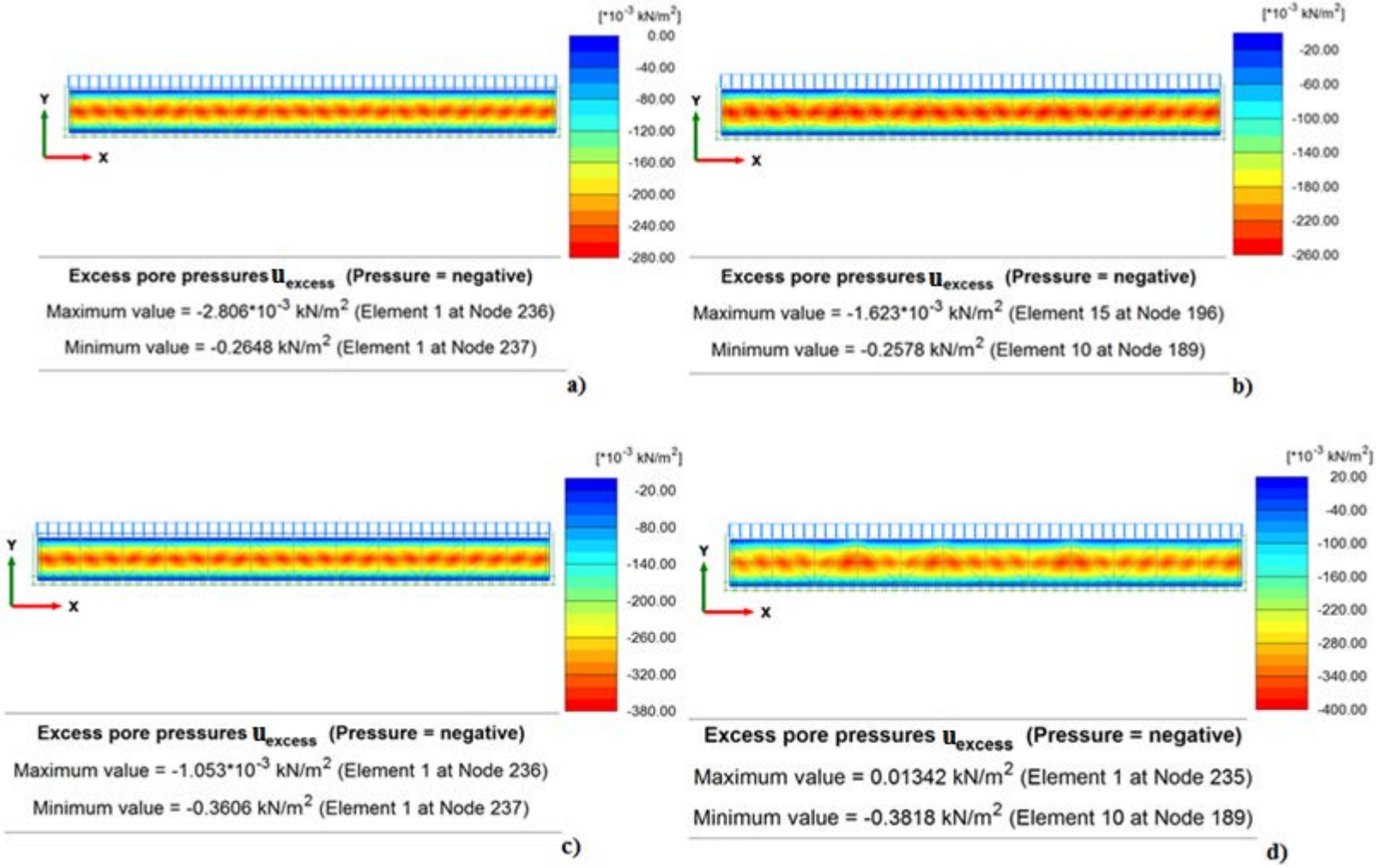

Figure F-7: Excess pore pressure at sample D/H ratio scale 11 at; a and c) Plastic-Consolidation simulation model at 55kPa and 110kPa and b and d) Consolidation simulation model at 55kPa and 110kPa respectively